Deciphering the Role of the Endometrial Microenvironment and Inflammation in Adverse Pregnancy Outcomes and Tumorigenesis

Dissertation

der Mathematisch-Naturwissenschaftlichen Fakultät

der Eberhard Karls Universität Tübingen

zur Erlangung des Grades eines

Doktors der Naturwissenschaften

(Dr. rer. nat.)

vorgelegt von

M.Sc. Janet Pushpa Raja Xavier

aus

Madurai, Indien

Tübingen

2024

Gedruckt mit Genehmigung der Mathematisch-Naturwissenschaftlichen Fakultät der Eberhard Karls Universität Tübingen.

Tag der mündlichen Qualifikation:	19.11.2024
Dekan:	Prof. Dr. Thilo Stehle
1. Berichterstatter/-in:	Prof. Dr. med. Sara Y. Brucker
2. Berichterstatter/-in:	Prof. Dr. Robert Feil

Preface

This dissertation introduces novel mechanistic pathways governing endometrial physiology and identifies their potential role in the pathogenesis of preeclampsia and tumorigenesis. The study was conducted from June 2019 until May 2024 under the supervision of Prof. Dr. med. Sara Y. Brucker and Dr. Madhuri S Salker in the Department of Women's Health at the University Women's Hospital, Tübingen. Prof. Dr. med. Sara Y. Brucker, Medical Director, University Women's Hospital, Tübingen and Prof. Dr. Robert Feil head of the Department of Signal Transduction & Transgenic Models at the Interfaculty Institute for Biochemistry, were members of the doctoral committee.

Acknowledgements

I am pleased to express my gratitude to my supervisor, Prof. Dr. med. Sara Y. Brucker, for granting me this wonderful opportunity to conduct my doctoral research under her guidance. Your scientific input and expertise have profoundly enriched my research endeavors over the years.

I am immensely thankful to Dr. Madhuri S. Salker for her valuable scientific guidance and throughout my journey on this fascinating project. Your belief in me, coupled with your advice, has helped me to navigate through obstacles and evolve into a successful scientist.

I would like to acknowledge Prof. Dr. Robert Feil for his contributions as the member of my doctoral committee. Thank you for your helpful advice and support throughout the years. I want to express my sincere thanks and appreciation to our laboratory head, Dr. André Koch, for his unwavering support and guidance during my PhD journey. Your willingness to share your valuable scientific insights and words of encouragement were immensely helpful.

I want to extend my appreciation to all the members of the Salker research group for fostering a supportive and inspiring environment. Your contribution and encouragement have been invaluable, and I am grateful for the opportunity to have been a part of such a wonderful team. Further, I want to acknowledge everyone from FFG research institute, who has played a role, big or small, in shaping my research journey. I am also thankful to all collaborators for their exceptional contributions to the projects.

I am thankful for the love and support of my friends, who have stood by me through thick and thin, making difficult times bearable and joyful moments even brighter. Thank you for being my second family, a source of warmth and support away from home.

I want to express my deepest gratitude to my family. To my parents, sister, and my extended family, thank you for your belief in me and the endless encouragement you have provided. Your support has been a constant source of strength throughout my life, shaping me into the person I am today. I am profoundly grateful for your unconditional love and guidance.

Lastly, I want to thank my dear husband, John, for always helping me to prioritize what matters the most and for being my pillar of strength. Thank you for everything you bring into my life. Your encouragement, patience, and belief in me have been instrumental in reaching this milestone.

Table of Contents

1. Abbreviations

ABPs	Actin binding proteins
ACTG1	Actin gamma 1
Arp2/3	Actin related protein 2/3
cAMP	Cyclic adenosine monophosphate
CAPZA1	Capping actin protein of muscle z-line subunit alpha 1
COX2	Cyclooxygenase2
DCTN2	Dynactin subunit 2
EnCa	Endometrial cancer
EnSCs	Endometrial stromal cells
EGF	Epidermal growth factor
EGFL7	Epidermal growth factor like domain 7
EIS	Electrical impedance spectroscopy
EMT	Epithelial-to-mesenchymal transition
EVTs	Extra villous trophoblasts
ECM	Extracellular matrix
FGF	Fibroblast growth factor
F-actin	Filamentous actin
G-actin	Globular actin
GAPs	GTPase activating proteins
GDIs	GDP dissociation inhibitors
GEFs	Guanine nucleotide exchange factors
GTP	Guanosine triphosphate
HIFs	Hypoxia-inducible factors
HMG-CoA	3-hydroxy-3-methylglutaryl-coenzyme A
HUVECs	Human umbilical vein endothelial cells
ICC	Intrahepatic cholangiocarcinoma
IQGAP1	IQ motif containing GTPase activating protein 1
IUGR	Intrauterine growth restriction
LC-MS	Liquid chromatography mass spectrometry
LIMKs	Lim kinases

MAPK	Mitogen-activated protein kinase
MCP-1	Monocyte chemoattractant protein
MMP	Matrix metalloproteinase
PAK1	p21-activated kinases1
PE	Preeclampsia
PFN2	Profilin 2
PI3K	Phosphatidylinositol 3-kinase
PlGF	Placental growth factor
PGE_2	Prostaglandin 2
PPARγ	Peroxisome proliferator-activated receptor gamma
Rac1	Ras-related C3 botulinum toxin substrate 1
SGK1	Serum glucocorticoid regulated kinase 1
SMA	Smooth muscle actin
sEng	Soluble endoglin
sFlt1	Soluble fms-like tyrosine kinase-1
TUBA1A	Tubulin alpha 1A
TIMP	Tissue inhibitor of metalloproteinases
VEGF	Vascular endothelial growth factor
VEGFR-A	Vascular endothelial growth factor-A
VEGFR-C	Vascular endothelial growth factor-C
VEGFR-1	Vascular endothelial growth factor receptor-1
VEGFR-2	Vascular endothelial growth factor receptor-2
VSMC	Vascular smooth muscle cell
WAVE2	WASp Family Verprolin-homologous Protein-2
YWHAZ	Tryptophan 5-Monooxygenase Activation Protein Zeta

2. Summary

The decidual transformation during the menstrual cycle is pivotal in preparing the endometrium to support a healthy pregnancy[1,2]. This physiological adaptation of the endometrium involves changes in cell proliferation, morphology, mechanotransduction responses, immune cell modulation, and vascular remodelling[3,4]. Disruptions in these processes can result in pregnancy complications such as implantation failure, recurrent miscarriage, or preeclampsia, as well as contribute to cancer progression[4,5]. This underscores the importance of endometrial preconditioning occurring during each menstrual cycle in women's health.

Preeclampsia is an obstetric complication characterized by inadequate extravillous trophoblast invasion and abnormal placentation[6]. Identifying molecular targets for early detection and treatment of preeclampsia is crucial, considering its severe clinical outcomes and lack of preventative measures[7]. Emerging evidence indicate that endometrial factors (altered decidual mechanics and angiogenesis) play a role in the onset of preeclampsia[5,8-10]. Therefore, investigating the maternal decidual health before pregnancy becomes imperative to uncover novel molecular pathways associated with defective decidua formation, which could potentially contribute to the pathogenesis of preeclampsia.

PlGF, a pleiotropic cytokine, plays expanding roles in diverse biological processes, notably in disease advancement[11]. Anomalies in PlGF production within the endometrial stroma correlate with early pregnancy loss[12]. Elevated PlGF levels are associated with disruptions in cytoskeletal organization and aberrant angiogenesis across various tumor and disease pathologies[13,14]. This thesis aims to investigate the potential contribution of abnormal PlGF levels to the formation of defective decidua by influencing endometrial cellular mechanics and angiogenesis, with implications for preeclampsia pathogenesis. Additionally, it aims to explore if aberrant endometrial milieu influences the progression of cancer.

Earlier studies indicate a possible involvement of abnormal endometrial PlGF and altered decidual biomechanics in the development of preeclampsia[8,15,16]. This thesis (*Manuscript 1*) shows aberrant PlGF stimulation leads to increased Rac1 activity, actin polymerization, and cell stiffness in endometrial stromal cells *in vitro*. Furthermore, dysregulation of Rac1 and actin induced by abnormal PlGF can be mitigated by

treatment with the pharmacological drug pravastatin. Intriguingly, improved actin dynamics in the endometrium with pravastatin also enhances trophoblast cell invasion through endometrial cell monolayers.

Aberrant PlGF also activates anti-angiogenic pathways in endometrial stromal cells through the NFAT5-SGK1-VEGF-A signaling cascade (*Manuscript 2*), hindering normal angiogenic cues in endothelial cells by promoting hypersprouting and impairment of endothelial barrier function. Inhibition of SGK1 improves angiogenic effects and promotes placental cell invasion, implicating SGK1 as a key modulator of PlGF-NFAT5 mediated pathological angiogenic signaling.

Pathological angiogenesis is a key factor in fueling tumor growth and facilitating metastasis[17]. Increased NFAT5 expression was found to be correlated with more aggressive forms of endometrial cancer (*Manuscript 3*). *In vitro* NFAT5 overexpression influenced endometrial cancer cell activity with enhanced cell proliferation and migration. Intriguingly, increased NFAT5 expression triggered the activation of HIF-1α and COX2, fostering an inflammatory milieu within endometrial cancer cells. This environment is characterized by increased levels of PGE_2, likely exacerbating tumour aggressiveness.

Taken together, this thesis sheds light on how abnormal endometrial PlGF levels before pregnancy can disrupt mechanotransduction and uterine vessel development, contributing to impaired decidua formation. These novel maternal mechanistic pathways, which support defective decidua formation prior to conception, may potentially play a role in the manifestation of preeclampsia. Pravastatin emerges as a promising pharmacological candidate to reverse aberrant decidua, offering new therapeutic possibilities for managing preeclampsia. Furthermore, the shared involvement of NFAT5 in abnormal angiogenesis and carcinogenesis underscores the significance of pathological endometrial preconditioning in various endometrial pathologies.

3. Zusammenfassung

Die dezidуale Transformation während des Menstruationszyklus ist entscheidend für die Vorbereitung des Endometriums auf eine gesunde Schwangerschaft[1,2]. Diese Adaption umfasst Veränderungen der Zellproliferation und -morphologie, mechanotransduktive Reaktionen, das Immunsystem und die vaskuläre Umgestaltung[3,4]. Störungen können zu Implantationsversagen, Fehlgeburten oder Präeklampsie führen und Krebs fördern[4,5]. Dies unterstreicht die Bedeutung der Vorprägung des Endometriums für die Frauengesundheit.

Präeklampsie ist eine Schwangerschaftskomplikation, die durch unzureichende Invasion extravillöser Trophoblasten und abnormale Plazentation gekennzeichnet ist[6]. Die Identifikation molekularer Zielstrukturen für die Früherkennung und Behandlung von Präeklampsie ist, aufgrund der schwerwiegenden klinischen Folgen und der fehlenden präventiven Maßnahmen, entscheidend[7]. Neue Erkenntnisse deuten darauf hin, dass endometriale Faktoren beim Auftreten von Präeklampsie eine Rolle spielen könnten[5,8-10]. Daher ist die Untersuchung der Gesundheit des mütterlichen Endometriums vor der Schwangerschaft von entscheidender Bedeutung, um neue molekulare Signalwege aufzudecken, die mit der Bildung einer defekten Decidua in Verbindung stehen und möglicherweise zur Pathogenese der Präeklampsie beitragen könnten.

PlGF, ein pleiotropes Zytokin, spielt eine zunehmende Rolle in verschiedenen biologischen Prozessen, insbesondere im Progress von Krankheiten[11]. Anomalien in der PlGF-Produktion im endometrialen Stroma korrelieren mit frühem Schwangerschaftsverlust[12]. Erhöhte PlGF-Spiegel sind mit Störungen der zytoskelettalen Organisation und abnormer Angiogenese bei verschiedenen Tumor- und Krankheitspathologien assoziiert[13,14]. Ziel dieser Arbeit ist es, den potenziellen Beitrag abnormaler PlGF-Spiegel zur Bildung einer defekter Dezidua durch die Beeinflussung der zellulären Mechanik des Endometriums und der Angiogenese zu untersuchen, was Auswirkungen auf die Pathogenese der Präeklampsie hat. Darüber hinaus soll erforscht werden, ob ein abnormales endometriales Milieu den Progress von Krebs beeinflusst.

Frühere Forschungsarbeiten deuten auf eine mögliche Rolle von aberrantem endometrialem PlGF und abnormale dezidуale Biomechanik in der Pathogenese der

Präeklampsie hin[8,15,16]. Abnorme PlGF-Stimulation führt zu erhöhter Rac1-Aktivität, Aktinpolymerisation und Zellsteifigkeit in endometrialen Stromazellen. Zudem kann die durch abnormes PlGF hervorgerufene Dysregulation von Rac1 und Aktin durch die Behandlung mit dem pharmakologischen Medikament Pravastatin gemildert werden (*Manuscript 1*). Interessanterweise verbessert Pravastatin über die Aktindynamik im Endometrium auch die Invasion von Trophoblastenzellen durch endometriale Monolayer-Zellkulturen.

Aberrantes PlGF aktiviert auch anti-angiogene Wege in endometrialen Stromazellen durch die NFAT5-SGK1-VEGF-A-Signalkaskade (*Manuscript 2*), die normale angiogene Signale in Endothelzellen behindert, indem sie abnormes Sprossen und eine Beeinträchtigung der endothelialen Barrierefunktion fördert. Die Inhibition von SGK1 verbessert angiogene Effekte und fördert die Invasion von Plazentazellen, was auf eine Schlüsselrolle von SGK1 im PlGF-vermittelten pathologischen angiogenen Signalwegs hindeutet.

Die pathologische Angiogenese ist ein Schlüsselfaktor für Tumorwachstum und Metastasierung[17]. Es wurde festgestellt, dass eine erhöhte NFAT5-Expression mit aggressiveren Formen des Endometriumkarzinoms korreliert (*Manuscript 3*). In vitro beeinflusste die NFAT5-Überexpression die Aktivität von Endometriumkarzinomzellen, indem sie die Zellproliferation und -migration verstärkte. NFAT5-Überexpression induziert die Aktivierung von HIF-1α und COX2, welche zu einer erhöhten entzündlichen Mikroumgebung mit erhöhten PGE_2 Spiegeln in endometrialen Tumorzellen führt und somit zur Tumoraggressivität beitragen kann.

Zusammenfassend beleuchtet diese Dissertation, wie abnormale endometriale PlGF-Spiegel vor der Schwangerschaft die Mechanotransduktion und die Entwicklung der Uterusgefäße stören und so zur Beeinträchtigung der Dezidualbildung beitragen können. Neue maternale mechanistische Signalwege, die an der fehlerhaften Dezidualbildung vor der Empfängnis beteiligt sind, und ihre potenzielle Rolle bei der Manifestation von Präeklampsie werden beschrieben. Pravastatin erweist sich als vielversprechender pharmakologischer Kandidat, um diese dezidualen Mechanismen zu bekämpfen und bietet neue therapeutische Möglichkeiten zur Behandlung von Präeklampsie. Darüber hinaus unterstreicht die Beteiligung von NFAT5 an abnormaler Angiogenese und Karzinogenese die Bedeutung der pathologischen Vorprägung des Endometriums bei verschiedenen endometrialen Pathologien.

4. List of Publications

Manuscript 1: Excessive endometrial PlGF - Rac1 signaling underlies endometrial cell stiffness linked to pre-eclampsia.

Janet P. Raja Xavier, Carmela Rianna, Emily Hellwich, Iliana Nikolou, Aditya Kumar Lankapalli, Sara Y. Brucker, Yogesh Singh, Florian Lang, Tilman E. Schäffer, and Madhuri S. Salker

Commun Biol 7, 530 (2024); doi: 10.1038/s42003-024-06220-7; PMID: 38704457

Manuscript 2: Placental growth factor mediates pathological uterine angiogenesis by activating the NFAT5 - SGK1 signaling axis in the endometrium: Implications for preeclampsia development.

Janet P. Raja Xavier, Toshiyuki Okumura, Melina Apweiler, Yogesh Singh, Sara Y. Brucker, Satoru Takeda, Florian Lang, and Madhuri S. Salker

Biol Res. 2024 Aug 17;57(1):55. doi: 10.1186/s40659-024-00526-w; PMID: 39152497

Manuscript 3: Rel Family Transcription Factor NFAT5 Upregulates COX2 via HIF-1α Activity in Ishikawa and HEC1a Cells.

Toshiyuki Okumura, **Janet P. Raja Xavier**, Jana Pasternak, Zhiqi Yang, Cao Hang, Bakhtiyor Nosirov, Yogesh Singh, Jakob Admard, Sara Y. Brucker, Stefan Kommoss, Satoru Takeda, Annette Staebler, Florian Lang, and Madhuri S. Salker.

Int. J. Mol. Sci. 2024, 25(7), 3666; doi: 10.3390/ijms25073666; PMID: 38612478

5. Personal Contribution

Manuscript 1: Excessive endometrial PlGF - Rac1 signaling underlies endometrial cell stiffness linked to pre-eclampsia.

I was involved in designing the experiments and selecting methodologies. Additionally, I conducted all the methodologies expect for *in vitro* PlGF kinetic assay, acquired the data, performed data analysis, interpreted the results, data visualization and contributed to both manuscript writing and editing.

Manuscript 2: Placental growth factor mediates pathological uterine angiogenesis by activating the NFAT5-SGK1 signaling axis in the endometrium: Implications for pre-eclampsia development.

I contributed to research concepts, designed experiments, and selected methodologies. Furthermore, I executed all methodologies, curated the data, conducted data analysis, interpreted the results, data visualization and contributed to the writing of the original draft as well as manuscript editing.

Manuscript 3: Rel Family Transcription Factor NFAT5 Upregulates COX2 via HIF-1α Activity in Ishikawa and HEC1a Cells.

I conducted certain experimental methodologies, participated in data curation, performed data analysis, interpreted the data, and prepared figures. Additionally, I contributed to manuscript writing and participated in editing.

6. Introduction

6.1 Endometrial anatomy and physiology

The endometrium forms the innermost layer of the uterine wall, comprising two main layers: *the functionalis* and *the basalis*[3]. Positioned alongside the contractile myometrium, it is bordered by the outermost perimetrium, which connects to pelvic connective tissue and extends into the peritoneal cavity[18]. The endometrium comprises various cell types, including stromal cells, epithelial cells, vascular cells, and immune cells, along with glands that produce essential cues for supporting pregnancy[3] (*Figure 1*). Throughout the menstrual cycle, fluctuations in hormones such as estrogen, progesterone, luteinizing hormone, follicle-stimulating hormone, and growth factors like vascular endothelial growth factor (VEGF) and epidermal growth factor (EGF) induce changes in endometrial cellular proliferation, cell type distributions, and tissue architecture[3,19]. Estrogen promotes the growth of both stromal and epithelial cells, leading to the thickening of the endometrium in the proliferative phase[20]. Conversely, ovulation initiates a transition to a progesterone-dominant secretory phase[3]. Following ovulation, the glands become more tortuous and secrete various factors into their

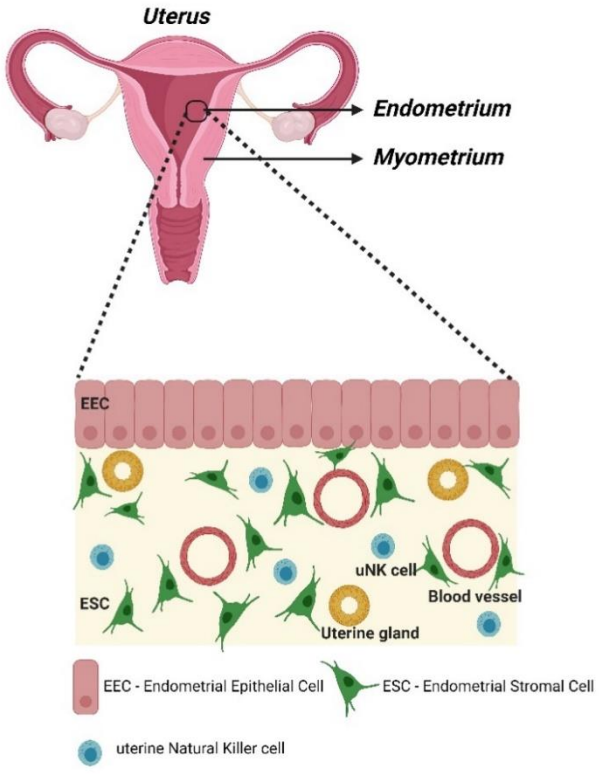

Figure 1.Schematic ross-section of the endometrium: The cross-section of the endometrium reveals a layer of columnar epithelium and connective tissue lining the uterine wall. The connective layer comprises stromal cells, vascular cells, uterine glands, and immune cells. Adapted from Lang et al., 2020[1]. The image was created with BioRender

lumens to support potential embryo implantation[3]. Critical to all phases of the menstrual cycle is the simultaneous growth and regression of the uterine vasculature that supplies the endometrium[21]. Endometrial blood vessels undergo significant morphological and functional changes throughout the three phases of the menstrual cycle[21]. In the absence of pregnancy, the decline of the progesterone-producing corpus luteum triggers hormone withdrawal, leading to focal shedding of the superficial layer of the endometrium (*the functionalis*) and exposure of the underlying layer (*the basalis*)[22]. Therefore, proper endometrial function necessitates the ability to regenerate from inflammatory tissue repair event occurring during each menstrual cycle[5].

6.2 Endometrial adaptions for a successful pregnancy

During both the programmed shedding and repair phases of menstrual cycle, as well as in early pregnancy, the endometrium undergoes substantial remodeling within its cellular compartments[23]. This process entails dynamic communication between uterine cells, endocrine factors, and immune cells within the uterus, which is vital for the effective shedding of the endometrium and its subsequent re-epithelialization following each menstrual cycle[3]. If pregnancy occurs instead, the endometrium undergoes further remodeling to facilitate implantation and support placenta and fetal development[24]. Therefore, the cyclic process of endometrial decidualization followed by menstrual shedding serves as a physiological preconditioning, preparing uterine tissue for the significant remodeling associated with successful embryo implantation and deep placentation during early pregnancy[2,25]. These physiological adaptations during endometrial repair involve various processes such as cell proliferation, migration, oxidative stress, decidualization, cytoskeletal changes, alterations in ECM composition, angiogenesis, and vascular remodeling to varying degrees[18,22,23,26] (*Figure 2*). The endometrium responds optimally to a range of hormonal (such as estrogen and progesterone), chemical (growth factors such as VEGF), and mechanical signals (such as cell stiffness and extracellular matrix elasticity) to fulfill these diverse functions[27,28].

6.2.1 Biomechanical adaptations of the endometrium

During the process of endometrial reconstruction following menstruation, the endometrium experiences crucial changes in its biomechanical characteristics. Across the menstrual cycle, changes in mechanobiology encompass alterations in basement membrane composition, remodeling of cytoskeletal proteins, and an overall shift in

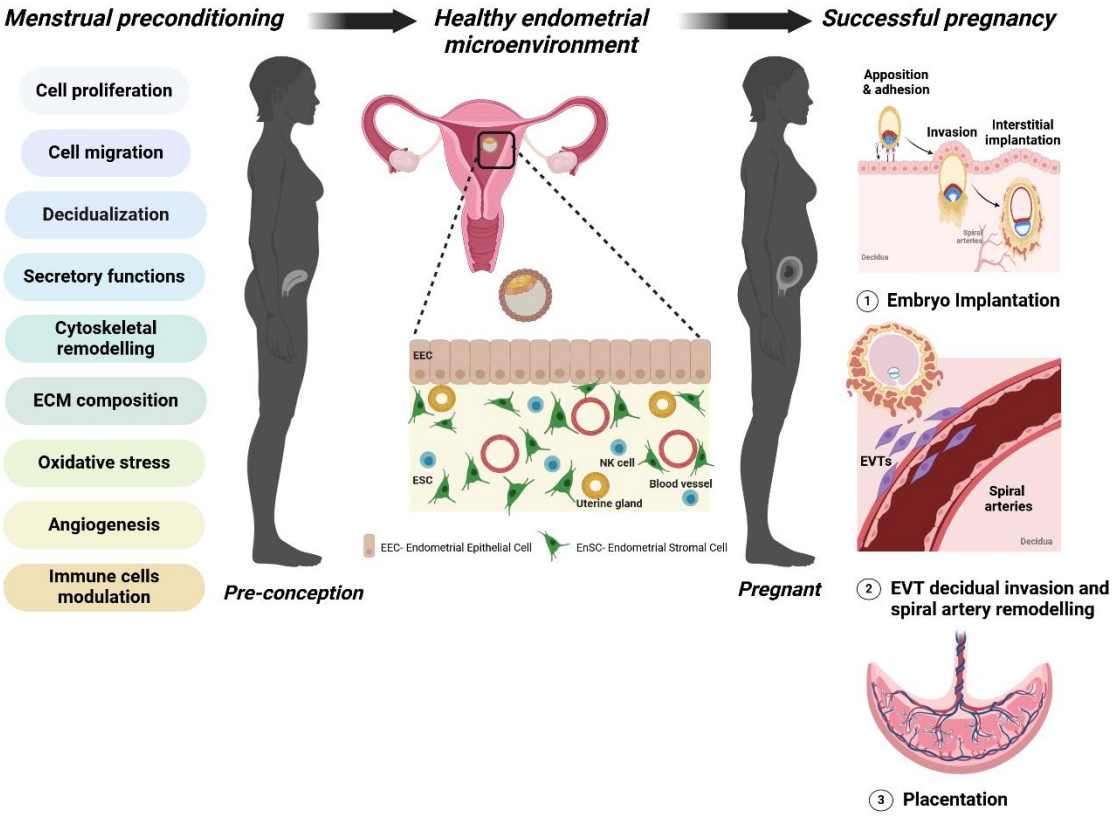

Figure 2. Endometrial cellular adaptions for a successful pregnancy: The endometrium undergoes extensive cellular and tissue modifications during menstrual repair and regeneration to maintain healthy microenvironment. These essential preconditioning mechanisms prepares the endometrium to accommodate early pregnancy events in case of a successful embryo implantation, thus rendering protection against abnormal pregnancy outcomes. The image was created with BioRender.

extracellular matrix composition[18]. Decidualization involves significant modifications in the extracellular matrix and the partial mesenchymal-epithelial transition of resident fibroblasts, leading to tissue softening[29]. During the mid-secretory phase, stromal edema and decreased fibrous components of the connective tissue compartment promote tissue loosening, facilitating implantation and aiding in physiological placentation[24]. Similarly, junctional adhesion, cytoskeletal rearrangement, and extracellular matrix stiffness regulate endometrial proliferation, differentiation, and blastocyst invasion during early pregnancy[18]. These preparatory changes modify the mechanical properties of the endometrium to enhance blastocyst adhesion and migration through the epithelial surface layer into the underlying connective tissue compartment[18,30]. Additionally, they support adequate invasion of extravillous trophoblasts (EVTs) into the decidua for spiral artery remodeling[18]. The mechanobiology of the endometrium during uterine repair is governed by various mechanotransduction pathways[5].

6.2.1.1 Rac1-PAK1 signaling effectors on cellular mechanobiology

Mechanical cues within the cellular microenvironment, including factors such as extracellular matrix properties, stretching, compression, actin turnover, cell stiffness, and shear stress, play a crucial role in maintaining homeostasis[31]. Disruption to these cellular mechanical properties interfere with mechanosensing and mechanotransduction signaling pathways, potentially driving various pathophysiologies[31,32].

Ras-related C3 botulinum toxin substrate 1 (Rac1) is a member of the Rho family of small GTPases, recognized as a key intracellular mechanotransduction mediator[33]. Rac1 can regulate multiple cell activities such as proliferation, migration, and differentiation as well as biological processes such as cytoskeletal dynamics, metabolism, and organ development[34]. The activation of Rho GTPases is positively mediated by guanine nucleotide exchange factors (GEFs) and the inactivation is regulated by GTPase activating proteins (GAPs) and GDP dissociation inhibitors (GDIs)[31]. Thus, activation of Rac1 occurs when it binds to GTP (guanosine triphosphate), leading to conformational changes that enable its interaction with downstream effector proteins, ultimately leading to the regulation of cellular processes[31]. Dysregulation of Rac1 signaling has been implicated in various diseases, including cancer, where Rac1 promotes tumour cell invasion and metastasis, as well as inflammatory and cardiovascular disorders[35-37].

Rac1 plays a pivotal role in regulating the actin cytoskeleton through various mechanisms[37]. One such mechanism involves Rac1 binding to WASp Family Verprolin-homologous Protein-2 (WAVE2) proteins, leading to the activation of the actin-nucleating protein, actin-related protein 2/3 (Arp2/3) complex[38]. Rac1 can also influence actin cytoskeleton dynamics by binding to p21-activated kinases (PAKs), which subsequently initiate cytoskeletal rearrangement by phosphorylating Lim kinases (LIMKs)[39]. Activation of the Rac1/PAK/WAVE2 axis initiates the growth of new branched filaments, facilitating dynamic cytoskeletal rearrangements. The regulation of actin by Rac1 is essential for various cellular processes, including cell-cell adhesion, early cell-ECM interactions, cell motility, and polarization[33]. These functions represent crucial outcomes of Rac1 signaling, highlighting its central role in coordinating cytoskeletal dynamics and cellular behavior.

6.2.1.2 Actin cytoskeleton

The actin cytoskeleton comprises filamentous actin (F-actin), formed by the polymerization of globular (G-actin) molecules, along with numerous actin-binding proteins (ABPs)[40]. These ABPs, regulated by the small GTPase signaling systems (such as RhoA, Rac1, and Cdc42), facilitate the assembly of actin filaments into various cytoskeletal structures[41]. These structures collectively form a mechanically robust actin cytoskeleton, characterized by interconnected networks of filaments with diverse arrangements and functions[42]. The architecture of the cytoskeleton governs the mechanical characteristics of the cell[42].

Actin filaments establish connections with focal adhesions at points of cell-substrate contact and adherens junctions at regions of cell-cell interaction[43]. These filaments serve essential functions in both detecting mechanical stimuli and producing contractile forces through association with the motor protein myosin II[44]. Additionally, actin filaments contribute to propelling the plasma membrane forward through polymerization-generated forces[44]. The forces generated, whether through actin polymerization or myosin II motor activity, are propagated throughout the cell and ultimately transmitted to adhesion sites[43]. Actin cytoskeletal remodelling has the potential to mediate mechanical stress-induced gene expression and plays crucial roles in mechanical force-induced cell proliferation, differentiation, and various physiological and pathophysiological processes, including embryogenesis, organogenesis, tissue homeostasis, organ size control and cancer progression[44-46].

6.2.2 Vascular adaptations of the endometrium

In healthy adult humans, physiological angiogenesis typically occurs infrequently, except during wound healing and within the female reproductive tract[47]. Particularly in the endometrium, the process of angiogenesis is tightly regulated throughout the reproductive period[47]. Throughout the menstrual cycle, the uterine vasculature undergoes dynamic changes in response to hormonal fluctuations and reproductive events[48]. Angiogenesis begins with the repair of the vascular bed post menstruation, followed by remarkable lengthening of spiral arteries and stromal proliferation[47]. Under estrogen influence in the proliferative phase of the cycle, vessel growth occurs, preparing the endometrium for potential implantation[21,49]. Enhanced angiogenesis and spiral artery growth, driven by increased estrogen and progesterone levels, lead to complex vessel remodeling[47]. When no implantation occurs, corpus luteum degeneration, coupled with decreased estrogen and progesterone levels, triggers

vasoconstriction of spiral arteries, causing endometrial ischemia and necrosis[28,50]. Thus, unlike conventional vascular beds, the endometrial vasculature demonstrates dynamic growth and regression throughout the menstrual cycle, marked by significant morphological and functional alterations. In the endometrium, a plethora of factors, both hormonal (VEGF, Thromospodin-1, etc.,) and non-hormonal (Hypoxia, MMPs, etc.,) have been identified to facilitate angiogenesis[51-54]. These factors are thought to foster endometrial angiogenesis by modulating the expression and function of angiogenic molecules within endometrial stromal cells[55]. Subsequently, these molecules act in a paracrine manner on endothelial cells to facilitate endometrial angiogenesis[55,56].

After successful implantation, the uterine arteries undergo crucial adaptations to accommodate the developing fetus[9]. These adjustments involve heightened blood flow, vasodilation, enhanced angiogenesis, remodeling of spiral arteries, and promotion of placental growth[9]. These vascular changes are vital for providing the placenta with sufficient nutrients and oxygen, essential for maintaining a healthy pregnancy[57]. Therefore, the quality of uterine vessels in the maternal microenvironment is paramount for achieving favorable pregnancy outcomes.

6.2.3 Consequences of abnormal endometrial adaptions

The cyclic nature of menstruation serves as a protective mechanism, shielding uterine tissues from the hyperinflammation and oxidative stress associated with early pregnancy events such as deep placentation[2]. Defective decidua, therefore, contributes to the establishment of a pathological maternal-fetal interface upon pregnancy[58]. This has relevant clinical consequences, ranging from recurrent implantation failure and pregnancy loss in early pregnancy to several serious complications of advanced gestation, such as miscarriage, preeclampsia (PE), intra-uterine growth restriction (IUGR), and still birth[58-61]. Recent evidence suggests that certain endometrial disorders, such as endometrial fibroids, chronic endometritis, and endometriosis, can negatively affect decidualization in the endometrium[62-64]. This may elucidate some aspects of the reduced reproductive outcomes in women associated with these conditions. Further research is required to fully comprehend the biomolecular mechanisms underlying defective decidualization, which impacts the endometrial microenvironment. Despite the clinical importance of the above stated complications and the knowledge on events related to uterine endometrial adaptations

pre-conception and early pregnancy, there is still a need for identifying new therapeutic targets. The complexity of endometrial microenvironment and the intricate interplay among different molecular regulators present a significant challenge in identifying pathological modulators.

6.3 Preeclampsia

6.3.1 Disease pathophysiology

PE is a pregnancy-related multisystem disorder, affects approximately 2% to 8% of pregnant women and poses significant both maternal and fetal mortality risks[6]. Hypertension and proteinuria are hallmark features, often accompanied by systemic organ dysfunction such as liver complications and cardiovascular diseases[6] (*Figure 3*). PE follows a two-stage model: abnormal placental development leads to poor perfusion and placental ischemia, causing maternal endothelial dysfunction and resulting in hypertension, proteinuria, and other systemic symptoms[65]. Currently, PE classification primarily relies on gestational age at diagnosis, distinguishing between early-onset and late-onset forms[66]. Early-onset PE is linked to defective placentation, while late-onset PE appears associated with maternal cardiovascular predisposition and issues related to maternal-fetal perfusion imbalance[66]. In normal pregnancy, trophoblast invasion into the decidualized endometrium prompts spiral artery remodeling, facilitating enhanced blood flow to the placenta[6]. However, in PE, inadequate trophoblast invasion results in incomplete spiral artery remodeling, leading to poor placentation[66]. Consequently, reported to increase placental ischemia, prompting increased secretion of angiogenic markers like soluble fms-like tyrosine kinase-1 (sFlt-1) and soluble endoglin (sEng) into the maternal circulation[66,67]. This dysregulation of angiogenic factors damages maternal endothelium, giving rise to the clinical manifestations of PE[67].

6.3.2 Etiology of PE

The biological mechanisms linking clinical findings to observed multi-organ dysfunction in PE remain largely elusive[68]. However, extensive literature highlights various risk factors associated with PE, shedding light on the diverse factors that increase the risk of developing PE syndromes. Some potential etiologies linked to PE manifestations

include uteroplacental ischemia, gestational diabetes mellitus, and maternal obesity[69-71].

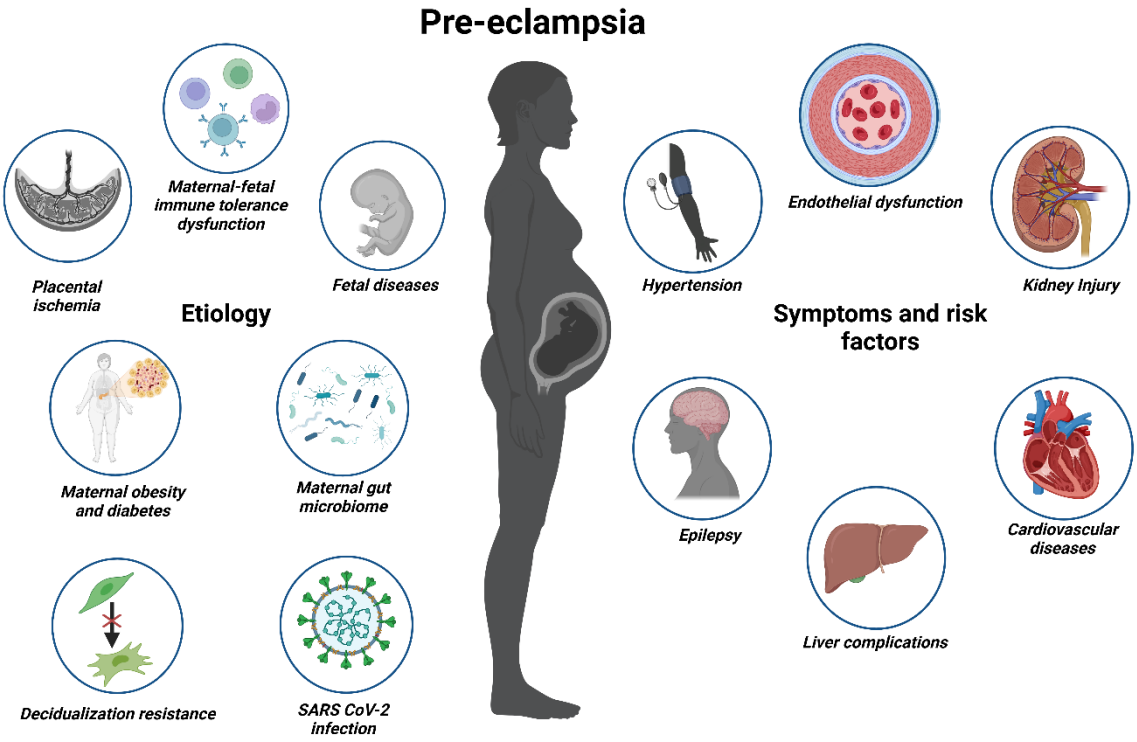

Figure 3. Pre-eclampsia etiology and symptoms: Pre-eclampsia is a multi-factorial pregnancy disorder with varying proposed etiology from placental, fetal and maternal origin. Hypertension is key feature of pre-eclampsia, involving various other symptoms and risk factors. Adapted from Jung et al., 2022 [72]. The Image was created in BioRender.

Notably, emerging research suggests a role for maternal gut dysbiosis in PE pathogenesis[73]. Moreover, recent reports indicate a possible association between SARS-CoV-2 infection and PE, although the underlying mechanisms remain unclear[74]. Other etiologic factors implicated in PE include the breakdown of maternal-fetal immune tolerance, endocrine disorders, placental aging, and fetal conditions such as ballantyne syndrome or mirror syndrome[72]. Recent research has highlighted significant maternal contributions to PE, particularly focusing on decidualization resistance and its role in PE pathophysiology. It's been observed that an impaired maternal microenvironment, characterized by defective decidua before pregnancy, serves as a precursor for PE development[8,75]. Despite these insights, the cause of deficient arterial invasion by EVTs leading to poor placentation remains unclear. Therefore, further comprehensive research is necessary to elucidate the complex mechanisms underlying the development of PE.

6.4 Placental growth factor

6.4.1 Structure and function

Placental growth factor (PlGF) is a pleiotropic cytokine belonging to the VEGF family, pivotal for angiogenesis and vasculogenesis[11]. While primarily synthesized in the placenta, PlGF is also expressed in various tissues like the heart, lungs, and kidneys. PlGF is a homodimeric glycoprotein, composed of two identical subunits held together by disulfide bonds[11]. Each subunit contains a conserved cysteine-knot motif typical of the VEGF family, crucial for receptor binding and activation[11]. Its biological actions are mediated through binding to its receptor, vascular endothelial growth factor receptor-1 (VEGFR-1), triggering downstream signaling pathways crucial for angiogenesis, endothelial cell proliferation, migration, and survival[76,77]. In addition to its direct effects on endothelial cells, PlGF indirectly influences angiogenesis by modulating other angiogenic factors like vascular endothelial growth factor-A (VEGF-A)[77]. It forms heterodimers with VEGF-A, enhancing its activity and promoting binding to vascular endothelial growth factor receptor-2 (VEGFR-2), the primary receptor for VEGF-A mediated angiogenesis[77]. Unlike VEGF, PlGF is prominently upregulated in pathological conditions, including hypoxia. Various stimuli such as inflammatory cytokines, growth factors, hormones, and oncogenes can induce PlGF expression in pathological states[11].

6.4.2 PlGF supports pathological angiogenesis

PlGF holds a crucial role in disease pathology, as its expression escalates in numerous pathological conditions, including various cancers, chronic inflammatory ailments, and diverse eye diseases (e.g. diabetic retinopathy)[78-80]. Inhibiting PlGF has shown promise in selectively curbing pathological angiogenesis while sparing physiological vessels, potentially mitigating side effects[11]. PlGF directly fosters vessel growth by influencing endothelial cell growth, migration, and survival, as well as vessel maturation[81]. It augments the proliferation and recruitment of smooth muscle cells and supports fibroblast proliferation, a hallmark of pathological angiogenesis[11]. Moreover, PlGF can heighten vascular permeability by disrupting endothelial cell junction integrity, facilitating the extravasation of plasma proteins and inflammatory cells into surrounding tissues, thereby promoting inflammatory responses[82]. Additionally, PlGF recruits circulating proangiogenic cells, like endothelial progenitor cells and myeloid cells, to angiogenic sites, aiding in the formation and stabilization of new blood vessels, further exacerbating pathological angiogenesis[77]. Furthermore, PlGF potentiates the

effects of VEGF- A, enhancing their binding to VEGFR-1 and VEGFR-2, consequently amplifying the signaling, and promoting pathologic angiogenic responses[77]. Hence, targeting PlGF signaling pathways emerges as a promising therapeutic strategy for inhibiting pathological angiogenesis across various diseases[83-85].

6.4.3 PlGF supports aberrant cytoskeletal remodeling

The understanding of PlGF in cellular mechanotransduction is still at infancy. Recent research suggests that PlGF may play a role in cellular mechanics, particularly through its involvement in cytoskeletal remodeling. PlGF has been found to enhance the motility of breast cancer cells by activating the phosphorylation of extracellular signal-regulated kinases (ERK1/2), which is associated with cytoskeletal rearrangement[13]. This indicates that PlGF signaling may influence the dynamic organization of the cytoskeleton, which is essential for cell movement and migration processes.

Furthermore, emerging evidence implicates PlGF in supporting the progression of intrahepatic cholangiocarcinoma (ICC) by promoting tumor desmoplasia. Desmoplasia refers to the abnormal accumulation of fibrous tissue within tumor microenvironments, leading to increased tissue stiffness[86]. PlGF appears to contribute to this process by promoting fibrosis and collagen deposition within ICC tumors, thereby creating a stiffer extracellular matrix (increased tissue stiffness) that supports tumor growth and invasion[86]. Overall, these findings highlight the diverse roles of PlGF in cancer progression, including its involvement in cytoskeletal remodeling and tumor desmoplasia. Further research into the mechanistic pathways underlying PlGF-mediated effects on cellular mechanotransduction and cytoskeletal remodeling could provide valuable insights.

6.5 Nuclear factor of activated T cell 5

6.5.1 NFAT5 as a transcription factor

Nuclear Factor of Activated T cell 5 (NFAT5) belongs to the Rel family of transcriptional regulators and possesses a DNA binding domain that shares sequence homology with the Rel homology domain (RHD)[87]. Unlike its counterparts (NFAT 1-4), NFAT5 lacks a calcineurin binding domain outside of its DNA binding domain[87]. The NFAT5 protein features a leucine-rich nuclear export sequence (NES) followed by a proline-rich transactivation domain (AD1) at the N-terminal[88]. Additionally, it harbors a low-complexity glutamine and serine/threonine-rich region (AD2 and AD3) at the C-terminal end. These three activation domains (AD1, AD2, and AD3) act in concert in response

to hypertonic signals[88] (*Figure 4*). NFAT5 undergoes regulation within approximately 30 minutes when a cell experiences hypertonic stress. Its phosphorylation is controlled

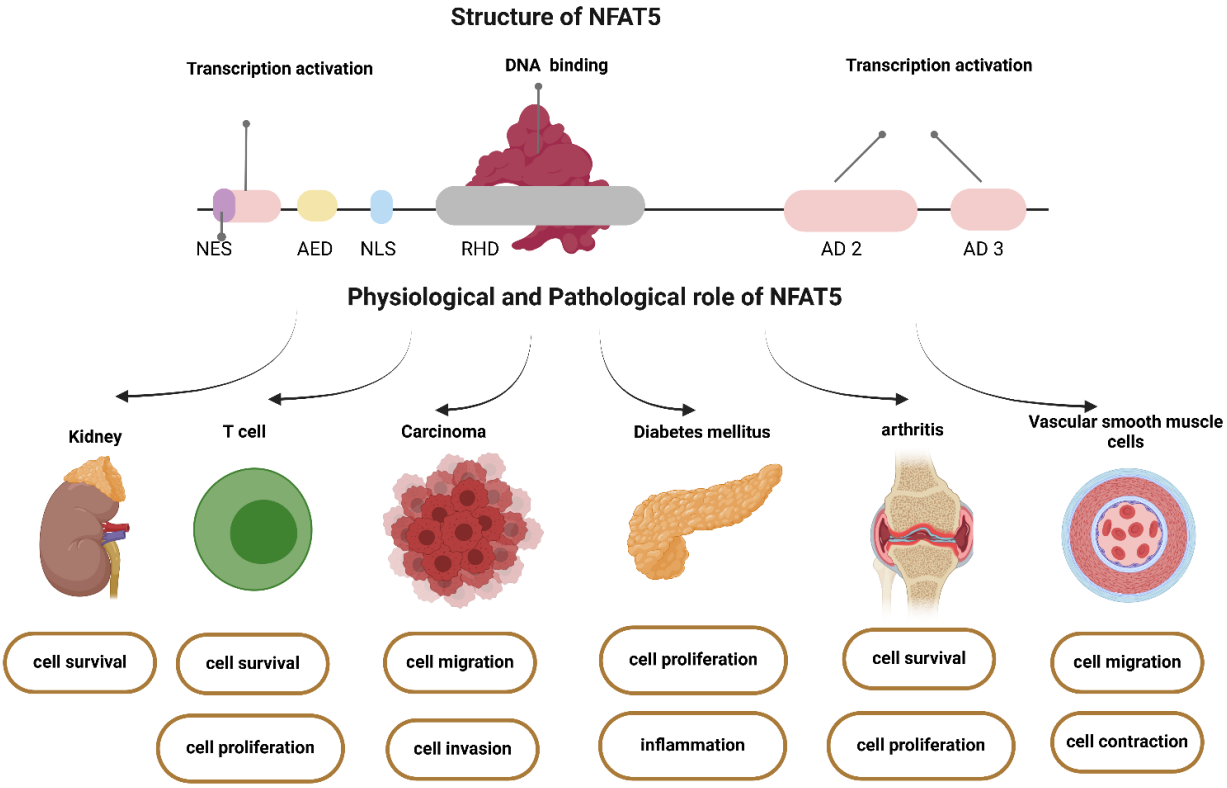

Figure 4. Structure and diverse roles of NFAT5: The structural domain organization of tonicity sensitive transcription factor NFAT5. NFAT5 contains nuclear export sequence (NES), auxiliary export domain (AED) and three transcription activation domains (AD1, AD2 and AD3). It also contains a nuclear localization signal (NLS) and Rel-homology domain for DNS binding (RHD). NFAT5 transcriptional activity regulates different physiological and pathological functions under hypertonic or non-hypertonic stimulus in different tissues. The image was created in BioRender.

by various kinases, with some such as p38 MAPK, protein kinase A, and Fyn playing a role in activating NFAT5[89,90]. Notably, NFAT5 stands out as the sole transcription factor known to undergo bidirectional nucleocytoplasmic trafficking[90]. Aside from hypertonicity, numerous tonicity-independent agents are known to stimulate NFAT5 activity[87]. These signals, like hypertonicity, elevate NFAT5 mRNA and protein levels. Reported tonicity-independent stimuli regulating NFAT5 transcriptional activity include ischemia, hypoxia, inflammatory stimuli, reactive oxygen species, and metabolic stress[87]. NFAT5 serves a protective role under normal conditions but can have detrimental effects in pathological conditions[89]. Its protective and pathological effects in response to various stressors are documented across different tissues (*Figure 4*). For instance, in the renal medulla, NFAT5 activation by local hypertonicity is crucial for its physiological function and for shielding the tissue from the adverse effects of hypertonicity[91]. Conversely, NFAT5 induction in response to non-hypertonic stimuli,

such as in tumors, has a pathogenic role in functions like cell migration and invasion, contributing to tumor metastasis[92]. Additionally, NFAT5 induction by autoimmune stress and metabolic stress is pathological in various tissues and cell types[93].

6.5.2 NFAT5 mediates pathological angiogenesis

NFAT5 transcription participates in mediating pro-angiogenic factors and tumor angiogenesis[92,94]. In diabetic complications such as nephropathy, retinopathy, and atherosclerosis, NFAT5 is known to play a pathogenic role, particularly in vascular complications. Under hypertonic conditions, NFAT5 promotes vascular remodeling by regulating the expression of tenascin-C and smooth muscle actin (SMA), thereby mediating vascular smooth muscle cell (VSMC) migration[95]. Moreover, NFAT5's transcriptional activity induces the expression of angiogenic factors like VEGF-A, which orchestrates neovascularization and edema in diabetic retinopathy[94]. NFAT5 also regulates genes such as vascular endothelial growth factor-C (VEGF-C), serum glucocorticoid regulated kinase 1 (SGK1), and cyclooxygenase 2 (COX2), which are responsible for abnormal vascular development in diabetes[88]. In early atherosclerosis stages, NFAT5 plays a pathogenic role by directing monocyte chemoattractant protein (MCP)-1, promoting macrophage migration and endothelial innate immune response, thereby contributing to lesion formation[96]. Knockdown of NFAT5 expression using siRNA reduces the expression of VEGF, PlGF, and fibroblast growth factor (FGF) in retinal epithelial cells, suggesting that NFAT5's transcriptional role is crucial for hyperosmolarity-induced expression of angiogenic stimulators in the pathophysiology of age-related macular degeneration[94,97]. Similarly, NFAT5 haploinsufficiency in animal models also results in diminished angiogenesis[98], emphasizing the importance of NFAT5 in pathological angiogenesis.

NFAT5 has been implicated in promoting tumor-driven angiogenesis in various cancer models. In breast cancer cells, NFAT5 increases the expression of the pro-angiogenic factor VEGF-A by interacting with STAT3 and binding to the promoter region of VEGF[99]. Elevated VEGF-A levels contribute to cell proliferation, migration, adhesion, and angiogenesis, fostering tumor progression[99]. Another study demonstrated a positive correlation between NFAT5 expression levels and glioblastoma grade. Additionally, silencing NFAT5 disrupted angiogenesis in glioblastoma by inhibiting the secretion of epidermal growth factor-like domain 7 (EGFL7)[92]. These findings

underscore the significant role of NFAT5 along with its downstream signaling effectors in driving tumor angiogenesis.

6.6 Tumorigenesis

6.6.1 Endometrial Cancer

Endometrial cancer (EnCa) is a common gynecological malignancy[100]. In recent years, there has been a notable increase in the incidence of EnCa, and projections indicate that this trend will continue to rise in the coming decades[100]. While it primarily affects women aged 65 - 79 years, there is a concerning increase in diagnoses among younger age groups (30 - 50 years)[101]. Several risk factors have been associated with endometrial cancer, including obesity, hormonal imbalances (such as estrogen dominance), diabetes, hypertension, genetic predisposition (e.g., Lynch syndrome), and certain reproductive factors (e.g., nulliparity)[102-104]. Endometrial cancer typically presents with abnormal uterine bleeding, such as irregular or heavy menstrual periods, bleeding between periods, or postmenopausal bleeding[101]. Treatment options for endometrial cancer depend on the stage and characteristics of the tumor but may include surgery (such as hysterectomy), radiation therapy, chemotherapy, hormone therapy, or targeted therapy[105]. The prognosis for endometrial cancer varies depending on factors such as the stage at diagnosis, tumor grade, and molecular characteristics[105].

EnCa is hormonally driven, primarily attributed to excessive estrogenic stimulation of the uterine endometrial lining, although estrogen-independent pathways also contribute to carcinogenesis[100]. This aberrant hormonal signaling triggers unchecked cell proliferation, leading to malignant transformation and potential metastasis[100]. EnCa progresses by acquiring six characteristic traits: sustained cell growth, evasion of growth suppression mechanisms, resistance to cell death, immortality, stimulation of new blood vessel formation (angiogenesis), and activation of pathways facilitating invasion and migration[104]. Unfortunately, prognosis for advanced-stage EnCa remains poor, highlighting the critical need for identifying novel molecular targets to improve patient outcomes.

6.6.2 Hypoxia and COX2 signaling in cancer progression

Hypoxia, or low oxygen levels, is a common feature of solid tumors due to rapid cell proliferation, inadequate blood supply, and aberrant tumor vasculature[106]. In response to hypoxia, cancer cells activate various adaptive mechanisms, including the

upregulation of COX2 pathway, which plays a significant role in cancer progression[107,108]. COX2 is an enzyme involved in the synthesis of prostaglandins, which are lipid mediators implicated in inflammation, angiogenesis, and tumor growth[109]. Under hypoxic conditions, cancer cells increase COX2 expression through the activation of hypoxia-inducible factors (HIFs), particularly HIF-1α[108]. The interaction between HIF-1α and COX2 in cancer is complex and multifaceted. HIF-1α can directly regulate COX2 expression under hypoxic conditions, leading to increased prostaglandin production and promoting tumor progression[110]. COX2 driven prostaglandin production stimulates the expression of pro-angiogenic factors like VEGF, fostering the formation of new blood vessels to nourish the tumor[111]. Additionally, COX2 mediated prostaglandin synthesis activates signaling pathways crucial for cancer cell survival and proliferation, such as the phosphatidylinositol 3-kinase (PI3K) and mitogen-activated protein kinase (MAPK) pathways[112,113]. Moreover, COX2 derived prostaglandins play a role in enhancing tumor cell invasion and metastasis by promoting epithelial-to-mesenchymal transition (EMT), enabling cancer cells to acquire invasive traits and migrate to distant sites[113,114]. Lastly, COX2 expression in tumor cells is associated with immune suppression, including the inhibition of T cell function and the promotion of regulatory T cell activity, aiding in tumor immune evasion[115]. Conversely, COX2 derived prostaglandins can also directly stabilize HIF-1α and enhance its transcriptional activity, creating a positive feedback loop that sustains tumor growth and aggressiveness[116]. Several researches corroborate the involvement of HIF-1α and COX2 in the pathogenesis of tumors such as ovarian cancer and breast cancer[108,117,118]. Presently, numerous COX2 inhibitors have been developed and investigated for their potential anticancer properties, either as standalone treatments or in combination with other therapeutic approaches[119,120]. Understanding the potential molecular targets regulating HIF-1α and COX2 in endometrial cancer will therefore offer insights into potential therapeutic strategies aimed at these pathways, ultimately enhancing patient outcomes.

7. Aim and Objectives

Inadequate endometrial preconditioning, characterized by insufficient or defective maturation of the decidua pre-conception and/or at early pregnancy, can adversely affect pregnancy outcomes[2]. Consequently, pathological decidua, including aberrant biomechanical and/or biochemical adaptations in the endometrium, may fail to provide protection against placentation-related disorders during pregnancy, such as PE[25].

Recent research suggests that endometrial determinants, such as defective decidualization accompanied with altered endometrial biomechanics, contribute to the etiology of PE[8,15]. These findings underscore the need for further investigation into the role of maternal factors in PE pathogenesis. The overall aim of this thesis was to elucidate the mechanistic pathways that cause defects in the endometrial microenvironment before conception and may serve as precursors to the pathophysiology of PE.

Low PlGF levels are connected to PE and serve as a clinical diagnostic marker for predicting the pathogenesis[121]. Nevertheless, it remains unclear whether dysregulated low PlGF levels are a cause or a consequence of PE progression. In the endometrium, maintaining a delicate equilibrium between the angiogenic and inflammatory functions of PlGF is considered essential for successful conception[122]. It's noteworthy that aberrant PlGF is reportedly linked with altered cellular stiffness and pathological angiogenesis[13,123].

This thesis aimed to investigate the association between aberrant PlGF levels and PE pregnancies, as well as to unravel the pathological pathways mediated by aberrant PlGF in the endometrium. The first objective was to delineate the PlGF-mediated Rac1 mechanical signal transduction pathway in the human endometrial stromal cells (EnSCs), which constitutes the decidua. Additionally, the study aimed to elucidate the impact of dysregulated PlGF-Rac1 signaling on endometrial cellular mechanics. Finally, the goal was to comprehend the effects of alterations in endometrial mechanical behaviour on EVT (BeWo) cell invasion.

The second objective of this thesis was to explore whether aberrant PlGF also contributes to pathological uterine angiogenesis by interrupting paracrine communication between endometrial stromal cells and endothelial cells. The initial aim was to characterize the PlGF-NFAT5 mediated angiogenic signaling cascade in stromal cells. Subsequently, the study aimed to validate its angiogenic potential on

human umbilical vein endothelial cells (HUVECs) by verifying various angiogenic checkpoints.

Given the shared pathways between pathological angiogenesis and tumorigenesis, the next goal was to investigate whether NFAT5 acts as a common molecular factor in disrupted uterine angiogenesis and the progression of endometrial tumours. To achieve this, the focus was on characterizing NFAT5's expression in endometrial carcinoma. After elucidating NFAT5's role in tumorigenesis, we aimed to establish a plausible signaling cascade activated by NFAT5 aberrations using an *in vitro* model of endometrial cancer cells. Enhancing our comprehension of these pathways will enable us to better understand the endometrial factors contributing to the etiology of PE. Ultimately, this could lead to therapeutic advancements targeting the endometrium before pregnancy to prevent PE, as well as facilitate the development of new biomarkers for identifying women at risk of developing endometrial cancer.

8. Results and Discussion

8.1 Study 1: Excessive endometrial PlGF - Rac1 signaling underlies endometrial cell stiffness linked to preeclampsia.

During early pregnancy, EVTs invade the endometrium and congregate around the spiral arteries, facilitating spiral artery remodelling[124]. The endometrial stromal cells at the decidua promotes EVT invasion to support ongoing pregnancy by modulating a delicate balance of actin cytoskeleton reorganization, whilst curbing excessive invasion at the maternal site[125,126]. However, in PE, shallow EVT invasion is observed[6], potentially due to a stiffer endometrial environment hindering proper invasion. Furthermore, PE is associated with impaired cytoskeleton rearrangements and increased arterial stiffness, although the functional mechanism remains elusive[127,128]. Intriguingly, PlGF plays a pivotal role in actin regulation and cytoskeletal rearrangement in breast cancer and leukemic cells, rendering them stiffer[13,14]. In line with this, this study aimed to uncover the molecular mechanisms by which PlGF influences endometrial cytoskeletal remodelling, shedding light on the role of altered maternal biomechanics in the pathogenesis of PE. Understanding these cellular mechanics is crucial for deciphering the pathophysiology of conditions such as PE and other pregnancy-related disorders (implantation failure, miscarriage, IUGR) where abnormal endometrial function contribute to adverse maternal and fetal outcomes. The findings presented here provides valuable insights into a novel relationship between maternal biomechanics prior to pregnancy and PE pathogenesis.

PE linked with altered endometrial mechanics.

The pathogenesis of PE is complex and not fully elucidated, but it is characterised by maternal uteroplacental malperfusion and abnormal adaptive placentation[6]. Recent studies indicate that PE could potentially be a disorder originating from defective decidua before pregnancy[8,15,129,130]. These authors demonstrated *in vitro* that EnSCs isolated from patients with a history of PE failed to undergo decidualization, indicating that a defect in decidual molecular process may contribute significantly to PE pathogenesis[8,15,130]. This suggests a pivotal role of maternal decidual in the development of PE. However, while these studies highlighted the importance of defective decidua in PE, it did not elucidate the specific molecular mechanisms underlying this defect.

To date, the biomarker sFLT1/PlGF is a well-established marker for diagnosing PE in asymptomatic pregnant women[131]. The sFLT1/PlGF ratio demonstrates a sensitivity of 66.2% and specificity of 83.1%[121,132]. However, its effectiveness is limited to only 4 weeks before the onset of PE symptoms[121]. As a result, there is currently a lack of highly sensitive and specific screening methods for diagnosing PE early in pregnancy, hampering early intervention to prevent maternal and fetal mortality and morbidity[7]. While indirect evidence suggests to a pathological role for PlGF in pregnancy[106,131,132], but the role of endogenous PlGF on non-endothelial cells prior to pregnancy, particularly in the decidua remains elusive. To this end, we first aimed to enhance our understanding on the relationship between endometrial PlGF levels and pregnancies affected by PE through *in silico* investigation.

We primarily assessed the expression kinetics of PlGF across the menstrual cycle (*GEO2052*)[133]. Whole-genome molecular phenotyping of human endometrial tissue allowed us to identify the molecular signature of PlGF across the menstrual cycle in normo-ovulatory women. We observe that *PlGF* expression is elevated during the proliferative phase of the cycle, with expression levels decreasing as the cycle progresses into the secretory phase (*Manuscript1, Figure S1a*). Subsequently, we examined the association between PE pathophysiology and altered levels of PlGF and cytoskeleton-activating Rho-GTPase target protein PAK1. Transcript analysis from uteroplacental units of 10 PE and 10 healthy pregnancy subjects revealed upregulation of *PlGF* and *PAK1* in PE term deciduas (*Manuscript 1, Figure S1b)* compared to healthy pregnancies (*GEO2548*)[16]. This evaluation gave as a positive correlation between abnormal endometrial PlGF and aberrant cellular mechanics in PE pathogenesis.

Furthermore, through *in silico* analysis of RNA sequencing data (*GSE172381*)[15], we observed transcriptomic alterations in endometrial biopsies from women with prior PE compared to controls. Gene ontology analysis highlighted dysregulation in pathways related to cell signaling, motility, cytoskeleton, extracellular matrix, and reproductive process (*Manuscript 1, Figure S1c*). Notably, 93 genes linked to extracellular matrix organization, cell motility, and cytoskeleton dynamics were identified (*Manuscript 1, Figure S1d*). Furthermore, analysis of bulk RNA-seq data (*GSE172381*) revealed differential expression of 593 genes in decidua from PE patients, particularly impacting actin dynamics and cytoskeleton signaling pathways. These results imply that changes

in the expression of extracellular matrix, cell motility, cell organization, and cytoskeletal components before pregnancy likely disturb the maternal microenvironment during early pregnancy and placentation, potentially playing a role in the development of PE. Overall, these *in silico* findings suggest a potential link between dysregulated decidual PlGF and altered endometrial mechanics preconception, likely contributing to PE pregnancy.

PlGF induces proteomic alterations involving regulators of cellular actin machinery and ECM organization.

Next, we aimed to investigate the potential effect of aberrant PlGF on endometrial stromal cellular mechanics *in vitro*. To this end, EnSCs were treated with PlGF at 20 ng/ml for 6 days. Initially, proteomic analysis was conducted by comparing protein expression patterns in control and PlGF-treated EnSCs to elucidate the effects at a global level. This analysis revealed 97 dysregulated proteins, with volcano plots illustrating 47 upregulated (blue) and 50 downregulated (red) proteins associated with PlGF treatment in EnSCs (*Manuscript 1, Figure 1a*). Upregulated proteins included those involved in actin cytoskeleton regulation (DCTN2, PFN2, RAP1B, CAPZA1), GTPase regulation (IQGAP1, ARHGAP1), and extracellular matrix organization (COL1A2, COL1A1, TUBA1A), while downregulated proteins included actin stabilizing proteins (CAPZB, CNN1, CALD1). Gene Ontology analysis of the protein signature identified biological processes associated with GTPase activity (*Manuscript 1, Figure 1b*). Additionally, validation of these findings through qPCR demonstrated that PlGF enhanced gene expression of ECM associated markers (*ACTA2, COL1A1, COL1A2, COL3A1, COL4A1*) and matrix metalloprotease markers (*MMP2, MMP9*) in EnSCs, confirming the increased ECM-associated transcriptome changes observed in the proteomics data upon PlGF treatment (*Manuscript 1, Figure S2)*. Overall, these findings suggest that PlGF induces an enhanced cellular mechanotransduction signal in EnSCs, with increased actin regulation and GTPase activation signaling pathways.

PlGF enhances expression of cytoskeletal regulators Rac1 and PAK1 in endometrial stromal cells.

Rac1, small Rho family GTPase protein together with its major downstream effector PAK1, has been identified as one of the central mediators in cytoskeletal remodelling, essential for defining cell's mechanical properties[134]. In keeping with our observations

from proteomic characterisation, we aimed to gain insights into the impact of PlGF on GTPase Rac1-dependent regulation in EnSCs *in vitro*. PlGF treatment resulted in a significant increase of both *Rac1* and *PAK1* transcript levels (Manuscript 1, Figure 2a-b) in EnSCs. Additionally, PlGF treatment led to a significant increase in both total and phospho-Rac1 protein levels (*Manuscript 1, Fig 2c-d and S3*).

Rac1 activation is known to initiate the phosphorylation of PAK1, which subsequently regulates the turnover of cellular actin dynamics[135]. Treatment with PlGF for 6 days resulted in an increase in both the total protein level and the phosphorylated levels of PAK1 in endometrial cells (*Manuscript 1, Figure 2c and 2e*). Further, to validate the activation of Rac1 protein, we employed Rac1 activation assay (immunoprecipitation). This assay determined Rac1 activity by quantifying the amount of GTP-bound (activated) Rac1 precipitated by a GST-PAK1 fusion protein. PlGF treatment significantly elevated Rac1 activity compared to the control group (*Manuscript 1, Figure 2f-g and S3*). These findings underscore the role of PlGF in enhancing Rac1 activity, likely contributing to the observed increase in PAK1 phosphorylation and indicating a potential mechanism for mediating cellular signaling and actin dynamics within the endometrium.

PlGF decreases actin depolymerization and augments cell stiffness in endometrial stromal cells.

Rac1 is pivotal in regulating actin polymerization, a fundamental cellular process governing morphology and movement[35,134]. This involves assembling actin monomers into filamentous structures, crucial for cell shape and motility[33,134]. To evaluate this, we subsequently examined the effects of PlGF treatment on stromal cells, focusing on changes in actin polymerization dynamics. Remarkably, both flow cytometry (*Manuscript 1, Figure 3a-b and S5*) and Western blotting analysis (*Manuscript 1, Figure 3c-d and S6a*) revealed that treatment of EnSCs with PlGF significantly reduced the ratio of soluble G-actin to filamentous F-actin, indicating enhanced actin filament polymerization. Fluorescent images depicting F-actin organization (*Manuscript 1, Figure 3e and S6b, red*) demonstrated substantial reorganization of the actin cytoskeleton, accompanied by increased cell area (*Manuscript 1, Figure 3f*) and increased fluorescence intensity (*Manuscript 1, Figure 3g*) under PlGF treatment in endometrial cells.

Actin polymerization is closely linked to cell stiffness, with changes in actin organization and dynamics impacting the mechanical properties of cells[136,137]. Increased actin polymerization typically leads to greater cell stiffness, as the polymerized actin filaments provide resistance to stress and help maintain cell shape[136,137]. To assess if PlGF induces structural alterations and affects mechanical stiffness in EnSCs, we utilized atomic force microscopy (AFM) based physical cellular characterization.

Subsequent imaging of individual cells using AFM in the force mapping mode allowed for the quantification of cell stiffness (*Manuscript 1, Figure 3h*). The comparison of mean stiffness demonstrated that PlGF-treated EnSCs exhibited significantly higher stiffness (mean stiffness = 4.94 kPa) compared to control cells (mean stiffness = 3.13 kPa). Additionally, to assess the impact of PlGF on stiffness alterations in a physiologically relevant setting, EnSCs were cultured on PDMS substrates with a bulk stiffness ranging from 1 to 2 kPa. Remarkably, even when seeded on soft PDMS gels, PlGF-treated EnSCs exhibited increased cellular stiffness compared to untreated EnSCs (*Manuscript 1, Figure S8*). Alterations in actin dynamics, particularly polymerization, have been associated with the formation of filaments with increased mechanical stability. Thus, our findings confirm that aberrant PlGF mediated disruption in actin polymerization can result in increased endometrial cell stiffness associated with altered cellular mechanics.

Cell biomechanics are pertinent across all tissues, with tissue stiffness varying significantly[138]. Human tissues span a wide range of stiffness, from soft tissues like the brain (~0.2 kPa) to rigid structures like bone (~10^6 kPa)[139]. The decidua biopsies typically exhibit a stiffness of around 1.2 kPa[140]. This decidual stiffness at the maternal fetal interface is known to support EVT invasion during early pregnancy. EVTs invade and aggregate around the decidua, initiating the remodelling of spiral arteries[124]. Once EVT cells reach the inner third of the myometrium, they cease migration and undergo differentiation into multinucleated giant cells[124]. Interestingly, smooth muscle tissue (myometrium) has a stiffness of approximately 5 kPa[139], five times that of the decidua and similar to the stiffness observed post-treatment with PlGF in EnSCs (4.9 kPa). This significant difference in stiffness across the uterine tissue may play a crucial role in regulating the behaviour and invasion depth of EVT cells as they navigate through the endometrial layers during pregnancy.

Taken together, we hypothesize that elevated levels of PlGF in the endometrium prior to pregnancy may lead to inadequate invasion of EVTs into the decidua due to increased stiffness at the maternal microenvironment. Insufficient EVT invasion thereby hinders remodeling of spiral arteries during early pregnancy events, contributing to pathogenesis of PE later in pregnancy.

Aberrant PlGF disrupts *in vitro* decidualization in stromal cells.

EnSCs undergo a crucial differentiation process known as decidualization, which is initiated by progesterone during the early secretory phase[25]. Decidualization involves various structural and functional changes in the endometrial stromal cells, leading to the formation of the decidua, a specialized tissue that provides a supportive environment for the developing embryo[141]. It is an essential physiological process for ensuring maternal-fetal interface integrity and physiological fetal development[25]. Therefore, we investigated the impact of abnormal PlGF levels on EnSCs during the process of decidualization *in vitro*. Our findings revealed that PlGF disrupted the decidualization potential of EnSCs, as evidenced by a decrease in transcript levels of decidual markers such as prolactin and insulin-like growth factor binding protein-1 (*Manuscript 1, Figure S9*). The decreased levels of decidualization markers were accompanied by a decrease in Rac1 activity (*Manuscript 1, Figure S10a*) and a reduction in the ratio of G- to F-actin (*Manuscript 1, Figure S10 b-c*), along with increased cell stiffness (*Manuscript 1, Figure S11*), observed in PlGF-treated decidualized EnSCs compared to decidualized EnSCs. These results confirm that abnormal PlGF levels in the endometrium hinder the decidualization process of EnSCs, leading to negative regulation of decidual markers, actin dynamics, and cell stiffness.

A significant reduction in cell stiffness and surface roughness in human endometrial stromal cells is reported following decidualization[142]. These morphodynamic and functional alterations are linked cytoskeletal actin reorganization [143]. Such alterations in the biophysical properties of the endometrial stromal cells following decidualization are believed to be critical in limiting trophoblast invasion beyond the endometrium. Hence, we hypothesize that abnormal levels of endometrial PlGF may disrupt the maternal microenvironment, affecting decidualization by interfering with cytoskeletal remodeling of stromal cells. This disruption in cytoskeletal dynamics within the decidua

may hinder critical early pregnancy events such as stromal cell migration, uterine immune and trophoblast cell invasion, thereby resulting in pathological placentation.

PlGF modulation of actin regulation is *via* Rac1, PAK1, and WAVE2 signaling pathways.

To unequivocally demonstrate the direct modulation of the Rac1-PAK1 signaling pathway by PlGF, EnSCs were initially treated with PlGF for 4 days. Subsequently, they were transfected with Rac1 and/or PAK1 siRNAs for 48 hours, followed by continued PlGF treatment for an additional 2 days (20 ng/ml). Efficient Rac1 gene silencing (40-50% silencing) was achieved, and co-treatment with PlGF further suppressed both total and phosphorylated Rac1 (50-60% silencing) and PAK1 protein expression in EnSCs (*Manuscript 1, Figure 4a-d and Fig S12*). Similarly, inhibition of PAK1 with siPAK1 (± PlGF) mirrored the effect of Rac1 gene silencing, significantly reducing total (40-50% silencing) and phosphorylated levels of PAK1 (50-60% silencing) protein activity, with and without the presence of PlGF (*Manuscript 1, Figure 4a, d-e and Fig S12*).

Activation of Rac1 is recognized for its pivotal role in regulating actin polymerization by engaging with the Arp2/3-mediated actin nucleation pathway via its effector protein WAVE2[144]. When Rac1 is activated, it promotes the activation of WAVE2, which in turn activates the Arp2/3 complex[38]. To assess the regulation of WAVE2 upon Rac1 activation, we employed siRNA transfection for WAVE2 with and without PlGF treatment. Our results demonstrated that PlGF significantly increased the protein levels of WAVE2 and the ARP2/3 ratio in EnSCs (*Manuscript 1, Figure 4f-g and Figure S13*). Furthermore, silencing of Rac1 or WAVE2 with or without PlGF treatment led to a reduction in the expression levels of these proteins, confirming their activation through the Rac1 signaling cascade. Notably, silencing WAVE2 with or without PlGF did not show an additional effect on PAK1 activity levels (*Manuscript 1, Figure 4a-e*), indicating that WAVE2 downstream activity in modulating actin nucleation operates independently of PAK1.

Next, we also explored whether loss of Rac1/PAK1 or WAVE2 can affect G/F actin. Remarkably, silencing Rac1/PAK1 or WAVE2 with or without PlGF treatment resulted in a significant increase in the ratio of monomeric G-actin to filamentous F-actin, as detected by flow cytometry (*Manuscript 1, Figure 5a*). This alteration in the G/F actin

ratio with siRNAs, irrespective of PlGF treatment, was also confirmed by Western blot analysis of G and F actin protein lysates (*Manuscript 1, Figure 5b-c and Figure S13*). These findings not only validate the inhibitory effect of siRac1, siPAK1, and siWAVE2 but also support the PlGF-mediated activation of the Rac1-PAK1 signaling axis and its downstream impact on endometrial actin dynamics. These observations confirm the activation of the Rac1-PAK1 signaling cascade by PlGF and its subsequent effect on endometrial actin modulation.

Pravastatin counteracts PlGF-induced changes in endometrial actin dynamics and improve BeWo cell invasion.

Pravastatin belongs to the class of drugs known as statins, known for reducing cholesterol levels in individuals at risk of cardiovascular disease[145]. Statins function by inhibiting the enzyme HMG-CoA reductase, which is integral to the synthesis of cholesterol[145]. In rodent models of PE, pravastatin, administered early in pregnancy, restored angiogenic balance and normalized endothelial function[146,147]. Several clinical studies have investigated pravastatin use in pregnant women at high risk of PE. In a double-blind, placebo-controlled trial involving 1120 women screened for term PE, those given 20 mg daily pravastatin from 35-37 weeks gestation until delivery showed no significant difference compared to the placebo group[148]. Another study administered 10mg daily pravastatin during early pregnancy (12-16 weeks), demonstrating a notable reduction in the incidence and severity of PE[149]. Although concerns regarding statin teratogenicity persist[150], above studies suggests no increased risk of congenital anomalies with statin exposure during pregnancy[148,149]. These retrospective clinical trials found no identifiable safety risks associated with pravastatin. While promising, further research is needed to confirm the necessity of statins for treating and preventing PE and to assess potential teratogenic effects if prescribed during early pregnancy.

Rac1 undergoes post-translational modification by geranylgeranyl diphosphate (GGPP), affecting its subcellular localization[151]. Statins, by inhibiting mevalonate synthesis upstream of cholesterol and GGPP production, can impede with Rac1's isoprenylation[152]. Similarly, statins are known to influence the rearrangement of F-actin, affecting cofilin, a protein involved in cell shape and motility regulation[153]. Pravastatin and simvastatin reportedly downregulate pY14-caveolin, disrupting actin interactions[154]. The above evidence indicates a potential link between statins and the regulation of actin dynamics.

Based on the aforementioned reports, we wanted to explore whether the activation of Rac1 induced by PlGF and the resulting alterations in actin dynamics in EnSCs could be reversed pharmacologically with pravastatin. Thus, we evaluated the effects of pravastatin (10 µM) on Rac1 activity in EnSCs with and without PlGF treatment. Our findings demonstrate that pravastatin counteracts the effects of PlGF on actin levels by restoring the ratio of G- and F-actin levels, as confirmed by both flow cytometry and Western blotting. Overall, these results indicate that pravastatin treatment for 24 hours rescues the alterations induced by PlGF in EnSCs, with levels nearly returning to control (untreated) (*Manuscript 1, Figure 6a–g and Figure S14*). Additionally, we observed an inhibitory effect of pravastatin on PlGF-induced Rac1-GTP levels (*Manuscript 1, Figure 6h-i and Figure S14*), indicating a decrease in Rac1 activity.

The biomechanical phenotype of endometrial stromal cells is crucial for supporting physiological EVT invasion within the confined 3D extracellular matrices of the decidua[155]. Impairment in EVT invasion is believed to play a significant role in the development of PE and its associated complications[6]. In line with this, we hypothesized that PlGF-induced alterations in stromal cell stiffness could hinder the normal invasion of EVTs (BeWo) through EnSCs. To investigate this, we utilized electrical impedance spectroscopy (EIS), which assesses cellular resistance to an applied electric current, reflecting cell stiffness and the integrity of cell junctions. To this end, EnSCs monolayers were formed in the presence or absence of PlGF treatment for 6 days with or without 24 h pravastatin (10 µM) treatment. Subsequently, BeWo cells were added, and invasion was monitored using EIS.

Our findings reveal that the resistance of stromal monolayers treated with PlGF was significantly higher compared to the control, indicating a reduction in BeWo invasion through EnSCs (*Manuscript 1, Figure 6j*). The changes in actin dynamics and increased cellular stiffness provide a rationale for the inhibited invasion of BeWo cells through PlGF-primed endometrial stromal monolayers. Remarkably, the diminished BeWo invasion in PlGF-treated EnSCs was reversed by pravastatin treatment (*Manuscript 1, Figure 6j*). These findings collectively suggest a clear beneficial effect of pravastatin in inhibiting PlGF-mediated Rac1 activation, reverting actin polymerization to normal levels, and improving BeWo cell invasion through endometrial cells.

Pravastatin reverses PlGF-induced alterations in cell and ECM proteome of endometrial stromal cells.

To comprehensively understand the impact of pravastatin on PlGF mediated cellular mechanics in EnSCs, we employed quantitative proteomic analysis. Proteomic analysis comparing protein expression in PlGF (n=3) and PlGF + pravastatin (n=3) treated EnSCs revealed 95 dysregulated proteins. Volcano plots (*Manuscript 1, Figure 7a*) showed 55 upregulated (orange) and 40 downregulated (violet) proteins associated with pravastatin treatment in PlGF-treated EnSCs. Upregulated proteins included those involved in actin cytoskeleton regulation and stabilization (e.g., ACTG1 and CAPZB), while downregulated proteins encompassed actin cytoskeleton and extracellular matrix remodelling proteins (e.g., CNN2, COL1A1, COL1A2, COL6A, TUBA1A). Gene Ontology analysis identified pathways linked to GTP binding, intracellular transport, and cytoplasmic translation associated with pravastatin treatment in PlGF-treated EnSCs (*Manuscript 1, Figure 7b*). Thus, proteomic analysis suggests that pravastatin treatment reverses actin regulation, extracellular matrix remodelling mechanics, and cell stiffness, while suppressing GTPases pathway activity in PlGF-treated EnSCs. Thus, we propose that pravastatin may serve as a promising pharmacological candidate to counteract abnormal PlGF induced aberrant Rac1 signaling. Furthermore, it could potentially mitigate abnormal cell stiffness, facilitating proper EVT invasion into the maternal microenvironment. This intervention holds promise for preventing shallow placentation, a key contributor to the pathogenesis of PE.

In conclusion, this study sheds light on an underlying transcriptomic anomaly related to cytoskeletal-actin dynamics in PE, as inferred from publicly available datasets. This anomaly may contribute to the maternal manifestations of shallow or impaired placentation observed in PE. Moreover, our *in vitro* investigation unveils a previously unrecognized function of PlGF in promoting the expression and activity of the small G-protein Rac1 and its downstream kinase PAK1, leading to enhanced actin polymerization and increased cellular stiffness. The alteration in cell stiffness induced by PlGF likely impedes EVT invasion, potentially contributing to insufficient uterine artery remodeling observed in PE pregnancies. Our findings represent a significant advancement towards understanding the maternal molecular mechanisms underlying PE pathogenesis.

By elucidating the role of PlGF in modulating Rac1-PAK1 signaling and its downstream effects on cytoskeletal dynamics and cell stiffness, our study provides valuable insights into potential therapeutic targets for PE. This study also highlights pravastatin as a potential pharmacological candidate capable of reversing cellular actin abnormalities and improving EVT invasion ability. These insights may pave the way for the development of novel approaches aimed at early risk assessment and intervention for PE, thus improving maternal and fetal health outcomes.

8.2 Study 2: Placental growth factor mediates pathological uterine angiogenesis by activating the NFAT5-SGK1 signaling axis in the endometrium: Implications for preeclampsia development.

Angiogenesis is closely associated with the physiological changes that take place in the endometrium during each menstrual cycle[48,156]. This process is tightly regulated by the paracrine communication between EnSCs and endothelial cells[56,157]. During early pregnancy, the uterine spiral arteries undergo extensive remodelling to accommodate the increased demands of the growing fetus and ensure physiological placentation[158]. Pregnancy-associated vascular transformations at the decidua are critical for a healthy pregnancy outcome, highlighting the importance of endometrial vascular health pre-conception[159]. Any molecular aberration in these processes can lead to complications in pregnancy including miscarriage or PE[159]. PE is characterized by abnormal spiral artery remodelling, angiogenic imbalance and impaired placentation, with its underlying cause remaining elusive[160]. PlGF, a known VEGF homolog is implicated in pathological angiogenesis and inflammation[11,161-163]. Our previous study describes regulation of PlGF across the menstrual cycle and demonstrated its role in altering endometrial cellular mechanics as seen in PE pregnancies, when dysregulated (*Manuscript 1*). In this study, we aimed to examine whether aberrant endometrial PlGF contributes to pathological uterine angiogenesis by disrupting EnSCs and endothelial paracrine communication. Our findings unravel an anti-angiogenic pathway mediated by PlGF in endometrial stromal cells and decipher the PlGF's paracrine responsiveness on endothelial angiogenic ability. This study emphasizes abnormal uterine angiogenesis prior to pregnancy as an important endometrial determinant in the pathogenesis of PE.

PlGF induces tonicity independent activation of NFAT5 in endometrial stromal cells.

NFAT5 is a member of the Rel family of transcriptional activators[92,164]. Originally identified as a transcription factor responsive to osmotic stress, NFAT5 has broader implications beyond osmoregulation, influencing various physiological processes including development, immune response, and cellular stress[87,93,165-167]. A recent study unveiled that the transcriptional activity of NFAT5 drives the production of angiogenic factors, leading to neovascularization and the development of angiogenesis-associated edema[94]. Intriguingly, in retinal pigment epithelial cells, dysregulated PlGF signaling through NFAT5 activity results in abnormal vessel formation in diabetic

retinopathy[97]. These findings suggest a potential role for the PlGF-NFAT5 axis in blood vessel development, emphasizing the need for further investigation into its role in endometrial angiogenesis.

We first investigated the spatio-temporal expression pattern of NFAT5 in the endometrium through *in silico* analysis. *NFAT5* expression was notably higher during the proliferative phase (*Manuscript 2, Figure S1a*) compared to the late secretory phase of the menstrual cycle (*GEO 2052*). Single-cell analysis further confirmed elevated *NFAT5* expression in the stromal population, along with other endometrial cell types and EVTs (*Manuscript 2, Figure S1b & c*). According to data from the Human Protein Atlas, NFAT5 is widely expressed throughout the endometrium, with particularly intense staining observed in the perivascular area and blood vessels (*Manuscript 2, Figure S1d*). Following this, we explored the potential involvement of NFAT5 in the etiology of PE. For this purpose, we manually analysed *NFAT5* expression levels from gene expression studies conducted on first-trimester decidua samples obtained from both pre-symptomatic women who later developed PE and healthy pregnancies (*GEO 3467*). Our analysis revealed upregulated *NFAT5* transcripts in the decidua of pre-symptomatic women who subsequently developed PE (*Manuscript 2, Figure S1e*). These findings collectively suggest that endometrial NFAT5 expression peaks during the proliferative phase and is associated with the onset of PE before symptom onset.

Next, we aimed to establish a putative association between PlGF and NFAT5 regulation in endometrial stromal cells. EnSCs were subjected to varying concentrations of PlGF (ranging from 2.5 to 50 ng/ml) for 6 days. Transcript analysis revealed a notable increase in *NFAT5* mRNA expression specifically at a PlGF concentration of 20 ng/ml compared to other concentrations tested (*Manuscript 2, Figure S2a*). Time course analysis demonstrated that *NFAT5* gene expression peaked after 6 days of treatment with PlGF (20 ng/ml) (Manuscript 2, Figure 1a). All subsequent experiments utilized PlGF at a concentration of 20 ng/ml for a treatment duration of 6 days in EnSCs. Consistent with mRNA findings, PlGF significantly elevated NFAT5 protein levels in EnSCs, confirming tonicity-independent activation of NFAT5 (*Manuscript 2, Figure 1b-c and Figure S2b*). Additionally, PlGF-induced NFAT5 spatial regulation was examined using immunofluorescence. Endogenous NFAT5, initially localized in the cytosol of untreated EnSCs, translocated to the nucleus upon

PlGF treatment (*Manuscript 2, Figure 1d*). NFAT5 is activated under hyperosmotic cellular stress (Hyp Osm); hence, we verified its transcriptional activity in EnSCs by exposing them to Hyp Osm (800 mOsm/ml) medium for 3 hours as a positive control (*Manuscript 2,* Figure S3a-c). Taken together, these findings elucidate the unique regulation of tonicity-independent NFAT5 activation in the endometrium. Moreover, the observed increase in NFAT5 immunoreactivity in endometrial tissues during the proliferative phase of the menstrual cycle, particularly in the perivascular region around blood vessels, highlights its significance in influencing uterine vessel formation.

NFAT5 activation, regulated by p38 MAPK, induces SGK1 expression in endometrial stromal cells.

Further, we aimed to decipher signaling downstream cascade modulated upon PlGF-NFAT5 activation in EnSCs. p38 MAPK is recognized for its role in activating NFAT5 transcriptional activity under hypertonic conditions[90]. To confirm its involvement as an upstream regulator of NFAT5 in a tonicity independent environment, we examined the protein levels of total and phosphorylated p38 MAPK after PlGF treatment. We observed increased levels of total p38 MAPK protein, along with a significant upregulation of phosphorylated p38 MAPK (*Manuscript 2, Figure 2a-c and Figure S4*). NFAT5 acts as a regulator for various angiogenic mediators and factors, including SGK1, HIF-1α, and VEGF-A[97,168-170]. Subsequently, we conducted a series of experiments to determine if PlGF indeed contributed to the activation of these downstream targets. Our findings revealed a significant upregulation of both total and phosphorylated SGK1 protein levels in PlGF-treated stromal cells (*Manuscript 2, Figure 2a, d-e*). SGK1 is known to stimulate HIF-1α, a key modulator in angiogenic signaling. We observed elevated levels of *HIF-1α* transcripts upon PlGF treatment in stromal cells (*Manuscript 2, Figure 2f*). Additionally, PlGF exerted a robust stimulating effect on HIF-1α promoter activity, as demonstrated by luciferase assays in EnSCs (*Manuscript 2, Figure 2g*).

To further confirm the angiogenic pathway facilitated by NFAT5 activation, we assessed both intracellular and secreted levels of the pro-angiogenic factor VEGF-A. Prior research has highlighted the involvement of VEGF in the initial angiogenic events linked to the postmenstrual regeneration of the endometrium[171,172]. PlGF-induced NFAT5 stimulation in EnSCs led to a significant increase in cellular VEGF-A protein (*Manuscript 2, Figure 2a-h*). Surprisingly, however, the secreted levels of VEGF-A

protein in the EnSCs supernatant were decreased compared to untreated control levels (*Manuscript 2, Figure 2i*).

The decline in secreted levels of VEGF-A despite elevated intracellular and cellular VEGF-A levels poses an intriguing observation. It is thought that intracellularly activated VEGF-A (in EnSCs) might engage in intracrine signaling by interacting with receptors located within the cell, leading to a reduction in the secretion of VEGF-A[173,174]. Additionally, it can be postulated that an autocrine signaling mechanism could be activated in EnSCs, wherein secreted VEGF-A initiates a negative feedback loop by binding to its extracellular receptors, thereby decreasing the availability of VEGF-A in the CM[175,176]. Another potential mechanism could involve the activation of HIF-1α-mediated transcriptional activity, which regulates the secretion of both PlGF and VEGF-A[177,178]. Consequently, secreted PlGF, upon HIF-1α activation in EnSCs, might act as an antagonist to VEGF-A, forming biologically inactive PlGF/VEGF heterodimers and further attenuating VEGF-A secretion[123]. However, these proposed mechanisms necessitate further characterization to understand their complete regulatory roles. Overall, these findings highlight the aberrant PlGF-mediated angiogenic signaling axis in EnSCs involving NFAT5 and SGK1 targets, marked by a decrease in the secretion of the proangiogenic factor VEGF-A.

Secretome analysis unveils pathological angiogenic signaling in PlGF treated CM.

To comprehensively assess the global effect of PlGF on angiogenic mediators in EnSCs, we employed proteomic analysis to examine the secreted factors. Supernatant (CM) from EnSCs treated with or without PlGF for 6 days was analysed using liquid chromatography mass spectrometry (LC-MS) (*Manuscript 2, Figure 3a*). A comparison between control CM (Con-CM, n=3) and PlGF-treated CM (PlGF-CM, n=3) identified 32 dysregulated secreted proteins. Volcano plots depicted the differentially regulated proteins, with 18 upregulated (in green) and 14 downregulated (in orange) proteins associated with PlGF treatment in EnSCs (*Manuscript 2, Figure 3b*). Some of the significantly upregulated proteins in PlGF-treated CM included components associated with actin and ECM, such as ECM-1, ACTA1, PFN1, COL1A2, MMP2, and tissue inhibitors of metalloproteinases (TIMP2). Conversely, significantly downregulated proteins included AHNAK, FLNA, and YWHAZ. Although proteins like COL2A6, COL6A3, and COL3A1 were not differentially expressed based on our study

thresholds, modest yet significant changes in their expressions were observed. Thus, the proteomic analysis of stromal cell secretome upon PlGF stimulation revealed an upregulation of numerous ECM associated biomolecules. This finding aligns with our previous study, where we observed PlGF-induced increases in both type I collagen and cell stiffness through enhanced actin polymerization (*Manuscript 1*). Such ECM remodelling proteins have known to play a vital role in angiogenesis by directly influencing endothelial cell phenotypes and functions[179]. For instance, type I collagen is reported to significantly impact endothelial cell morphogenesis by suppressing cAMP-dependent protein kinase A and inducing actin polymerization[180]. Additionally, matrix metalloproteinases (MMPs) act as key inflammatory mediators, regulating endothelial proliferation and survival during pathological vessel remodelling[181].

Gene Ontology (GO) analysis of the protein signature associated with PlGF-treated CM identified pathways related to structural remodelling, ECM modification, and pathological vessel development. Intriguingly, we also observed activation of pathways associated with pathological angiogenesis, such as atherosclerosis and hypertrophic cardiomyopathy, in the stromal secretome induced by aberrant PlGF signaling. Acute atherosis lesions, resembling early stages of atherosclerosis, have been reported in the walls of spiral arteries in the uteroplacental circulation in some cases of PE[128,182]. Therefore, we hypothesize that the altered composition of ECM-associated proteins, along with angiogenic imbalances (low VEGF-A) in PlGF-treated conditioned media, creates a pathological inflammatory-like microenvironment that likely modulates pathological angiogenic behaviour in endothelial cells.

PlGF-treated CM induces abnormal hypersprouting behaviour in HUVECs.

During endometrial sprouting angiogenesis, growth factors and cytokines released from the stroma and surrounding uterine microenvironment stimulate the quiescent endothelial cells lining the vasculature[47,56,183]. This stimulation prompts the endothelial cells to degrade the extracellular matrix and invade the surrounding tissue, ultimately leading to the formation of new capillaries[47]. Hence, we aimed to better elucidate the effects of PlGF-induced secreted factors (low VEGF-A and high ECM remodelling proteins) on the angiogenic behaviour of HUVECs. To test this conjecture, we treated HUVECs with CM collected from untreated or PlGF-treated EnSCs (*Manuscript 2, Figure 4a*). Subsequently, we assessed the impact on angiogenic processes in HUVECs using various functional assays. PlGF-CM significantly enhanced cell

proliferation in HUVECs, as indicated by the BrdU ELISA assay (*Manuscript 2, Figure 4b*). Furthermore, a wound healing scratch assay utilizing GFP-labelled HUVECs revealed reduced cell migration upon treatment with PlGF-CM (*Manuscript 2, Figure 4c-d*), while the *in vitro* tube formation assay showed no significant change in tube length between Con-CM and PlGF-CM treatments on HUVECs (*Manuscript 2, Figure 4e-f*). However, PlGF-CM-treated HUVECs exhibited an increased number of endothelial cell branches, indicative of abnormal hypersprouting behaviour (*Manuscript 2, Figure 4e-g*), a phenotype associated with pathological angiogenesis. VEGF-A exhibits concentration-dependent activity in inducing endothelial cell proliferation, thereby promoting sprouting and anastomosis through a VEGF/Notch-dependent mechanism[184,185]. In our study, low VEGF-A in PlGF-CM exerted negative angiogenic modulation in HUVECs, inhibiting proliferation, migration, and inducing pathological hypersprouting.

VEGF-A and Notch signaling pathways often interact coordinately to fine-tune angiogenesis and vascular development[185,186]. To investigate the involvement of Notch signaling in the anti-angiogenic effects of PlGF-CM on HUVECs, we examined the gene expression levels of key Notch signaling effectors, including Notch receptors *(Notch 1* and *Notch 2*), ligands (*Dll4* and *Jagged-1*), and target genes (*Hey 1* and *Hes1*), which were downregulated in PlGF-CM-treated HUVECs (*Manuscript 2, Figure 4h-l and Figure S5a*). Moreover, protein analysis confirmed enhanced VEGFR2 expression and decreased levels of VEGFR1 and VEGF-A in PlGF-CM-treated HUVECs (*Manuscript 2, Figure 4m-n and Figure S5b*), supporting the modulation of hypersprouting *via* repression of Notch signaling and upregulation of VEGFR2. Consistent with the reported results, diminished expression of Notch and VEGFR1 was observed in the endothelial cells of the decidua, linked with early pregnancy loss[187]. The above data also validates the interplay between the stromal and endothelial compartments, facilitating cell-cell communication to regulate endometrial angiogenic function.

Endothelial barrier function is critical for vascular resistance and permeability regulation defining the vessel integrity during angiogenesis[188]. We evaluated the endothelial barrier function of the HUVECs using EIS approach. EIS measurements demonstrated an increase in cell index in HUVECs treated with PlGF-CM, indicating enhanced junctional resistance and decreased permeability between endothelial cells

(*Manuscript 2, Figure 4o*). Reduced levels of VEGF-A and elevated ECM-associated biomolecules in PlGF-CM likely compromised barrier function in HUVECs, leading to heightened cell impedance, diminished permeability, and increased vascular stiffness. Collectively, these findings suggest that dysregulated PlGF-NFAT5-SGK1 signaling in stromal cells mediates adverse angiogenic effects on HUVECs through alterations in the secretome signature, notably impacting Notch signaling pathway and endothelial barrier function.

Enhanced secretion of VEGF-A observed in EnSCs upon SGK1 silencing.

Endometrial SGK1 is integral to endometrial physiology and crucial for maintaining pregnancy[1]. It is recognized to play a mechanistic role in maintaining the functional reproductive axis[1,189]. Hence, we investigated whether SGK1 acts as a pivotal regulator in the stroma-endothelial paracrine pathway upon PlGF stimulation. Efficient SGK1 gene silencing employing siRNA significantly reduced both total and phosphorylated SGK1 protein expression levels in EnSCs (*Manuscript 2, Figure 5a-c and Figure S6*). Similarly, inhibition of SGK1 with PlGF mirrored the effects observed with gene silencing, leading to a significant decrease in both total and phosphorylated levels of SGK1 protein (Manuscript 2, Figure 5a-c). Notably, silencing of SGK1 transcripts resulted in a significant reduction in HIF-1α mRNA levels and promoter activity in EnSCs (Manuscript 2, Figure 5d-e). This effect was also observed in EnSCs treated with siSGK1+PlGF (Manuscript 2, Figure 5d-e). Interestingly, diminished SGK1 expression in EnSCs did not significantly alter total VEGF-A levels as detected by western blotting (Manuscript 2, Figure 5a and f). However, SGK1 silencing led to improved secretion of VEGF-A in the CM characterized by ELISA (*Manuscript 2, Figure 5g*), and the VEGF-A protein signature (both total and secreted) remained consistent also in sample groups where siSGK1 inhibition was combined with PlGF treatment in EnSCs (Man*uscript 2, Figure 5a, f-g*). These findings highlight the important molecular role of SGK1 in aiding angiogenic paracrine communication pathway in the endometrium.

Suppression of SGK1 in endometrial stromal cells improves angiogenic activity in HUVECs.

To verify the functional relevance of SGK1 in modulating the paracrine mechanism, HUVECs were exposed to CM from EnSCs with SGK1 inhibition, with or without PlGF

treatment. The siSGK1 ± PlGF-CM treatments reduced cell proliferation and enhanced cell migration in HUVECs compared to controls (*Manuscript 2, Figure 6a-c*). Moreover, the tube formation capacity of HUVECs was enhanced with siSGK1 ± PlGF-CM, accompanied by a decrease in the number of branches (*Manuscript 2, Figure 6d-e*). Notably, siSGK1 ± PlGF-CM treatment upregulated notch signaling components (*Notch 1* and *Notch 2* receptors, *Dll4* and *Jagged-1* Notch ligands, and *Hey 1* and *Hes1* Notch target genes), indicating restoration of Notch signaling function upon SGK1 inhibition (*Manuscript 2, Figure S7*). Correspondingly, the protein expression levels of VEGFR1/2 and VEGF-A in HUVECs were normalized with siSGK1 ± PlGF-CM treatment (*Manuscript 2, Figure 6f-g and Figure S8*). These data confirm that SGK1 inhibition in EnSCs enhances the secretion of angiogenic cues, mitigating the hypersprouting phenotype in HUVECs. Furthermore, cellular impedance analysis with EIS demonstrated improved endothelial barrier function, with increased cell permeability observed under the influence of both siSGK1 ± PlGF-CM (*Manuscript 2, Figure 6h).* HUVECs treated with VEGF-A (40 ng/ml for 24 h) served as a positive control for permeability stimulation.

Establishment of a low-resistance vascular system is essential for adequate spiral artery remodelling by invading EVTs[190]. Effective trophoblast invasion of maternal spiral arteries is imperative for normal placentation[124]. Shallow or inadequate invasion of maternal vessels is associated with PE[6]. We hypothesized that aberrant PlGF signaling in endometrial stromal cells produces cues that could hinder adequate trophoblast invasion. BeWo invasion was hampered and associated with high resistance (i.e., higher cell index) in HUVECs treated with PlGF-CM compared to Con-CM treated HUVECs (*Manuscript 2, Figure 6i*). The elevated vascular resistance and stiffness observed at the junctional interface of PlGF-CM HUVECs likely explains the impeded BeWo cell invasion. Thus, we posit aberrant levels of endometrial PlGF may contribute to the formation of high-resistant vessels in the endometrium, leading to inadequate trophoblast invasion, as evident in PE placentas. Interestingly, SGK1 inhibition improved the poor BeWo invasion driven by PlGF-CM through the HUVEC monolayer, as evidenced by the decrease in cell impedance values (*Manuscript 2, Figure 6i*).

Taken together, this study explores the role of SGK1 as a central mediator in the PlGF-induced anti-angiogenic pathway, by facilitating hypoxia promotion and differential

regulation angiogenic factors in endometrial cells. PE placentas are reported to have increased expression of HIF-1α, known to modulate sFlt-1 and sEng production and thereby contribute to angiogenic imbalance[191,192]. Moreover, HIF-1α overexpression has been linked to a HELLP syndrome-like phenotype and fetal growth restriction in pregnant mice[193]. These findings help us identify the potential involvement of dysregulated endometrial SGK1 in exacerbating hypoxia during uterine vascularization and placentation, as observed in PE.

Furthermore, the siSGK1+PlGF-CM improved endothelial migration, restored normal tube formation ability, enhanced vascular permeability, and improved BeWo invasion similar to Con-CM. These observations reinforce the pivotal role of endometrial SGK1 in modulating inflammation like anti-angiogenic cues in pathological vessel development. Our findings here are consistent with other reports emphasizing the key role of SGK1 in modulating inflammation in vascular disorders. Xi et al. provided evidence for SGK1's involvement in hypoxia-induced pulmonary hypertension by triggering a pro-inflammatory response. Absence of SGK1 mitigated the pro-inflammatory reaction induced by hypoxia and ameliorated arterial remodelling[194]. Similarly, Baban et al. demonstrated that activation of SGK1 signaling enhanced pro-survival pathways associated with inflammation, thus mitigating adverse cardiac remodelling in ischemia-reperfusion injury[195]. Therefore, results presented in this study highlights the prospect for selective inhibition of SGK1 in endometrial stroma to reverse the pathological switch activated by aberrant PlGF, identifying SGK1 as an attractive therapeutic target.

Our collective findings presented in this study lend support to the hypothesis that dysregulated endometrial PlGF may disrupt the coordinated physiological angiogenesis, leading to inadequate modification of spiral arteries and hindering trophoblast invasion, thereby contributing to the development of PE (*Manuscript 2, Figure 7*). In line with this, Doppler studies have revealed an increased uterine artery pulsatility index during early gestation, offering potential predictive value for a substantial proportion of PE cases (50%) later in pregnancy[196]. Intriguingly, further Doppler ultrasound examinations have linked endometriosis during the late secretory phase with heightened sub-endometrial blood flow[197]. The inverse relationship between pre-pregnancy perfusion levels and the likelihood of pregnancy complications, although not thoroughly examined, may also have implications for other

conditions such as abnormal uterine bleeding, polycystic ovary syndrome, unexplained infertility and pregnancy complications. However, while we highlight abnormal stromal PlGF as key molecule, it is important to acknowledge other contributing factors, including inadequate decidualization, aberrant uNK cell function, impaired trophoblast interaction, trophoblast cell death, and epigenetic alterations, or a combination thereof, may also play a role in disrupting maternal spiral artery transformation and leading to multifactorial pathogenesis such as PE.

In conclusion, our findings shed light on the emerging potential and advancements in understanding the PlGF-NFAT5-SGK1 signaling pathway in endometrial stromal cells and implications in uterine angiogenesis. While further exploration of the extensive implications of PlGF is warranted, this study highlights NFAT5 and SGK1 as promising targets for therapeutic interventions aimed at enhancing vascularization prior to pregnancy and mitigating adverse pregnancy outcomes such as PE.

Drawing from the insights gained from the aforementioned studies, we propose that local endometrial disruptions, such as abnormal stromal cellular mechanics (*Manuscript 1*) and /or poor-quality uterine vessels pre-conception (*Manuscript 2*), can trigger a chain reaction leading to reduced placental function, causing PE progression later in pregnancy. These studies also decipher aberrant PlGF mediated pathways driving these abnormal endometrial functions. Intriguingly, our findings are supported by recent research utilizing single-cell transcriptomics to examine distinct molecular profiles of PE subtypes[198]. This analysis revealed imbalances in angiogenic and extracellular matrix function in placentas from early-onset PE. Notably, stromal cells and vasculature displayed an inflamed, stressed, anti-angiogenic environment specifically in early-onset PE cases. Thus, we speculate that PE is primarily a disease of impaired endometrial preconditioning, potentially offering protection against pathological microenvironment.

8.3 Study 3: Rel Family Transcription Factor NFAT5 Upregulates COX2 via HIF-1α Activity in Ishikawa and HEC1a Cells

NFAT5 is a multifaceted protein involved in stress responses, with diverse functions in physiological and pathological processes[89]. Its role in pathological angiogenesis, particularly in diseases like cancer and diabetic retinopathy[88,91,92,99], has garnered significant research attention recently. Our previous study (*Manuscript 2*) unraveled NFAT5's unique ability to activate an anti-angiogenic inflammation pathway in endometrial stromal cells, supporting the development of pathological blood vessels. Inflammation and pathological angiogenesis are pivotal in cancer development, from the initiation of carcinogenesis, tumor *in situ* and advanced stages of cancer[17,199]. It's well-established that sustained angiogenesis and cancer-related inflammation share signaling pathways and molecules[17]. Hypoxia, in conjunction with angiogenesis, can also activate other cancer-specific biological pathways[17,200]. The angiogenic-inflammatory switch confers greater advantages to tumors beyond angiogenesis alone, driving the acquisition of tumor hallmarks and progression to advanced stages[17]. Given these findings, NFAT5 emerges as a potential player in tumor progression, warranting further investigation into its signaling axis and role in endometrial cancer (EnCa). To this end, we hypothesize that dysregulated NFAT5 transcriptional activation, contributing to pathological angiogenesis and inflammation cascade in the endometrium, may serve as a driving force for cancer initiation. Thus, in this study we aimed explored whether NFAT5 is expressed in human endometrial cancer tissue, whether NFAT5 expression in endometrial cancer cells is sensitive to HIF-1α. The findings presented here unveil NFAT5's novel role in EnCa and suggest a putative link between NFAT5 activation and the HIF-1α/COX2 signaling axis in tumor progression.

Enhanced NFAT5 staining in higher grade EnCa.

NFAT5's role in cancer pathogenesis is not as extensively studied as other transcription factors, emerging evidence suggests its potential impact on tumor development. Research has delved into its involvement in breast cancer, renal cell carcinoma, and glioblastoma. In breast cancer cells, NFAT5 has been implicated in promoting cell survival and proliferation by facilitating the secretion of pro-angiogenic factors[99]. Moreover, in renal cell carcinoma, elevated NFAT5 expression levels have been associated with various clinicopathological features, including tumor stage, grade, and metastasis[91]. These findings suggest that NFAT5 may play a role in the aggressiveness and progression of tumor pathophysiology. In keeping with these

observations, we aimed to investigate NFAT5 regulation in endometrial tumors. NFAT5 expressional analysis in EnCa tissues were demonstrated with a total of 26 EnCa cases selected at random (*Manuscript 3, Table 1*). Among these cases, 15 were over the age of 60, and the majority exhibited a post-menopausal status. Of the cases examined, 24 were classified as endometrioid histotype, while two were classified as serous histotype. Immunostaining was conducted on formalin-fixed, paraffin-embedded (FFPE) archival tissue samples collected from varying endometrial tumor grades. The results, as depicted in immunohistochemistry (*Manuscript 3, Figure 1a and Table 1*), revealed that in low-grade (G1, G2) endometrial cancer tissue, NFAT5 staining exhibited low to intermediate cytoplasmic intensity (score 1) within the tumor cells, contrasting with the moderate staining observed in neighboring endothelial cells (score 2). Conversely, high-grade endometrioid carcinomas (G3) displayed a robust and block-like homogeneous NFAT5 expression pattern, particularly evident in the perivascular region and at the leading edge.

In benign endometrium, we observed intense NFAT5 expression (score 3) in proliferating glands, while non-proliferating cells in the secretory phase exhibited reduced or low expression (score 1). A significant correlation was noted between higher grade tumors and intense NFAT5 staining. Furthermore, cases diagnosed with pT1b and higher, indicating invasion into the outer half of the myometrium, showed a significant association with increased NFAT5 staining. Additionally, an increase in NFAT5 staining was significantly linked to metastasis. The staining pattern of NFAT5 was consistent in both G1 and G3 cases examined in this study (*Manuscript 3, Figure S1*). Moreover, analysis of total RNA extracted from the same FFPE blocks via qRT-PCR revealed significantly higher *NFAT5* transcript levels in G3 (aggressive) tumor tissues compared to low-grade G1 tumor tissues (*Manuscript 3, Figure 1b*). Thus, this study report that the NFAT5 expression is significantly elevated in the more aggressive (G3) endometrial cancer tissues compared to the corresponding non-tumor, low-grade (G1) tissues. Interestingly, we show a positive correlation between increased NFAT5 staining and tumor metastasis. Nevertheless, it should be noted that our study utilized a small proof-of-concept cohort, highlighting the need for larger clinical cohorts to validate our findings.

NFAT5 overexpression in Ishikawa cells regulated transcriptome HIF1A and COX2.

RNA-sequencing was performed to gain further insight on NFAT5 overexpression and to establish a comprehensive analysis of aberrantly expressed genes after NFAT5 overexpression in Ishikawa cells, a well-defined endometrial adenocarcinoma cell line model. Using thresholds of FDR < 0.05 and log2FC ≥ 0.3 (which corresponds to an actual fold change of ≥ 1.23), we identified 57 genes with significant alterations following NFAT5 overexpression in Ishikawa cells (*Manuscript 3, Figure 2a*). Among these, 37 genes exhibited upregulation while 20 genes showed downregulation.

In keeping with its recognized function, many of the NFAT5-regulated genes were associated with osmoregulation and/or facilitating cell survival in hypertonic conditions. Examples include aldo-keto reductase family 1-member b (*AKR1B1*), ATPase Na+/K+ transporting subunit beta 1 (*ATP1B1*), and solute carrier family 6 member 12 (*SLC6A12*). Significantly upregulated genes following NFAT5 overexpression in Ishikawa cells include leucine-rich repeat containing G protein-coupled receptor 6 (*LGR6*) (log2FC = 1.749), *NFAT5* itself (log2FC = 2.705), prostaglandin-endoperoxide synthase 2 (*PTGS2*, encoding COX2 protein) (log2FC = 0.320), angiogenin (*ANG*) (log2FC = 0.566) and netrin 4 (*NTN4*) (log2FC = 0.476). Similarly, NFAT5 overexpression in Ishikawa cells resulted in downregulation of genes such as ankyrin repeat domain 1 (*ANKRD1*) (log2FC = −0.855), a transcription factor known to positively regulate apoptosis, and amine oxidase copper containing 3 (*AOC*3) (log2FC = −0.358), whose low levels are associated with poor prognosis in cancers.

Although *HIF1A* (log2FC = 0.104, FDR < 0.05) and estrogen receptor 1 (*ESR1*) (log2FC = −0.22, FDR < 0.05) did not meet the criteria for differential expression in this study, we observed modest yet significant changes in their expression levels following NFAT5 overexpression. Further, employing Ingenuity Pathway Analysis (IPA) highlighted a robust correlation with the activation of PTGS2 (COX2) signaling following NFAT5 overexpression in Ishikawa cells. (*Manuscript 3, Figure S2*). Collectively, these findings indicate an increase in *HIF1A* and *PTGS2* transcripts upon NFAT5 overexpression in Ishikawa cells.

NFAT5 expression is sensitive to hypoxia/NFAT5-HIF-1α-COX2 signaling axis in endometrial cancer cells.

Hypoxia serves as a mechanism that propels the acquisition of aggressive tumor characteristics[201]. Thus, we assessed whether induction of NFAT5 expression in

Ishikawa cells is responsive to hypoxia. Cells were treated with dimethyloxalylglycine (DMOG), a cell-permeable prolyl-4-hydroxylase (PHD) inhibitor. DMOG is known to suppress PHD activity, thereby stabilizing HIF-1α levels and mimicking a hypoxic environment both *in vitro* and *in vivo*.

Ishikawa cells treated with DMOG for 24 h resulted in a significant increase in *NFAT5* transcript levels. The increase in *NFAT5* transcript levels induced by DMOG treatment was mirrored by a significant rise in NFAT5 protein abundance in Ishikawa cells (*Manuscript 3, Figure 3a and b*). Further, we investigated whether heightened expression of NFAT5 can activate the HIF-1α signaling axis in Ishikawa cells. NFAT5 transfection led to the upregulation of *NFAT5* transcripts, accompanied by a significant increase in *HIF1A* and *PTGS2* gene expression (*Manuscript 3, Figure 3c*). The impact of NFAT5 transfection on *NFAT5* and *PTGS2* transcript levels corresponded to a similar elevation in NFAT5 and COX2 protein abundance as well (*Manuscript 3, Figure 3d*).

Furthermore, transfection of NFAT5 in Ishikawa cells demonstrated a pronounced stimulatory effect on HIF-1α promoter activity, as indicated by hypoxia response elements (HRE)-luciferase assay (*Manuscript 3, Figure 3e*). It is recognized that HIF-1α plays a pivotal role in maintaining oxygen homeostasis within the tumor microenvironment, with the ability to enhance COX2 expression through transcriptional regulation[108,202]. COX2 serves as a significant mediator of pro-tumorigenic inflammation. It exhibits upregulation across various cancer types and plays a crucial role in tumor progression[203,204]. In line with this, this study reported an increase in *PTGS2* transcript levels followed by an elevation in COX2 protein abundance upon DMOG treatment in Ishikawa cells (*Manuscript 3, Figure 3f and g*). Overall, these findings suggest a significant interplay between NFAT5 and the HIF-1α signaling axis in Ishikawa cells. Considering this sensitivity of NFAT5 expression to hypoxia, we propose that the localized hypoxic conditions within advanced cancer tissues may contribute to the upregulation of NFAT5 expression as seen in higher grade EnCa.

Overexpression of NFAT5 drives aggressive cellular phenotype.

Next, we evaluated the potential impact of NFAT5 overexpression on endometrial cancer biology on assessing cell cycle progression, proliferation, and migration in Ishikawa cells transfected with an NFAT5 plasmid. Analysis of the cell cycle profile

revealed a higher proportion of cells in the S phase upon NFAT5 overexpression, indicating an increase in DNA replication compared to the control (*Manuscript 3, Figure 4a*). Further, NFAT5 overexpression led to a significant increase in cell proliferation and enhancement in cell migration in Ishikawa cells following NFAT5 overexpression, as determined by BrdU ELISA and wound healing assay respectively (*Manuscript 3, Figure 4 b-d*). These findings collectively suggest that NFAT5 overexpression may contribute to a more aggressive cellular phenotype in Ishikawa cells through activation of hypoxia and inflammatory milieu, characterized by increased DNA replication, proliferation, and migration.

HIF-1α activation through NFAT5 with DMOG establishes positive feedback loop between NFAT5 and HIF-1α.

To investigate the potential positive feedback loop between NFAT5 and hypoxia, Ishikawa cells were transfected with an NFAT5 overexpression plasmid followed by treatment with DMOG, or DMOG treatment alone. As a result, significantly higher levels of *NFAT5* and *PTGS2* transcripts were observed compared to cells treated with DMOG alone (*Manuscript 3, Figure 5a*). Correspondingly, the combined effect of NFAT5 transfection and DMOG treatment led to a similar increase in NFAT5 and COX2 protein abundance compared to cells treated with DMOG alone (*Manuscript 3, Figure 5b–d and Figure S4*). Next, HIF-1α promoter activity was quantified using dual-luciferase reporter assays following 24 h of NFAT5 transfection and/or DMOG treatment. Both NFAT5 transfection and DMOG treatment exerted a strong stimulatory effect on HIF-1α promoter activity. Furthermore, the activation of HIF-1α *via* NFAT5 with DMOG amplifies this response, establishing a positive feedback loop (*Manuscript 3, Figure 5e*).

It is widely acknowledged that inflammation is a crucial and an enabling characteristic of tumorigenesis[205]. COX2 plays a pivotal role in the synthesis of prostanoids, including prostaglandins, prostacyclin, and thromboxane, from the precursor arachidonic acid[109]. Prostaglandins, in particular, stimulate the release of proinflammatory chemokine[206]. In this we study report, elevated HIF-1α and COX2 activity was corroborated by an increase in secreted levels of COX2 metabolite PGE_2 in NFAT5 transfected Ishikawa cells, with a significant difference observed in cells subjected to combined NFAT5 transfection and DMOG treatment (*Manuscript 3, Figure 5f*). These results collectively suggest a potential positive feedback loop between NFAT5 and hypoxia, mediated by

increased HIF-1α promoter activity, and elevated secretion of inflammatory mediator PGE_2 in Ishikawa cells.

The potential synergistic role of COX2 in endometrial tumor progression and metastasis mediated by NFAT5 transcription, underscores COX2 as a promising therapeutic target. Given the close association between chemoresistance, hypoxia, and COX2 overexpression in various tumor models[108,119,207], inhibiting COX2 activity could improve the efficacy of cancer therapies such as chemotherapy and radiation. Moreover, selective inhibition of COX2 with nimesulide has shown promise in reducing tumor formation in a mouse model of hypoxic tumors[120]. However, further investigation is needed to validate these findings in human subjects.

Based on the aforementioned results, we propose that overexpression of NFAT5 may play a significant role in the progression of endometrial cancer (EnCa), however the precise mechanism underlying the putative factors driving elevated NFAT5 expression in the endometrium still remains unclear. Several potential risk factors are associated with EnCa, such as obesity, poor diet, and a sedentary lifestyle can likely modulate NFAT5 overexpression in the endometrium to drive tumorigenesis[102,104,208]. Indeed, a high-salt diet has been demonstrated to elevate NFAT5 levels, leading to the activation of macrophages and the promotion of fibrin deposition[209]. Additionally, excessive salt intake has been reported to modulate the expression of several pro-inflammatory cytokines, including TNF, IL-6, and PGE_2, through NFAT5-mediated transcriptional activity[210].

Similarly, increased uptake of glucose has been associated with heightened NFAT5 levels, observed in conditions like diabetic retinopathy and diabetes mellitus[211,212]. Elevated NFAT5 levels are also linked to obesity development and insulin resistance. NFAT5 has been shown to epigenetically suppress the transcriptional activity of peroxisome proliferator-activated receptor gamma (PPARγ), a critical regulator of nutrient and energy metabolism[213]. Consequently, it is plausible that in obese individuals with enhanced adipose tissue, factors such as hypoxia and insulin resistance may contribute to increased NFAT5 expression. Therefore, excessive consumption of dietary salt, sugar, or fat could potentially upregulate NFAT5, fostering local inflammation and creating a microenvironment conducive to tumorigenesis.

Our previous study (*Manuscript 2*) identifies aberrant endometrial PlGF as a possible mediator of tonicity-independent induction of NFAT5 transcriptional activation supporting pathological angiogenesis. It is noteworthy that PlGF has been linked to inflammation in diet-induced obese mouse models[214]. Increased systemic PlGF levels have been associated with obesity in patients with pancreatic and breast cancer, as well as in various mouse models of these cancers[76]. Interestingly, elevated PlGF expression is observed both systemically and locally within tumors in high-grade endometrial carcinomas[215]. Taken together, this suggests a complex interplay between pathological angiogenesis and the tumor microenvironment in the development and progression of endometrial cancer. This raises an intriguing possibility of investigating the role of the PlGF-NFAT5 signaling axis in the pathogenesis of endometrial tumors.

In addition to dietary or lifestyle factors, genetic predisposition to dysregulated NFAT5 activity could also represent a significant risk factor. Single-nucleotide polymorphisms (SNPs) located in NFAT5 introns have been to be associated with increased risk of conditions such as high blood pressure, diabetes mellitus, diabetic nephropathy, and inflammation, suggesting that genetic variation in NFAT5 transcription may contribute to pathological phenotypes[88,89,216,217]. Further investigation is needed to confirm these findings in the context of endometrial cancer (EnCa).

Our previous study (*Manuscript 2*) have highlighted the potential role of abnormal PlGF in triggering NFAT5-HIF-1α mediated pathological vessel formation in the endometrium, thereby supporting poor EVT invasion, a key contributor to the manifestation of PE. Interestingly, in the current study, we have highlighted NFAT5-HIF-1α as key players in endometrial cancer progression. These findings prompt speculation about a putative link between preeclampsia and its increased risk of endometrial cancer. A recent study provides only limited evidence suggesting a weak association between PE and an elevated risk of any endometrial neoplasia[218]. However, varying definitions of PE, lack of subgroup analysis and absence of diverse population cohort limits its findings. Therefore, new investigations into the long-term impacts of PE may offer insights into the understudied biological mechanisms of endometrial carcinogenesis and identify key endometrial determinants for diverse pathologies.

Taken together, our findings in this study suggest that elevated NFAT5 levels are associated with more aggressive forms of endometrial cancer. Additionally, NFAT5

overexpression triggers the activation of HIF-1α and COX2, leading to increased PGE_2 levels in endometrial cancer cells, potentially fueling tumor aggressiveness. Despite the elusive mechanism driving abnormal NFAT5 expression in endometrial tumor tissues, the development of selective COX2 inhibitors as anti-cancer therapies present a promising avenue for treating endometrial cancer.

9. General discussion

Establishing a healthy pregnancy often occurs even before implantation and placentation, with the physiological formation of the decidua playing a pivotal role[25]. Referred to as the endometrial preconditioning, the dynamics of endometrial tissue following each menstrual cycle are crucial for creating an optimal environment for embryo implantation and subsequent placental development[2]. However, when the endometrial microenvironment is impaired, hindering the maternal "soil" from undergoing necessary tissue modifications, it can lead to aberrations with trophoblast invasion, placentation, and result in adverse pregnancy outcomes[8,219].

Pregnancy disorders such as PE present a complex challenge affecting both maternal and fetal health[6]. Early identification of women at risk of PE is crucial to mitigate both short- and long-term adverse effects[68]. Managing PE requires careful monitoring, timely intervention, and sometimes early delivery to ensure the best possible outcomes[68]. Thus, PE places a significant economic burden too[65]. However, a major challenge lies in the fact that the onset of clinical manifestations of PE often occurs long after its underlying etiology has begun[65]. Consequently, current diagnostic strategies, which rely on biomarkers of placental dysfunction, have shown limited success[220]. This underscores the importance of reexamining the fundamental factors driving PE pathogenesis.

This thesis investigates endometrial biomechanics (*Manuscript 1*)[221] and vascular health (*Manuscript 2*) (*Raja Xavier et al., accepted*) before conception, with an emphasis on elucidating pathways involved in pathological endometrial microenvironment that contributes to the progression of PE. Specifically, the studies outlined here reveal potential maternal therapeutic targets prior to pregnancy to alleviate adverse pregnancy outcomes. This thesis has also identified a shared molecular factor (NFAT5) that can contribute to different endometrial disorders, such as pathological vessel development, and the advancement of endometrial tumors (*Manuscript 3*)[222]. Thus, any dysregulation in endometrial biology disrupts its physiological preconditioning mechanism, thereby compromising its ability to provide protection against pathological manifestations such as PE or the initiation of tumorigenesis. Together, these studies highlight the importance of a healthy endometrial microenvironment for enhancing the quality of life in women.

A notable limitation of this thesis is the lack of validation for its findings in either *in vivo* models or patient cohorts. While animal models in PE research are valuable, they hold drawbacks, including species differences, limited reproducibility, and limited translation to humans[223]. These include species differences that can lead to varied physiological responses, limited reproducibility of results across different studies, and challenges in translating findings to human clinical scenarios. The complexity of human pregnancy and placentation processes is not fully replicated in animal models, making it difficult to draw definitive conclusions about the efficacy and safety of potential treatments based solely on animal data[224]. Consequently, validation in human subjects is crucial for confirming the clinical relevance of these findings. Research involving human subjects with PE can provide valuable insights into the clinical presentation, progression, and management of the disease. However, studying the molecular pathology of fetal placental and maternal decidual tissues post-delivery may not provide comprehensive insights into the origin of impaired placentation. This is due to the occurrence of critical events such as trophoblast invasion and spiral artery remodeling during the first half of pregnancy. Post-delivery samples, while useful for certain analyses, do not capture these early events, making it challenging to draw comprehensive conclusions about the origin and early development of placental abnormalities.

Acquiring first-trimester human placenta and decidua for studying these early placentation events poses significant challenges due to ethical, logistical, and technical constraints. Ethically, obtaining tissues from early pregnancies requires consent and often involves sensitive situations such as miscarriages or elective terminations. Logistically, accessing these tissues at precisely the right developmental stages requires coordinated efforts between researchers and clinical teams. Technically, preserving the integrity of these delicate tissues for molecular and histological analyses requires specialized techniques and immediate processing, adding another layer of complexity. These challenges highlight the need for innovative approaches and technologies to study early placentation events in human pregnancies. Developing non-invasive or minimally invasive methods to monitor and analyze early placental development, as well as improving *in vitro* models that mimic these early processes, could provide valuable alternatives. Despite these difficulties, advancing our understanding of the early molecular and cellular events in PE is crucial for identifying

biomarkers and therapeutic targets that could lead to earlier diagnosis and more effective prevention and treatment strategies.

As the understanding of PE evolves, there is a growing recognition of the maternal factors contributing to its progression[8]. Investigating the endometrial biology in women with a history of PE offers a promising avenue for research and clinical insights. These studies can shed light on how aberrant endometrial factors influence crucial early pregnancy events like EVT invasion and spiral artery remodeling, processes vital for establishing a healthy placental environment. By dissecting the molecular and cellular mechanisms underlying these events in women with prior PE, researchers can uncover potential biomarkers and therapeutic targets for future intervention strategies. Additionally, such studies enable the development of personalized approaches to manage recurrent PE, allowing for tailored interventions based on individual endometrial and placental characteristics. Ultimately, these endeavors hold the promise of improving maternal and fetal outcomes by enhancing our understanding of PE pathogenesis and facilitating the implementation of targeted preventive and therapeutic measures.

Taken together, currently significant findings have been made in understanding the maternal contribution to PE and the role of decidualization resistance in its pathophysiology. However, the molecular mechanisms underlying pathological decidua prior to pregnancy have remained largely unexplored. This thesis fills this research gap by unveiling new insights into the mechanisms that may contribute to a deficient endometrium before pregnancy. Consequently, this study reinforces the concept of aberrant endometrial factors preceding the onset of PE. Additionally, this thesis emphasizes the necessity for novel decidua-based diagnostic approaches for PE to be implemented pre-conception. Since decidualization occurs during the human menstrual cycle independent of conception, it presents an opportune window for early assessment. Developing a molecular test to characterize endometrial tissue before pregnancy could facilitate prospective risk screening for this condition and implementing preventive measures, thus potentially averting the onset of this detrimental disease.

Early identification of women at risk of PE is crucial for mitigating both short- and long-term adverse effects for the mother and fetus. In the short term, it allows for vigilant monitoring and timely interventions, such as antihypertensive medications and

corticosteroids, to prevent severe complications and ensure the best outcomes for both. In the long term, it reduces the risk of chronic health issues for the mother and developmental complications for the baby. Early identification also enables preventive measures like lifestyle changes and low-dose aspirin therapy, further reducing the incidence and severity of PE.

In conclusion, the outcomes of this thesis underscore the vital significance of a healthy endometrial microenvironment in averting adverse pregnancy outcomes and tumorigenesis. This research, centered on maternal factors impacting early pregnancy phases, notably endometrial preconditioning, lays the groundwork for pioneering diagnostic and therapeutic approaches. These novel strategies have the potential to markedly enhance maternal and fetal health outcomes, alleviating the impact of pregnancy-related conditions such as PE and understanding the risk between complicated pregnancies and tumorigenesis. The incorporation of pre-conception diagnostics and tailored therapies presents a promising trajectory for obstetric and gynecological care, offering the prospect of enhancing the overall well-being of women globally.

10. References

1 Lang, F., Rajaxavier, J., Singh, Y., Brucker, S. Y. & Salker, M. S. The Enigmatic Role of Serum & Glucocorticoid Inducible Kinase 1 in the Endometrium. *Frontiers in cell and developmental biology* **8**, 556543-556543 (2020). https://doi.org:10.3389/fcell.2020.556543

2 Brosens, J. J., Parker, M. G., McIndoe, A., Pijnenborg, R. & Brosens, I. A. A role for menstruation in preconditioning the uterus for successful pregnancy. *Am J Obstet Gynecol* **200**, 615.e611-616 (2009). https://doi.org:10.1016/j.ajog.2008.11.037

3 Critchley, H. O. D., Maybin, J. A., Armstrong, G. M. & Williams, A. R. W. Physiology of the Endometrium and Regulation of Menstruation. *Physiological Reviews* **100**, 1149-1179 (2020). https://doi.org:10.1152/physrev.00031.2019

4 Jain, V., Chodankar, R. R., Maybin, J. A. & Critchley, H. O. D. Uterine bleeding: how understanding endometrial physiology underpins menstrual health. *Nat Rev Endocrinol* **18**, 290-308 (2022). https://doi.org:10.1038/s41574-021-00629-4

5 Zhang, T. *et al.* Extracellular matrix stiffness mediates uterine repair via the Rap1a/ARHGAP35/RhoA/F-actin/YAP axis. *Cell Commun Signal* **21**, 22 (2023). https://doi.org:10.1186/s12964-022-01018-8

6 Jena, M. K., Sharma, N. R., Petitt, M., Maulik, D. & Nayak, N. R. Pathogenesis of Preeclampsia and Therapeutic Approaches Targeting the Placenta. *Biomolecules* **10** (2020). https://doi.org:10.3390/biom10060953

7 Khan, B., Allah Yar, R., Khakwani, A. K., Karim, S. & Arslan Ali, H. Preeclampsia Incidence and Its Maternal and Neonatal Outcomes With Associated Risk Factors. *Cureus* **14**, e31143 (2022). https://doi.org:10.7759/cureus.31143

8 Garrido-Gomez, T. *et al.* Defective decidualization during and after severe preeclampsia reveals a possible maternal contribution to the etiology. *Proc Natl Acad Sci U S A* **114**, E8468-e8477 (2017). https://doi.org:10.1073/pnas.1706546114

9 Zhang, P. Decidual vasculopathy and spiral artery remodeling revisited II: relations to trophoblastic dependent and independent vascular transformation. *The Journal of Maternal-Fetal & Neonatal Medicine*, 1-7 (2020). https://doi.org:10.1080/14767058.2020.1718646

10 Plaisier, M. Decidualisation and angiogenesis. *Best Pract Res Clin Obstet Gynaecol* **25**, 259-271 (2011). https://doi.org:10.1016/j.bpobgyn.2010.10.011

11 Dewerchin, M. & Carmeliet, P. PlGF: a multitasking cytokine with disease-restricted activity. *Cold Spring Harb Perspect Med* **2** (2012). https://doi.org:10.1101/cshperspect.a011056

12 Binder, N. K. *et al.* Placental Growth Factor Is Secreted by the Human Endometrium and Has Potential Important Functions during Embryo Development and Implantation. *PLoS One* **11**, e0163096 (2016). https://doi.org:10.1371/journal.pone.0163096

13 Taylor, A. P., Leon, E. & Goldenberg, D. M. Placental growth factor (PlGF) enhances breast cancer cell motility by mobilising ERK1/2 phosphorylation and cytoskeletal rearrangement. *Br J Cancer* **103**, 82-89 (2010). https://doi.org:10.1038/sj.bjc.6605746

14 Casalou, C., Fragoso, R., Nunes, J. F. M. & Dias, S. VEGF/PLGF induces leukemia cell migration via P38/ERK1/2 kinase pathway, resulting in Rho

GTPases activation and caveolae formation. *Leukemia* **21**, 1590-1594 (2007). https://doi.org:10.1038/sj.leu.2404668
15 Garrido-Gomez, T. *et al.* Disrupted PGR-B and ESR1 signaling underlies defective decidualization linked to severe preeclampsia. *Elife* **10** (2021). https://doi.org:10.7554/eLife.70753
16 Herse, F. *et al.* Dysregulation of the circulating and tissue-based renin-angiotensin system in preeclampsia. *Hypertension* **49**, 604-611 (2007). https://doi.org:10.1161/01.Hyp.0000257797.49289.71
17 Aguilar-Cazares, D. *et al.* Contribution of Angiogenesis to Inflammation and Cancer. *Front Oncol* **9**, 1399 (2019). https://doi.org:10.3389/fonc.2019.01399
18 Sternberg, A. K., Buck, V. U., Classen-Linke, I. & Leube, R. E. How Mechanical Forces Change the Human Endometrium during the Menstrual Cycle in Preparation for Embryo Implantation. *Cells* **10** (2021). https://doi.org:10.3390/cells10082008
19 Massimiani, M. *et al.* Molecular Signaling Regulating Endometrium-Blastocyst Crosstalk. *Int J Mol Sci* **21** (2019). https://doi.org:10.3390/ijms21010023
20 Gellersen, B. & Brosens, J. J. Cyclic decidualization of the human endometrium in reproductive health and failure. *Endocr Rev* **35**, 851-905 (2014). https://doi.org:10.1210/er.2014-1045
21 Smith, S. K. Regulation of angiogenesis in the endometrium. *Trends in Endocrinology & Metabolism* **12**, 147-151 (2001). https://doi.org:https://doi.org/10.1016/S1043-2760(01)00379-4
22 Massri, N., Loia, R., Sones, J. L., Arora, R. & Douglas, N. C. Vascular changes in the cycling and early pregnant uterus. *JCI Insight* **8** (2023). https://doi.org:10.1172/jci.insight.163422
23 Maenhoudt, N., De Moor, A. & Vankelecom, H. Modeling Endometrium Biology and Disease. *J Pers Med* **12** (2022). https://doi.org:10.3390/jpm12071048
24 Huang, C. C. *et al.* Establishment of the fetal-maternal interface: developmental events in human implantation and placentation. *Front Cell Dev Biol* **11**, 1200330 (2023). https://doi.org:10.3389/fcell.2023.1200330
25 Ng, S.-W. *et al.* Endometrial Decidualization: The Primary Driver of Pregnancy Health. *International journal of molecular sciences* **21**, 4092 (2020). https://doi.org:10.3390/ijms21114092
26 Zhang, C. *et al.* Oxidative stress on vessels at the maternal-fetal interface for female reproductive system disorders: Update. *Front Endocrinol (Lausanne)* **14**, 1118121 (2023). https://doi.org:10.3389/fendo.2023.1118121
27 Hu, X. *et al.* Cyclical endometrial repair and regeneration: Molecular mechanisms, diseases, and therapeutic interventions. *MedComm (2020)* **4**, e425 (2023). https://doi.org:10.1002/mco2.425
28 Makieva, S. *et al.* Inside the Endometrial Cell Signaling Subway: Mind the Gap(s). *Int J Mol Sci* **19** (2018). https://doi.org:10.3390/ijms19092477
29 Zhang, X. H. *et al.* The mesenchymal-epithelial transition during in vitro decidualization. *Reprod Sci* **20**, 354-360 (2013). https://doi.org:10.1177/1933719112472738
30 O'Connor, B. B., Pope, B. D., Peters, M. M., Ris-Stalpers, C. & Parker, K. K. The role of extracellular matrix in normal and pathological pregnancy: Future applications of microphysiological systems in reproductive medicine. *Exp Biol Med (Maywood)* **245**, 1163-1174 (2020). https://doi.org:10.1177/1535370220938741

31 Di, X. *et al.* Cellular mechanotransduction in health and diseases: from molecular mechanism to therapeutic targets. *Signal Transduct Target Ther* **8**, 282 (2023). https://doi.org:10.1038/s41392-023-01501-9
32 Martino, F., Perestrelo, A. R., Vinarský, V., Pagliari, S. & Forte, G. Cellular Mechanotransduction: From Tension to Function. *Front Physiol* **9**, 824 (2018). https://doi.org:10.3389/fphys.2018.00824
33 Chung, C. Y., Lee, S., Briscoe, C., Ellsworth, C. & Firtel, R. A. Role of Rac in controlling the actin cytoskeleton and chemotaxis in motile cells. *Proc Natl Acad Sci U S A* **97**, 5225-5230 (2000). https://doi.org:10.1073/pnas.97.10.5225
34 Kunschmann, T. *et al.* The Small GTPase Rac1 Increases Cell Surface Stiffness and Enhances 3D Migration Into Extracellular Matrices. *Sci Rep* **9**, 7675 (2019). https://doi.org:10.1038/s41598-019-43975-0
35 Ma, N., Xu, E., Luo, Q. & Song, G. Rac1: A Regulator of Cell Migration and a Potential Target for Cancer Therapy. *Molecules* **28** (2023). https://doi.org:10.3390/molecules28072976
36 Shi, Y. *et al.* Rac1-Mediated DNA Damage and Inflammation Promote Nf2 Tumorigenesis but Also Limit Cell-Cycle Progression. *Dev Cell* **39**, 452-465 (2016). https://doi.org:10.1016/j.devcel.2016.09.027
37 Nohata, N. *et al.* Temporal-specific roles of Rac1 during vascular development and retinal angiogenesis. *Dev Biol* **411**, 183-194 (2016). https://doi.org:10.1016/j.ydbio.2016.02.005
38 Chen, B. *et al.* Rac1 GTPase activates the WAVE regulatory complex through two distinct binding sites. *Elife* **6** (2017). https://doi.org:10.7554/eLife.29795
39 Sells, M. A. *et al.* Human p21-activated kinase (Pak1) regulates actin organization in mammalian cells. *Curr Biol* **7**, 202-210 (1997). https://doi.org:10.1016/s0960-9822(97)70091-5
40 Izdebska, M., Zielińska, W., Hałas-Wiśniewska, M. & Grzanka, A. Involvement of Actin and Actin-Binding Proteins in Carcinogenesis. *Cells* **9** (2020). https://doi.org:10.3390/cells9102245
41 Filić, V. *et al.* Regulation of the Actin Cytoskeleton via Rho GTPase Signalling in Dictyostelium and Mammalian Cells: A Parallel Slalom. *Cells* **10** (2021). https://doi.org:10.3390/cells10071592
42 Fletcher, D. A. & Mullins, R. D. Cell mechanics and the cytoskeleton. *Nature* **463**, 485-492 (2010). https://doi.org:10.1038/nature08908
43 Bachir, A. I., Horwitz, A. R., Nelson, W. J. & Bianchini, J. M. Actin-Based Adhesion Modules Mediate Cell Interactions with the Extracellular Matrix and Neighboring Cells. *Cold Spring Harb Perspect Biol* **9** (2017). https://doi.org:10.1101/cshperspect.a023234
44 Cronin, N. M. & DeMali, K. A. Dynamics of the Actin Cytoskeleton at Adhesion Complexes. *Biology (Basel)* **11** (2021). https://doi.org:10.3390/biology11010052
45 Parker, F., Baboolal, T. G. & Peckham, M. Actin Mutations and Their Role in Disease. *Int J Mol Sci* **21** (2020). https://doi.org:10.3390/ijms21093371
46 Li, M. *et al.* Roles of the cytoskeleton in human diseases. *Mol Biol Rep* **50**, 2847-2856 (2023). https://doi.org:10.1007/s11033-022-08025-5
47 Maas, J. W. *et al.* Endometrial angiogenesis throughout the human menstrual cycle. *Hum Reprod* **16**, 1557-1561 (2001). https://doi.org:10.1093/humrep/16.8.1557

48 Rogers, P. A., Donoghue, J. F., Walter, L. M. & Girling, J. E. Endometrial angiogenesis, vascular maturation, and lymphangiogenesis. *Reprod Sci* **16**, 147-151 (2009). https://doi.org:10.1177/1933719108325509
49 Qi, R., Li, T. C. & Chen, X. The role of the renin-angiotensin system in regulating endometrial neovascularization during the peri-implantation period: literature review and preliminary data. *Ther Adv Endocrinol Metab* **11**, 2042018820920560 (2020). https://doi.org:10.1177/2042018820920560
50 Smith, S. K. Angiogenesis, vascular endothelial growth factor and the endometrium. *Hum Reprod Update* **4**, 509-519 (1998). https://doi.org:10.1093/humupd/4.5.509
51 Möller, B., Lindblom, B. & Olovsson, M. Expression of the vascular endothelial growth factors B and C and their receptors in human endometrium during the menstrual cycle. *Acta Obstet Gynecol Scand* **81**, 817-824 (2002). https://doi.org:10.1034/j.1600-0412.2002.810903.x
52 Machado, D. E., Berardo, P. T., Palmero, C. Y. & Nasciutti, L. E. Higher expression of vascular endothelial growth factor (VEGF) and its receptor VEGFR-2 (Flk-1) and metalloproteinase-9 (MMP-9) in a rat model of peritoneal endometriosis is similar to cancer diseases. *J Exp Clin Cancer Res* **29**, 4 (2010). https://doi.org:10.1186/1756-9966-29-4
53 Yu, X., Gao, C., Dai, C., Yang, F. & Deng, X. Endometrial injury increases expression of hypoxia-inducible factor and angiogenesis in the endometrium of women with recurrent implantation failure. *Reprod Biomed Online* **38**, 761-767 (2019). https://doi.org:10.1016/j.rbmo.2018.12.027
54 Iruela-Arispe, M. L., Porter, P., Bornstein, P. & Sage, E. H. Thrombospondin-1, an inhibitor of angiogenesis, is regulated by progesterone in the human endometrium. *J Clin Invest* **97**, 403-412 (1996). https://doi.org:10.1172/jci118429
55 Print, C. *et al.* Soluble factors from human endometrium promote angiogenesis and regulate the endothelial cell transcriptome. *Hum Reprod* **19**, 2356-2366 (2004). https://doi.org:10.1093/humrep/deh411
56 Ahn, J. *et al.* Three-dimensional microengineered vascularised endometrium-on-a-chip. *Hum Reprod* **36**, 2720-2731 (2021). https://doi.org:10.1093/humrep/deab186
57 Mori, M., Bogdan, A., Balassa, T., Csabai, T. & Szekeres-Bartho, J. The decidua-the maternal bed embracing the embryo-maintains the pregnancy. *Semin Immunopathol* **38**, 635-649 (2016). https://doi.org:10.1007/s00281-016-0574-0
58 Staff, A. C. *et al.* Failure of physiological transformation and spiral artery atherosis: their roles in preeclampsia. *Am J Obstet Gynecol* **226**, S895-s906 (2022). https://doi.org:10.1016/j.ajog.2020.09.026
59 Audette, M. C. & Kingdom, J. C. Screening for fetal growth restriction and placental insufficiency. *Semin Fetal Neonatal Med* **23**, 119-125 (2018). https://doi.org:10.1016/j.siny.2017.11.004
60 Burton, G. J. & Jauniaux, E. Pathophysiology of placental-derived fetal growth restriction. *Am J Obstet Gynecol* **218**, S745-s761 (2018). https://doi.org:10.1016/j.ajog.2017.11.577
61 Gibbins, K. J. *et al.* Findings in Stillbirths Associated with Placental Disease. *Am J Perinatol* **37**, 708-715 (2020). https://doi.org:10.1055/s-0039-1688472
62 Lisiecki, M., Paszkowski, M. & Woźniak, S. Fertility impairment associated with uterine fibroids - a review of literature. *Prz Menopauzalny* **16**, 137-140 (2017). https://doi.org:10.5114/pm.2017.72759

63 Wu, D. *et al.* Chronic endometritis modifies decidualization in human endometrial stromal cells. *Reprod Biol Endocrinol* **15**, 16 (2017). https://doi.org:10.1186/s12958-017-0233-x
64 Cai, X. *et al.* Endometrial stromal PRMT5 plays a crucial role in decidualization by regulating NF-κB signaling in endometriosis. *Cell Death Discov* **8**, 408 (2022). https://doi.org:10.1038/s41420-022-01196-x
65 Chang, K. J., Seow, K. M. & Chen, K. H. Preeclampsia: Recent Advances in Predicting, Preventing, and Managing the Maternal and Fetal Life-Threatening Condition. *Int J Environ Res Public Health* **20** (2023). https://doi.org:10.3390/ijerph20042994
66 Han, L., Holland, O. J., Da Silva Costa, F. & Perkins, A. V. Potential biomarkers for late-onset and term preeclampsia: A scoping review. *Front Physiol* **14**, 1143543 (2023). https://doi.org:10.3389/fphys.2023.1143543
67 Rana, S., Lemoine, E., Granger, J. P. & Karumanchi, S. A. Preeclampsia. *Circulation Research* **124**, 1094-1112 (2019). https://doi.org:10.1161/CIRCRESAHA.118.313276
68 Rana, S., Lemoine, E., Granger, J. P. & Karumanchi, S. A. Preeclampsia: Pathophysiology, Challenges, and Perspectives. *Circ Res* **124**, 1094-1112 (2019). https://doi.org:10.1161/circresaha.118.313276
69 Bakrania, B. A. *et al.* Preeclampsia: Linking Placental Ischemia with Maternal Endothelial and Vascular Dysfunction. *Compr Physiol* **11**, 1315-1349 (2020). https://doi.org:10.1002/cphy.c200008
70 McElwain, C. J., Tuboly, E., McCarthy, F. P. & McCarthy, C. M. Mechanisms of Endothelial Dysfunction in Pre-eclampsia and Gestational Diabetes Mellitus: Windows Into Future Cardiometabolic Health? *Front Endocrinol (Lausanne)* **11**, 655 (2020). https://doi.org:10.3389/fendo.2020.00655
71 Abraham, T. & Romani, A. M. P. The Relationship between Obesity and Pre-Eclampsia: Incidental Risks and Identification of Potential Biomarkers for Pre-Eclampsia. *Cells* **11** (2022). https://doi.org:10.3390/cells11091548
72 Jung, E. *et al.* The etiology of preeclampsia. *Am J Obstet Gynecol* **226**, S844-s866 (2022). https://doi.org:10.1016/j.ajog.2021.11.1356
73 Tang, R. *et al.* The Gut Microbiota Dysbiosis in Preeclampsia Contributed to Trophoblast Cell Proliferation, Invasion, and Migration via lncRNA BC030099/NF-κB Pathway. *Mediators Inflamm* **2022**, 6367264 (2022). https://doi.org:10.1155/2022/6367264
74 Celewicz, A. *et al.* SARS CoV-2 infection as a risk factor of preeclampsia and pre-term birth. An interplay between viral infection, pregnancy-specific immune shift and endothelial dysfunction may lead to negative pregnancy outcomes. *Ann Med* **55**, 2197289 (2023). https://doi.org:10.1080/07853890.2023.2197289
75 Garrido-Gómez, T., Castillo-Marco, N., Cordero, T. & Simón, C. Decidualization resistance in the origin of preeclampsia. *Am J Obstet Gynecol* **226**, S886-s894 (2022). https://doi.org:10.1016/j.ajog.2020.09.039
76 Incio, J. *et al.* PlGF/VEGFR-1 Signaling Promotes Macrophage Polarization and Accelerated Tumor Progression in Obesity. *Clin Cancer Res* **22**, 2993-3004 (2016). https://doi.org:10.1158/1078-0432.Ccr-15-1839
77 Tjwa, M., Luttun, A., Autiero, M. & Carmeliet, P. VEGF and PlGF: two pleiotropic growth factors with distinct roles in development and homeostasis. *Cell Tissue Res* **314**, 5-14 (2003). https://doi.org:10.1007/s00441-003-0776-3

78 Ruggiero, D. *et al.* Genetics of PlGF plasma levels highlights a role of its receptors and supports the link between angiogenesis and immunity. *Sci Rep* **11**, 16821 (2021). https://doi.org:10.1038/s41598-021-96256-0
79 Luttun, A. *et al.* Revascularization of ischemic tissues by PlGF treatment, and inhibition of tumor angiogenesis, arthritis and atherosclerosis by anti-Flt1. *Nat Med* **8**, 831-840 (2002). https://doi.org:10.1038/nm731
80 Li, X. *et al.* Placental Growth Factor Contributes to Liver Inflammation, Angiogenesis, Fibrosis in Mice by Promoting Hepatic Macrophage Recruitment and Activation. *Front Immunol* **8**, 801 (2017). https://doi.org:10.3389/fimmu.2017.00801
81 Mac Gabhann, F. & Popel, A. S. Model of competitive binding of vascular endothelial growth factor and placental growth factor to VEGF receptors on endothelial cells. *Am J Physiol Heart Circ Physiol* **286**, H153-164 (2004). https://doi.org:10.1152/ajpheart.00254.2003
82 Cai, J. *et al.* Placenta growth factor-1 exerts time-dependent stabilization of adherens junctions following VEGF-induced vascular permeability. *PLoS One* **6**, e18076 (2011). https://doi.org:10.1371/journal.pone.0018076
83 Raevens, S. *et al.* Placental growth factor inhibition targets pulmonary angiogenesis and represents a therapy for hepatopulmonary syndrome in mice. *Hepatology* **68**, 634-651 (2018). https://doi.org:10.1002/hep.29579
84 Hu, J. *et al.* Apolipoprotein A1 suppresses the hypoxia-induced angiogenesis of human retinal endothelial cells by targeting PlGF. *Int J Ophthalmol* **16**, 33-39 (2023). https://doi.org:10.18240/ijo.2023.01.05
85 Luttun, A., Tjwa, M. & Carmeliet, P. Placental growth factor (PlGF) and its receptor Flt-1 (VEGFR-1): novel therapeutic targets for angiogenic disorders. *Ann N Y Acad Sci* **979**, 80-93 (2002). https://doi.org:10.1111/j.1749-6632.2002.tb04870.x
86 Aoki, S. *et al.* Placental growth factor promotes tumour desmoplasia and treatment resistance in intrahepatic cholangiocarcinoma. *Gut* **71**, 185-193 (2022). https://doi.org:10.1136/gutjnl-2020-322493
87 Halterman, J. A., Kwon, H. M. & Wamhoff, B. R. Tonicity-independent regulation of the osmosensitive transcription factor TonEBP (NFAT5). *Am J Physiol Cell Physiol* **302**, C1-C8 (2012). https://doi.org:10.1152/ajpcell.00327.2011
88 Cen, L., Xing, F., Xu, L. & Cao, Y. Potential Role of Gene Regulator NFAT5 in the Pathogenesis of Diabetes Mellitus. *J Diabetes Res* **2020**, 6927429 (2020). https://doi.org:10.1155/2020/6927429
89 Choi, S. Y., Lee-Kwon, W. & Kwon, H. M. The evolving role of TonEBP as an immunometabolic stress protein. *Nature Reviews Nephrology* **16**, 352-364 (2020). https://doi.org:10.1038/s41581-020-0261-1
90 Zhou, X. How do kinases contribute to tonicity-dependent regulation of the transcription factor NFAT5? *World J Nephrol* **5**, 20-32 (2016). https://doi.org:10.5527/wjn.v5.i1.20
91 Chernyakov, D. *et al.* Loss of RANBP3L leads to transformation of renal epithelial cells towards a renal clear cell carcinoma like phenotype. *J Exp Clin Cancer Res* **40**, 226 (2021). https://doi.org:10.1186/s13046-021-01982-y
92 Yu, H. *et al.* Transcription Factor NFAT5 Promotes Glioblastoma Cell-driven Angiogenesis via SBF2-AS1/miR-338-3p-Mediated EGFL7 Expression Change. *Frontiers in Molecular Neuroscience* **10** (2017). https://doi.org:10.3389/fnmol.2017.00301

93 Lee, N., Kim, D. & Kim, W. U. Role of NFAT5 in the Immune System and Pathogenesis of Autoimmune Diseases. *Front Immunol* **10**, 270 (2019). https://doi.org:10.3389/fimmu.2019.00270
94 Veltmann, M. *et al.* Osmotic Induction of Angiogenic Growth Factor Expression in Human Retinal Pigment Epithelial Cells. *PLoS One* **11**, e0147312 (2016). https://doi.org:10.1371/journal.pone.0147312
95 Scherer, C. *et al.* Arterial wall stress controls NFAT5 activity in vascular smooth muscle cells. *J Am Heart Assoc* **3**, e000626 (2014). https://doi.org:10.1161/jaha.113.000626
96 Lin, X. C. *et al.* NFAT5 promotes arteriogenesis via MCP-1-dependent monocyte recruitment. *J Cell Mol Med* **24**, 2052-2063 (2020). https://doi.org:10.1111/jcmm.14904
97 Hollborn, M. *et al.* Osmotic regulation of NFAT5 expression in RPE cells: The involvement of purinergic receptor signaling. *Mol Vis* **23**, 116-130 (2017).
98 Yoon, H. J. *et al.* NF-AT5 is a critical regulator of inflammatory arthritis. *Arthritis Rheum* **63**, 1843-1852 (2011). https://doi.org:10.1002/art.30229
99 Amara, S., Alotaibi, D. & Tiriveedhi, V. NFAT5/STAT3 interaction mediates synergism of high salt with IL-17 towards induction of VEGF-A expression in breast cancer cells. *Oncol Lett* **12**, 933-943 (2016). https://doi.org:10.3892/ol.2016.4713
100 Makker, V. *et al.* Endometrial cancer. *Nat Rev Dis Primers* **7**, 88 (2021). https://doi.org:10.1038/s41572-021-00324-8
101 Constantine, G. D., Kessler, G., Graham, S. & Goldstein, S. R. Increased Incidence of Endometrial Cancer Following the Women's Health Initiative: An Assessment of Risk Factors. *J Womens Health (Larchmt)* **28**, 237-243 (2019). https://doi.org:10.1089/jwh.2018.6956
102 Ali, A. T. Risk factors for endometrial cancer. *Ceska Gynekol* **78**, 448-459 (2013).
103 Wong, A. & Ngeow, J. Hereditary Syndromes Manifesting as Endometrial Carcinoma: How Can Pathological Features Aid Risk Assessment? *Biomed Res Int* **2015**, 219012 (2015). https://doi.org:10.1155/2015/219012
104 Onstad, M. A., Schmandt, R. E. & Lu, K. H. Addressing the Role of Obesity in Endometrial Cancer Risk, Prevention, and Treatment. *J Clin Oncol* **34**, 4225-4230 (2016). https://doi.org:10.1200/jco.2016.69.4638
105 Kuhn, T. M., Dhanani, S. & Ahmad, S. An Overview of Endometrial Cancer with Novel Therapeutic Strategies. *Curr Oncol* **30**, 7904-7919 (2023). https://doi.org:10.3390/curroncol30090574
106 Laviv, Y., Wang, J. L., Anderson, M. P. & Kasper, E. M. Accelerated growth of hemangioblastoma in pregnancy: the role of proangiogenic factors and upregulation of hypoxia-inducible factor (HIF) in a non-oxygen-dependent pathway. *Neurosurg Rev* **42**, 209-226 (2019). https://doi.org:10.1007/s10143-017-0910-4
107 Chen, Z., Han, F., Du, Y., Shi, H. & Zhou, W. Hypoxic microenvironment in cancer: molecular mechanisms and therapeutic interventions. *Signal Transduct Target Ther* **8**, 70 (2023). https://doi.org:10.1038/s41392-023-01332-8
108 Ding, Y. *et al.* Hypoxia-induced HIF1α dependent COX2 promotes ovarian cancer progress. *J Bioenerg Biomembr* **53**, 441-448 (2021). https://doi.org:10.1007/s10863-021-09900-9

109 Alexanian, A. & Sorokin, A. Cyclooxygenase 2: protein-protein interactions and posttranslational modifications. *Physiol Genomics* **49**, 667-681 (2017). https://doi.org:10.1152/physiolgenomics.00086.2017
110 Lee, J. J. *et al.* Hypoxia activates the cyclooxygenase-2-prostaglandin E synthase axis. *Carcinogenesis* **31**, 427-434 (2010). https://doi.org:10.1093/carcin/bgp326
111 Costa, C. *et al.* Cyclo-oxygenase 2 expression is associated with angiogenesis and lymph node metastasis in human breast cancer. *J Clin Pathol* **55**, 429-434 (2002). https://doi.org:10.1136/jcp.55.6.429
112 Sobolewski, C., Cerella, C., Dicato, M., Ghibelli, L. & Diederich, M. The role of cyclooxygenase-2 in cell proliferation and cell death in human malignancies. *Int J Cell Biol* **2010**, 215158 (2010). https://doi.org:10.1155/2010/215158
113 Greenhough, A. *et al.* The COX-2/PGE2 pathway: key roles in the hallmarks of cancer and adaptation to the tumour microenvironment. *Carcinogenesis* **30**, 377-386 (2009). https://doi.org:10.1093/carcin/bgp014
114 Zhang, X., Qu, P., Zhao, H., Zhao, T. & Cao, N. COX-2 promotes epithelial-mesenchymal transition and migration in osteosarcoma MG-63 cells via PI3K/AKT/NF-κB signaling. *Mol Med Rep* **20**, 3811-3819 (2019). https://doi.org:10.3892/mmr.2019.10598
115 Yaqub, S. *et al.* Regulatory T cells in colorectal cancer patients suppress anti-tumor immune activity in a COX-2 dependent manner. *Cancer Immunol Immunother* **57**, 813-821 (2008). https://doi.org:10.1007/s00262-007-0417-x
116 Liu, X. H. *et al.* Prostaglandin E2 induces hypoxia-inducible factor-1alpha stabilization and nuclear localization in a human prostate cancer cell line. *J Biol Chem* **277**, 50081-50086 (2002). https://doi.org:10.1074/jbc.M201095200
117 Maroni, P. *et al.* Nuclear co-localization and functional interaction of COX-2 and HIF-1α characterize bone metastasis of human breast carcinoma. *Breast Cancer Res Treat* **129**, 433-450 (2011). https://doi.org:10.1007/s10549-010-1240-1
118 Schoos, A., Gabriel, C., Knab, V. M. & Fux, D. A. Activation of HIF-1α by δ-Opioid Receptors Induces COX-2 Expression in Breast Cancer Cells and Leads to Paracrine Activation of Vascular Endothelial Cells. *J Pharmacol Exp Ther* **370**, 480-489 (2019). https://doi.org:10.1124/jpet.119.257501
119 Gonzalez-Angulo, A. M., Fuloria, J. & Prakash, O. Cyclooxygenase 2 inhibitors and colon cancer. *Ochsner J* **4**, 176-179 (2002).
120 Li, X. H. *et al.* Nimesulide inhibits tumor growth in mice implanted hepatoma: overexpression of Bax over Bcl-2. *Acta Pharmacol Sin* **24**, 1045-1050 (2003).
121 Zeisler, H. *et al.* Predictive Value of the sFlt-1:PlGF Ratio in Women with Suspected Preeclampsia. *N Engl J Med* **374**, 13-22 (2016). https://doi.org:10.1056/NEJMoa1414838
122 Nejabati, H. R., Latifi, Z., Ghasemnejad, T., Fattahi, A. & Nouri, M. Placental growth factor (PlGF) as an angiogenic/inflammatory switcher: lesson from early pregnancy losses. *Gynecol Endocrinol* **33**, 668-674 (2017). https://doi.org:10.1080/09513590.2017.1318375
123 Eriksson, A. *et al.* Placenta growth factor-1 antagonizes VEGF-induced angiogenesis and tumor growth by the formation of functionally inactive PlGF-1/VEGF heterodimers. *Cancer Cell* **1**, 99-108 (2002). https://doi.org:10.1016/s1535-6108(02)00028-4
124 Pollheimer, J., Vondra, S., Baltayeva, J., Beristain, A. G. & Knöfler, M. Regulation of Placental Extravillous Trophoblasts by the Maternal Uterine

Environment. *Front Immunol* **9**, 2597 (2018). https://doi.org:10.3389/fimmu.2018.02597
125 Davila, J. *et al.* Rac1 Regulates Endometrial Secretory Function to Control Placental Development. *PLoS Genet* **11**, e1005458-e1005458 (2015). https://doi.org:10.1371/journal.pgen.1005458
126 Tu, Z. *et al.* Uterine RAC1 via Pak1-ERM signaling directs normal luminal epithelial integrity conducive to on-time embryo implantation in mice. *Cell Death & Differentiation* **23**, 169-181 (2016). https://doi.org:10.1038/cdd.2015.98
127 Agalakova, N. I. *et al.* Canrenone Restores Vasorelaxation Impaired by Marinobufagenin in Human Preeclampsia. *International journal of molecular sciences* **23**, 3336 (2022). https://doi.org:10.3390/ijms23063336
128 Kim, J. Y. & Kim, Y. M. Acute Atherosis of the Uterine Spiral Arteries: Clinicopathologic Implications. *J Pathol Transl Med* **49**, 462-471 (2015). https://doi.org:10.4132/jptm.2015.10.23
129 Conrad, K. P., Rabaglino, M. B. & Post Uiterweer, E. D. Emerging role for dysregulated decidualization in the genesis of preeclampsia. *Placenta* **60**, 119-129 (2017). https://doi.org:10.1016/j.placenta.2017.06.005
130 Garrido-Gomez, T. *et al.* Preeclampsia: a defect in decidualization is associated with deficiency of Annexin A2. *Am J Obstet Gynecol* **222**, 376.e371-376.e317 (2020). https://doi.org:10.1016/j.ajog.2019.11.1250
131 Dröge, L. A. *et al.* Prediction of Preeclampsia-Related Adverse Outcomes With the sFlt-1 (Soluble fms-Like Tyrosine Kinase 1)/PlGF (Placental Growth Factor)-Ratio in the Clinical Routine: A Real-World Study. *Hypertension* **77**, 461-471 (2021). https://doi.org:10.1161/hypertensionaha.120.15146
132 Nikuei, P. *et al.* Diagnostic accuracy of sFlt1/PlGF ratio as a marker for preeclampsia. *BMC Pregnancy and Childbirth* **20**, 80 (2020). https://doi.org:10.1186/s12884-020-2744-2
133 Talbi, S. *et al.* Molecular phenotyping of human endometrium distinguishes menstrual cycle phases and underlying biological processes in normo-ovulatory women. *Endocrinology* **147**, 1097-1121 (2006). https://doi.org:10.1210/en.2005-1076
134 Sit, S.-T. & Manser, E. Rho GTPases and their role in organizing the actin cytoskeleton. *Journal of Cell Science* **124**, 679-683 (2011). https://doi.org:10.1242/jcs.064964
135 Shin, Y. J., Kim, E. H., Roy, A. & Kim, J.-H. Evidence for a Novel Mechanism of the PAK1 Interaction with the Rho-GTPases Cdc42 and Rac. *PLOS ONE* **8**, e71495 (2013). https://doi.org:10.1371/journal.pone.0071495
136 Salker, M. S. *et al.* LeftyA decreases Actin Polymerization and Stiffness in Human Endometrial Cancer Cells. *Scientific Reports* **6**, 29370 (2016). https://doi.org:10.1038/srep29370
137 Kang, H. *et al.* Identification of cation-binding sites on actin that drive polymerization and modulate bending stiffness. *Proceedings of the National Academy of Sciences* **109**, 16923-16927 (2012). https://doi.org:doi:10.1073/pnas.1211078109
138 Mierke, C. T. Editorial: Biomechanical Properties of Cells and Tissues and Their Impact on Cellular Adhesion and Motility. *Front Cell Dev Biol* **8**, 475 (2020). https://doi.org:10.3389/fcell.2020.00475
139 Vining, K. H. & Mooney, D. J. Mechanical forces direct stem cell behaviour in development and regeneration. *Nat Rev Mol Cell Biol* **18**, 728-742 (2017). https://doi.org:10.1038/nrm.2017.108

140 Abbas, Y. *et al.* Tissue stiffness at the human maternal-fetal interface. *Hum Reprod* **34**, 1999-2008 (2019). https://doi.org:10.1093/humrep/dez139
141 Sang, Y., Li, Y., Xu, L., Li, D. & Du, M. Regulatory mechanisms of endometrial decidualization and pregnancy-related diseases. *Acta Biochimica et Biophysica Sinica* **52**, 105-115 (2020). https://doi.org:10.1093/abbs/gmz146
142 Pan-Castillo, B. *et al.* Morphophysical dynamics of human endometrial cells during decidualization. *Nanomedicine* **14**, 2235-2245 (2018). https://doi.org:10.1016/j.nano.2018.07.004
143 Ihnatovych, I., Livak, M., Reed, J., de Lanerolle, P. & Strakova, Z. Manipulating actin dynamics affects human in vitro decidualization. *Biol Reprod* **81**, 222-230 (2009). https://doi.org:10.1095/biolreprod.108.074666
144 Goley, E. D. & Welch, M. D. The ARP2/3 complex: an actin nucleator comes of age. *Nature Reviews Molecular Cell Biology* **7**, 713-726 (2006). https://doi.org:10.1038/nrm2026
145 Hirota, T., Fujita, Y. & Ieiri, I. An updated review of pharmacokinetic drug interactions and pharmacogenetics of statins. *Expert Opin Drug Metab Toxicol* **16**, 809-822 (2020). https://doi.org:10.1080/17425255.2020.1801634
146 Bauer, A. J. *et al.* Pravastatin Attenuates Hypertension, Oxidative Stress, and Angiogenic Imbalance in Rat Model of Placental Ischemia-Induced Hypertension. *Hypertension* **61**, 1103-1110 (2013). https://doi.org:10.1161/HYPERTENSIONAHA.111.00226
147 Garrett, N. *et al.* Pravastatin therapy during preeclampsia prevents long-term adverse health effects in mice. *JCI Insight* **3** (2018). https://doi.org:10.1172/jci.insight.120147
148 Döbert, M. *et al.* Pravastatin Versus Placebo in Pregnancies at High Risk of Term Preeclampsia. *Circulation* **144**, 670-679 (2021). https://doi.org:10.1161/CIRCULATIONAHA.121.053963
149 Costantine, M. M. *et al.* A randomized pilot clinical trial of pravastatin versus placebo in pregnant patients at high risk of preeclampsia. *American Journal of Obstetrics and Gynecology* **225**, 666.e661-666.e615 (2021).
150 Chang, J.-C. *et al.* Perinatal Outcomes After Statin Exposure During Pregnancy. *JAMA Network Open* **4**, e2141321-e2141321 (2021). https://doi.org:10.1001/jamanetworkopen.2021.41321
151 Abdrabou, A. & Wang, Z. Post-Translational Modification and Subcellular Distribution of Rac1: An Update. *Cells* **7** (2018). https://doi.org:10.3390/cells7120263
152 Zeiser, R. *et al.* Regulation of different inflammatory diseases by impacting the mevalonate pathway. *Immunology* **127**, 18-25 (2009). https://doi.org:10.1111/j.1365-2567
153 Lin, L. P., Yu, T. Y., Chang, H. N., Tsai, W. C. & Pang, J. S. Simvastatin Downregulates Cofilin and Stathmin to Inhibit Skeletal Muscle Cells Migration. *Int J Mol Sci* **23** (2022). https://doi.org:10.3390/ijms23052848
154 Menter, D. G. *et al.* Differential effects of pravastatin and simvastatin on the growth of tumor cells from different organ sites. *PLoS One* **6**, e28813 (2011). https://doi.org:10.1371/journal.pone.0028813
155 Matsuzaki, S. Mechanobiology of the female reproductive system. *Reprod Med Biol* **20**, 371-401 (2021). https://doi.org:10.1002/rmb2.12404
156 Vento-Tormo, R. *et al.* Single-cell reconstruction of the early maternal-fetal interface in humans. *Nature* **563**, 347-353 (2018). https://doi.org:10.1038/s41586-018-0698-6

157 Gnecco, J. S. *et al.* Compartmentalized Culture of Perivascular Stroma and Endothelial Cells in a Microfluidic Model of the Human Endometrium. *Ann Biomed Eng* **45**, 1758-1769 (2017). https://doi.org:10.1007/s10439-017-1797-5
158 Varberg, K. M. & Soares, M. J. Paradigms for investigating invasive trophoblast cell development and contributions to uterine spiral artery remodeling. *Placenta* **113**, 48-56 (2021). https://doi.org:10.1016/j.placenta.2021.04.012
159 Boeldt, D. S. & Bird, I. M. Vascular adaptation in pregnancy and endothelial dysfunction in preeclampsia. *J Endocrinol* **232**, R27-r44 (2017). https://doi.org:10.1530/joe-16-0340
160 Huppertz, B. The Critical Role of Abnormal Trophoblast Development in the Etiology of Preeclampsia. *Curr Pharm Biotechnol* **19**, 771-780 (2018). https://doi.org:10.2174/1389201019666180427110547
161 Apicella, I., Cicatiello, V., Acampora, D., Tarallo, V. & De Falco, S. Full Functional Knockout of Placental Growth Factor by Knockin with an Inactive Variant Able to Heterodimerize with VEGF-A. *Cell Rep* **23**, 3635-3646 (2018). https://doi.org:10.1016/j.celrep.2018.05.067
162 Lennikov, A. *et al.* Synergistic interactions of PlGF and VEGF contribute to blood-retinal barrier breakdown through canonical NFκB activation. *Exp Cell Res* **397**, 112347 (2020). https://doi.org:10.1016/j.yexcr.2020.112347
163 Kang, M. *et al.* Placental growth factor (PlGF) is linked to inflammation and metabolic disorders in mice with diet-induced obesity. *Endocrine Journal* **65**, 437-447 (2018). https://doi.org:10.1507/endocrj.EJ17-0363
164 Cheung, C. Y. *et al.* Unconventional tonicity-regulated nuclear trafficking of NFAT5 mediated by KPNB1, XPOT and RUVBL2. *J Cell Sci* **135** (2022). https://doi.org:10.1242/jcs.259280
165 Jeong, G. R. *et al.* Inflammatory signals induce the expression of tonicity-responsive enhancer binding protein (TonEBP) in microglia. *J Neuroimmunol* **295-296**, 21-29 (2016). https://doi.org:10.1016/j.jneuroim.2016.04.009
166 Muhammad, K. *et al.* NFAT5 Controls the Integrity of Epidermis. *Front Immunol* **12**, 780727 (2021). https://doi.org:10.3389/fimmu.2021.780727
167 Zhao, G. *et al.* NFAT5-Mediated Signalling Pathways in Viral Infection and Cardiovascular Dysfunction. *Int J Mol Sci* **22** (2021). https://doi.org:10.3390/ijms22094872
168 Sahu, I. *et al.* NFAT5-sensitive Orai1 expression and store-operated Ca(2+) entry in megakaryocytes. *Faseb j* **31**, 3439-3448 (2017). https://doi.org:10.1096/fj.201601211R
169 Kumar, R. *et al.* NFAT5, which protects against hypertonicity, is activated by that stress via structuring of its intrinsically disordered domain. *Proceedings of the National Academy of Sciences* **117**, 20292-20297 (2020). https://doi.org:doi:10.1073/pnas.1911680117
170 Chen, S. *et al.* Tonicity-dependent induction of Sgk1 expression has a potential role in dehydration-induced natriuresis in rodents. *The Journal of Clinical Investigation* **119**, 1647-1658 (2009). https://doi.org:10.1172/JCI35314
171 Fan, X. *et al.* VEGF blockade inhibits angiogenesis and reepithelialization of endometrium. *Faseb j* **22**, 3571-3580 (2008). https://doi.org:10.1096/fj.08-111401
172 Girling, J. E. & Rogers, P. A. Regulation of endometrial vascular remodelling: role of the vascular endothelial growth factor family and the angiopoietin-TIE

signalling system. *Reproduction* **138**, 883-893 (2009). https://doi.org:10.1530/rep-09-0147
173 Bhattacharya, R. *et al.* Intracrine VEGF signalling mediates colorectal cancer cell migration and invasion. *Br J Cancer* **117**, 848-855 (2017). https://doi.org:10.1038/bjc.2017.238
174 Wiszniak, S. & Schwarz, Q. Exploring the Intracrine Functions of VEGF-A. *Biomolecules* **11** (2021). https://doi.org:10.3390/biom11010128
175 Koch, K. R. *et al.* Autocrine impact of VEGF-A on uveal melanoma cells. *Invest Ophthalmol Vis Sci* **55**, 2697-2704 (2014). https://doi.org:10.1167/iovs.13-13254
176 Lee, S. *et al.* Autocrine VEGF signaling is required for vascular homeostasis. *Cell* **130**, 691-703 (2007). https://doi.org:10.1016/j.cell.2007.06.054
177 Tudisco, L. *et al.* Epigenetic control of hypoxia inducible factor-1α-dependent expression of placental growth factor in hypoxic conditions. *Epigenetics* **9**, 600-610 (2014). https://doi.org:10.4161/epi.27835
178 Lazzara, F. *et al.* Stabilization of HIF-1α in Human Retinal Endothelial Cells Modulates Expression of miRNAs and Proangiogenic Growth Factors. *Front Pharmacol* **11**, 1063 (2020). https://doi.org:10.3389/fphar.2020.01063
179 Mongiat, M., Andreuzzi, E., Tarticchio, G. & Paulitti, A. Extracellular Matrix, a Hard Player in Angiogenesis. *Int J Mol Sci* **17** (2016). https://doi.org:10.3390/ijms17111822
180 Whelan, M. C. & Senger, D. R. Collagen I initiates endothelial cell morphogenesis by inducing actin polymerization through suppression of cyclic AMP and protein kinase A. *J Biol Chem* **278**, 327-334 (2003). https://doi.org:10.1074/jbc.M207554200
181 Wang, X. & Khalil, R. A. Matrix Metalloproteinases, Vascular Remodeling, and Vascular Disease. *Adv Pharmacol* **81**, 241-330 (2018). https://doi.org:10.1016/bs.apha.2017.08.002
182 Pitz Jacobsen, D. *et al.* Acute Atherosis Lesions at the Fetal-Maternal Border: Current Knowledge and Implications for Maternal Cardiovascular Health. *Front Immunol* **12**, 791606 (2021). https://doi.org:10.3389/fimmu.2021.791606
183 Ma, Q. *et al.* Extracellular vesicles secreted by human uterine stromal cells regulate decidualization, angiogenesis, and trophoblast differentiation. *Proc Natl Acad Sci U S A* **119**, e2200252119 (2022). https://doi.org:10.1073/pnas.2200252119
184 Blanco, R. & Gerhardt, H. VEGF and Notch in tip and stalk cell selection. *Cold Spring Harb Perspect Med* **3**, a006569 (2013). https://doi.org:10.1101/cshperspect.a006569
185 Akil, A. *et al.* Notch Signaling in Vascular Endothelial Cells, Angiogenesis, and Tumor Progression: An Update and Prospective. *Front Cell Dev Biol* **9**, 642352 (2021). https://doi.org:10.3389/fcell.2021.642352
186 Chen, W. *et al.* The endothelial tip-stalk cell selection and shuffling during angiogenesis. *J Cell Commun Signal* **13**, 291-301 (2019). https://doi.org:10.1007/s12079-019-00511-z
187 Cöl-Madendag, I., Madendag, Y., Altinkaya, S., Bayramoglu, H. & Danisman, N. The role of VEGF and its receptors in the etiology of early pregnancy loss. *Gynecol Endocrinol* **30**, 153-156 (2014). https://doi.org:10.3109/09513590.2013.864272
188 Claesson-Welsh, L., Dejana, E. & McDonald, D. M. Permeability of the Endothelial Barrier: Identifying and Reconciling Controversies. *Trends Mol Med* **27**, 314-331 (2021). https://doi.org:10.1016/j.molmed.2020.11.006

189 Salker, M. S. *et al.* Deregulation of the serum- and glucocorticoid-inducible kinase SGK1 in the endometrium causes reproductive failure. *Nature Medicine* **17**, 1509-1513 (2011). https://doi.org:10.1038/nm.2498
190 Sato, Y., Fujiwara, H. & Konishi, I. Mechanism of maternal vascular remodeling during human pregnancy. *Reprod Med Biol* **11**, 27-36 (2012). https://doi.org:10.1007/s12522-011-0102-9
191 Sánchez-Elsner, T., Botella, L. M., Velasco, B., Langa, C. & Bernabéu, C. Endoglin expression is regulated by transcriptional cooperation between the hypoxia and transforming growth factor-beta pathways. *J Biol Chem* **277**, 43799-43808 (2002). https://doi.org:10.1074/jbc.M207160200
192 Nevo, O. *et al.* Increased expression of sFlt-1 in in vivo and in vitro models of human placental hypoxia is mediated by HIF-1. *Am J Physiol Regul Integr Comp Physiol* **291**, R1085-1093 (2006). https://doi.org:10.1152/ajpregu.00794.2005
193 Tal, R. *et al.* Effects of hypoxia-inducible factor-1alpha overexpression in pregnant mice: possible implications for preeclampsia and intrauterine growth restriction. *Am J Pathol* **177**, 2950-2962 (2010). https://doi.org:10.2353/ajpath.2010.090800
194 Xi, X. *et al.* SGK1 Mediates Hypoxic Pulmonary Hypertension through Promoting Macrophage Infiltration and Activation. *Anal Cell Pathol (Amst)* **2019**, 3013765 (2019). https://doi.org:10.1155/2019/3013765
195 Baban, B., Liu, J. Y. & Mozaffari, M. S. SGK-1 regulates inflammation and cell death in the ischemic-reperfused heart: pressure-related effects. *Am J Hypertens* **27**, 846-856 (2014). https://doi.org:10.1093/ajh/hpt269
196 Plasencia, W., Maiz, N., Bonino, S., Kaihura, C. & Nicolaides, K. H. Uterine artery Doppler at 11 + 0 to 13 + 6 weeks in the prediction of pre-eclampsia. *Ultrasound Obstet Gynecol* **30**, 742-749 (2007). https://doi.org:10.1002/uog.5157
197 Xavier, P., Beires, J., Barros, H. & Martinez-de-Oliveira, J. Subendometrial and intraendometrial blood flow during the menstrual cycle in patients with endometriosis. *Fertil Steril* **84**, 52-59 (2005). https://doi.org:10.1016/j.fertnstert.2005.01.114
198 Admati, I. *et al.* Two distinct molecular faces of preeclampsia revealed by single-cell transcriptomics. *Med* **4**, 687-709.e687 (2023). https://doi.org:10.1016/j.medj.2023.07.005
199 Greten, F. R. & Grivennikov, S. I. Inflammation and Cancer: Triggers, Mechanisms, and Consequences. *Immunity* **51**, 27-41 (2019). https://doi.org:10.1016/j.immuni.2019.06.025
200 Muz, B., de la Puente, P., Azab, F. & Azab, A. K. The role of hypoxia in cancer progression, angiogenesis, metastasis, and resistance to therapy. *Hypoxia (Auckl)* **3**, 83-92 (2015). https://doi.org:10.2147/hp.S93413
201 Li, Y., Zhao, L. & Li, X. F. Hypoxia and the Tumor Microenvironment. *Technol Cancer Res Treat* **20**, 15330338211036304 (2021). https://doi.org:10.1177/15330338211036304
202 Rani, S., Roy, S., Singh, M. & Kaithwas, G. Regulation of Transactivation at C-TAD Domain of HIF-1α by Factor-Inhibiting HIF-1α (FIH-1): A Potential Target for Therapeutic Intervention in Cancer. *Oxid Med Cell Longev* **2022**, 2407223 (2022). https://doi.org:10.1155/2022/2407223
203 Liu, B., Qu, L. & Yan, S. Cyclooxygenase-2 promotes tumor growth and suppresses tumor immunity. *Cancer Cell International* **15**, 106 (2015). https://doi.org:10.1186/s12935-015-0260-7

204 Hashemi Goradel, N., Najafi, M., Salehi, E., Farhood, B. & Mortezaee, K. Cyclooxygenase-2 in cancer: A review. *J Cell Physiol* **234**, 5683-5699 (2019). https://doi.org:10.1002/jcp.27411
205 Zhao, H. *et al.* Inflammation and tumor progression: signaling pathways and targeted intervention. *Signal Transduction and Targeted Therapy* **6**, 263 (2021). https://doi.org:10.1038/s41392-021-00658-5
206 Ricciotti, E. & FitzGerald, G. A. Prostaglandins and inflammation. *Arterioscler Thromb Vasc Biol* **31**, 986-1000 (2011). https://doi.org:10.1161/atvbaha.110.207449
207 Xu, H. *et al.* CXCR2 promotes breast cancer metastasis and chemoresistance via suppression of AKT1 and activation of COX2. *Cancer Letters* **412**, 69-80 (2018). https://doi.org:https://doi.org/10.1016/j.canlet.2017.09.030
208 Wang, X., Glubb, D. M. & O'Mara, T. A. Dietary Factors and Endometrial Cancer Risk: A Mendelian Randomization Study. *Nutrients* **15** (2023). https://doi.org:10.3390/nu15030603
209 Ma, P. *et al.* NFAT5 directs hyperosmotic stress-induced fibrin deposition and macrophage infiltration via PAI-1 in endothelium. *Aging (Albany NY)* **13**, 3661-3679 (2020). https://doi.org:10.18632/aging.202330
210 Schröder, A. *et al.* Impact of salt and the osmoprotective transcription factor NFAT-5 on macrophages during mechanical strain. *Immunol Cell Biol* **99**, 84-96 (2021). https://doi.org:10.1111/imcb.12398
211 Madonna, R. *et al.* High glucose-induced hyperosmolarity contributes to COX-2 expression and angiogenesis: implications for diabetic retinopathy. *Cardiovasc Diabetol* **15**, 18 (2016). https://doi.org:10.1186/s12933-016-0342-4
212 Hernández-Ochoa, E. O. *et al.* Elevated extracellular glucose and uncontrolled type 1 diabetes enhance NFAT5 signaling and disrupt the transverse tubular network in mouse skeletal muscle. *Exp Biol Med (Maywood)* **237**, 1068-1083 (2012). https://doi.org:10.1258/ebm.2012.012052
213 Lee, H. H. *et al.* TonEBP in Myeloid Cells Promotes Obesity-Induced Insulin Resistance and Inflammation Through Adipose Tissue Remodeling. *Diabetes* **71**, 2557-2571 (2022). https://doi.org:10.2337/db21-1099
214 Kang, M. *et al.* Placental growth factor (PlGF) is linked to inflammation and metabolic disorders in mice with diet-induced obesity. *Endocr J* **65**, 437-447 (2018). https://doi.org:10.1507/endocrj.EJ17-0363
215 Coenegrachts, L. *et al.* Increased expression of placental growth factor in high-grade endometrial carcinoma. *Oncol Rep* **29**, 413-418 (2013). https://doi.org:10.3892/or.2012.2178
216 Packialakshmi, B. *et al.* NFAT5 contributes to the pathogenesis of experimental autoimmune encephalomyelitis (EAE) and decrease of T regulatory cells in female mice. *Cell Immunol* **375**, 104515 (2022). https://doi.org:10.1016/j.cellimm.2022.104515
217 Padmanabhan, S., Caulfield, M. & Dominiczak, A. F. Genetic and molecular aspects of hypertension. *Circ Res* **116**, 937-959 (2015). https://doi.org:10.1161/circresaha.116.303647
218 Jordao, H. *et al.* Pre-eclampsia during pregnancy and risk of endometrial cancer: a systematic review and meta-analysis. *BMC Womens Health* **23**, 259 (2023). https://doi.org:10.1186/s12905-023-02408-x
219 Ticconi, C., Di Simone, N., Campagnolo, L. & Fazleabas, A. Clinical consequences of defective decidualization. *Tissue Cell* **72**, 101586 (2021). https://doi.org:10.1016/j.tice.2021.101586

220 MacDonald, T. M., Walker, S. P., Hannan, N. J., Tong, S. & Kaitu'u-Lino, T. J. Clinical tools and biomarkers to predict preeclampsia. *EBioMedicine* **75**, 103780 (2022). https://doi.org:10.1016/j.ebiom.2021.103780
221 Raja Xavier, J. P. *et al.* Excessive endometrial PlGF- Rac1 signalling underlies endometrial cell stiffness linked to pre-eclampsia. *Communications Biology* **7**, 530 (2024). https://doi.org:10.1038/s42003-024-06220-7
222 Okumura, T. *et al.* Rel Family Transcription Factor NFAT5 Upregulates COX2 via HIF-1α Activity in Ishikawa and HEC1a Cells. *Int J Mol Sci* **25** (2024). https://doi.org:10.3390/ijms25073666
223 Bakrania, B. A., George, E. M. & Granger, J. P. Animal models of preeclampsia: investigating pathophysiology and therapeutic targets. *Am J Obstet Gynecol* **226**, S973-s987 (2022). https://doi.org:10.1016/j.ajog.2020.10.025
224 Costa, J. *et al.* The Role of the 3Rs for Understanding and Modeling the Human Placenta. *J Clin Med* **10** (2021). https://doi.org:10.3390/jcm10153444

Appendix

Published Manuscripts

Manuscript 1: Excessive endometrial PlGF- Rac1 signaling underlies endometrial cell stiffness linked to pre-eclampsia.

Janet P. Raja Xavier, Carmela Rianna, Emily Hellwich, Iliana Nikolou, Aditya Kumar Lankapalli, Sara Y. Brucker, Yogesh Singh, Florian Lang, Tilman E. Schäffer, and Madhuri S. Salker

Commun Biol 7, 530 (2024); doi: 10.1038/s42003-024-06220-7; PMID: 38704457

Manuscript 2: Placental growth factor mediates pathological uterine angiogenesis by activating the NFAT5-SGK1 signaling axis in the endometrium: Implications for pre-eclampsia development.

Janet P. Raja Xavier, Toshiyuki Okumura, Melina Apweiler, Yogesh Singh, Sara Y. Brucker, Satoru Takeda, Florian Lang, and Madhuri S. Salker

Biol Res. 2024 Aug 17;57(1):55. doi: 10.1186/s40659-024-00526-w; PMID: 39152497

Manuscript 3: Rel Family Transcription Factor NFAT5 Upregulates COX2 via HIF-1α Activity in Ishikawa and HEC1a Cells.

Toshiyuki Okumura, **Janet P. Raja Xavier**, Jana Pasternak, Zhiqi Yang, Cao Hang, Bakhtiyor Nosirov, Yogesh Singh, Jakob Admard, Sara Y. Brucker, Stefan Kommoss, Satoru Takeda, Annette Staebler, Florian Lang, and Madhuri S. Salker.

Int. J. Mol. Sci. 2024, 25(7), 3666; doi: 10.3390/ijms25073666; PMID: 38612478

communications biology

Article

https://doi.org/10.1038/s42003-024-06220-7

Excessive endometrial PlGF- Rac1 signalling underlies endometrial cell stiffness linked to pre-eclampsia

Check for updates

Janet P. Raja Xavier[1], Carmela Rianna[2], Emily Hellwich[2], Iliana Nikolou[1], Aditya Kumar Lankapalli[3], Sara Y. Brucker[1], Yogesh Singh[1,4], Florian Lang[5], Tilman E. Schäffer[2] & Madhuri S. Salker[1]

Cell stiffness is regulated by dynamic interaction between ras-related C3 botulinum toxin substrate 1 (Rac1) and p21 protein-activated kinase 1 (PAK1) proteins, besides other biochemical and molecular regulators. In this study, we investigated how the Placental Growth Factor (PlGF) changes endometrial mechanics by modifying the actin cytoskeleton at the maternal interface. We explored the global effects of PlGF in endometrial stromal cells (EnSCs) using the concerted approach of proteomics, atomic force microscopy (AFM), and electrical impedance spectroscopy (EIS). Proteomic analysis shows PlGF upregulated RhoGTPases activating proteins and extracellular matrix organization-associated proteins in EnSCs. Rac1 and PAK1 transcript levels, activity, and actin polymerization were significantly increased with PlGF treatment. AFM further revealed an increase in cell stiffness with PlGF treatment. The additive effect of PlGF on actin polymerization was suppressed with siRNA-mediated inhibition of Rac1, PAK1, and WAVE2. Interestingly, the increase in cell stiffness by PlGF treatment was pharmacologically reversed with pravastatin, resulting in improved trophoblast cell invasion. Taken together, aberrant PlGF levels in the endometrium can contribute to an altered pre-pregnancy maternal microenvironment and offer a unifying explanation for the pathological changes observed in conditions such as pre-eclampsia (PE).

Pregnancy is dependent on the transformation of the endometrium, a process driven by the differentiation of endometrial stromal cells (EnSCs) into specialized decidual cells[1]. The decidua contributes to early nutrient exchange, production of cytokines, and growth factors as well as supports the development of new blood vessels, modulates extravillous trophoblast (EVT) invasion, and acts as a protective barrier against infections and maternal host immune responses[2]. Disturbances in the uterine microenvironment are associated with miscarriages and third-trimester perinatal morbidity and mortality caused by pre-eclampsia (PE) and intrauterine growth restriction, small-for-gestational age, pre-term birth, and stillbirth[3–5]. It is increasingly evident that abnormal levels of inflammatory and growth/signaling factors produced in the decidua during early pregnancy play a decisive role in the deregulation of the local microenvironment leading to several disorders of pregnancy[6,7]. The endometrial contribution to the etiology of PE remains elusive. A recent study, albeit at the transcriptomic level, highlighted the role of poor decidualisation in PE[8]. However, the exact molecular mechanism of how a defective endometrial microenvironment in pre-pregnancy can lead to pregnancies complicated by PE remains unclear.

Placental Growth Factor (PlGF) was first identified in the placenta and is up-regulated in several pathological conditions such as tumor malignancy, sepsis, arthritis, and diabetic retinopathy[9–12]. PlGF primarily exerts its action on endothelial cells[13], but a plethora of studies now support the role of PlGF in non-endothelial tissues including the liver, skeleton, and thyroid[14–17]. PlGF is present in the human endometrium, exhibiting temporal changes across the menstrual cycle and reinforces uterine angiogenesis[15]. Expression of PlGF has been reported in the decidua, placenta, uterine natural killer cells, and trophoblasts cells[15]. An intricate balance between its angiogenic and inflammatory roles in the endometrium is considered important for successful conception[14]. Several studies show up-regulation of endometrial PlGF causes switching of the controlled uterine angiogenesis to a severe inflammation cascade

[1]Department of Women's Health, University of Tübingen, Tübingen, Germany. [2]Institute of Applied Physics, University of Tübingen, Tübingen, Germany. [3]Department of Biology, Ineos Oxford Institute of Antimicrobial Research, Oxford, UK. [4]Institute of Medical Genetics and Applied Genomics, University of Tübingen, Tübingen, Germany. [5]Department of Physiology, University of Tübingen, Tübingen, Germany. e-mail: madhuri.salker@med.uni-tuebingen.de

leading to tissue damage and early pregnancy losses[14]. It was further shown that PlGF modifies cellular motility and adhesion with important roles in early pregnancy[15]. Low levels of PlGF are associated with PE and used as a clinical diagnostic marker for PE prediction[13,18], but it remains uncertain whether dysregulated low PlGF level is a cause or consequence of PE progression.

Ras-related C3 botulinum toxin substrate 1 (Rac1) is a major player of the Rho family of small GTPases that controls multiple cell signalling pathways such as cytoskeleton organization, cell proliferation, apoptosis and immune activation[19]. The major downstream cellular target of activated Rac1 is p21(Rac1)-activated kinase (PAK1)[20] and activation of this pathway reverses the process of polymerization brought on by ARP2/3 activity, converting F-actin filaments into G-actin monomers[21]. The actin cytoskeleton provides the structural scaffold for a cell and principally determines its mechanical properties. Consequently, any alteration of actin polymerization is anticipated to modify cell stiffness[22,23]. Regulatory proteins of the actin cytoskeleton including Rac1 play a pivotal role during implantation[24]. Therefore, the ability of endometrial cells to support the ongoing pregnancy requires a delicate balance of reorganization of the actin cytoskeleton to promote EVT invasion and to restrict over invasion[25,26]. Interestingly, PlGF plays a pivotal role in actin regulation and cytoskeletal rearrangement in breast cancer and leukemic cells making them stiffer[16,27]. Furthermore, PE is associated with impaired cytoskeleton rearrangements and increased arterial stiffness[28,29]. However, a functional mechanism has not been directly investigated. During early pregnancy, EVTs invade the endometrium cluster around the spiral arteries and induce their remodelling[30]. Differences in stiffness within the endometrium could influence EVT migration. Given that PE is characterized by shallow EVT invasion, it is tempting to speculate that a stiffer endometrium prior to pregnancy may indeed contribute to the pathogenesis of PE in part by hindering invasion.

Taken together, here we postulate that excessive PlGF levels in the endometrium contribute to impaired cytoskeletal rearrangements and stiffness and thus participate in the pathophysiology of PE. To test this hypothesis, manual mining of RNA sequencing (RNA-seq) data shows that at a pathway level, several biological processes including extracellular structure, actin, and cell-matrix organization were affected in the decidua prior to the onset of PE. We, therefore, sought to determine whether high PlGF affects the actin turnover and cell stiffness of EnSCs. We report that high PlGF (20 ng/ml for 6 days) leads to dynamic changes in the mechanical cellular properties in EnSCs. We provide evidence that PlGF increases Rac1 activity, PAK1 phosphorylation, actin polymerization, and cell stiffness. Lastly, we show that PlGF-induced Rac1 and actin dysregulation can be improved with the pharmacological substance pravastatin. Interestingly, improved endometrial actin dynamics with pravastatin also enhanced trophoblast (BeWo) cell invasion through endometrial cell monolayers.

Results

PlGF induces proteome changes, pointing to the regulators of cellular actin machinery and ECM organization

To verify the expression kinetics of PlGF across the menstrual cycle, we performed *insilico* analysis (*GEO2052*). Whole genome molecular phenotyping of human endometrial tissue enabled the identification of PlGF molecular signature across the menstrual cycle in normo-ovulatory women. We observe that PlGF is higher in the proliferative phase (n = 4) with expression levels declining across the secretory phase (n = 6) of the cycle (Fig S1a). Next, we explored whether PE pathophysiology is associated with dysregulated levels of endometrial PlGF and cytoskeleton-activating Rho-GTPases proteins like PAK1. We verified their expression levels obtained from microarray and gene expression studies in uteroplacental units from 10 preeclamptic women and 10 women with healthy pregnancies. We found that PlGF and PAK1 transcripts were upregulated in term decidua's (Fig S1b) of preeclamptic women (*GEO2548*) compared to the decidua from healthy pregnancies.

Furthermore, we mined a publicly available RNA sequencing array (in silico analysis, *GSE172381*) from endometrial biopsies obtained from women who developed PE in a previous pregnancy (n = 24) and controls who never had PE ($n = 16$). We verified transcriptomic alterations in the endometrium from patients with a history of PE. Gene Ontology analysis of the gene signature identified six classes and 43 enriched biological processes (FDR < 0.05). These pathways were mainly associated with cell signalling, cell motility, cytoskeleton extracellular matrix, and reproductive process (Fig S1c). These pathways are hallmarks of impaired endometrial function and PE pathogenesis. We identified 93 genes representative of the altered pathways in PE participating in the extracellular matrix organization, cell motility, and in cytoskeleton (Fig S1d). These *insilico* findings discussed above provided us with a positive cue for a possible correlation between dysregulated decidual PlGF and altered endometrial mechanics as observed in PE pathogenesis.

To identify a putative link between endometrial cells and cell stiffness, EnSCs were treated with PlGF (20 ng/ml for 6 days). The cells were then harvested for proteomics. Proteomic analysis was performed by comparing protein expression patterns in control ($n = 3$) and PlGF ($n = 3$) treated EnSCs. This comparison revealed a total of 97 dysregulated proteins. Differentially regulated proteins were shown in volcano plots as seen in Fig. 1a. A total of 47 upregulated (blue) and 50 (red) downregulated differentially regulated proteins were identified as being associated with PlGF treatment in EnSCs. Upregulated proteins include those involved in actin cytoskeleton regulation, such as DCTN2, PFN2, RAP1B, and CAPZA1; and proteins associated with GTPase regulation (IQGAP1 and ARHGAP1), and extracellular matrix organization proteins (COL1A2, COL1A1, and TUBA1A). Some of the downregulated proteins include actin-stabilizing proteins such as CAPZB, CNN1, and CALD1. Gene Ontology analysis of the protein signature associated with PlGF treatment in EnSCs also identified biological process associated with GTPases activity (Fig. 1b). Further to validate the above finding, we studied the effect of PlGF on ECM markers of EnSCs with qPCR. We show that PlGF enhanced gene expression of ECM-associated markers (*ACTA2, COL1A1, COL1A2, COL3A1, COL4A1*) and matrix metalloprotease markers (*MMP2 and MMP9*) in EnSCs confirming the increased ECM associated transcriptome changes as seen in proteomics data (Fig S2a, b). These findings suggested that PlGF exerts a pro-stiffness phenotype with actin regulation and GTPases activation signaling pathway being one of the most common GO terms.

PlGF upregulates cytoskeletal regulators Rac1 and PAK1 in endometrial stromal cells

Next, we investigated to gain insights into the effect of PlGF on small G protein or GTPase Rac1-dependent regulation of actin organization and polymerization in endometrial stromal cells. Rac1-PAK1 cellular signaling pathway accounts for a pivotal role in the reorganization of the actin filaments, hence the effect of PlGF on Rac1 expression and activity was verified. PlGF treatment (20 ng/ml for 6 days) was followed by a significant increase of both Rac1 ($^*p < 0.05$) and PAK1 ($p < 0.05$) transcript levels normalized to L19 transcript levels (Fig. 2a, b). Moreover, PlGF treatment was also followed by a significant increase in total ($^{**}p < 0.01$) and phosphor-Rac1 ($^{***}p < 0.001$) protein levels (Fig. 2c–e and Supplementary information).

Rac1 activation is known to trigger phosphorylation of PAK1, which in turn regulates the actin turnover dynamics. As shown in Fig. 2c –g and Supplementary information treatment with PlGF for 6 days increased PAK1 total protein level and phosphorylated levels ($^*p < 0.05$), pointing to an increase of PAK1 activity in endometrial cells. Further, to validate the activation of Rac1 protein, Rac1 activation assay (immunoprecipitation) was employed. Rac1 activity was assayed by determining the amount of GTP-bound (activated) Rac1 that was precipitated by a GST-PAK1 fusion protein. As evident in Fig. 2h, i and Supplementary information, PlGF treatment dramatically increased the activity of Rac1(GTP) ($^*p < 0.05$) compared to control. Actin regulator Rac1 acts as a key molecule in

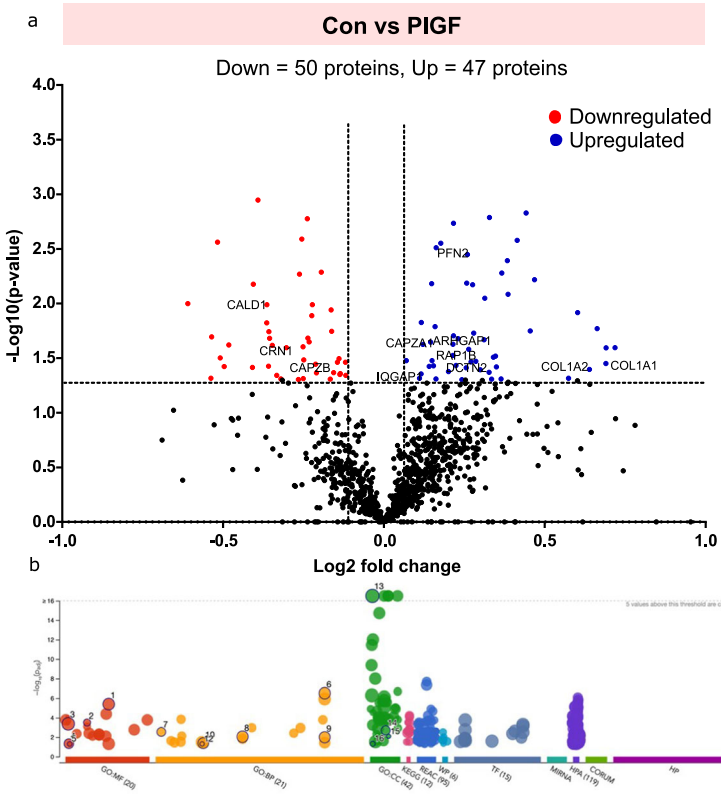

ID	Source	Term ID	Term Name	p_{adj} (query_1)
1	GO:MF	GO:0043168	Anion binding	4.011×10^{-6}
2	GO:MF	GO:0016628	Oxidoreductase activity, acting on the CH-CH...	3.089×10^{-4}
3	GO:MF	GO:0003824	Catalytic activity	4.207×10^{-4}
4	GO:MF	GO:0003924	GTPase activity	4.710×10^{-2}
5	GO:MF	GO:0004069	L-aspartate:2-oxoglutarate aminotransferase a...	4.97×10^{-2}
6	GO:BP	GO:1901566	Organonitrogen compound biosynthetic process	3.133×10^{-7}
7	GO:BP	GO:0002181	Cytoplasmic translation	2.876×10^{-3}
8	GO:BP	GO:0044281	Small molecule metabolic process	8.930×10^{-3}
9	GO:BP	GO:1901565	Organonitrogen compound catabolic process	1.013×10^{-2}
10	GO:BP	GO:0019752	Carboxylic acid metabolic process	4.126×10^{-2}
11	GO:BP	GO:0019751	Glutamate catabolic process to 2-oxoglutarate	4.886×10^{-2}
12	GO:BP	GO:0019750	Glutamate catabolic process to aspartate	4.886×10^{-2}
13	GO:CC	GO:0005737	Cytoplasm	7.735×10^{-20}
14	GO:CC	GO:0044391	Ribosomal subunit	2.007×10^{-3}
15	GO:CC	GO:0070381	Endosome to plasma membrane tranport vesi...	8.175×10^{-3}
16	GO:CC	GO:0005785	Signal recognition particle receptor complex	4.873×10^{-2}

Fig. 1 | Protein expression profile of EnSCs cell lysates treated with PlGF. a Volcano plot showing upregulated (blue) and downregulated (red) proteins in PlGF-treated EnSCs ($n = 3$) compared to untreated EnSCs ($n = 3$) (control). Each point represents one protein; black points are the rest of the proteins obtained in the global proteomic analysis. The significance threshold range is 0.05 and the fold change threshold is −1 and +1. **b** Gene Ontology analysis of the protein signature associated with PlGF treatment in EnSCs shows enriched biological processes.

regulating cell migration[31]. Thereby, we studied the migratory potential of PlGF-treated EnSCs using a wound healing assay. PlGF treatment enhanced cell migration in EnSCs (Fig S3a, b) without a change in cell proliferation (Fig S3c, d) as verified by a BrdU proliferation ELISA and MTS.

PlGF downregulates actin depolymerization and augments cell stiffness in endometrial stromal cells

Activation of Rac1 in cells decreases the G/F actin ratio, which in turn enhances cellular stiffness. To test this, we next investigated whether the marked alterations of cell stiffness following PlGF treatment in stromal cells were marked by respective alterations with actin polymerization dynamics. Interestingly, as evident from both flow cytometry (Fig. 3a, b and S4, $^{*}p < 0.05$) and western blotting analysis (Fig. 3c, d and Supplementary information, $^{**}p < 0.01$), a 6-day treatment of EnSCs with PlGF significantly decreased the ratio of soluble G-actin over filamentous F-actin, reflecting the polymerization of actin filaments. Fluorescent images of F-actin organization (Fig. 3e and S5, red) and its concomitant changes under PlGF treatment show a profound reorganization of the actin cytoskeleton with an increased cell area (Fig. 3f, $^{**}p < 0.01$) and enhanced fluorescence intensity (Fig. 3g, $^{***}p < 0.001$).

Filamentous actin (F-actin) is a structural cytoskeleton protein known to play an important role in maintaining cellular and tissue structure. To determine whether PlGF induces structural changes and modifies mechanical stiffness in EnSCs, atomic force microscopy (AFM) was performed on live EnSCs after treatment with PlGF for 6 days (20 ng/ml). Individual cells were subsequently imaged with AFM in the force mapping mode to quantify the cell stiffness (Fig. 3h). Comparison of the mean stiffness revealed that PlGF-treated EnSCs are significantly stiffer ($\langle E \rangle = 4.94$ kPa) than the control cells ($\langle E \rangle = 3.13$ kPa) (Fig. 3i, $^{****}p < 0.0001$). EGF, a known Rac1 activator, was used as a positive control for an increase in cell stiffness (Fig S6). Additionally, to infer the change in stiffness in a more relevant physiological environment, EnSCs were seeded onto PDMS substrates (bulk stiffness 1–2 kPa) and subjected to PlGF treatment as described above. We observed PlGF-treated EnSCs seeded on top of a soft substrate as PDMS gels, still showed an increase in cellular stiffness compared to untreated EnSCs (Fig S7).

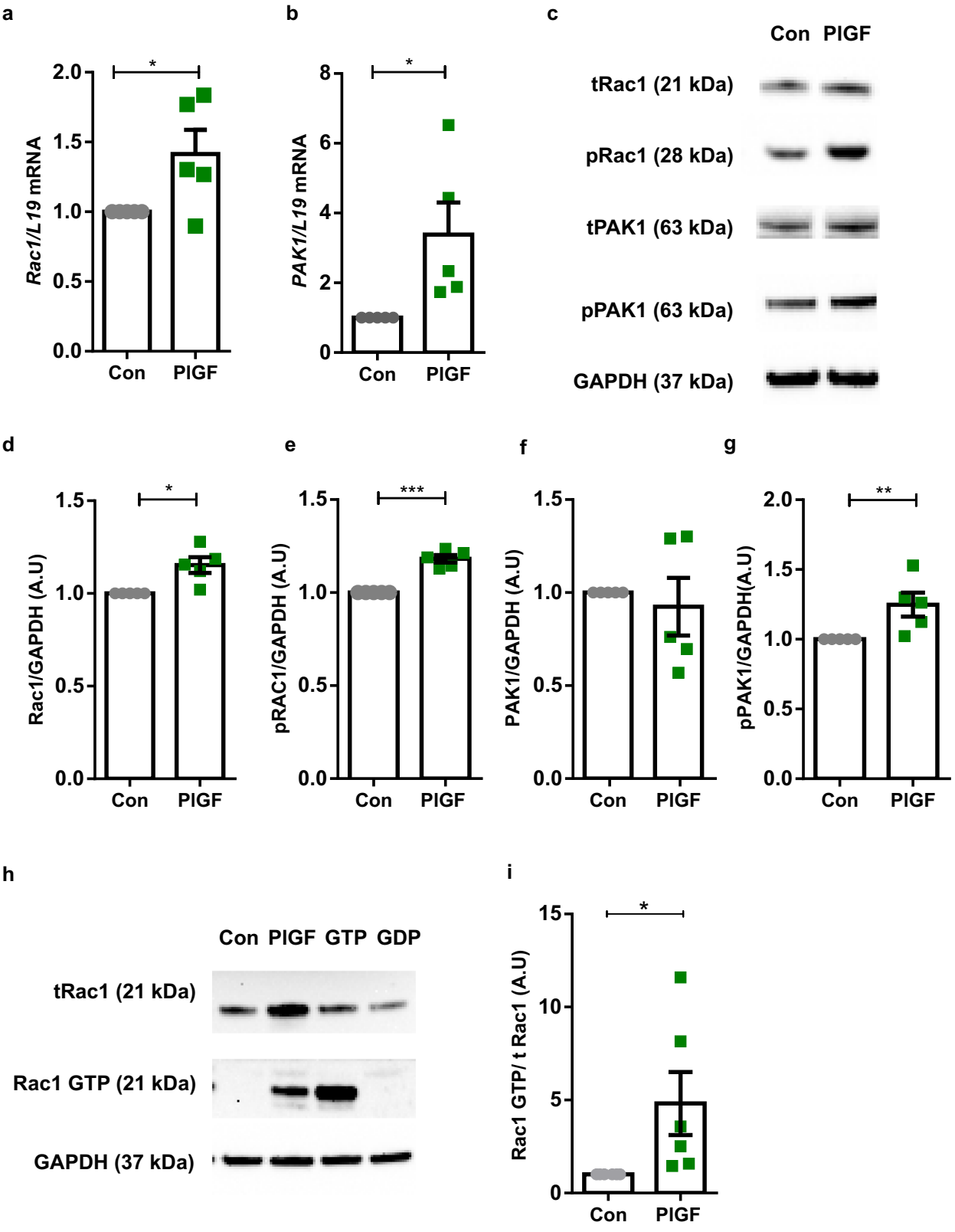
a
b
c
Rac1/L19 mRNA
PAK1/L19 mRNA
Con
PIGF
tRac1 (21 kDa)
pRac1 (28 kDa)
tPAK1 (63 kDa)
pPAK1 (63 kDa)
GAPDH (37 kDa)
d
e
f
g
Rac1/GAPDH (A.U)
pRAC1/GAPDH (A.U)
PAK1/GAPDH (A.U)
pPAK1/GAPDH(A.U)
h
i
Con PIGF GTP GDP
Rac1 GTP (21 kDa)
Rac1 GTP/ t Rac1 (A.U)

Fig. 2 | Effect PlGF on transcript and protein levels of Rac1 and PAK1 cytoskeletal regulators. a Arithmetic mean ± SEM of Rac1 transcript level in EnSCs on treatment with PlGF ($n = 5$, $^{*}p < 0.05$). **b** Arithmetic mean ± SEM of PAK1 transcripts levels in EnSCs on treatment with PlGF ($n = 5$, $^{*}p < 0.05$). **c** Original western blots representing total and phosphorylated levels of Rac1 and PAK1 targets with GAPDH used as a loading control. **d** Arithmetic mean ± SEM of protein levels of total Rac1 in untreated and PlGF-treated EnSCs ($n = 5$, $^{*}p < 0.05$,). **e** Arithmetic mean ± SEM of protein levels of phosphorylated Rac1in untreated and PlGF-treated EnSCs ($n = 5$, $^{***}p < 0.01$). **f** Arithmetic mean ± SEM of protein levels of total PAK1 in untreated and PlGF-treated EnSCs. **g** Arithmetic mean ± SEM of protein levels of phosphorylated PAK1 in untreated and PlGF-treated EnSCs ($n = 5$, $^{**}p < 0.01$). **h** Original western blots of total Rac1, Rac1 GTP, and GAPDH from Rac1 Pull down assay. **i** Arithmetic mean ± SEM of protein levels of activated form of Rac1, as Rac1GTP normalised to total Rac1($n = 6$, $^{*}p < 0.05$) in EnSCs on treatment with PlGF and untreated controls. All the above data represented here is normalized to control samples. The statistical significance was tested with an Unpaired *t*-test with Welch's correction.

EnSCs undergo a differentiation process termed decidualization, initiated by progesterone during the early secretory phase[3,32]. Decidualization of stromal cells is critical to regulate trophoblast invasion to mediate pregnancy establishment and progression[1,32]. Therefore, we evaluated the effect of aberrant PlGF on EnSCs during decidualization in vitro. Further, we verified the effect of PlGF on actin regulators and cell stiffness of decidualized EnSCs. Our results show that PlGF impaired the decidualization potential in EnSCs with a decrease in transcript levels of markers such as prolactin and insulin-like growth factor binding protein-1 (Fig S8). The reduced decidualization markers were accompanied by decrease in Rac1 activity (Fig S9a) and a decrease in G/F actin ratio (Fig S9b, c) with increased cell stiffness (Fig S10) in PlGF-treated decidualized EnSCs compared to decidualized EnSCs. These results confirm that aberrant PlGF levels in the endometrium would impede the decidualizing behaviour of EnSCs with negative regulation of decidual markers, actin dynamics and cell stiffness.

PlGF influence on endometrial actin regulation is mediated by Rac1, PAK1 and WAVE2 signalling effectors

To prove unequivocally that PlGF directly modulates the Rac1-PAK1 signaling pathway, EnSCs were first treated with PlGF for 4 days followed by transfection with Rac1, PAK1, and/or WAVE2 siRNAs for 48 h, and then continued with PlGF treatment for 2 more days (20 ng/ml). Rac1 gene silencing was efficient (40-50% silencing) and co-treatment with PlGF further suppressed both total and phosphorylated Rac1 (50-60% silencing) and PAK1 protein expression in EnSCs (Fig. 4a–d and Supplementary information, $^{*}p < 0.05$, $^{**}p < 0.01$, $^{***}p < 0.001$). Similarly, inhibition of PAK1 with siPAK1 (± PlGF) again paralleled the effect of Rac1 gene silencing, significantly downregulating total (40-50% silencing) and phosphorylated levels of PAK1(50-60% silencing) protein activity with and without PlGF (Fig. 4a, d, e and Supplementary information, $^{**}p < 0.01$).

Further, we investigated the influence of PlGF on Rac1 regulatory proteins responsible for actin nucleation and turnover such as WAVE2 and ARP2/3. We demonstrated that, PlGF significantly increased protein levels of WAVE2 and ARP2/3 ratio in EnSCs (Fig. 4f, g and Supplementary information, $^{*}p < 0.05$, $^{**}p < 0.01$). Further, silencing of Rac1 or WAVE2 with and without PlGF treatment, was also followed by a decrease in expression levels of these proteins validating their activation through Rac1 signaling cascade. However, silencing WAVE2 with and without PlGF, did not have an additional effect on PAK1 activity levels (Fig. 4a–e, $^{**}p < 0.01$), highlighting WAVE2 downstream activity to be independent of PAK1 in modulating actin nucleation.

We next explored whether loss of Rac1/PAK1 or WAVE2 can affect G/F actin. Strikingly, silencing of Rac1/PAK1 or WAVE2 with and without PlGF was also followed by a significant increase of soluble G-actin over filamentous F-actin (flow cytometry; Fig. 5a, $^{*}p < 0.5$, $^{***}p < 0.001$). This effect on reverting G and F actin ratio levels with siRNAs with or without PlGF was also evidenced with Western blot analysis measuring the pan actin levels of G and F actin protein lysates (Fig. 5b, c and Supplementary information, $^{*}p < 0.5$, $^{***}p < 0.001$). Thus, the above-presented results confirm the inhibitory effect of siRac1, siPAK1, and siWAVE2. Further, it validates the PlGF-mediated activation of Rac1-PAK1 signaling axis and its downstream effect on endometrial actin dynamics.

Pravastatin reverses PlGF-induced endometrial actin dynamics and improves BeWo cell invasion

We next examined if PlGF-induced Rac1 activation and altered actin dynamics in EnSCs could be pharmacologically reversed. Therefore, we assessed the activity of pravastatin drug on Rac1 mechanism with and without PlGF treatment. We show pravastatin reverts back to the effect of PlGF on actin levels by increasing G and F actin ratio levels, as evidenced by both flow cytometry and Western blotting respectively. Taken together these results confirm that PlGF-treated EnSCs can be recused after a 24 h treatment with pravastatin, with levels almost reaching control (untreated) levels (Fig. 6a–g and Supplementary information), $^{*}p < 0.5$, $^{**}p < 0.01$, $^{***}p < 0.001$, $^{****}p < 0.0001$). Similarly, we also show an inhibitory effect of pravastatin on PlGF-induced Rac1-GTP (Fig. 6h–I and Supplementary information) levels.

Tight junctions, which connect adjacent cells, control the barrier of a tissue layer. PE is characterized by poor EVT invasion through the stroma to the spiral arteries[30]. We hypothesised that PlGF can impede normal invasion of BeWo through EnSCs. To test this, we used electrical impedance spectroscopy (EIS), which can measure (electrical) resistance which reflects the tightness of the junctions. To this end, EnSCs monolayers were formed in the presence or absence of PlGF for 6 days with or without 24 h pravastatin (10 μM) treatment. Following this BeWo cells were added and the invasion was monitored with EIS.

We show that the resistance of PlGF-treated stromal monolayer was higher compared to the control pointing to a reduced BeWo invasion (Fig. 6j, $^{***}p < 0.0001$). Strikingly, the reduced BeWo invasion in PlGF-treated EnSCs was reversed by pravastatin treatment (Fig. 6j, $^{****}p < 0.0001$). Collectively, these results indicate a clear beneficial effect of pravastatin in inhibiting PlGF-mediated Rac1 activation and normalising actin levels with improved BeWo cell invasion through the endometrial cells.

Pravastatin reverts the PlGF-modified cell and ECM proteome in endometrial stromal cells

To investigate the comprehensive effect of PlGF and drug pravastatin in EnSCs, we utilized a quantitative proteomic approach. Proteomic analysis was performed by comparing protein expression patterns in PlGF ($n = 3$) and PlGF + pravastatin ($n = 3$) treated EnSCs. This comparison revealed a total of 95 dysregulated proteins. Differentially regulated proteins were shown in volcano plots as seen in Fig. 7a. A total of 55 upregulated (orange) and 40 (violet) downregulated differentially regulated proteins were identified as being associated with pravastatin treatment in PlGF-treated EnSCs. The heatmap describes the differentially regulated proteins expressed in different treatment groups (Con/PlGF/Prav/PlGF+Prav) in EnSCs following global proteomic analysis (Fig S11). Some of the upregulated proteins were involved in actin cytoskeleton regulation and stabilization such as ACTG1 and CAPZB. Some of the downregulated proteins included actin cytoskeleton and extracellular matrix remodelling proteins such as CNN2, COL1A1, COL1A2, COL6A, and TUBA1A. Gene Ontology analysis of the protein signature associated with pravastatin treatment in PlGF-treated EnSCs identified pathways associated with GTP binding, intracellular transport and cytoplasmic translation (Fig. 7b). Thus, the proteomic analysis pointed to a reversal of actin regulation, extracellular matrix remodelling mechanics and cell-

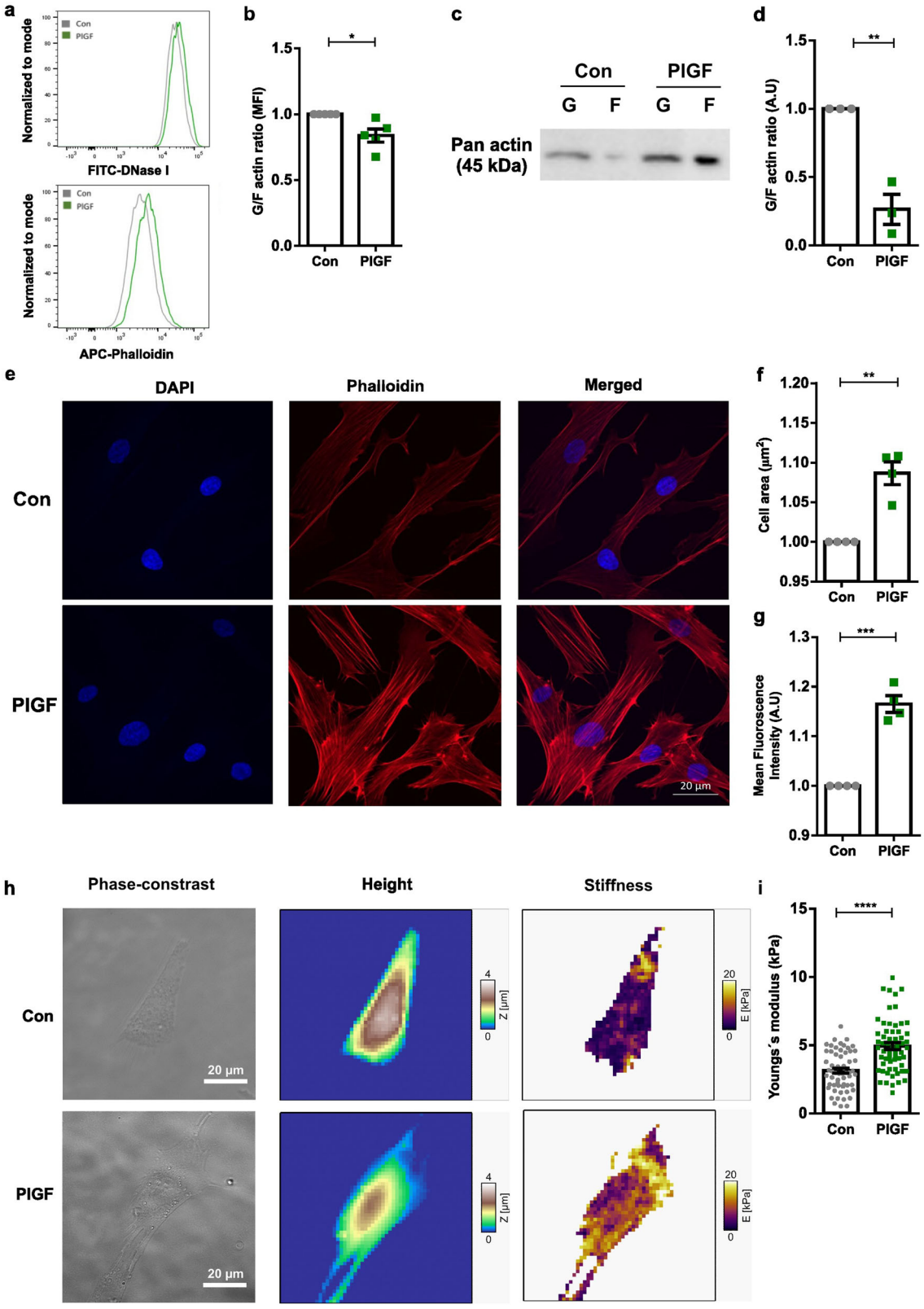

stiffness with the absence of GTPases pathway activity with pravastatin treatment on PlGF treated EnSCs.

Discussion

PE is a disorder that affects 3–5% of pregnant women and is a leading cause of maternal and neonatal mortality and morbidity[33,34]. The principal features include a new onset of hypertension and proteinuria. Currently, the only definitive cure is delivery.

The pathogenesis of PE is multifactorial and is incompletely understood but appears to be a consequence of maternal uteroplacental malperfusion and abnormal adaptive placentation[35,36]. Recent studies suggest that PE might in fact be a disorder of the decidua prior to

Fig. 3 | Effect of PlGF on actin polymerization and cell stiffness in EnSCs. **a** Representative original histogram of DNaseI (G-actin; Left) and Phalloidin (F-actin; Right) binding in EnSCs after 6 days of treatment without and with PlGF. **b** Arithmetic means ± SEM of mean fluorescence intensity (MFI) of G-actin over F-actin ratio in EnSCs after 6 days of treatment without and with PlGF ($n = 5$, $^{*}p < 0.05$). **c** Representative original western blot of soluble G-actin and filamentous F-actin in human endometrial EnSCs after 6 days of treatment with PlGF. **d** Arithmetic mean ± SEM of G-actin over F-actin ratio in EnSCs after 6 days treatment with PlGF ($n = 3$, $^{**}p < 0.01$). **e** Original immunofluorescence images of eflour650-phalloidin binding to F-actin (red) and DAPI staining for cell nuclei (blue) in EnSCs treated with or without PlGF. **f** Arithmetic mean ± SEM individual cells were measured) of cell area (μm^2) measured in EnSCs post treatment with PlGF ($n = 4$, $^{**}p < 0.01$). **g** Arithmetic mean ± SEM of mean fluorescence intensity (MFI) measured from immunofluorescence images in EnSCs post-treatment with PlGF ($n = 4$, $^{***}p < 0.001$). All the above data represented here are normalized to control cells. The statistical significance was tested with an Unpaired *t*-test with Welch's correction. **h** AFM analysis of cell stiffness and cell morphology in untreated EnSCs and cells treated with PlGF for 6 days at 20 ng/ml. Representative optical phase contrast images, height images, and AFM stiffness images measuring the Young's modulus. **i** Arithmetic mean ± SEM of Young's modulus (cell stiffness) ($n = 60$, $^{****}p < 0.0001$). The statistical significance was tested with a non-parametric Mann-Whitney U test.

pregnancy[3,8]. These authors demonstrated in vitro that EnSCs isolated from patients with a history of PE failed to decidualize and that a decidual molecular defect is an important contributor in PE, suggesting a pivotal role of the maternal decidua in the development of PE pathogenesis. However, this study did not provide any molecular mechanism causing defective decidua.

The well-established marker for PE diagnosis in asymptomatic pregnant women is the use of the biomarker sFLT1/PlGF. The sFLT1/PlGF ratio shows a sensitivity of 66.2% and a specificity of 83.1%[18,37]. However, its use is effective only 4 weeks before PE symptoms manifest. Therefore, during early pregnancy, there is an absence of screening methods (both highly sensitive and specific) to diagnose PE earlier and therefore avoid mortality and morbidity. Indirect evidence points to a pathological role for PlGF in pregnancy[38–40], but the role of endogenous PlGF on non-endothelial cells prior to pregnancy, specifically in modulating the decidua remains unknown.

To identify the involvement of altered cellular mechanics in the decidua in PE progression, we performed manual mining of bulk RNA-seq from endometrial biopsies (*GSE172381*)[8]. 593 genes were identified to be differentially expressed in the decidua from patients with a history of PE compared to the women with healthy pregnancies. Remarkably, according to gene enrichment analysis, actin dynamics and cytoskeleton signalling pathways were highly dysregulated. Thus, the altered expression of extracellular matrix, cell motility, cell component organisation, and cytoskeletal components, prior to pregnancy could disturb the microenvironment at the maternal interface during early pregnancy and placentation contributing to the development of PE.

The main aim of this study has been to investigate the effect of PlGF on endometrial cellular mechanics. Our study revealed that PlGF affect cellular actin regulation and ECM machinery at a global level employing proteomics. Further, PlGF influences stromal cells showed a variety of protein cargo, including cell signalling molecules, factors that maintain cell polarity, intracellular transport mediators, and actin-modulating proteins such as Rho GTPases activating protein. Rac1, a member of the Rho family of small GTPases controls a wide array of cellular functions. In response to diverse signals, it converts from an inactive GDP-bound form to an active GTP-bound form. Rac1 signalling has been directly implicated in the regulation of cell motility, such as migration and invasion[41–43], and is therefore an important regulator of actin cytoskeleton organization[44]. In our study, we show that following PlGF treatment there is a significant up-regulation of Rac1 activity and even accounts for the observed actin reorganization, followed by cell stiffening. Rac1 activation is further recognised to regulate actin polymerization interacting with the Arp2/3-mediated actin nucleation pathway through its target WAVE2 to improve actin nucleation. In our study however, we observed a PlGF-induced increase of Rac1 phosphorylation a regulator of both PAK1 and WAVE2, indicating activation of both of these signalling effectors in endometrial stromal cells. In line with this, we observed the reorganization of the actin filaments network towards the polymerization of F-actin filaments. Since modification of actin dynamics through polymerization has been reported to account for filaments of higher mechanical stability[45], our observations on cell stiffening in response to PlGF treatment may directly be correlated to the observed PlGF-induced actin depolymerization. Moreover, siRNA targeting either Rac1, PAK1, and WAVE2 or in combination with PlGF did not increase these targets. This observation confirms that PlGF is a target of the Rac1/PAK1 signalling cascade (Fig. 8).

Cell biomechanics is relevant for all tissues and the stiffness of most human tissues diverges greatly from the brain (soft, ~0.2 kPa) to bone (rigid, ~10^6 kPa)[46]. The decidua (biopsies) has a stiffness of around 1.2 kPa[47]. During early pregnancy, EVTs invade and congregate around the decidua and induce the remodeling of the spiral arteries. Modifications in stiffness within the endometrium could thereby impact EVT invasion, and the most notable change in stiffness that they will encounter is when only they approach the myometrium, the smooth muscular layer beneath the decidua. It is interesting to point out that the stiffness of smooth muscle tissue is ~5 kPa, five times that of decidua, which is similar to the stiffness observed post-treatment with PlGF in EnSCs (4.9 kPa). Once EVT cells arrive at the (inner third) myometrium, they halt their migration and differentiate into multinucleated giant cells. Taken together, we speculate that, prior to pregnancy, increased levels of PlGF in the endometrium could result in an under-invasion of EVT pathology in decidua due to the enhanced stiffness. Increased stiffness in the endometrium hence interferes with the decidualization function of the stromal cells and prevents or hampers EVT migration, therefore preventing effective remodelling of spiral arteries, resulting in PE pathogenesis later on in pregnancy.

Statins (HMG-CoA reductase inhibitors) are widely used and are effective in preventing cardiovascular mortality and morbidity[48]. In rodent models of PE, pravastatin administered in early pregnancy was able to restore angiogenic imbalance and re-establish normal endothelial function[49,50]. These preliminary animal studies provide a strong rationale for the use of pravastatin in the prevention of PE in humans. It is noteworthy to point out two recent clinical trials using pravastatin. In 2021, Döbert et al., performed a double-blind, placebo-controlled trial in 1120 women[51]. Women screened for term PE were given 20 mg daily dose of pravastatin for 35–37 weeks gestation until delivery. They found no difference between the pravastatin and placebo group. In, another study performed during the early phase of pregnancy (12–16 weeks) women were given 10 mg per day pravastatin until delivery[52]. Although the numbers were limited, this study showed a significant reduction in incidence and severity of PE when pravastatin was administered earlier in pregnancy during EVT invasion and thus placental formation. The use of statins in pregnancy is highly debated because of its possible teratogenicity[53]. However recent studies suggest that statin exposure during pregnancy is not associated with an increased risk of congenital anomaly in humans[53,54]. The above-mentioned retrospective clinical trials with use of pravastatin for PE prevention or treatment also showed no identifiable safety risks associated with pravastatin in their cohorts[51,52]. Whilst this clinical trial is very encouraging, further studies are warranted to support the necessity of statins for the treatment and prevention of PE pathogenesis and possible teratogenicity if prescribed in early pregnancy.

Rac1 is post-translationally modified by an isoprenyl lipid group, specifically geranylgeranyl diphosphate (GGPP), which is thought to regulate its subcellular localization[55,56]. Statins are known to inhibit mevalonate synthesis upstream of both cholesterol and GGPP synthesis,

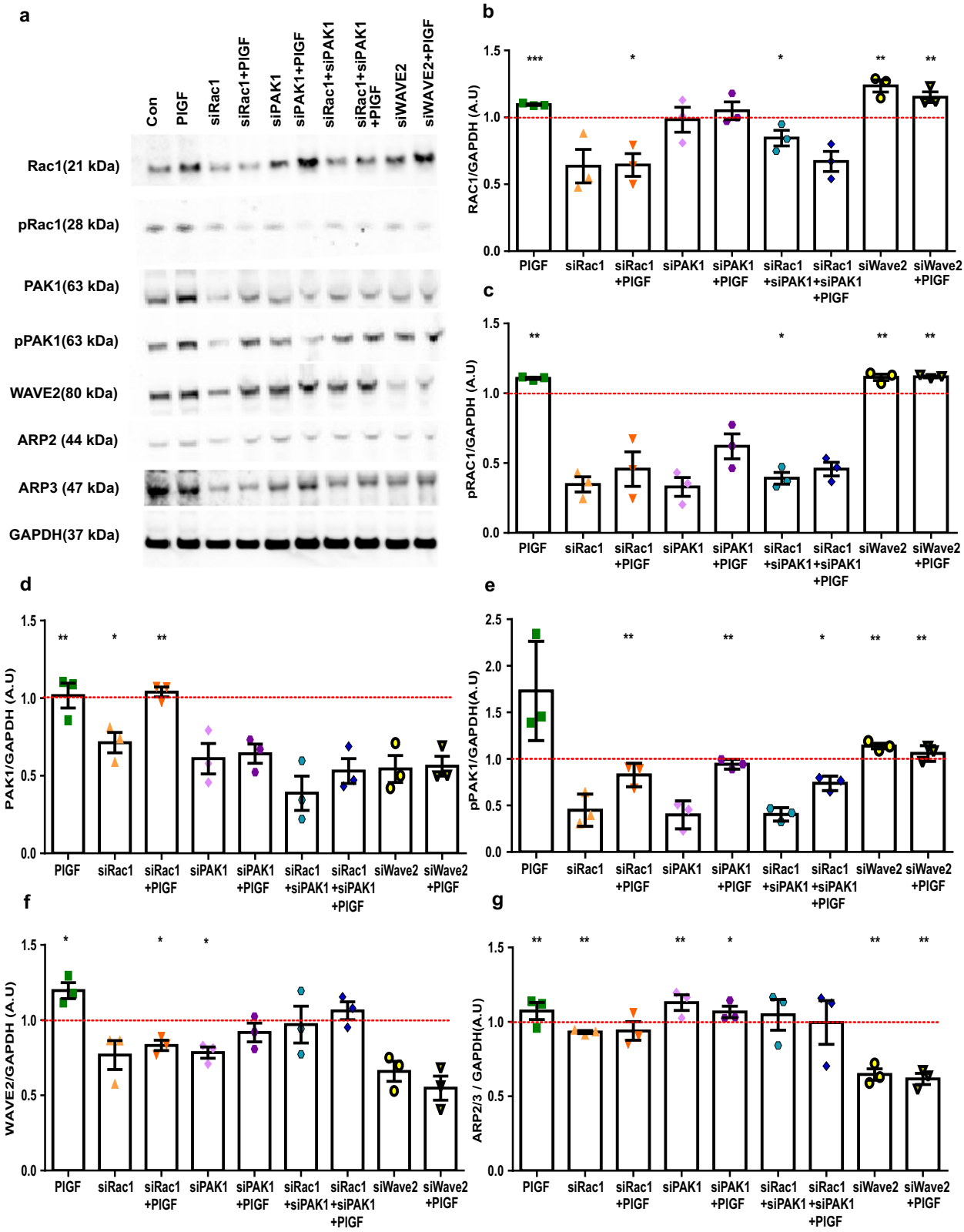

and thus, statins can inhibit the isoprenylation of cytoskeletal regulator Rac1[57]. Studies also support a potential link between statins and actin modulation[58–61]. Statins are reported to affect the rearrangement of F-actin with a regulatory effect on cofilin, an actin-binding protein involved in the control of cell shape and motility[60]. Similarly, pravastatin and simvastatin are known to downregulate pY14-caveolin, which indicates a loss of actin interactions[58]. Recently, Sarkar et al. reported that lovastatin induces significant polymerization of the actin cytoskeleton in regulating the dynamics of the serotonin1A receptor[59]. Thus, playing a major role in the modulation of cognitive and behavioural functions[59]. In our study, we report an inhibitory effect of pravastatin on Rac1 activation, reverting actin polymerization to normal levels and improving

Fig. 4 | Effect of siRNA on PlGF-activated Rac1-PAK1 signaling cascade in EnSCs. a Original western blots of total and phosphorylated levels of Rac1, pRac1, PAK1and pPAK1, WAVE2, and ARP2/3 targets with GAPDH as loading control. **b** Arithmetic means ± SEM of protein levels of total Rac1 in siRNA Rac1/PAK1/WAVE2 or in combination with and without PlGF treatment ($n = 3$, $^{*}p < 0.05$, $^{**}p < 0.01$, $^{***}p < 0.001$). **c** Arithmetic means ± SEM of protein levels of phosphorylated Rac1 in siRNA Rac1/PAK1/WAVE2 or in combination with and without PlGF treatment ($n = 3$, $^{*}p < 0.05$, $^{**}p < 0.01$). **d** Arithmetic means ± SEM of protein levels of total PAK1 in siRNA Rac1/PAK1/WAVE2 or in combination with and without PlGF treatment ($n = 3$, $^{*}p < 0.05$, $^{**}p < 0.01$). **e** Arithmetic means ± SEM of protein levels of phosphorylated PAK1 in siRNA Rac1/PAK1/WAVE2 or in combination with and without PlGF treatment ($n = 3$, $^{*}p < 0.05$, $^{**}p < 0.01$). **f** Arithmetic means ± SEM of protein levels of WAVE2 in siRNA Rac1/PAK1/WAVE2 or in combination with and without PlGF treatment ($n = 3$, $^{*}p < 0.05$). **g** Arithmetic means ± SEM of protein levels of ARP2 over ARP3 ratio in siRNA Rac1/PAK1/WAVE2 or in combination with and without PlGF treatment ($n = 3$, $^{*}p < 0.05$, $^{**}p < 0.01$). All the above data represented here is normalized to control cells. The control is represented as red dotted lines in the graphs. The statistical significance was tested between control and treated samples with an Unpaired t-test with Welch's correction.

trophoblast cell invasion through EnSCs monolayer. Additionally, our proteomic analysis confirms this inhibitory action of pravastatin on PlGF-treated EnSCs, with downregulating a few actin-regulating targets, ECM modulating proteins, and reversing GTPases activity. Thereby, we postulate that pravastatin could be a potential pharmacological candidate to reverse altered Rac1 signaling and further could potentially reduce decidual cell stiffness, allowing proper EVT invasion into the maternal microenvironment, thus preventing shallow placentation which is the main driver of PE.

However, given the non-cholesterol pleiotropic effects of statins such as reduction of inflammatory mediators, inhibiting the T-helper cell immune responses or nitric oxide synthases[62,63], which in turn may impact on decidualisation and pregnancy itself, well-planned research is required to validate its use in humans. Despite that, these studies demonstrate the equipoise necessary to approve a trial of prophylactic pravastatin either prior to pregnancy and/or in early pregnancy to prevent PE.

In conclusion, this study highlights an underlying transcriptomic defect of cytoskeletal-actin dynamics (using publicly available data sets) that may explain the maternal role of shallow or impaired placentation seen in PE. The present study further describes a previously uncharacterised function of PlGF in upregulating the expression and activity of the small G-protein Rac1 and of the kinase PAK1 with subsequent actin polymerization as well as the increase of cell stiffness. Our work is an important step towards the development of novel approaches that facilitate an early evaluation of the risk for PE and to treat this detrimental disease. Thus, this unique role of PlGF may provide avenues to pursue new therapeutic agents or non-invasive strategies capable of curtailing pregnancy disorders such as PE.

Methods

Cell lines

Human EnSCs (#T0533, Applied Biological Materials Inc)[23,64,65] were cultured at 37 °C in a humidified 5% CO_2 atmosphere in DMEM/F-12 medium (#11039-021, Invitrogen) containing 10% (v/v) dextran-coated charcoal striped (#C6241, Sigma) fetal bovine serum (#10270-106, Invitrogen). Human BeWo cells (#86082803, Sigma)[66,67], a human trophoblast cell line, were cultured in DMEM/F-12 medium (#11039-021, Invitrogen) containing 10% (v/v) fetal bovine serum (#10270-106, Invitrogen).

Cell culture treatment and transfection

EnSCs were subjected to treatment with PlGF (#P1588, Sigma) at a concentration of 20 ng/ml for 6 days[68]. For decidualization, EnSCs were treated with 0.5 µM 8-Bromoadenosine-3',5'-cyclic monophosphate sodium salt (cAMP) (#1140, Tocris) and 1 µM Medroxyprogesterone 17-acetate (MPA) (#M6013, Sigma) for 6 days[69]. The cell culture medium was replaced every 48 h with fresh treatment media. The experimental groups are indicated as control (untreated EnSCs), PlGF, cAMP+MPA, and cAMP+MPA+ PlGF.

Where indicated, EnSCs were treated with pravastatin (Pravastatin sodium salt hydrate, #P4498, Sigma) with or without PlGF treatment at 10 µM for 24 h[70]. The experimental groups are classified as control (untreated EnSCs), PlGF, pravastatin (Prav), and pravastatin + PlGF (Prav + PlGF). Epidermal Growth factor (EGF) was used as a positive control for Rac1 activation. (#324831, Sigma) at a concentration of 100 ng/ml for 24 h[71].

For gene silencing, EnSCs were treated with siRNAs[72], such as siRac1 (50 nM, #L-003560-00-0010, Dharmacon), siPAK1 (20 µM, #L-003521-00-0010, Dharmacon), and siWAVE2 (5 nM, #s55787, ThermoFisher Scientific). The siRNAs were transfected with Lipofectamine RNAiMAX (#13778075, ThermoFisher Scientific) for 48 h with and without combination with PlGF treatment.

Preparation of cell lysate for proteomic analysis

For proteome analyses, cell suspensions were prepared from EnSCs treated with and without PlGF(20 ng/ml for 6 days). Cells were lysed by adding lysis buffer [5% 1 M Tris/HCl pH 7,4, 2% 5 M NaCl, 1% Triton X 100, 1% PMSF, 4% protease inhibitor cocktail (Sigma-Aldrich, St. Louis, USA)] on ice. Ten micrograms of each sample were digested in solution with trypsin. After desalting using C18 stage tips, extracted peptides were separated on an Easy-nLC 1200 system coupled to a Q Exactive HFX mass spectrometer (Thermo Fisher Scientific). The peptide mixtures were separated using a 90 minutes segmented gradient from 10-33-50-90% of HPLC solvent B (80% acetonitrile in 0.1% formic acid) in HPLC solvent A (0.1% formic acid) at a flow rate of 200 nl/min. The 12 most intense precursor ions were sequentially fragmented in each scan cycle using higher energy collisional dissociation (HCD) fragmentation. Acquired MS spectra were processed with MaxQuant software package version 1.6.7.0 with integrated Andromeda search engine[73] Database search was performed against a target-decoy Homo sapiens database obtained from Uniprot, containing 103.859 protein entries and 286 commonly observed contaminants. Peptide, protein, and modification site identifications were reported at a false discovery rate (FDR) of 0.01, estimated by the target/decoy approach. The LFQ (Label-Free Quantification) algorithm was enabled, as well as match between runs and LFQ protein intensities was used for relative protein quantification. Data analysis was performed using Perseus[74] and STRING v11 database.

Quantitative Real-time PCR (qRT-PCR)

Total RNA was extracted from EnSCs cultures using Trizol (#15596026, Invitrogen) based on a phenol-chloroform extraction approach. Equal amounts of total RNA (1 µg) were reverse transcribed by using the Maxima h Minus method (#M1681, ThermoFisher Scientific), and the resulting cDNA was used as a template in qRT-PCR analysis. The gene-specific primer pairs were designed using the Primerblast (NCBI) software and purchased from Sigma. Detection of gene expression was performed using the PowerUp SYBR Green Master Mix (#A25742, ThermoFisher Scientific), and quantitative RT-PCR was performed on a QuantStudio 3 Real-Time PCR system (#A28567, ThermoFisher Scientific). L19 was used to normalize variances in input cDNA. The expression levels of the samples are given as arbitrary units defined by the $^{\Delta\Delta}$Ct method. All measurements were performed in triplicate. Melting curve analysis confirmed the amplification specificity of the genes. Sequences of human primers used for qRT-PCR are available on request.

Western Blotting

Whole cell protein lysates were extracted from EnSCs using hot 1X Laemmli buffer (final concentration) with a cell scraper post treatment[23]. Protein

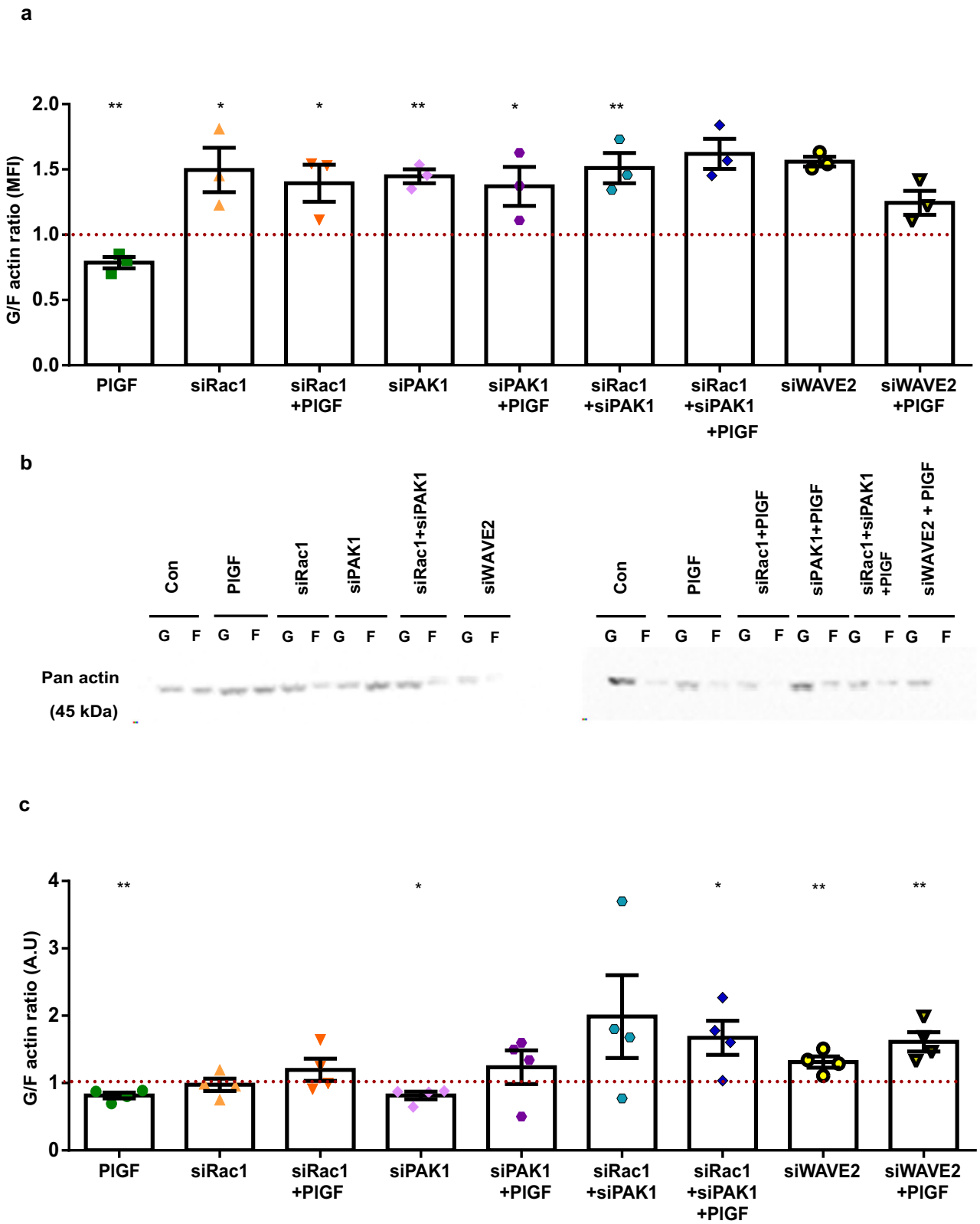

Fig. 5 | Effect of PlGF on endometrial actin dynamics under the influence of siRac1 siPAK1 and siWAVE2. a Arithmetic means ± SEM of G-actin over F-actin ratio in stromal cells after 6 days treatment with PlGF ± siRNAs transfections ($n = 3$, $^{*}p < 0.05$, $^{**}p < 0.01$). **b** Representative original western blot of soluble G-actin and filamentous F-actin in human endometrial stromal cells after 6 days of treatment with PlGF ± siRNAs transfections. **c** Arithmetic means ± SEM of G-actin over F-actin ratio in stromal cells after 6 days treatment with PlGF ± siRNAs transfections ($n = 4$, $^{*}p < 0.05$ $^{**}p < 0.01$). All the above data represented here is normalized to control cells. The control is represented as dotted lines in the graphs. The statistical significance was tested with an Unpaired t-test with Welch's correction.

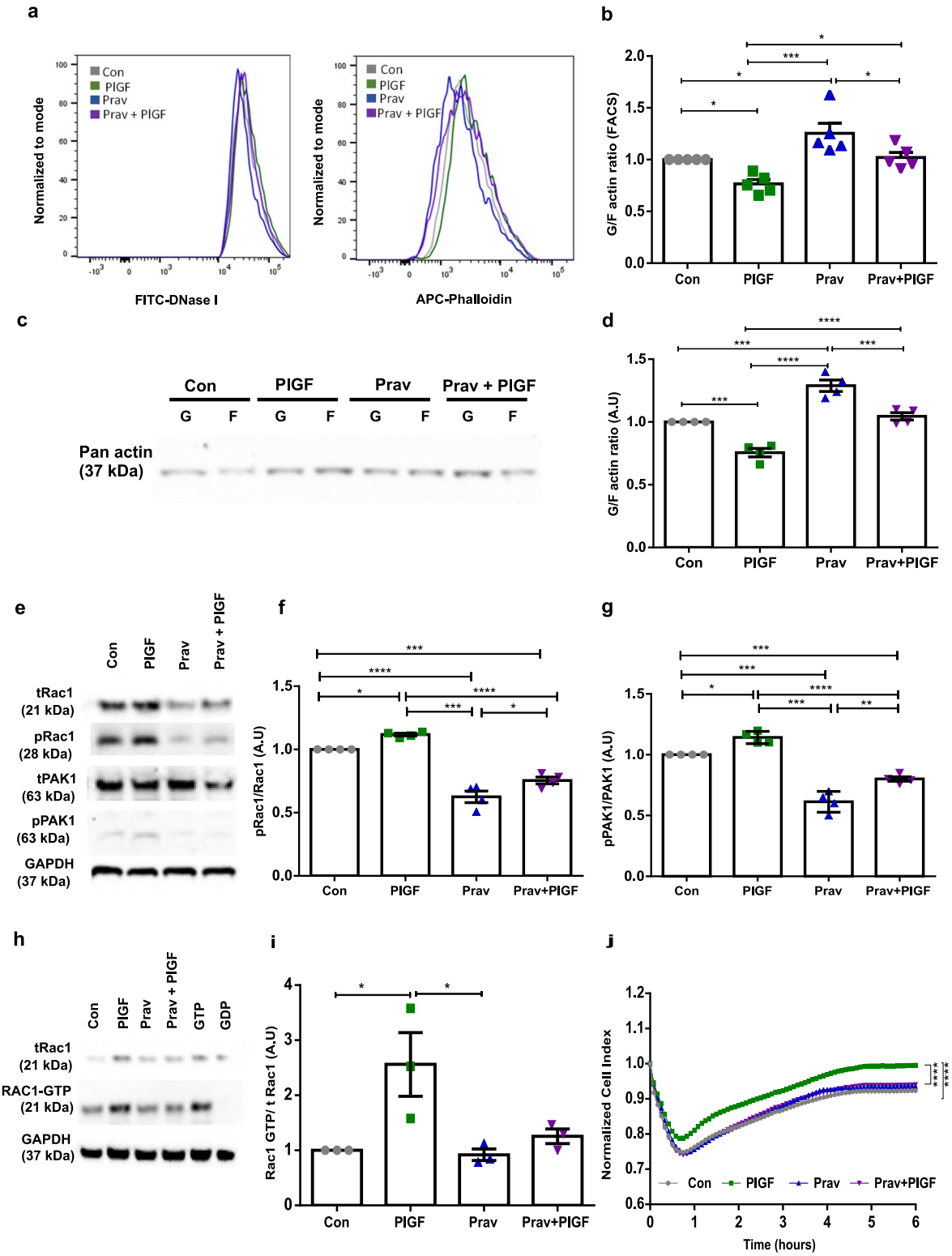

lysates were then loaded onto 4-12% Bis tris mini protein gels (#NW04120BOX, ThermoFisher Scientific) using the XCell SureLock® Mini-Cell apparatus (Invitrogen) followed by electrophoresis. The protein from the gel was then transferred onto a nitrocellulose membrane (#GE10600003, Amersham Biosciences) using a semi-dry transfer approach. After incubation with 5% non-fat milk in TBS-T (10 mM Tris, pH 8.0, 150 mM NaCl, 0.5% Tween 20) for 60 min, the membrane was washed twice with TBS-T and incubated with primary antibodies against Rac1 (1:1000, #2465 s, Cell Signaling Technology), phospho Rac1 (1:500, #2461 S, Cell Signaling Technology), PAK1 (1:500, 51137-1-AP, Protein Tech), phospho PAK1 (1:1000, #2601, Cell Signaling Technology), WAVE2 (1:1000,#3659 s, Cell Signaling Technology), ARP2 (1:1000, #3128 s, Cell

Fig. 6 | Pharmacological inhibition of PlGF-induced Rac1 activation with pravastatin. a Representative original histogram of DNaseI (G-actin; Left) and Phalloidin (F-actin; Right) binding in EnSCs after 6 days of treatment with PlGF ± pravastatin (10 mM, 24 h). **b** Arithmetic mean ± SEM of G-actin over F-actin ratio in EnSCs after 6 days treatment with PlGF ± pravastatin (24 h) ($n = 5$, $^{*}p < 0.05$, $^{***}p < 0.001$). **c** Representative original western blot of soluble G-actin over filamentous F-actin in human EnSCs after 6 days treatment with PlGF ± pravastatin (24 h). **d** Arithmetic mean ± SEM of G-actin and F-actin ratio in stromal cells after 6 days treatment with PlGF ± pravastatin (24 h) ($n = 4$, $^{***}p < 0.001$, $^{****}p < 0.0001$). **e** Original western blots of total and phosphorylated levels of Rac1 and PAK1 targets with GAPDH used as loading control. **f** Arithmetic mean ± SEM of protein ratio of phosphorylated Rac1/ total Rac1 in total lysate of endometrial stromal cells treated with PlGF± pravastatin (24 h) ($n = 5$, $^{*}p < 0.05$, $^{***}p < 0.001$, $^{****}p < 0.0001$). **g** Arithmetic mean ± SEM of *p*rotein ratio of phosphorylated PAK1/total PAK1 protein levels in total lysate of endometrial stromal cells treated with PlGF± pravastatin (24 h) ($n = 5$, $^{*}p < 0.05$, $^{**}p < 0.01$, $^{***}p < 0.001$, $^{****}p < 0.0001$). **h** Original western blots of total Rac1, Rac1 GTP, and GAPDH from Rac1 pull-down assay. **i** Arithmetic mean ± SEM of protein levels of activated form of Rac1 as Rac1GTP normalised to total Rac1in total lysate of endometrial stromal cells treated with PlGF± pravastatin (24 h) ($n = 3$, $^{*}p < 0.05$). All the above data represented here is normalized to control cells. The statistical significance was tested with an Unpaired *t*-test with Welch's correction. **j** Normalized cell index values of EnSCs monolayer to BeWo addition time point, cell index refers to the resistance in EnSCs layer post BeWo invasion for 6 h. EnSCs were under 6 days of treatment with PlGF ± pravastatin (24 h) ($n = 3$, $^{****}p < 0.0001$). The statistical significance for EIS analysis was tested at 5 h when the impedance was almost reaching a threshold, with an Unpaired *t*-test with Welch's correction.

Signaling Technology), ARP3 (1:1000,#4738 s, Cell Signaling Technology) or GAPDH (1:1000, #5174, Cell Signaling Technology) at 4 °C for overnight. The concentrations of the antibodies employed in the study are as per the manufacturer's instructions.

Post overnight incubation with primary antibodies, membranes were washed with TBS-T and incubated with HRP-conjugated anti-rabbit secondary (1:2000, #7074 s, Cell Signaling Technology) antibody for 1 h in room temperature. Post-secondary antibody incubation, blots were washed with TBS-T and developed with the ECL system (#R-03031-D25, Advansta) according to the manufacturer's protocols. The fluorescence signals were obtained with an iBright CL1000 (ThermoFisher Scientific), and the intensities were assessed by a densitometry analysis to measure the relative expression of the target proteins using GAPDH as a control by ImageJ software.

Active Rac1 pull-down assay

Rac1 pull down assays were performed using a Rac1 Activity Assay kit (#16118, ThermoFisher Scientific) to monitor Rac1 small GTPase activation as per manufacturer instruction.

Measurement of the G/F actin ratio by Triton X-100 fractionation

To quantify the effect of PlGF on actin polymerization in EnSCs, cells were incubated with actin extraction buffer and processed for G and F-actin protein lysates[22]. Bradford assay was performed to obtain protein concentration and equal volumes of each fraction were boiled with 1X Lamelli Buffer at 95 °C for 15 min. Proteins were separated on 10% SDS-polyacrylamide gels and transferred to PVDF membranes (#GE10600029, Amersham Biosciences). Non-specific binding sites were blocked by 1 h incubation at room temperature with 5% non-fat dry milk in TBS-T. The membranes were incubated overnight at 4 °C with primary antibodies against Pan-actin rabbit monoclonal antibodies (1:1000, #D18C11, Cell Signaling Technology). Post incubation with primary antibody, membranes were washed with TBS-T and incubated with HRP-conjugated anti-rabbit secondary (1:2000, #7074 s, Cell Signaling Technology) antibodies for 1 hour in room temperature. Antibody binding was detected post-developing with the ECL system (#R-03031-D25, Advansta) according to the manufacturer's protocols. The fluorescence signals were obtained with an iBright CL1000 (ThermoFisher Scientific), and the intensities were assessed by a densitometry analysis to measure the relative expression of the pan- actin by ImageJ software.

G/F actin ratio by Flow cytometry

To study the influence of PlGF treatment on G/F action ratio with flow cytometry, post treatment with PlGF (20 ng/ml for 6 days), EnSCs (≈1.0×10^5 cells) were first fixed with 4% paraformaldehyde (PFA) and then permeabilised with 1x Permeabilization buffer (#00-8333-56, eBioscience) and subsequently stained with 10 µl of fluorescent DNAse1-Alexaflour-488 (#D12371, Thermofisher Scientific) (5 mg/ml) for detection of G-actin and 1 µl fluorescent Phalloidin-eFluor® 660 (1000x) (1:1000, #50655905, Thermofisher Scientific) for detection of F-actin. The quantitative measure of the respective fluorescent labels was measured using green (FL-1) and red channel (FL-4) on a BD LSRFortessa™ Cell Analyzer (BD Biosciences) and the analysis was performed using Flowjo software (Flowjo LLC, USA). The ratio of G/F is calculated from the geometric mean values.

Immunofluorescence

For immunolabelling of cells, EnSCs (5000 cells) were seeded on glass chamber slides (#94.6170.402, Sarstedt) and cultured in 10% DCC FBS containing DMEM medium. Post treatment with PlGF (20 ng/ml for 6 days) in 2% DCC FBS medium, the cells were fixed with 4% paraformaldehyde for 15 min, washed with PBS, and permeabilized for 15 min in 0.1% Triton X-100/PBS. The samples were then blocked with 5% BSA in 0.1% TritonX-100/PBS for 1 h at RT and washed with PBS. The cells were then stained for F-actin with eflour 660-phalloidin (1:1000, #50655905, ThermoFisher Scientific) for 30 min at RT. Post incubation, slides were washed again with PBS, dehydrated, air-dried, and mounted using ProLong Gold antifade reagent containing DAPI (#P36931, Invitrogen). Fluorescence was detected with LSM 800 confocal laser scanning microscope (Zeiss). The images were captured using oil immersion, 40x objective lens. Scale bar - 20 µm. Mean fluorescence intensities were calculated using ImageJ software.

Atomic force microscopy (AFM)

AFM experiments on live EnSCs were carried out with a commercial AFM setup (MFP3D, Asylum Research, Santa Barbara, USA) with cells seeded on culture dishes at a density of $5{\times}10^4$ cells/cm². EnSCs were treated with either 20 ng/ml PlGF, decidualization treatment (cAMP+MPA), or 100 ng/ml EGF as a positive control for 6 days or 24 h, respectively, in a 2% DCC FBS treatment medium.

Additionally, AFM measurements were performed on cells seeded onto a polydimethylsiloxane (PDMS) substrate as described in Kenry et al.,[75](CY52-276, Dow Corning, Toray, Japan). The two components, A and B, were mixed for 15 min at a weight ratio of 6:5. The mixture was then degassed in a vacuum chamber, poured into Petri dishes, and cured in an oven at 80 °C for 12 h, to yield soft substrates with a bulk elastic modulus of 1–3 kPa[75]. EnSCs were seeded on these soft substrates at a density of $2{\times}10^4$ cells/cm² and were subjected to PlGF or/and decidualization treatment as described above.

Single EnSCs were imaged with AFM in the force mapping mode. To study cell stiffness, maps of 10×10 force indentation curves were recorded on a 5 × 5 µm² scan area on the central region of cells using a pyramidal tip (Bio-MLCT, cantilever C, spring constant 0.01 N/m, side angle 35°, Bruker AXS S.A.S., Champs-sur-Marne, France). The maximum deflection was set to 100 nm, resulting in an indentation depth of typically 400–600 nm, which is much smaller than the cell height, thereby an influence of the underlying stiff substrate on the measured Young's modulus was avoided[76]. Additionally, to display the whole cell body, we performed maps of 30 × 30 or 50 × 50 force indentation curves on an 80 × 80 µm² or 90×90 µm² scan area. Force-indentation curves were fitted with

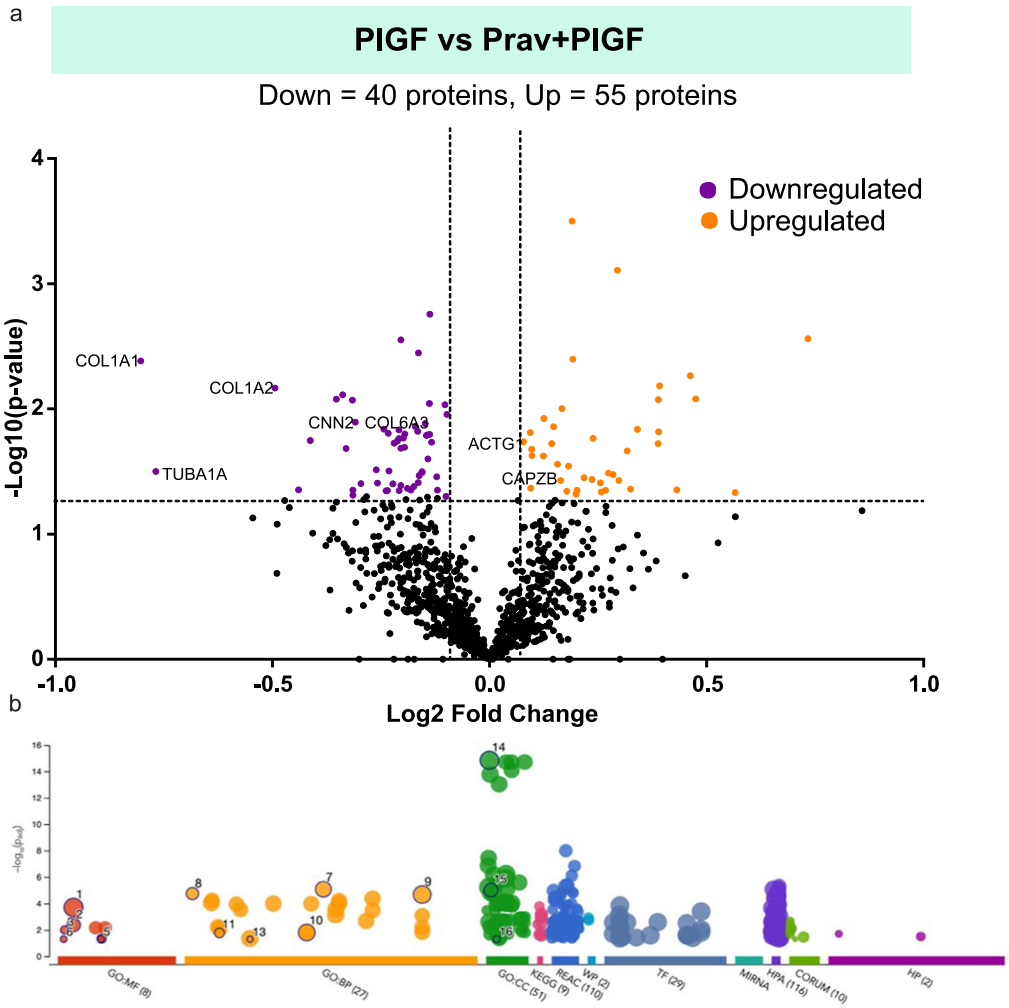

ID	Source	Term ID	Term Name	p_{adj} (query_1)
1	GO:MF	GO:0005515	Protein binding	$1.995x10^{-4}$
2	GO:MF	GO:0005525	GTP binding	$4.116x10^{-3}$
3	GO:MF	GO:0004298	Threonine-type endopeptidase activity	$1.025x10^{-2}$
4	GO:MF	GO:0031489	Myosin V binding	$4.674x10^{-2}$
5	GO:MF	GO:0030942	Endoplasmic reticulum signal peptide binding	$4.995x10^{-2}$
6	GO:MF	GO:0004069	L-aspartate:2-oxoglutarate aminotransferase a...	$4.995x10^{-2}$
7	GO:BP	GO:0046907	Intracellular transport	$8.253x10^{-6}$
8	GO:BP	GO:0002181	Cytoplasmic translation	$1.734x10^{-5}$
9	GO:BP	GO:1901564	Organonitrogen compound metabolic process	$2.072x10^{-5}$
10	GO:BP	GO:0044260	Cellular macromolecule metabolic process	$1.581x10^{-2}$
11	GO:BP	GO:0009065	Glutamine family amino acid catabolic process	$1.702x10^{-2}$
12	GO:BP	GO:0019551	Glutamate catabolic process to 2-oxoglutarate	$4.979x10^{-2}$
13	GO:BP	GO:0019550	Glutamate catabolic process to aspartate	$4.979x10^{-2}$
14	GO:CC	GO:0005737	cytoplasm	$1.434x10^{-15}$
15	GO:CC	GO:0005925	Focal adhesion	$9.550x10^{-6}$
16	GO:CC	GO:0030905	Retromer, tubulation complex	$4.995x10^{-2}$

Fig. 7 | Mass spectroscopy analysis for the effect of pravastatin on PlGF-induced protein machinery. a Volcano plot showing upregulated (orange) and down-regulated (violet) proteins in PlGF + pravastatin (n = 3) treated EnSCs compared to PlGF treatment ($n = 3$). Each point represents one protein; black points are the rest of the proteins obtained in the global proteomic analysis. The significance threshold range is 0.05 and the fold change threshold is -1 and +1. **b** Gene Ontology analysis of the protein signature associated with PlGF + pravastatin treatment in EnSCs shows enriched biological processes.

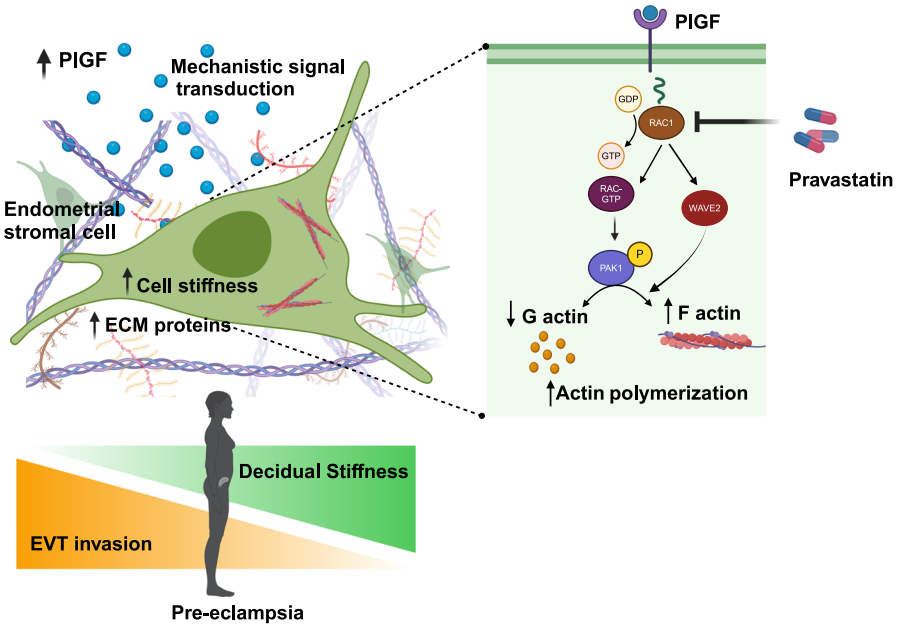

Fig. 8 | Graphical abstract describing the effect of pathological PlGF levels in altered endometrial cytoskeletal dynamics. Excessive endometrial PlGF promotes Rac1 activity by modulating Rac1-GDP conversion to Rac1-GTP in EnSCs. Rac1 activation upregulates its downstream targets PAK1 and WAVE2, leading to alterations in G and F-actin organisation and turn over with an effect on an increase in cell stiffness. High levels of PlGF also alter the cell's microenvironment with an increase in ECM-associated proteins altering endometrial biomechanics at a global cellular level. Dysregulation of endometrial/decidual mechanobiology with an increase in cell and ECM stiffness will impede EVT invasion during early pregnancy, leading to shallow placentation as seen in pre-eclampsia. Excessive PlGF-induced cell stiffness dysregulation in the endometrium could be pharmacologically reversed with a potential therapeutic target, pravastatin. The figure was created using BioRender.

the pyramidal Sneddon model[77] to calculate the Young´s modulus, E. Data were analysed with the data analysis package Igor Pro (Wavemetrics, Lake Oswego, OR, USA). The mean value of all Young´s modulus values on a cell was considered representative of that cell.

Electrical Impedance spectroscopy (EIS)

The invasion of BeWo through the stromal monolayer was studied with EIS measurements. The E-16 plates were coated with 0.1% gelatin and let to incubate for an hour at 37 °C. Next, 100 µl of 2% DCC FBS DMEM was added to E16 plate for background measurement. The plate was mounted onto the xCELLigence RTCA (Agilent, Germany) for background reading. Later, EnSCs were trypsinized and 3000 cells per well were added to the E16 plates and kept for incubation at 37 °C for cells to equilibrate and adhere. Post 24 h, the cells were treated with respective treatment conditions (Con/PlGF/Prav/Prav+PlGF) as mentioned above for 6 days. Ten hours prior treatment endpoint, E16 plates containing cells were clamped again onto the xCELLigence RTCA and placed in the incubator at 37 °C. Live cell impedance was monitored every 15 min for a total period of 10 h to ensure stromal cell monolayer formation.

Post treatment time point, the cell index measurement was paused and 2500 BeWo cells per 100 µl of 10% FBS DMEM were added. EIS cell index measurement was continued to monitor to the BeWo invasion through EnSCs monolayer. Live cell impedance was monitored every 5 min for a total period of 6 hours. Data is represented as normalized cell index relative to the time point BeWo cells were added to the EnSCs monolayer. Data acquisition and data analysis was performed using RTCA Software Pro (Agilent, Germany).

Wound healing scratch assay

EnSCs were seeded in a six-well plate at a concentration of 200×10^3 cells per well. After reaching 100% confluency, the wells were scratched in the centre vertically with a 200 µL tip to create a wound area. Cells were treated with either PlGF (20 ng/ml) for 6 days or/and thymidine (2 mm; #T1895, Sigma) for 42 h or remained untreated. Pictures were then taken immediately at 0 h using the EVOS M7000 cell imaging system (ThermoFisher Scientific) at an objective 4X. The cells were then allowed to incubate at 37 °C in a humidified 5% CO_2 atmosphere with the treatment medium for the next 24 h. Post incubation, cell migration was monitored by taking pictures at 24 h. Assessment of percentage of wound healing was quantified using the ImageJ software and presented as fold change.

BrdU cell proliferation assay

The effect of PlGF on EnSCs proliferation was measured using BrdU cell proliferation assay (#QIA58, Sigma). Briefly after the treatment of EnSCs with PlGF (20 ng/ml) for 6 days or/and thymidine (2 mm; #T1895, Sigma) for 42 h, cells were immunolabelled for BrdU and incubated for an additional 24 h. Incorporated BrdU was detected by the BrdU Cell Proliferation Assay as instructed in the manufacture protocol.

In silico data analysis

In silico analysis was performed on open-access gene-expression data. To study the kinetics of PlGF expression levels across the menstrual cycle, we obtained analysis of the normal endometrium at distinct phases of the menstrual cycle (*GDS2052*). To investigate PlGF and PAK1 mRNA levels in term preeclampsia, we obtained PAK1 gene activity data in human decidua of preeclamptic women and healthy pregnant women (*GDS2548*). Lastly, to understand the maternal influence on PE pathogenesis, transcriptomic profiling of decidua from previous healthy and preeclamptic pregnancies were studied (*GSE172381*).

Statistics and Reproducibility

Data are provided as means ± SEM, and n represents the number of independent experiments. Data provided here were tested for significance using student's unpaired two-tailed t-test with Welch's correction approach and nonparametric Mann-Whitney U test methods. PlGF treated samples were normalized to the control. Results with $p < 0.05$ were considered statistically significant. Figures and statistical analysis were made in Graphpad Prism (USA) or with R.

Reporting summary

Further information on research design is available in the Nature Portfolio Reporting Summary linked to this article.

Data availability

Proteomics data have been submitted to the PRoteomics IDEntification database (PRIDE) with accession number PXD050237. The source data behind the graphs in the figures can be found in Supplementary data 2, the uncropped, original Western blots are shown in Supplementary Fig. S12.

Received: 26 April 2023; Accepted: 19 April 2024;
Published online: 04 May 2024

References

1. Ng, S.-W. et al. Endometrial decidualization: the primary driver of pregnancy health. *Int J. Mol. Sci.* **21**, 4092 (2020).
2. Tong, J. et al. Decidualization and related pregnancy complications. *Maternal Fetal Med.* **4**, 24–35 (2022).
3. Garrido-Gomez, T. et al. Preeclampsia: a defect in decidualization is associated with deficiency of Annexin A2. *Am. J. Obstet. Gynecol.* **222**, 376.e371–376.e317 (2020).
4. Garrido-Gomez, T. et al. Defective decidualization during and after severe preeclampsia reveals a possible maternal contribution to the etiology. *Proc. Natl Acad. Sci. USA* **114**, E8468–e8477 (2017).
5. El-Azzamy, H. et al. Dysregulated uterine natural killer cells and vascular remodeling in women with recurrent pregnancy losses. *Am. J. Reprod. Immunol.* **80**, e13024 (2018).
6. Zhang, X. & Wei, H. Role of decidual natural killer cells in human pregnancy and related pregnancy complications. *Front. Immunol.* **12**, 728291 (2021).
7. Sun, F., Wang, S. & Du, M. Functional regulation of decidual macrophages during pregnancy. *J. Reprod. Immunol.* **143**, 103264 (2021).
8. Garrido-Gomez, T. et al. Disrupted PGR-B and ESR1 signaling underlies defective decidualization linked to severe preeclampsia. *Elife* **10**, e70753 (2021).
9. Dewerchin, M. & Carmeliet, P. PlGF: a multitasking cytokine with disease-restricted activity. *Cold Spring Harb. Perspect. Med* **2**, a011056 (2012).
10. De Falco, S. The discovery of placenta growth factor and its biological activity. *Exp. Mol. Med.* **44**, 1–9 (2012).
11. Aoki, S. et al. Placental growth factor promotes tumour desmoplasia and treatment resistance in intrahepatic cholangiocarcinoma. *Gut* **71**, 185 (2022).
12. Nguyen, Q. D. et al. Placental growth factor and its potential role in diabetic retinopathy and other ocular neovascular diseases. *Acta Ophthalmol.* **96**, e1–e9 (2018).
13. Chau, K., Hennessy, A. & Makris, A. Placental growth factor and pre-eclampsia. *J. Hum. Hypertens.* **31**, 782–786 (2017).
14. Nejabati, H. R., Latifi, Z., Ghasemnejad, T., Fattahi, A. & Nouri, M. Placental growth factor (PlGF) as an angiogenic/inflammatory switcher: lesson from early pregnancy losses. *Gynecol. Endocrinol.* **33**, 668–674 (2017).
15. Binder, N. K. et al. Placental growth factor is secreted by the human endometrium and has potential important functions during embryo development and implantation. *PLOS ONE* **11**, e0163096 (2016).
16. Taylor, A. P., Leon, E. & Goldenberg, D. M. Placental growth factor (PlGF) enhances breast cancer cell motility by mobilising ERK1/2 phosphorylation and cytoskeletal rearrangement. *Br. J. Cancer* **103**, 82–89 (2010).
17. Kang, M. et al. Placental growth factor (PlGF) is linked to inflammation and metabolic disorders in mice with diet-induced obesity. *Endocr. J.* **65**, 437–447 (2018).
18. Nikuei, P. et al. Diagnostic accuracy of sFlt1/PlGF ratio as a marker for preeclampsia. *BMC Pregnancy Childbirth* **20**, 80 (2020).
19. Sit, S.-T. & Manser, E. Rho GTPases and their role in organizing the actin cytoskeleton. *J. Cell Sci.* **124**, 679–683 (2011).
20. Shin, Y. J., Kim, E. H., Roy, A. & Kim, J.-H. Evidence for a novel mechanism of the PAK1 interaction with the Rho-GTPases Cdc42 and Rac. *PLOS ONE* **8**, e71495 (2013).
21. Gomez, T. M. & Letourneau, P. C. Actin dynamics in growth cone motility and navigation. *J. Neurochem.* **129**, 221–234 (2014).
22. Salker, M. S. et al. LeftyA decreases Actin polymerization and stiffness in human endometrial cancer cells. *Sci. Rep.* **6**, 29370 (2016).
23. Alauddin, M. et al. Gut bacterial metabolite urolithin a decreases actin polymerization and migration in cancer cells. *Mol. Nutr. Food Res.* **64**, 1900390 (2020).
24. Grewal, S., Carver, J. G., Ridley, J. & Mardon, J. Implantation of the human embryo requires Rac1-dependent endometrial stromal cell migration. *Proc. Natl Acad. Sci.* **105**, 16189–16194 (2008).
25. Davila, J. et al. Rac1 regulates endometrial secretory function to control placental development. *PLoS Genet* **11**, e1005458–e1005458 (2015).
26. Tu, Z. et al. Uterine RAC1 via Pak1-ERM signaling directs normal luminal epithelial integrity conducive to on-time embryo implantation in mice. *Cell Death Differ.* **23**, 169–181 (2016).
27. Casalou, C., Fragoso, R., Nunes, J. F. M. & Dias, S. VEGF/PLGF induces leukemia cell migration via P38/ERK1/2 kinase pathway, resulting in Rho GTPases activation and caveolae formation. *Leukemia* **21**, 1590–1594 (2007).
28. Agalakova, N. I. et al. Canrenone restores Vasorelaxation impaired by Marinobufagenin in human preeclampsia. *Int J. Mol. Sci.* **23**, 3336 (2022).
29. Kim, S. et al. Longitudinal change in arterial stiffness after delivery in women with preeclampsia and normotension: a prospective cohort study. *BMC Pregnancy Childbirth* **20**, 685–685 (2020).
30. Pollheimer, J., Vondra, S., Baltayeva, J., Beristain, A. G. & Knöfler, M. Regulation of Placental Extravillous Trophoblasts by the maternal uterine environment. *Front Immunol.* **9**, 2597 (2018).
31. Ma, N., Xu, E., Luo, Q. & Song, G. Rac1: A regulator of cell migration and a potential target for cancer therapy. *Molecules* **28**, 2976 (2023).
32. Sang, Y., Li, Y., Xu, L., Li, D. & Du, M. Regulatory mechanisms of endometrial decidualization and pregnancy-related diseases. *Acta Biochim. et. Biophys. Sin.* **52**, 105–115 (2020).
33. Rana, S., Lemoine, E., Granger, J. P. & Karumanchi, S. A. Preeclampsia. *Circ. Res.* **124**, 1094–1112 (2019).
34. Roberts, J. M. et al. Subtypes of Preeclampsia: Recognition and determining clinical usefulness. *Hypertension* **77**, 1430–1441 (2021).
35. Jena, M. K., Sharma, N. R., Petitt, M., Maulik, D. & Nayak, N. R. Pathogenesis of Preeclampsia and therapeutic approaches targeting the placenta. *Biomolecules* **10**, 953 (2020).
36. Tomimatsu, T. et al. Preeclampsia: Maternal systemic vascular disorder caused by generalized endothelial dysfunction due to placental antiangiogenic factors. *Int J. Mol. Sci.* **20**, 4246 (2019).
37. Zeisler, H. et al. Predictive value of the sFlt-1:PlGF ratio in women with suspected Preeclampsia. *N. Engl. J. Med* **374**, 13–22 (2016).
38. Dröge, L. A. et al. Prediction of Preeclampsia-related adverse outcomes with the sFlt-1 (Soluble fms-Like Tyrosine Kinase 1)/PlGF (Placental Growth Factor)-Ratio in the clinical routine: a real-world study. *Hypertension* **77**, 461–471 (2021).
39. Laviv, Y., Wang, J. L., Anderson, M. P. & Kasper, E. M. Accelerated growth of hemangioblastoma in pregnancy: the role of proangiogenic factors and upregulation of hypoxia-inducible factor (HIF) in a non-oxygen-dependent pathway. *Neurosurg. Rev.* **42**, 209–226 (2019).
40. Stepan, H., Hund, M. & Andraczek, T. Combining biomarkers to predict pregnancy complications and redefine Preeclampsia. *Hypertension* **75**, 918–926 (2020).
41. Fionda, C. et al. Cereblon regulates NK cell cytotoxicity and migration via Rac1 activation. *Eur. J. Immunol.* **51**, 2607–2617 (2021).
42. Kunschmann, T. et al. The small GTPase Rac1 increases cell surface stiffness and enhances 3D migration into extracellular matrices. *Sci. Rep.* **9**, 7675 (2019).
43. Zhang, L., Liang, H. & Xin, Y. Cucurbitacin E inhibits esophageal carcinoma cell proliferation, migration, and invasion by suppressing Rac1 expression through PI3K/AKT/mTOR pathway. *Anticancer Drugs* **31**, 847–855 (2020).
44. Yamaguchi, H. & Condeelis, J. Regulation of the actin cytoskeleton in cancer cell migration and invasion. *Biochim. Biophys. Acta* **1773**, 642–652 (2007).
45. Kita, K. et al. Cytoskeletal Actin structure in Osteosarcoma cells determines metastatic phenotype via regulating cell stiffness, migration, and transmigration. *Curr. Issues Mol. Biol.* **43**, 1255–1266 (2021).

46. Vining, K. H. & Mooney, D. J. Mechanical forces direct stem cell behaviour in development and regeneration. *Nat. Rev. Mol. Cell Biol.* **18**, 728–742 (2017).
47. Abbas, Y. et al. Tissue stiffness at the human maternal-fetal interface. *Hum. Reprod.* **34**, 1999–2008 (2019).
48. Hirota, T., Fujita, Y. & Ieiri, I. An updated review of pharmacokinetic drug interactions and pharmacogenetics of statins. *Expert Opin. Drug Metab. Toxicol.* **16**, 809–822 (2020).
49. Bauer, A. J. et al. Pravastatin attenuates hypertension, oxidative stress, and angiogenic imbalance in rat model of placental ischemia-induced hypertension. *Hypertension* **61**, 1103–1110 (2013).
50. Garrett, N. et al. Pravastatin therapy during preeclampsia prevents long-term adverse health effects in mice. *JCI Insight* **3**, e120147 (2018).
51. Döbert, M. et al. Pravastatin Versus Placebo in pregnancies at high risk of term preeclampsia. *Circulation* **144**, 670–679 (2021).
52. Costantine, M. M. et al. A randomized pilot clinical trial of pravastatin versus placebo in pregnant patients at high risk of preeclampsia. *Am. J. Obstet. Gynecol.* **225**, 666.e661–666.e615 (2021).
53. Chang, J.-C. et al. Perinatal outcomes after statin exposure during pregnancy. *JAMA Netw. Open* **4**, e2141321–e2141321 (2021).
54. Karalis, D. G., Hill, A. N., Clifton, S. & Wild, R. A. The risks of statin use in pregnancy: A systematic review. *J. Clin. Lipido.* **10**, 1081–1090 (2016).
55. Abdrabou, A. & Wang, Z. Post-translational modification and subcellular distribution of Rac1: An update. *Cells* **7**, 263 (2018).
56. Scott-Solomon, E. & Kuruvilla, R. Prenylation of Axonally translated Rac1 controls NGF-dependent Axon growth. *Dev. Cell* **53**, 691–705.e697 (2020).
57. Zeiser, R. et al. Regulation of different inflammatory diseases by impacting the mevalonate pathway. *Immunology* **127**, 18–25 (2009).
58. Menter, D. G. et al. Differential effects of pravastatin and simvastatin on the growth of tumor cells from different organ sites. *PLoS One* **6**, e28813 (2011).
59. Sarkar, P. & Chattopadhyay, A. Statin-induced increase in actin polymerization modulates GPCR dynamics and compartmentalization. *Biophys. J.* **122**, 1938–1955 (2023).
60. Lin, L. P., Yu, T. Y., Chang, H. N., Tsai, W. C. & Pang, J. S. Simvastatin downregulates Cofilin and Stathmin to inhibit skeletal muscle cells migration. *Int J. Mol. Sci.* **23**, 2848 (2022).
61. Rodríguez-Expósito, R. L. et al. Statins Induce Actin Cytoskeleton disassembly and an apoptosis-like process in Acanthamoeba spp. *Antibiotics* **11**, 280 (2022).
62. Khan, M. A. Therapeutic implications of statins beyond lipid lowering: In the perspective of their effects on the antigen presentation, T cells and NKT cells. *Int J. Health Sci.* **15**, 1–2 (2021).
63. Satny, M., Hubacek, J. A. & Vrablik, M. Statins and inflammation. *Curr. Atheroscler. Rep.* **23**, 80 (2021).
64. Tang, W., Chen, O., Yao, F. & Cui, L. miR-455 targets FABP4 to protect human endometrial stromal cells from cytotoxicity induced by hydrogen peroxide. *Mol. Med. Rep.* **20**, 4781–4790 (2019).
65. Alauddin, M. et al. Annexin A7 regulates endometrial receptivity. *Front Cell Dev. Biol.* **8**, 770 (2020).
66. Correia Carreira, S., Cartwright, L., Mathiesen, L., Knudsen, L. E. & Saunders, M. Studying placental transfer of highly purified non-dioxin-like PCBs in two models of the placental barrier. *Placenta* **32**, 283–291 (2011).
67. Khare, M., Taylor, A. H., Konje, J. C. & Bell, S. C. Delta9-tetrahydrocannabinol inhibits cytotrophoblast cell proliferation and modulates gene transcription. *Mol. Hum. Reprod.* **12**, 321–333 (2006).
68. Chau, K., Xu, B., Hennessy, A. & Makris, A. Effect of placental growth factor on trophoblast-endothelial cell interactions in vitro. *Reprod. Sci.* **27**, 1285–1292 (2020).
69. Mak, I. Y. et al. Regulated expression of signal transducer and activator of transcription, Stat5, and its enhancement of PRL expression in human endometrial stromal cells in vitro. *J. Clin. Endocrinol. Metab.* **87**, 2581–2588 (2002).
70. Lin, S. J. et al. Pravastatin induces thrombomodulin expression in TNFalpha-treated human aortic endothelial cells by inhibiting Rac1 and Cdc42 translocation and activity. *J. Cell Biochem.* **101**, 642–653 (2007).
71. Itoh, R. E. et al. Phosphorylation and activation of the Rac1 and Cdc42 GEF Asef in A431 cells stimulated by EGF. *J. Cell Sci.* **121**, 2635–2642 (2008).
72. Anderson, E. M. et al. Experimental validation of the importance of seed complement frequency to siRNA specificity. *RNA* **14**, 853–861 (2008).
73. Cox, J. & Mann, M. MaxQuant enables high peptide identification rates, individualized p.p.b.-range mass accuracies and proteome-wide protein quantification. *Nat. Biotechnol.* **26**, 1367–1372 (2008).
74. Tyanova, S. et al. The Perseus computational platform for comprehensive analysis of (prote)omics data. *Nat. Methods* **13**, 731–740 (2016).
75. Kenry, M. C. L., Nai, M. H., Cheong, F. C. & Lim, C. T. Viscoelastic effects of silicone gels at the micro- and nanoscale. *Procedia IUTAM* **12**, 20–30 (2015).
76. Santos, J. A. C., Rebêlo, L. M., Araujo, A. C., Barros, E. B. & de Sousa, J. S. Thickness-corrected model for nanoindentation of thin films with conical indenters. *R. Soc. Chem.* **8**, 4441 (2012).
77. Bilodeau, G. G. Regular pyramid punch problem. *J. Appl. Mech.* **59**, 519–523 (1992).

Acknowledgements

This work was supported by funding to M.S.S by Else Kröner-Fresenius-Stiftung (EKFS), intramural funds of Tübingen University the IZKF, the Athene award by the Federal Ministry of Education and Research (BMBF) and the Baden-Württemberg Ministry of Science as part of the Excellence Strategy of the German Federal and State Governments and by the Margarete von Wrangell (MvW 31-7635.41/118/3) habilitation scholarship co-funded by the Ministry of Science, Research and the arts (MWK) of the state of Baden-Württemberg and by the European Social Funds and the Open Access Publishing Fund of Tübingen University. The work described in this paper was partially conducted in the framework of the Graduate School 2543/1 "Intraoperative Multisensory Tissue Differentiation in Oncology" (project A4) funded by the German Research Foundation (DFG - Deutsche Forschungsgemeinschaft). We also acknowledge the support from the Open Access Publication Fund of the University of Tübingen. We thank Dr. Ana Velic from Proteome Center Tübingen (PCT) for performing the mass spec experiments and Quantitative Biology Centre Tübingen (Qbic) for proteomic data storage. We would like to thank Apl. Prof. Dr. Dorothea Alexander-Friedrich from the Department of Dental Medicine for providing access to the EIS equipment and Ms. Birgit Fehrenbacher from the Department of Dermatology for her kind help on confocal microscopy imaging.

Author contributions

M.S.S. designed the study and wrote the first draft. J.P.R.X, C.R., E.H., and I.N. performed the experiments and analyzed the data. A.K. and Y.S. performed bioinformatic analysis, data analysis, and figure preparation. M.S.S and J.P.R.X edited and drafted the manuscript. M.S.S, T.E.S., F.L, and S.Y.B provided advice, equipment, resources, and funds. All authors of the manuscript have read, edited, and agreed to its content.

Funding

Open Access funding enabled and organized by Projekt DEAL.

Competing interests

The authors declare no competing interests.

Additional information

Supplementary information The online version contains supplementary material available at https://doi.org/10.1038/s42003-024-06220-7.

Correspondence and requests for materials should be addressed to Madhuri S. Salker.

Peer review information *Communications Biology* thanks Lusine Aghajanova and the other, anonymous, reviewer(s) for their contribution to the peer review of this work. Primary Handling Editors: X Frank Zhang and Manuel Breuer.

Excessive endometrial PlGF- Rac1 signalling underlies endometrial cell stiffness linked to pre-eclampsia.

Supplementary Figures

Fig S1

a

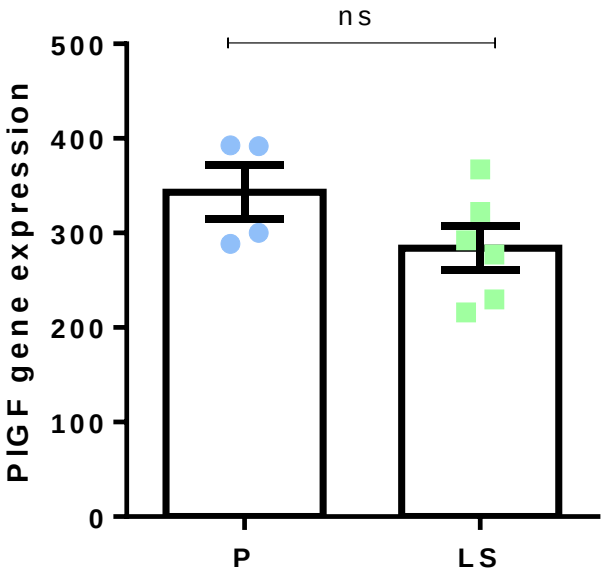

b

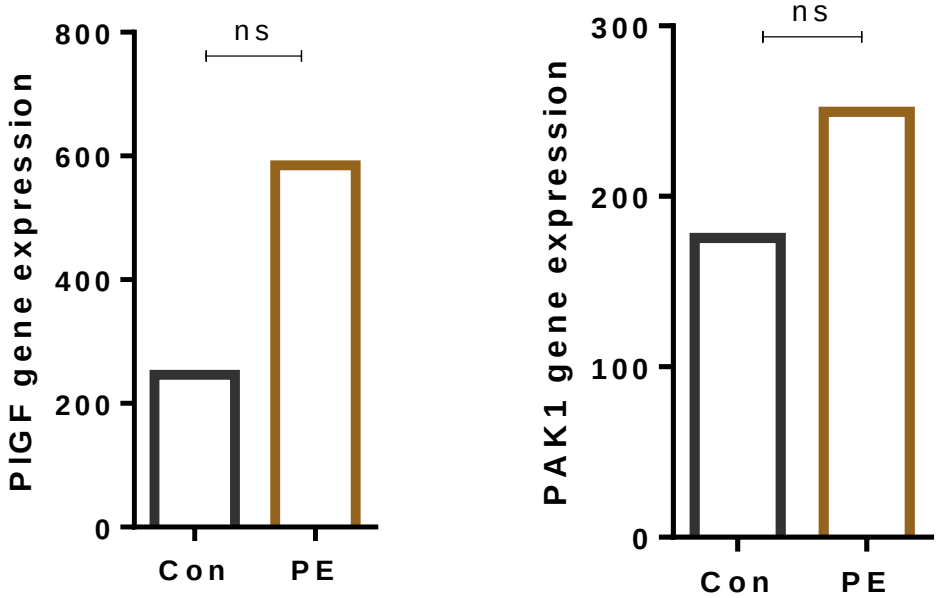

FigS1: a. Expression kinetics of PlGF across the menstrual cycle in the proliferative (P) phase (n=4) and late secretory (LS) phase (n=6) (*GDS2052*). Statistical significance was tested with unpaired t test and found to be non-significant. b. PlGF and PAK1 transcripts in term decidua's of preeclamptic women (n=10) compared to the decidua from healthy (n=10) pregnant women (*GEO2548*). The GEO dataset for the control and diseased samples were retrieved using the GEO2R query bioconductor package. Gene expression value was represented as average value pooled from all 10 samples respectively. Statistical significance was tested with unpaired t test. The gene expressions between control and PE are not statistically significant but show both upregulated PlGF and PAK1 gene expression pattern in PE decidua's compared to healthy pregnant tissue samples.

Fig S1

c

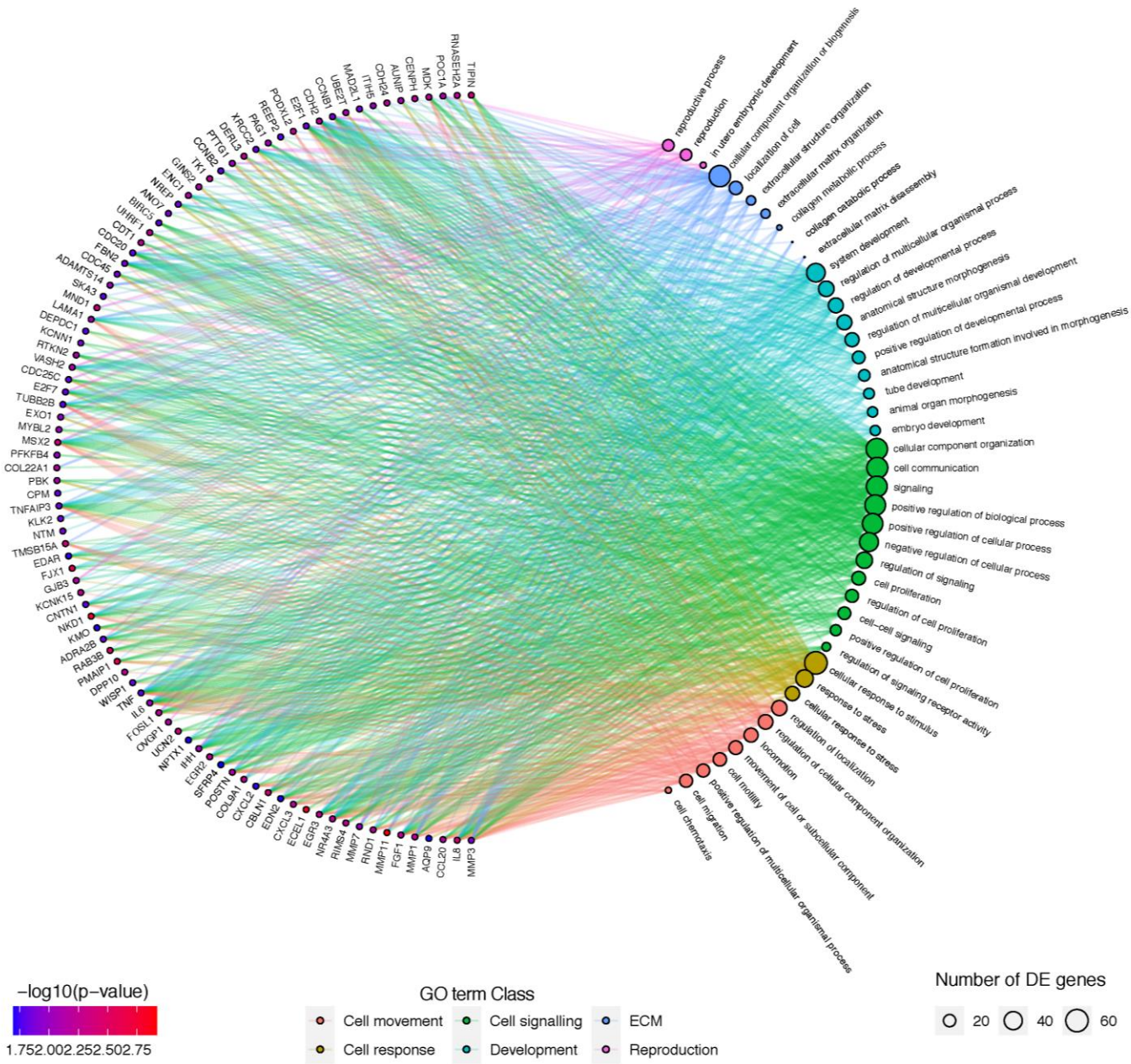

FigS1c. Gene ontology analysis from RNA sequencing array (RNA-seq, *GSE172381*) from endometrial biopsies obtained from women who had severe PE in a previous pregnancy (n = 24).

Fig S1

d

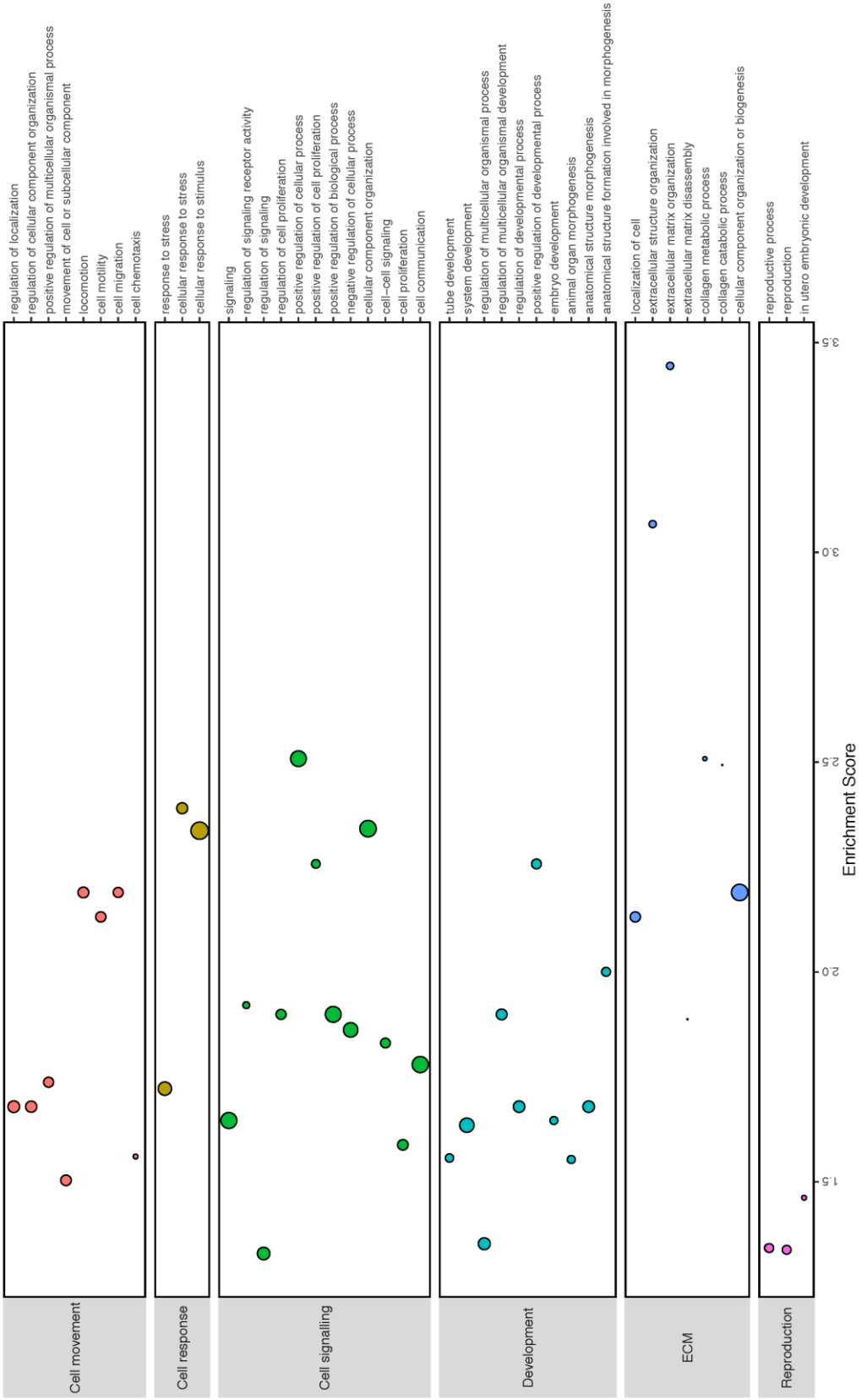

FigS1d: Enriched biological process from GO analysis from RNA sequencing array (RNA-seq, *GSE172381*) from endometrial biopsies obtained from women who had severe PE in a previous pregnancy (n = 24).

Fig S2

a

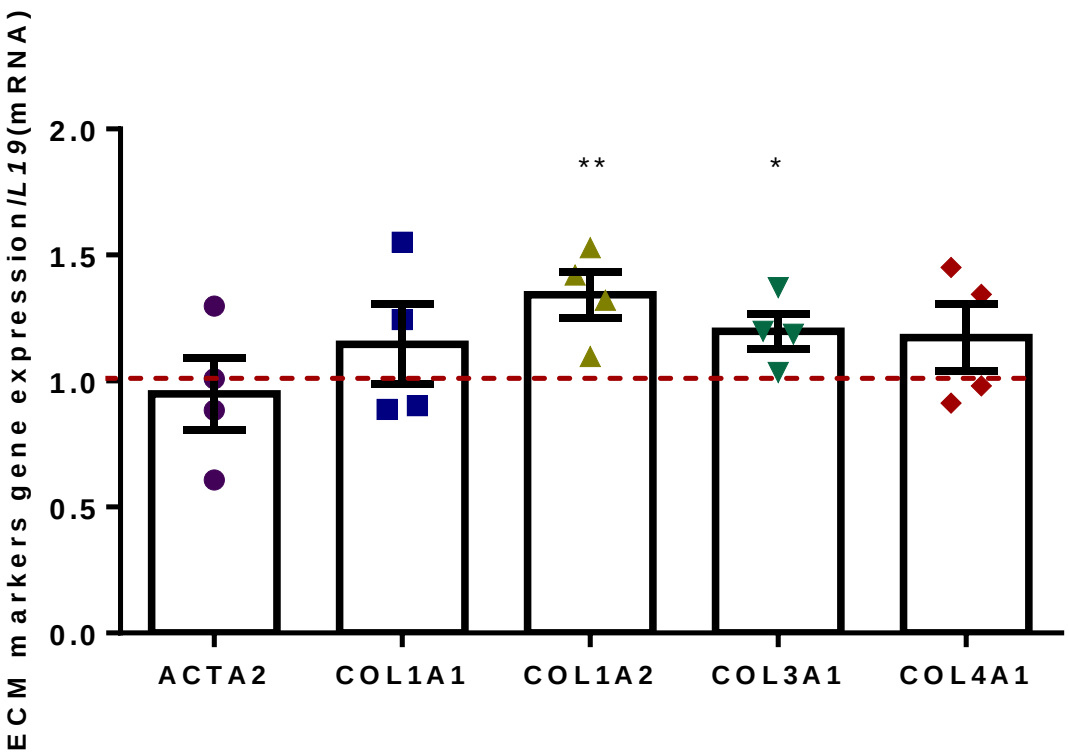

b

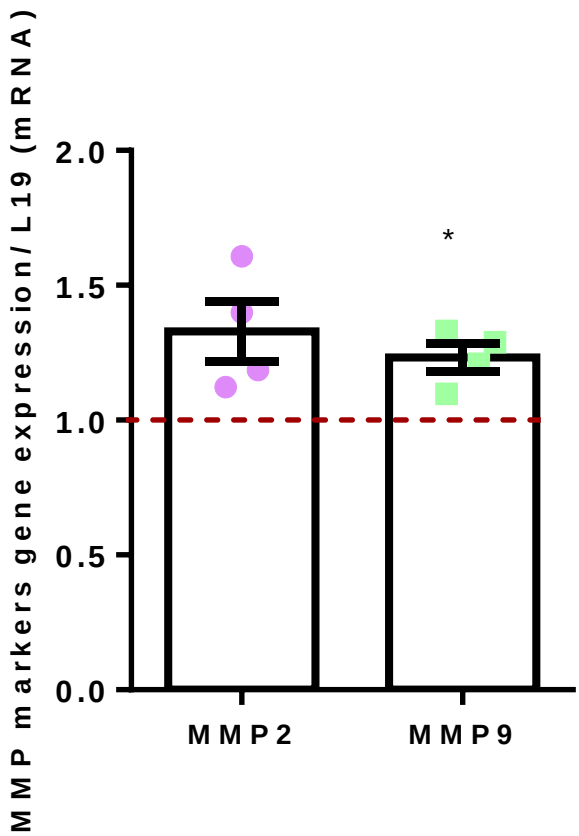

Fid S2: a) Arithmetic mean ± SEM of ECM markers transcript level in EnSCs on treatment with PlGF (n=4, *, p<0.05, **, p< 0.01). (b) Arithmetic mean ± SEM of MMP markers gene expression levels in EnSCs on treatment with PlGF (n=4, *, p<0.05). All the above data represented here is normalized to control cells. An unpaired t test with Welch's correction was used to test for statistical significance.

Fig S3

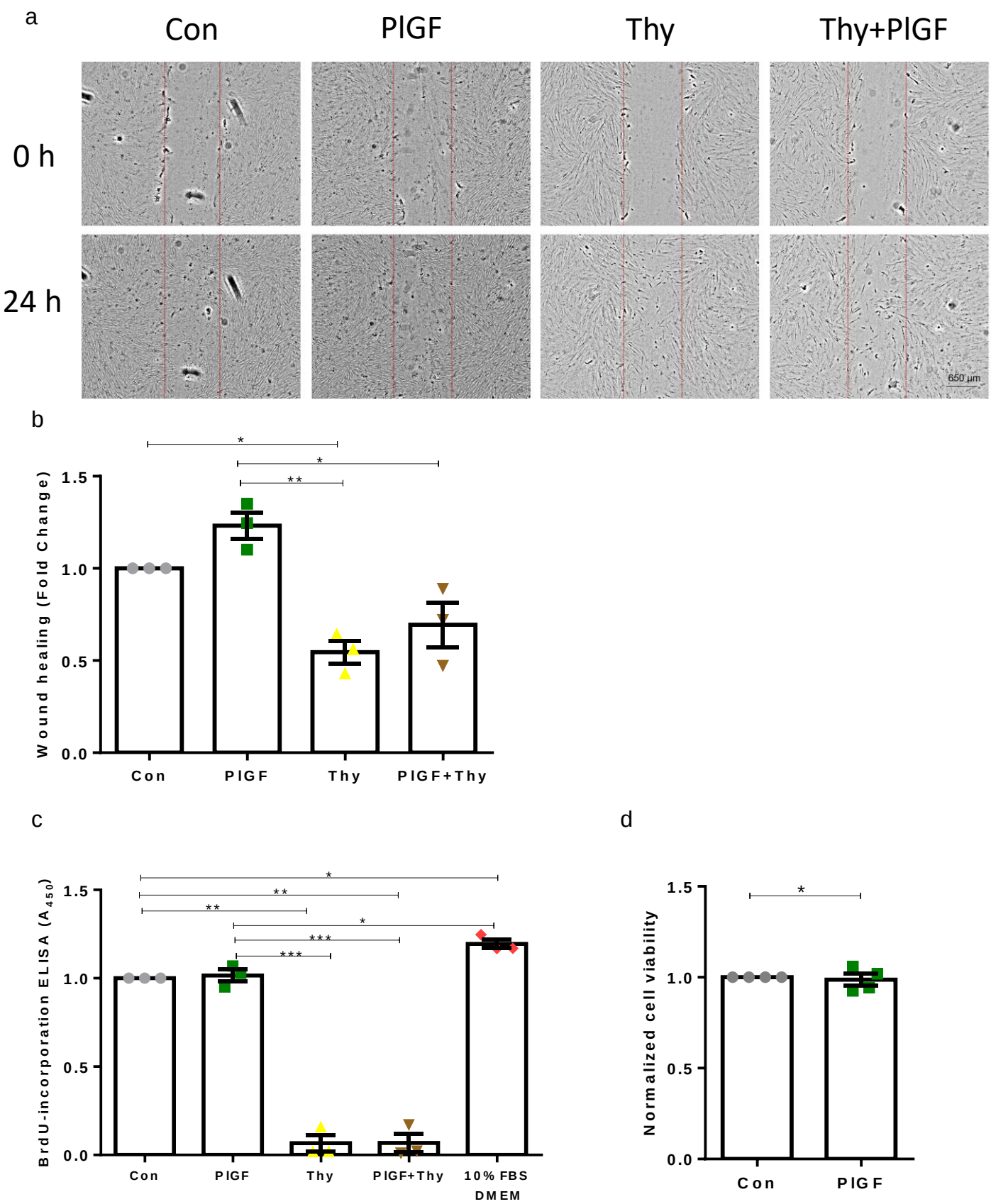

Fig S3 : a) Bright field images of wound healing scratch assay evaluated at 0h and 24 h. b) Arithmetic mean ± SEM of wound healing rate on EnSCs treated with PlGF ± thymidine (thy). c) Arithmetic mean ± SEM of BrdU cell proliferation assay on EnSCs treated with PlGF ± thymidine (thy). d) Arithmetic mean ± SEM of MTS cell viability assay on EnSCs treated with PlGF. All the above data represented here is normalized to control cells. An unpaired t test with Welch's correction was used to test for statistical significance

Fig S4

a

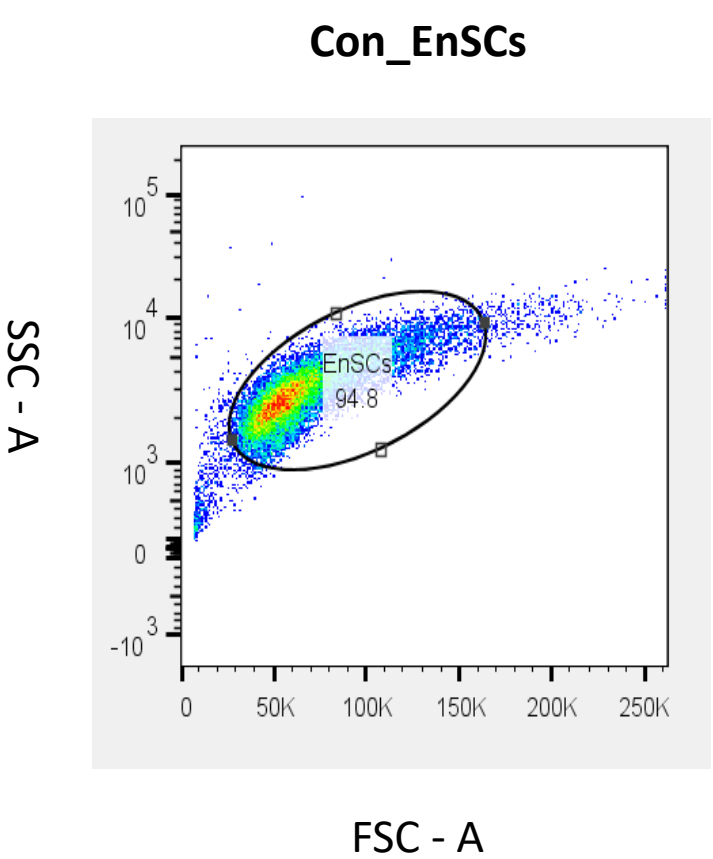

b

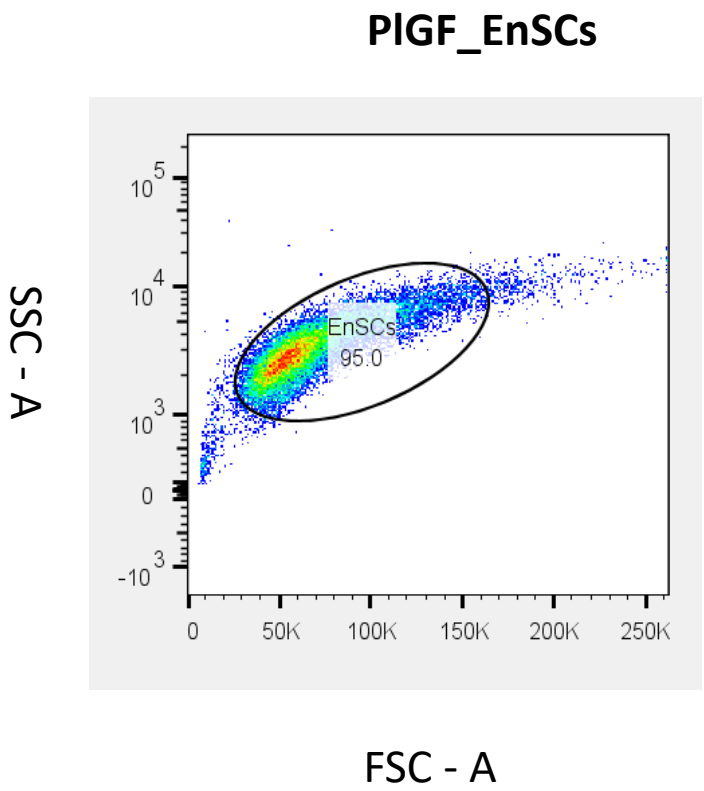

Fig S4: Gating strategy for single cells, illustrated in human endometrial stromal cell (EnSCs) population: Forward (FSC-A) and side scatter (SSC-A) are adjusted to minimize events on the axes, resulting in a single-cell population including > 80 % of total cells (a- Con, b- PlGF). Each dot or point on the plot represents an individual cell that has passed through the laser. Gating strategy has been applied on EnSCs population to exclude debris, dead cells and doublets. Cells gated on FSC-A versus SSC-A result in histograms specific to fluorophores (DNase I and Phalloidin) as depicted in both Figure 3a and 6a.

Fig S5

a

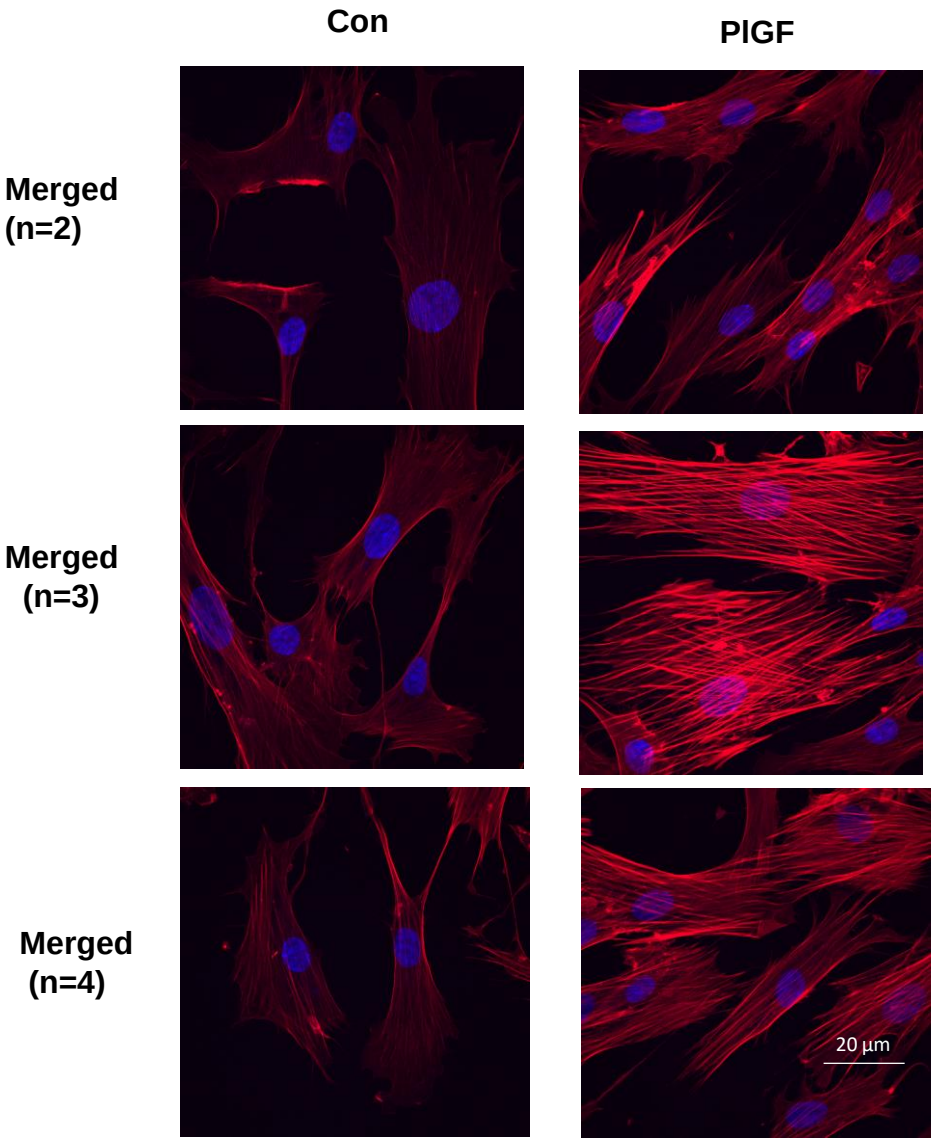

Fig S5: a. Representative immunofluoroscence images of EnSCs stained for phalloidin (F actin-red) and DAPI (nucleus – blue).

Fig S6

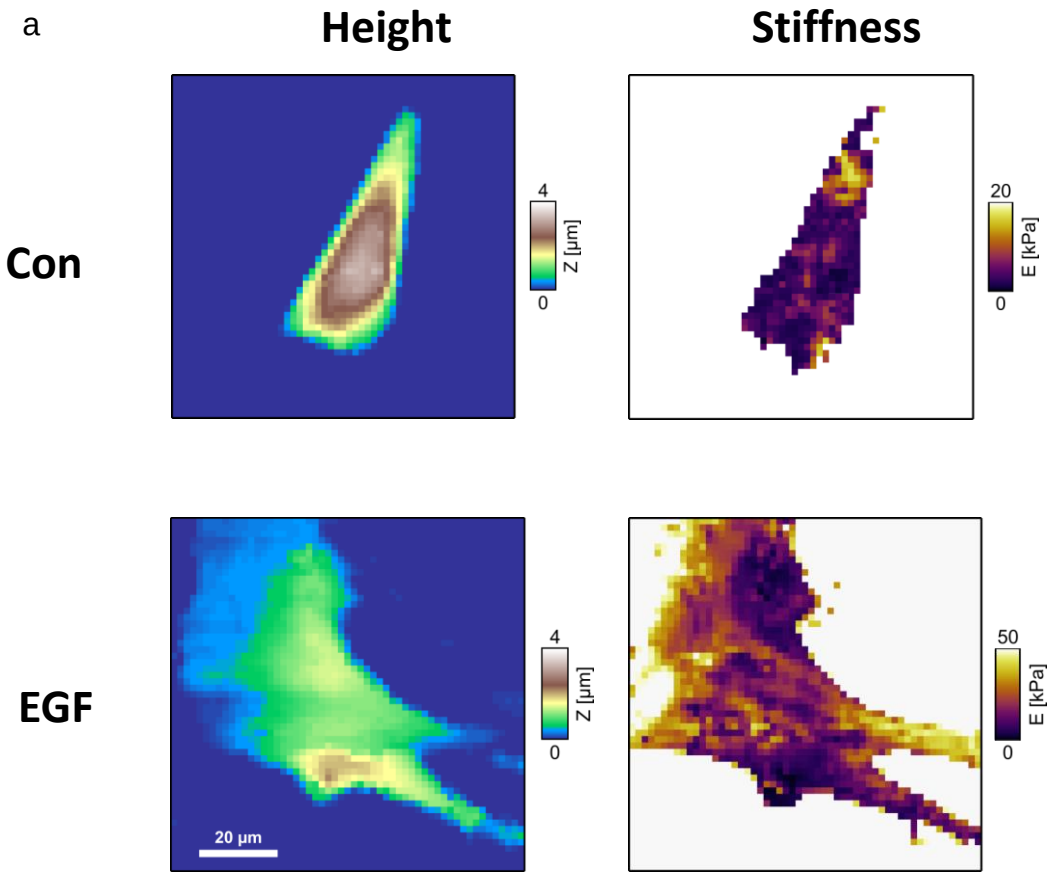

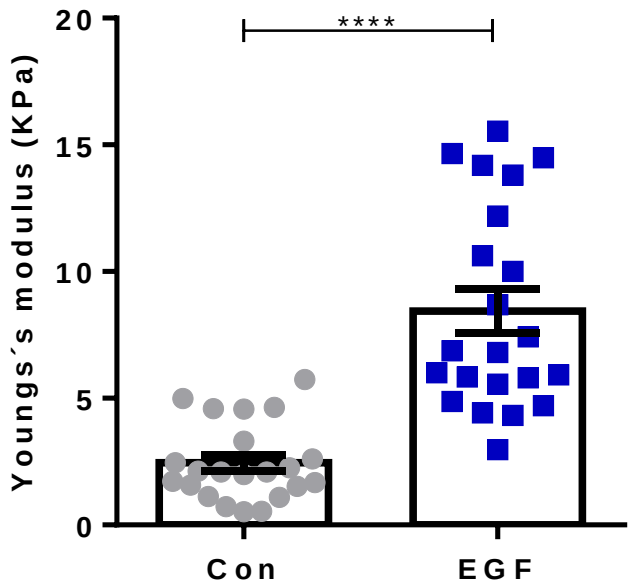

Fig S6 : a. AFM analysis of cell stiffness and cell morphology in EnSCs treated with EGF (100 ng/ml) for 24 hours. Representative height images and AFM stiffness images measuring the Young's modulus. (b) Arithmetic mean ± SEM of Young's modulus (cell stiffness. Non-parametric Mann-Whitney analysis was used to test for statistical significance.

Fig S7

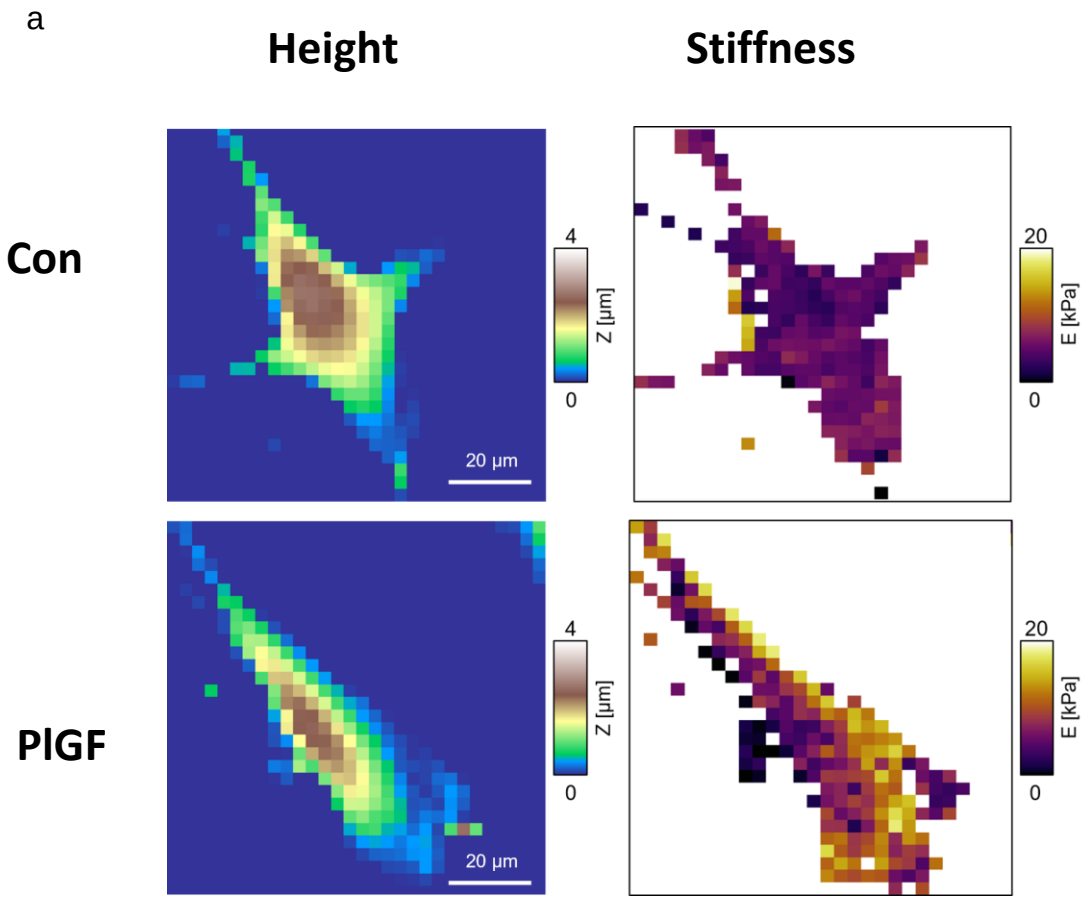

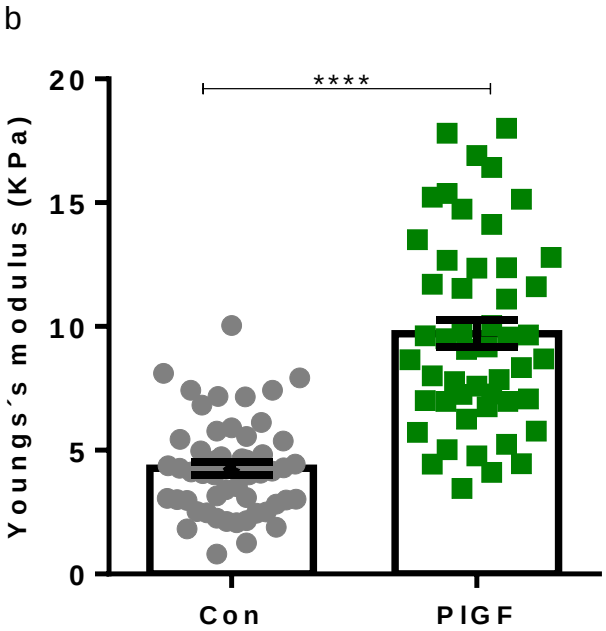

Fig S7 : a. AFM analysis of cell stiffness and cell morphology of EnSCs grown on PDMS coated petridishes. EnSCs were treated with PlGF (20 ng/ml) for 6 days, Representative height images and AFM stiffness images measuring the Young's modulus. (b) Arithmetic mean ± SEM of Young's modulus (cell stiffness). Non-parametric Mann-Whitney analysis was used to test for statistical significance.

Fig S8

a

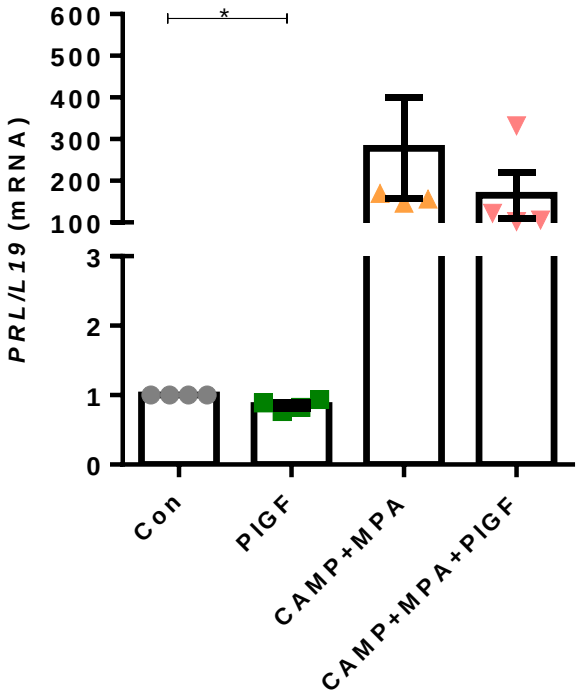

b

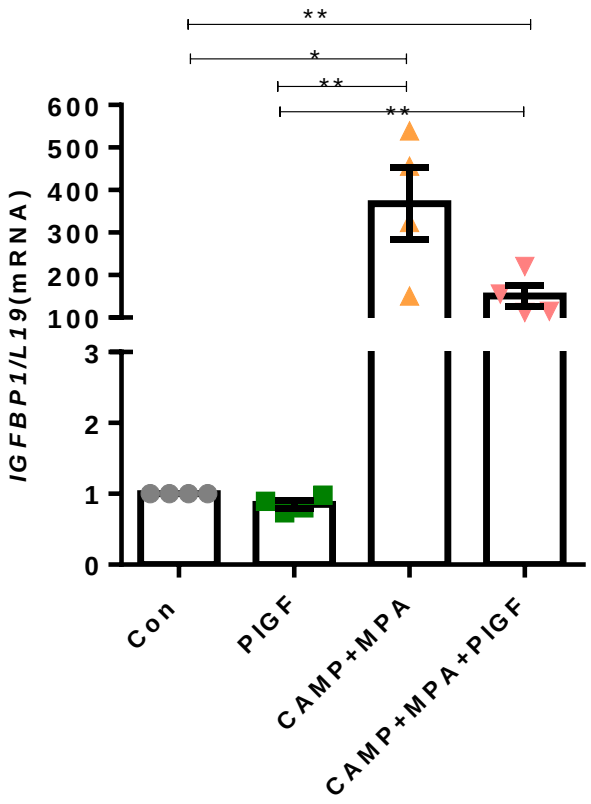

Fig S8: a) Arithmetic mean ± SEM of PRL transcript levels in EnSCs on treatment with PlGF±cAMP+MPA (n=4, *, p<0.05). (b) Arithmetic mean ± SEM of IGFBP1 transcript levels in EnSCs on treatment with PlGF±cAMP+MPA (n=4, *, p<0.05, **, p<0.01). All the above data represented here is normalized to control cells. An unpaired t test with Welch's correction was used to test for statistical significance.

Fig S9

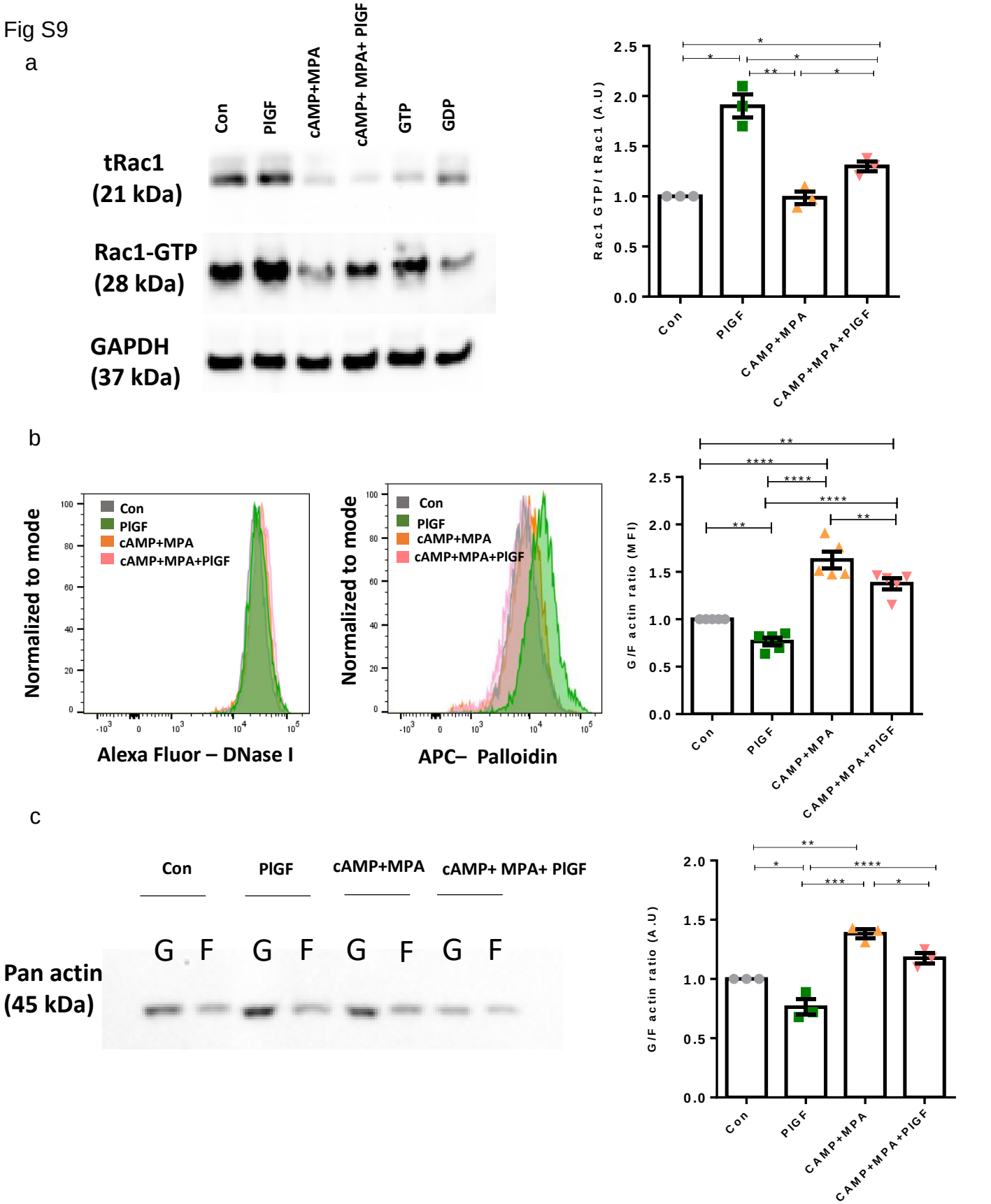

Fig S9 : a) Original WBs of tRac1,Rac1-GTP and arithmetic mean ± SEM of Rac1GTP levels / tRac1 ratio in EnSCs after 6 days treatment with PlGF ± cAMP+MPA. All the above data represented here is normalized to control cells. b) Representative original histogram of DNaseI (G-actin; Left) and Phalloidin (F-actin; Right) binding in EnSCs after 6 days treatment with PlGF ± cAMP+MPA and arithmetic mean ± SEM of G-actin over F-actin ratio in EnSCs after 6 days treatment with PlGF ± cAMP+MPA. c) Original western blots and arithmetic mean ± SEM of G-actin over F-actin ratio in EnSCs after 6 days treatment with PlGF ± cAMP+MPA. An unpaired t test with Welch's correction was used to test for statistical significance

Fig S10

a

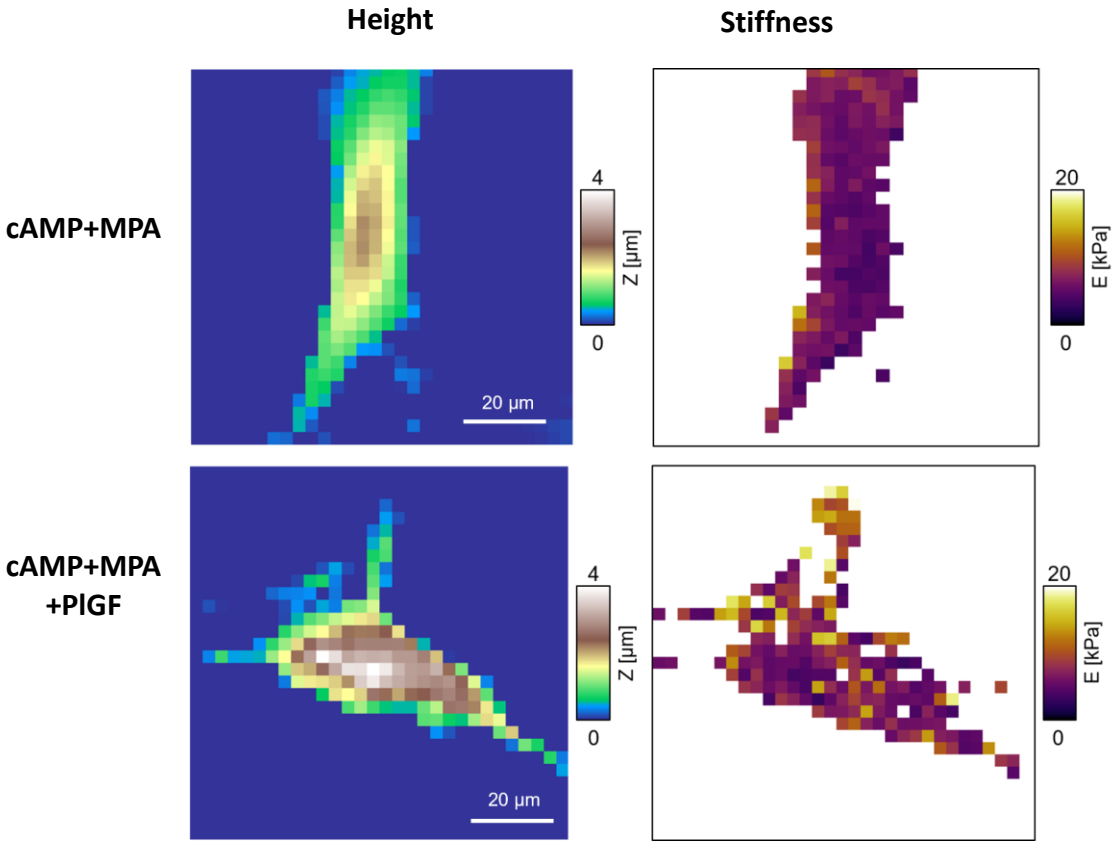

b

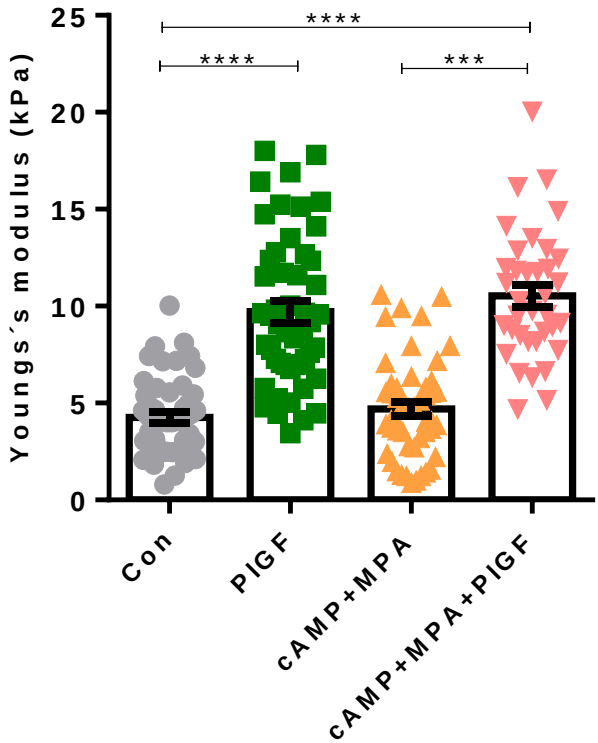

Fig S10: a. AFM analysis of cell stiffness and cell morphology of EnSCs grown on PDMS coated petridishes. EnSCs were treated with cAMP+MPA with or without PlGF for 6 days, Representative height images and AFM stiffness images measuring the Young's modulus. (b) Arithmetic mean ± SEM of Young's modulus (cell stiffness). Non-parametric Mann-Whitney analysis was used to test for statistical significance.

Fig S11

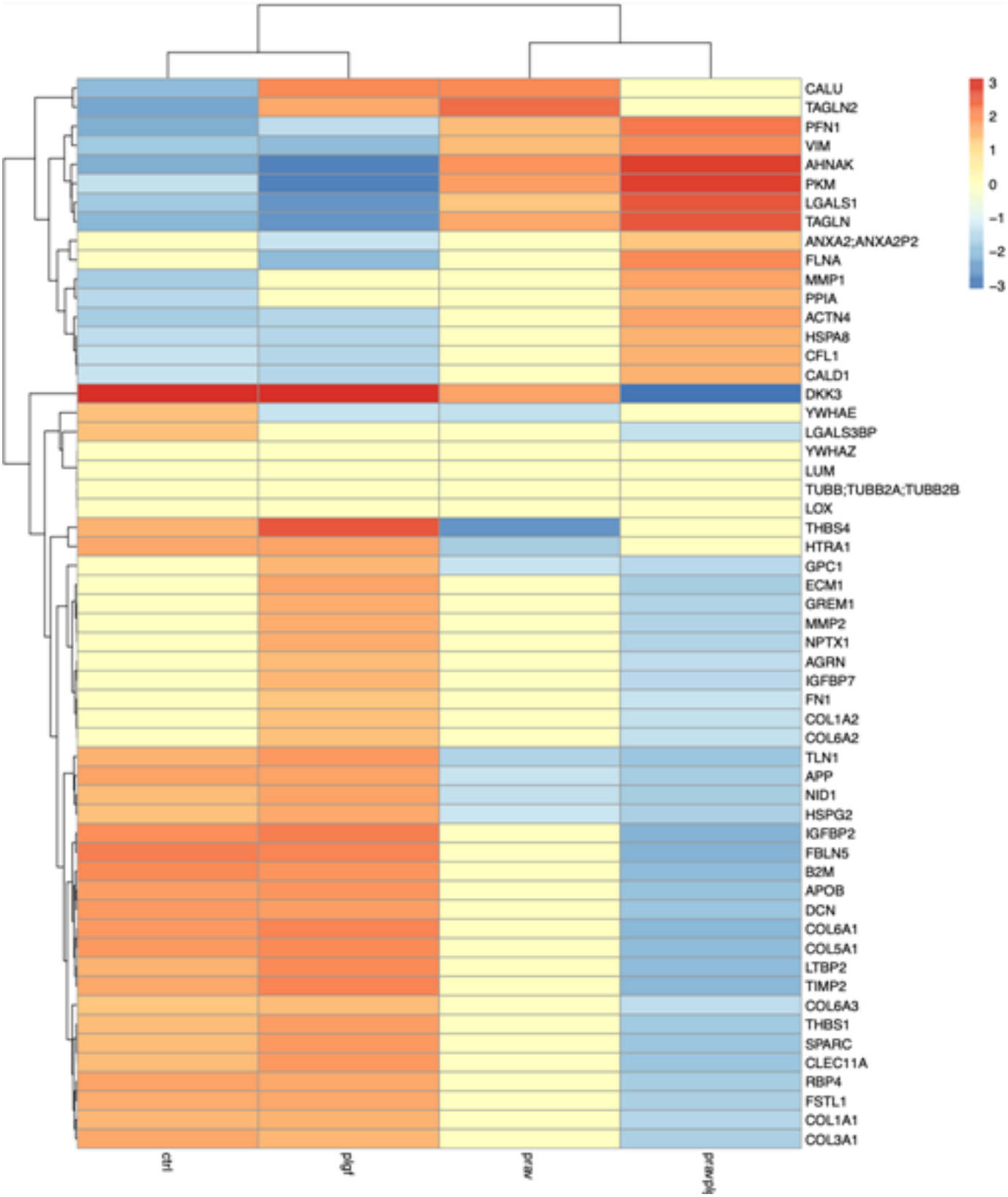

Fig S11: Heatmap showing the differentially regulated proteins expressed in different treatment group (Con/PlGF/Prav/PlGF+Prav) in EnSCs following global proteomic analysis.

Excessive endometrial PlGF- Rac1 signalling underlies endometrial cell stiffness linked to pre-eclampsia.

Supplementary Information

Original Western blots

Fig S12 Original western blot membranes of represented blots in figure 2c and 2h.

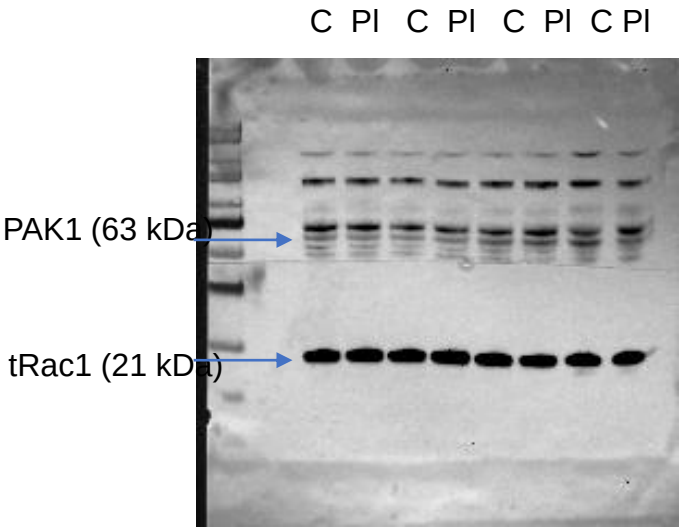

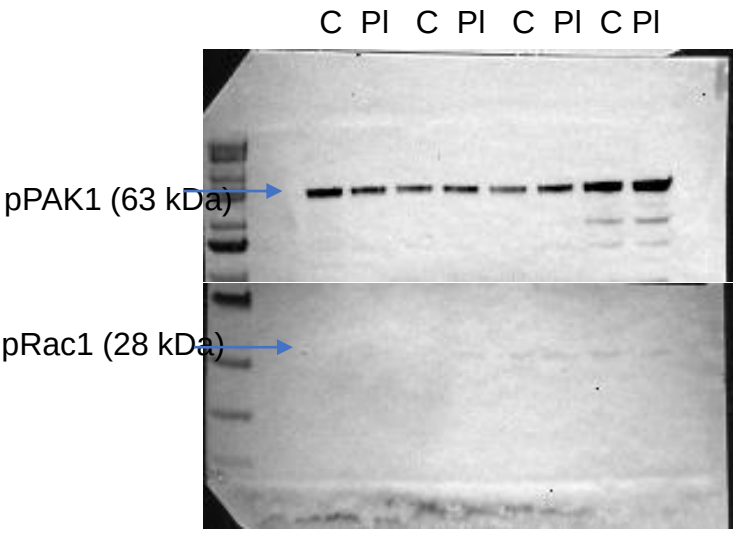

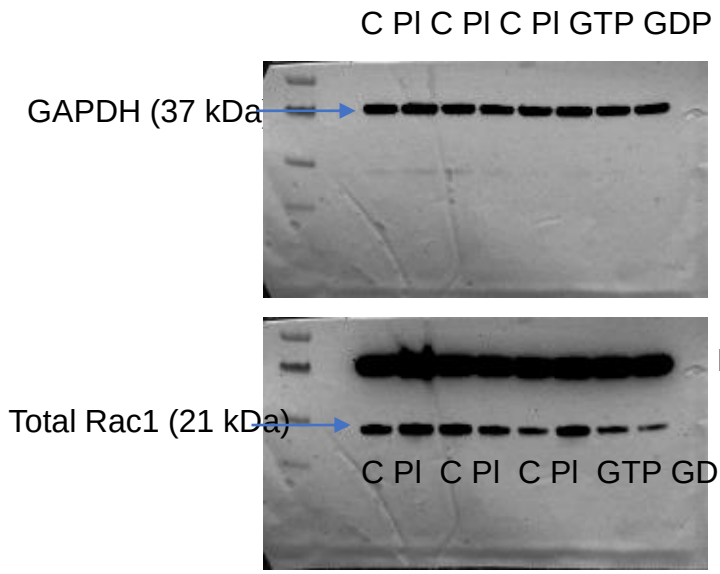

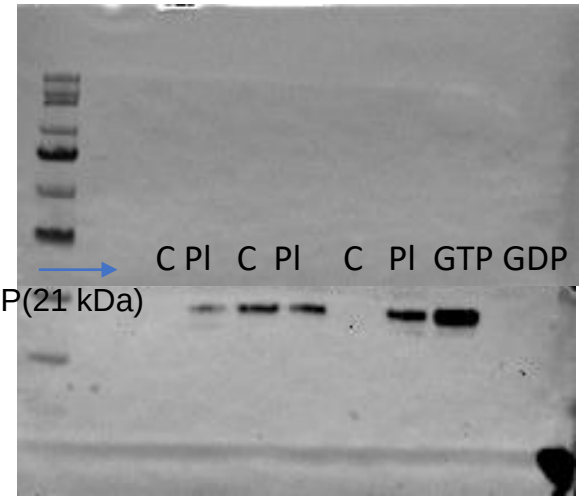

Original western blot membranes of represented blots in figure 3c

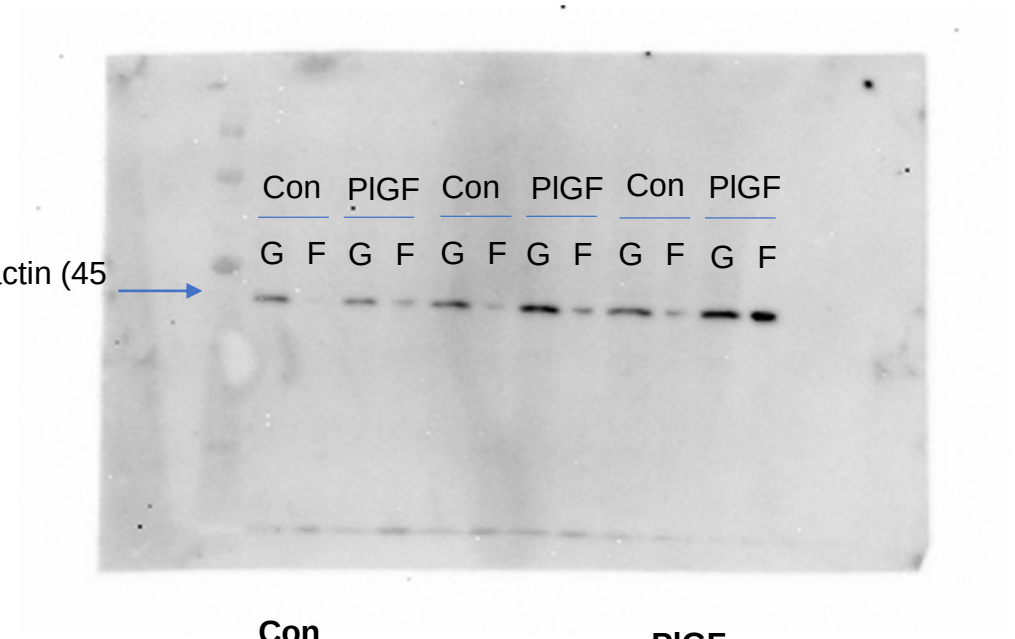

Original western blot membranes of the represented blots in figure 4a.

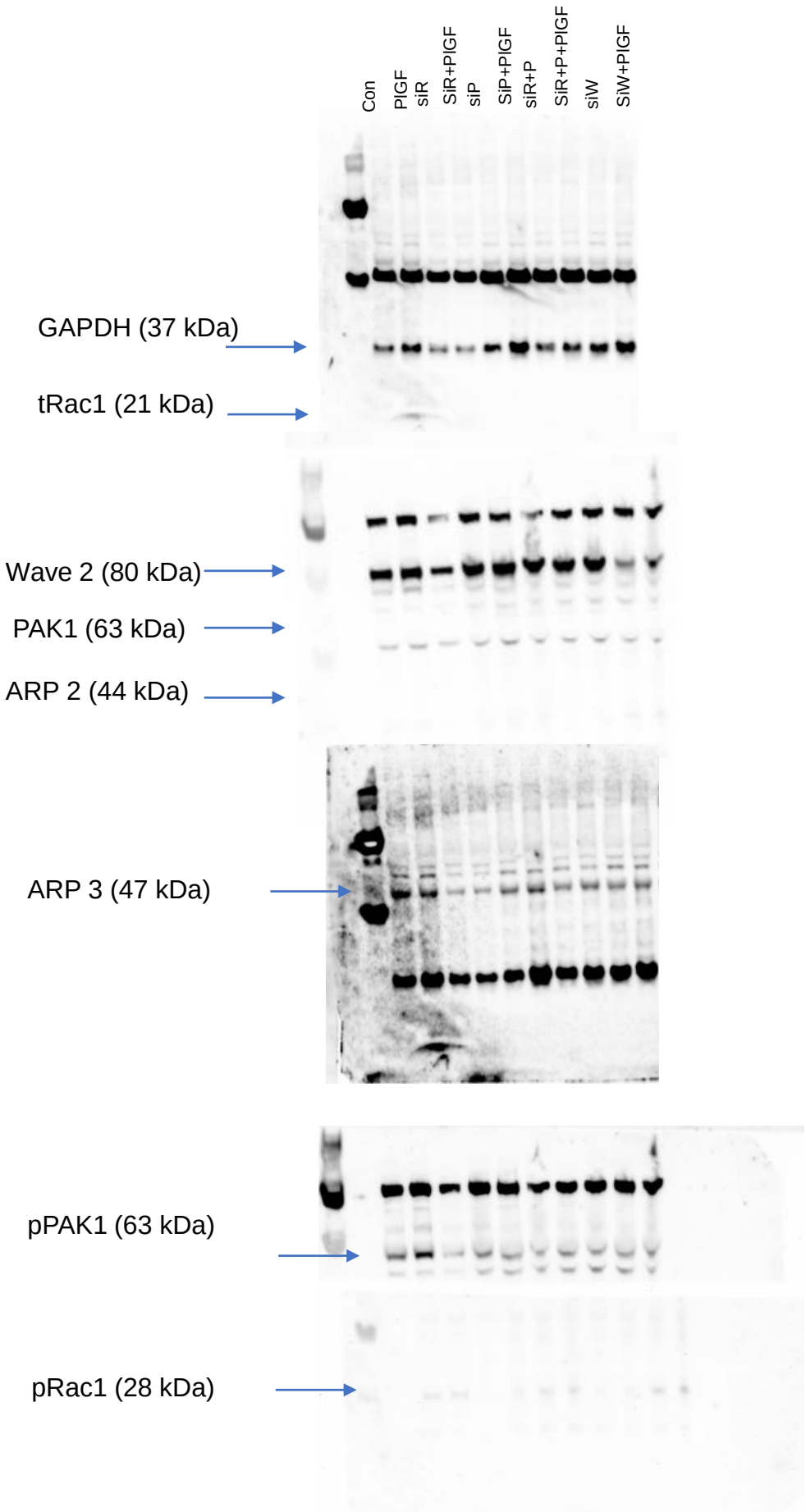

Original western blot membranes of represented blots in figure 5b.

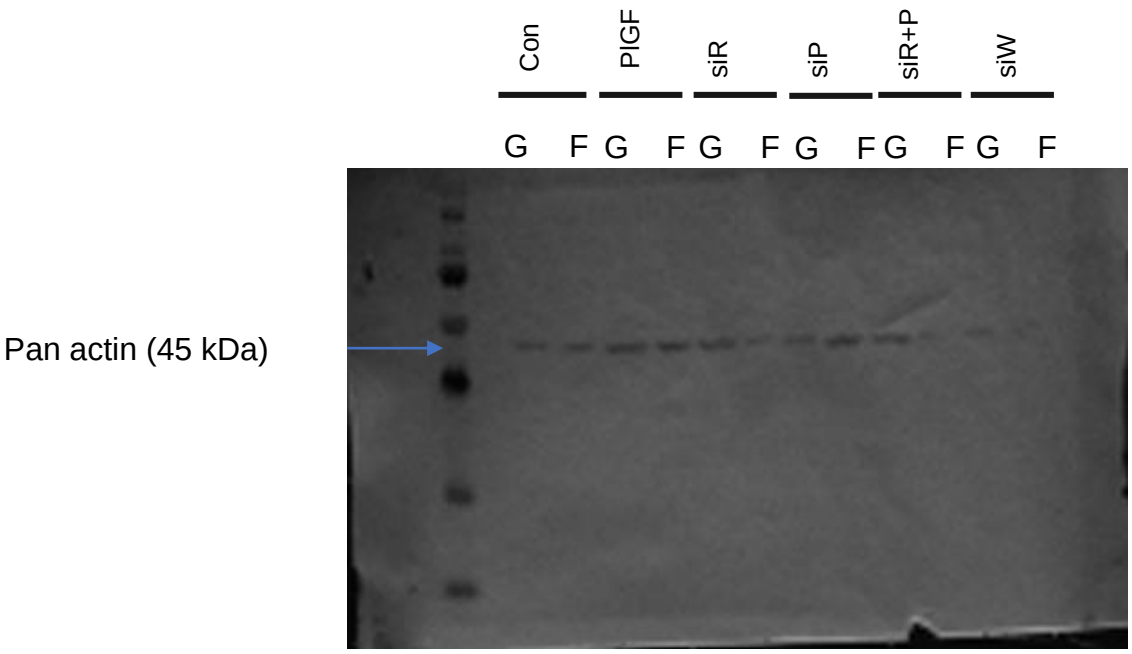

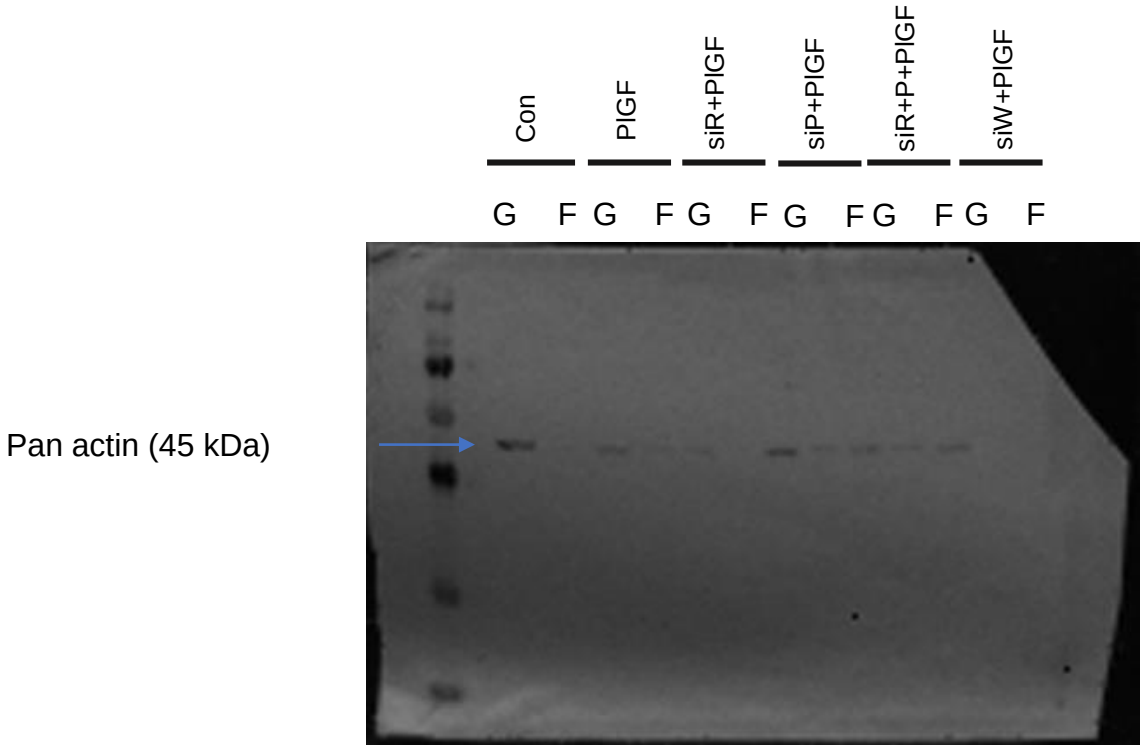

Original western blot membranes of represented blots in figure 6c and 6e.

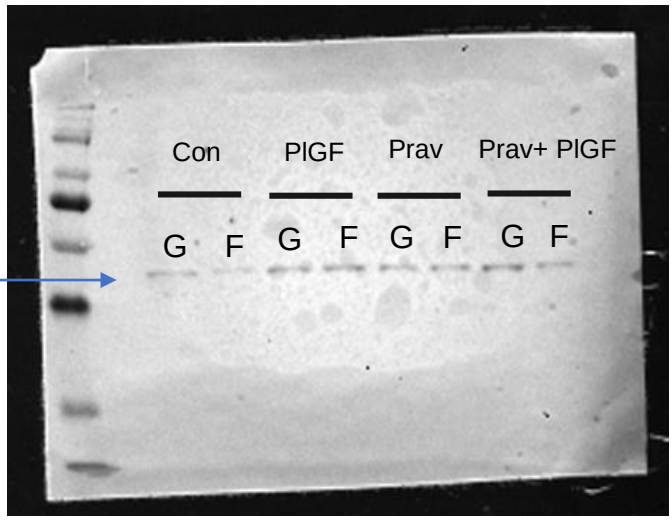

Pan actin (45 kDa)

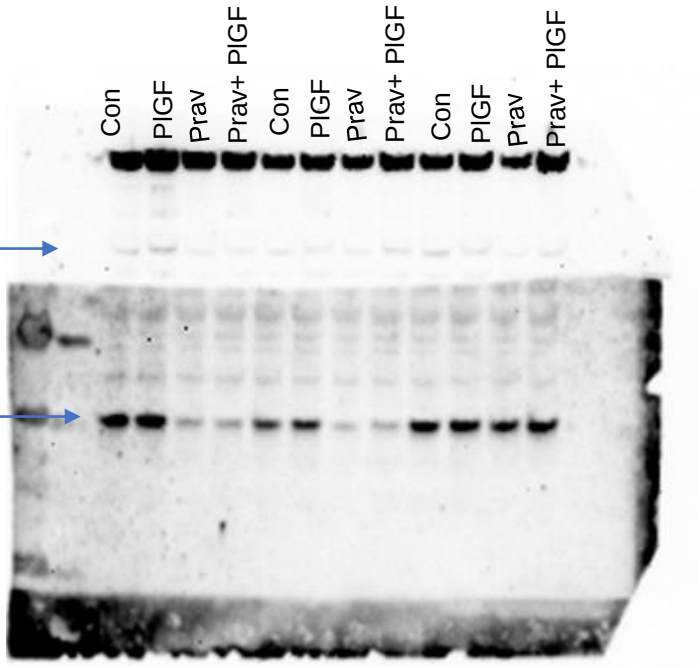

pPAK1(63 kDa)

pRac1(28 kDa)

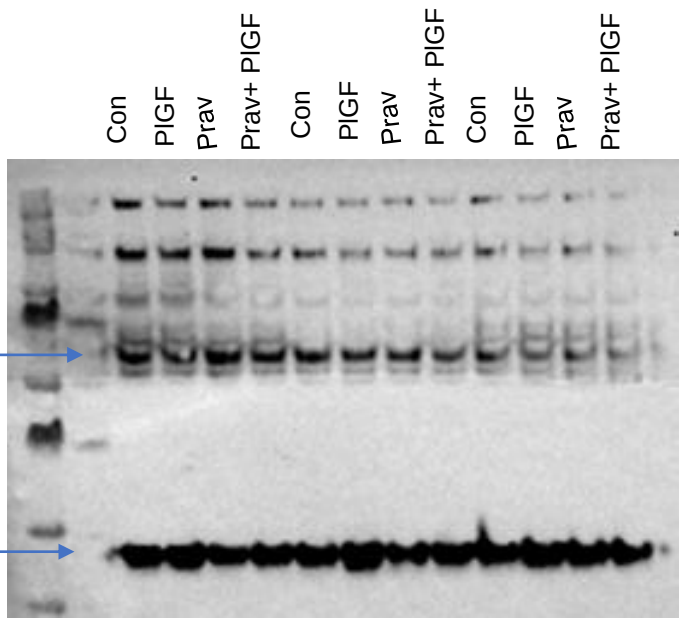

PAK1(63 kDa)

Rac1(21 kDa)

Biological Research

RESEARCH ARTICLE Open Access

Placental growth factor mediates pathological uterine angiogenesis by activating the NFAT5-SGK1 signaling axis in the endometrium: implications for preeclampsia development

Janet P. Raja Xavier[1], Toshiyuki Okumura[2], Melina Apweiler[1], Nirzari A. Chacko[1], Yogesh Singh[1,3], Sara Y Brucker[1], Satoru Takeda[2], Florian Lang[4] and Madhuri S Salker[1*]

Abstract

After menstruation the uterine spiral arteries are repaired through angiogenesis. This process is tightly regulated by the paracrine communication between endometrial stromal cells (EnSCs) and endothelial cells. Any molecular aberration in these processes can lead to complications in pregnancy including miscarriage or preeclampsia (PE). Placental growth factor (PlGF) is a known contributing factor for pathological angiogenesis but the mechanisms remain poorly understood. In this study, we investigated whether PlGF contributes to pathological uterine angiogenesis by disrupting EnSCs and endothelial paracrine communication. We observed that PlGF mediates a *tonicity-independent* activation of nuclear factor of activated T cells 5 (NFAT5) in EnSCs. NFAT5 activated downstream targets including SGK1, HIF-1α and VEGF-A. In depth characterization of PlGF - conditioned medium (CM) from EnSCs using mass spectrometry and ELISA methods revealed low VEGF-A and an abundance of extracellular matrix organization associated proteins. Secreted factors in PlGF-CM impeded normal angiogenic cues in endothelial cells (HUVECs) by downregulating Notch-VEGF signaling. Interestingly, PlGF-CM failed to support human placental (BeWo) cell invasion through HUVEC monolayer. Inhibition of SGK1 in EnSCs improved angiogenic effects in HUVECs and promoted BeWo invasion, revealing SGK1 as a key intermediate player modulating PlGF mediated anti-angiogenic signaling. Taken together, perturbed PlGF-NFAT5-SGK1 signaling in the endometrium can contribute to pathological uterine angiogenesis by negatively regulating EnSCs-endothelial crosstalk resulting in poor quality vessels in the uterine microenvironment. Taken together the signaling may impact on normal trophoblast invasion and thus placentation and, may be associated with an increased risk of complications such as PE.

Keywords PlGF, Endometrium, Placentation, Pregnancy, Preeclampsia, SGK1

*Correspondence:
Madhuri S Salker
madhuri.salker@med.uni-tuebingen.de
[1]Department of Women's Health, University of Tübingen, 72076Calwerstraße 7/6, Tübingen, Germany
[2]Department of Obstetrics and Gynaecology, Juntendo University School of Medicine, Tokyo, Japan
[3]Institute of Medical Genetics and Applied Genomics, University of Tübingen, Tübingen, Germany
[4]Department of Physiology, University of Tübingen, Tübingen, Germany

Introduction

Pregnancy-associated vascular transformations of the decidua are coordinated by complex cellular mechanisms to induce remodelling at the maternal-fetal interface, which are critical for a healthy pregnancy outcome [1, 2]. Angiogenesis is the development of new vessels from existing blood vessels. In the adult, (healthy) angiogenesis rarely occurs except during wound healing and during repair of the vascular bed after menstruation. Uterine angiogenesis within the decidua is coordinated by several factors secreted from stromal cells, surrounding the endometrial vessels [3, 4]. Any aberrations in remodelling of the uterine vasculature during early pregnancy results in miscarriage or pregnancy disorders such as preeclampsia (PE), fetal growth restriction (FGR) and intrauterine deaths (IUD) or stillbirths [5–7]. PE, a pregnancy-specific pathology is associated with hypertension and multiorgan dysfunction [8]. PE is reported to occur in 5 to 7% of all pregnancies globally, unfortunately this number is rising [9]. In 2022, pregnancies affected by PE were responsible for over 70,000 maternal deaths and 500,000 fetal deaths worldwide [9]. Insufficient vascularization within the uterine decidua, followed by poor placentation at the maternal-fetal interface contributes to ischemia, uteroplacental hypoxia, inflammation and elevated levels of oxidative stress [5, 10, 11]. Women diagnosed with a pre-eclamptic pregnancy are reported to be associated with 4-fold increased risk in future incident heart failure and a 2-fold increase in coronary heart diseases [12, 13]. Currently, there are no tests or treatments to predict the onset of preeclampsia or prevent it. Hence, there exists an urgent unmet clinical need to identify new molecular targets for early diagnosis and therapeutics in PE. Recent studies support that the pathophysiology of PE likely involves endometrial determinants in its pathogenesis [14–18]. Therefore, studying maternal uterine health prior to pregnancy is of importance to identify new molecular pathways driving adverse pregnancy outcomes such as PE.

After menstruation, one of the critical processes of the regenerating endometrium is the regrowth of blood vessels (angiogenesis) [19]. During each menstrual cycle and in early pregnancy, the uterine endothelium becomes activated and undergoes sprouting angiogenesis to increase the size and number of blood vessels in the endometrium [20]. The demand for angiogenic stimulus varies both spatially and temporally across the different menstrual phases [21, 22]. Endometrial stromal fibroblasts are known to secrete biochemical cues (growth factors and cytokines) to induce a pro-angiogenic response in endothelial cells of the spiral arterioles [19, 23, 24]. Employing a 3 dimensional (3D) bioengineered vascularized endometrium on-a-chip model, Ahn et al. highlighted the importance of endometrial stromal cells in stimulating angiogenesis in endothelial cells [23]. Stromal cells exhibit functionally directed proangiogenic cues in regulating microvascular network formation through neo-vessel sprouting of the endothelial cells [23, 25]. From a maternal standpoint, pregnancy is an example of extraordinary rapid histogenesis that is unrivalled in healthy adult tissues. This emphasizes the importance of signaling factors produced by the 'master' stromal cells within the uterine environment to influence dynamic angiogenesis processes within the endothelial compartment of spiral arteries. Hence, identifying molecular factors that deregulate the vascularized endometrial microenvironment prior to pregnancy and during early placentation is of critical importance.

Placental growth factor (PlGF) is found in the endometrial stroma and abnormal production of endometrial PlGF may result in pregnancy complications, though the mechanism is yet to be determined [26, 27]. The functional role of PlGF in various biological processes continues to expand, in particular its activity in disease progression [28, 29]. The interplay of PlGF as a pleiotropic cytokine is reported to augment ischemia, hypoxia, inflammatory or malignant processes [30–34]. PlGF shares a biochemical and functional relationship with vascular endothelial growth factor (VEGF-A), that is translated into high synergic activity in physiological and pathological angiogenesis [35, 36]. PlGF-VEGFR1 signaling is reported to modulate angiogenesis and tumour growth by regulating the Dll4-Notch pathway [34]. Inhibition of PlGF is further reported to selectively inhibit pathological angiogenesis [32, 37]. Soluble fms-like tyrosine kinase-1 (sFlt-1), is a circulating anti-angiogenic protein that acts by binding to the receptor binding domains of PlGF and to VEGF thereby preventing its interactions with endothelial receptors [38]. Circulating VEGF concentrations are low through pregnancy whilst free PlGF increases in normal pregnancies [38]. Therefore, free PlGF *a priori* is pivotal for maintaining vascular endothelial cell homeostasis [39].

PlGF is produced in many organs and cells including the human endometrium, decidua, placenta, uterine natural killer cells and trophoblasts cells [40]. Endometrial PlGF is higher in the proliferative phase with expression levels declining in the secretory phase, higher levels of PlGF were associated with implantation failure after IVF [41, 42]. Moreover, gene expression studies of the first trimester decidua prior to the onset of PE compared with healthy pregnancies reveals that local decidual PlGF levels are higher in the PE group [43]. Therefore, it is crucial to identify the underlying local factors that potentially contribute to the clinical manifestation of PE within the decidua. To the best of our knowledge, the potential role of endometrial PlGF- associated physiological

vessel development in the endometrium and its relation to pregnancy complications has not been investigated.

Nuclear factor of activated T cells (NFAT5) is part of the Rel family of transcriptional activators [44, 45]. It was originally characterized as a cell volume – regulated transcriptional factor activated by osmotic cell stress [44]. In addition to its well-known osmoprotective role, NFAT5 activation can be mediated independent from tonicity, thus having wider consequences on physiological functions such as development, immune function and cellular stress responses [46–51]. In a recent study, it was revealed that the transcriptional activity of NFAT5 mediates production of angiogenic factors causing neovascularization and angiogenesis associated oedema [52]. In retinal pigment epithelial cells aberrant PlGF signaling *via* NFAT5 activity causes abnormal vessel development in diabetic retinopathy [52]. NFAT5-inducible genes include serum glucocorticoid regulated kinase 1 (SGK1) [51, 53], which is a known activator of hypoxia inducible factor 1 subunit alpha (HIF-1α) proteins and subsequent VEGF-A formation and angiogenesis [54–58]. Thus, these findings so far point to a compelling potential role of PlGF-NFAT5-SGK1 in vessel remodelling and thus warrant further investigation in delineating this signaling axis and its role in endometrial angiogenesis.

In the present study, we studied the effect of PlGF mediated NFAT5 regulation in the endometrial stromal cells (EnSCs). Further, we identified a signaling downstream pathway involving PlGF-NFAT5-SGK1 activation in EnSCs. We also characterized the angiogenic factors secreted by the stromal cells upon PlGF mediated NFAT5 activation. To mimic the effect of secreted angiogenic cues on vessel formation ability we also demonstrated its responsiveness in endothelial (HUVECs) cells. Aberrant PlGF mediated secreted factors impaired trophoblast invasion through the HUVEC monolayer. Furthermore, angiogenic behaviour and trophoblast invasion were reversed by inhibiting SGK1.

Our study reveals that PlGF mediated NFAT5-SGK1 activation in endometrial stromal cells negatively regulate secretion of pro-angiogenic factors within the uterine microenvironment. Additionally, we show that the secreted angiogenic factors activate pathological pathway in endothelial cells resulting in impaired angiogenesis. In summary, aberrant endometrial PlGF expression could lead to dysregulated stromal-endothelial communication leading to poor trophoblast invasion.

Materials and methods

Cell culture

Primary human EnSCs (#T0533, Applied Biological Materials Inc) were cultured at 37 °C in a humidified 5% CO_2 atmosphere in DMEM/F-12 medium (#11039-021, Invitrogen) containing 10% (v/v) dextran coated charcoal stripped (#C6241, Sigma-Aldrich) fetal bovine serum (#10270-106, Invitrogen), 1% (v/v) antibiotic-antimycotic solution (#15240-062, Invitrogen) and 1% (v/v) L-glutamine (#25030-024, Invitrogen). Human umbilical vein endothelial cells (HUVECs) (#C-12,203, Sigma-Aldrich) and GFP-tagged HUVECs (#P20201, Innoprot) were cultured in endothelial growth medium (#C-22,010, PromoCell) with 1% (v/v) antibiotic-antimycotic solution (#15240-062, Invitrogen). Human trophoblast cell line, BeWo cells (#86,082,803, Sigma-Aldrich) were cultured in DMEM/F-12 medium (#11039-021, Invitrogen) containing 10% (v/v) fetal bovine serum (#10270-106, Invitrogen). All work was carried out in a Class I laminar flow hood. All cells were routinely tested for mycoplasma (every 3 months) and always gave a negative result.

Treatment and transfection of EnSCs

Before treatment or transfection of EnSCs, the culture medium was changed to fresh DMEM containing 2% (v/v) dextran coated charcoal stripped fetal bovine serum, 1% (v/v) antibiotic-antimycotic solution and 1% (v/v) L-glutamine for serum starvation. EnSCs were subjected to treatment with PlGF (#P1588, PlGF-1, Sigma-Aldrich) at a concentration of 20 ng/ml for 6 days [59]. The concentration was determined by a kinetic assay and time course experiments (Fig. 1 and Supplementary Fig. 1). For hyperosmolarity treatment in EnSCs, cells were treated with 800 mOsm in 2% DCC DMEM for 6 h. For gene silencing experiments, EnSCs were treated with siSGK1 (50 nM, #L-003027-00-0005, Dharmacon). The siRNAs were transfected with Lipofectamine RNAiMAX (#13,778,075, ThermoFisher Scientific) for 48 h with and without additional PlGF treatment. Stromal cell cultures were first treated with PlGF (20 ng/ml) for 4 days followed by transfection with SGK1 siRNA or in combination with PlGF for 48 h, and then continued with PlGF treatment for a further 2 days. The experimental groups are classified as Con (untreated EnSCs), PlGF, siSGK1 and siSGK1 + PlGF. Dimethyloxalylglycine, N-(Methoxyoxoacetyl)-glycine methyl ester (DMOG) (#D3695; Sigma-Aldrich) treatment in EnSCs was carried out for 24 h at a concentration of 0.5 mM.

Conditioned medium treatment of HUVECs

Post 6 days PlGF treatment in EnSCs, cell supernatant was collected as conditioned medium (CM). The control-CM (untreated) / PlGF-CM / siSGK1 CM / siSGK1 + PlGF CM were collected respectively and stored at -80 °C until processing. HUVECs were split and plated onto cell culture plates at a density as required. Post cell adhesion, the HUVECs were treated with respective conditioned medium diluted with HUVEC growth medium at 1:1 dilution factor and incubated at 37 °C for 48 h. HUVECs were treated with Dimethyloxalylglycine,

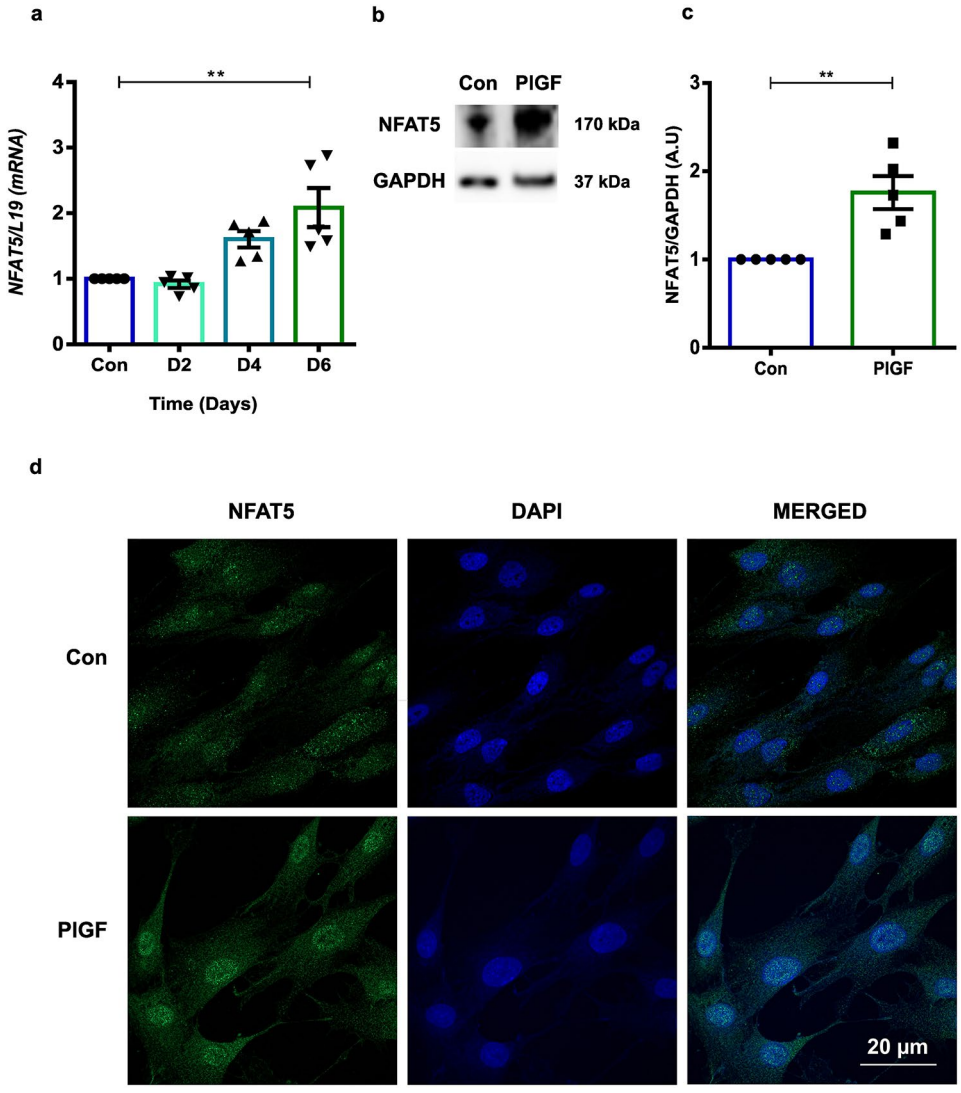

Fig. 1 PlGF activates NFAT5 expression and activity in EnSCs. (**a**) NFAT5 mRNA transcript kinetics in EnSCs treated with PlGF for 2, 4 and 6 days at a concentration of 20 ng/ml. *L19* was used as a housekeeping gene and the data was normalized to untreated (Con) ($n = 5$, **, $p < 0.01$). (**b**) Original Western blot analysis of NFAT5 protein with GAPDH as loading control in untreated (Con) and PlGF treated EnSCs. (**c**) Average NFAT5 protein levels after 6 days treatment with PlGF ($n = 5$, ** $p < 0.01$). The samples are represented after normalization with untreated control (Con). **d**) Immunofluorescence images confirms nuclear translocation of NFAT5 from the cytoplasm when activated by PlGF ($n = 3$). Scale bar: 20 µm. Data represented as arithmetic mean ± SEM. Significance was determined using student's unpaired two-tailed t-test with Welch's correction method. n represents the number of independent experiments (biological replicates)

N-(Methoxyoxoacetyl)-glycine methyl ester (DMOG) (#D3695; Sigma-Aldrich) to induce hypoxia for 24 h [60]. VEGF-A (#PHC9391, ThermoFisher Scientific) treatment was carried out for 24 h at a concentration of 40 ng/ml to induce vascular permeability [61]. The experimental groups in HUVECs are classified as Con-CM, PlGF-CM, siSGK1-CM and siSGK1 + PlGF-CM.

Quantitative real time-polymerase chain reaction (qRT-PCR)

Post treatment, cells were collected for downstream analysis of messenger RNA (mRNA) extraction and Quantitative Real-time PCR (qRT-PCR). Total RNA was extracted using TRizol™ reagent (#15,596,026, Invitrogen). One µg RNA was utilized to synthesize cDNA using the ThermoFisher Scientific Maxima™ H Minus cDNA Synthesis Master Mix with dsDNase (#M1681, Invitrogen). qRT-PCR was performed on the QuantStudio 3 Real-Time PCR System (Invitrogen) by using sets of gene-specific primers and the PowerUp™ SYBR® Green Master Mix (#A25742, Invitrogen). The relative differences in PCR product amounts were quantified by the $^{\Delta\Delta}C_T$ method, using ribosomal L19 (*L19*) as an internal housekeeping control [62]. Experiments were performed in triplicate (technical replicates). Melting curve was used to confirm amplification specificity. The gene expression levels of

the samples are provided as arbitrary units defined by the $^{\Delta\Delta}C_t$ method. All the gene-specific primers used in this study were designed using primeblast (NCBI) and purchased from Sigma-Aldrich. The primer sequence can be provided on request.

Western blotting

Whole cell protein lysate was extracted from EnSCs cultured on 6-well plates (approx. 1×10^6 at time of harvesting) using hot 1X Laemmli buffer with a cell scraper as previously reported [63]. Lamelli lysis buffer contains 0.5 M Tris hydrochloride (#9090.1, Roth) pH 6.8, 20% Sodium dodecyl sulfate (#151-21-3, Sigma-Aldrich), 0.1% Bromophenol blue (#34725-61-6, Serva),1% beta mercaptoethanol (#60-24-2, Sigma-Aldrich), and 20% glycerol (#56-81-5, Roth). Whole cell protein lysates were collected and heated at 95 °C for 3 min. Protein extracts were then loaded on to a 10% sodium dodecyl sulfate polyacrylamide gel (SDS-PAGE) using the XCell SureLock® Mini-Cell apparatus (Invitrogen) followed by electrophoresis. The protein from the gel was then transferred onto a nitrocellulose membrane (#10,600,003, GE HealthCare). After incubation with 5% non-fat milk or BSA in TBST (10 mM Tris, pH 8.0, 150 mM NaCl, 0.5% Tween 20) for 60 min, the membrane was washed once with TBST and incubated with primary antibodies against NFAT5 (1:2000, #NB20-3446, Novus Biologicals) [64], SGK1 (1:1000, #07-315, Merck) [65], phospho-SGK1 (1:1000, #36−002, Merck) [65], p38 MAPK (1:1000, #8690S, Cell Signaling Technologies) [66], phospho-p38 MAPK (1:1000, #4511, Cell Signaling Technologies) [66], VEGF-A (1:3000, #ab46154, abcam) [67], VEGFR1 (1:1000, #2893, Cell Signaling Technologies) [68], VEGFR2 (1:1000, #2479, Cell Signaling Technologies) [69], or GAPDH (1:1000, #5174, Cell Signaling Technologies) [70] at 4 °C for overnight. Membranes were then washed three times for 15 min and incubated with HRP-conjugated anti-rabbit secondary (1:2000, #7074s, Cell Signaling Technologies) [71] antibodies for 1 h in room temperature. Post-secondary antibody incubation, blots were washed with TBST three times for 15 min and developed with the ECL system (#R-03031-D25, Advansta) according to the manufacturer's protocols. The fluorescence signals were scanned with an iBright CL1000 (ThermoFisher Scientific), and the intensities were assessed by densitometry analysis to measure the relative expression of the target proteins using GAPDH as a loading control by ImageJ software [72].

Immunofluorescence

For immunolabelling of cells, EnSCs (5000 cells) were seeded on 4-well glass chamber slides (#94.6170.402, Sarstedt) and cultured in 10% DCC FBS containing DMEM medium. Post treatment with PlGF as described above, the cells were fixed with 4% paraformaldehyde for 15 min, washed with PBS, and permeabilized for 15 min in 0.1% Triton X-100/PBS. The samples were then blocked with 5% BSA in 0.1% TritonX-100/PBS for 1 h at RT and washed with PBS. The slides were then incubated with primary antibodies for NFAT5 (1:200, #NB20-3446, Novus Biologicals) [64] at 4 °C overnight. Subsequently, washed with PBS and incubated with FITC conjugated secondary antibody (#4412, Alexa Fluor 488 Conjugate, ThermoFisher Scientific) for 1 h at room temperature. Post incubation, slides were washed again with PBS, dehydrated, air-dried and mounted using ProLong Gold antifade reagent containing DAPI (#P36931, Invitrogen). Fluorescence was detected with LSM 800 confocal laser scanning microscope (Zeiss). The images were captured using oil immersion, 40x objective lens. Scale bar −20 µm. Mean fluorescence intensities were calculated using ImageJ software.

Luciferase reporter assay

EnSCs cells were seeded onto 24-well plates at a density of 5×10^4 cells/well with 10% DCC-FBS/DMEM and allowed to attach for 24 h. Post serum starvation, cells were transfected with HIF-1α vector (#87,261, Addgene) using Lipofectamine LTX with Plus reagent (#15,338,100, ThermoFisher Scientific) as per the manufacturer's instructions. After transfection for 24 h, cells were subjected to treatment with PlGF±siSGK1 as described above. The reporter activation was determined using the Dual-Luciferase Reporter Assay System (#E2920, Promega) according to the manufacturer's instructions.

Briefly, growth medium was removed and cells were washed with PBS. Subsequently, cells were lysed for 15 min at room temperature using 1X passive lysis buffer. Lysed cells were used for determination of luciferase activity. LAR II reagent was added to each well, and firefly luminescence was measured using a microplate reader (LUX VARIOSKAN, ThermoFisher Scientific). Next, Stop & Glo reagent was added to each well and renilla luciferase activity was measured using a microplate reader. Three replicate wells were used for each analysis, and the results were normalized to the activity of renilla luciferase.

ELISA

The secreted VEGF-A levels in PlGF-conditioned medium were measured with ELISA. Briefly, after the treatment of EnSCs with PlGF as described above, the conditioned medium was harvested and stored at -80 °C. The collected medium was processed with Human ELISA kit for VEGF-A (#BMS277-2, Invitrogen) following the manufacturer's instructions performed in biologically independent experiments (with three technical replicates).

Preparation of conditioned medium for proteomic analysis

For proteome analyses, conditioned medium (three biological replicates) was collected from EnSCs treated with and without PlGF as mentioned above. For precipitation of protein from conditioned medium, 100% acetone (ice cold): 100% MeOH (ice cold): protein solution was mixed at a ratio of 8:1:1, followed by incubation at -20 °C overnight. Post incubation the samples were washed (2X) at 2,500 g, 4 °C for 20 min. Post washing, the supernatant was then aspirated, and the pellet was air dried. After desalting using C18 stage tips, extracted peptides were separated on an Easy-nLC 1200 system coupled to a Q Exactive HFX mass spectrometer (ThermoFisher Scientific) as detailed in [73]. The peptide mixtures were separated using a 90 min segmented gradient from to 10-33-50-90% of HPLC solvent B (80% acetonitrile in 0.1% formic acid) in HPLC solvent A (0.1% formic acid) at a flow rate of 200 nl/min. The 12 most intense precursor ions were sequentially fragmented in each scan cycle using higher energy collisional dissociation (HCD) fragmentation. Acquired MS spectra were processed with MaxQuant software package version 1.6.7.0 with integrated Andromeda search engine [74]. A database search was performed against a target-decoy Homo sapiens database obtained from Uniprot, containing 103.859 protein entries and 286 commonly observed contaminants. Peptide, protein and modification site identifications were reported at a false discovery rate (FDR) of 0.01, estimated by the target/decoy approach and the fold change cut-off was set at $>\pm 1.0$ [75] The LFQ (Label-Free Quantification) algorithm was enabled, as well as match between runs and LFQ protein intensities were used for relative protein quantification. Data analysis was performed using Perseus [76], DEP and R packages.

BrdU cell proliferation

The effect of PlGF treated CM on HUVEC proliferation was measured using the BrdU cell proliferation assay on 96-well plates with 3000 cells (#QIA58, Sigma-Aldrich). Briefly after the treatment of HUVECs with respective CM for 48 h or/and thymidine (2 mM; #T1895, Sigma-Aldrich) for 42 h. Post treatment the cells were immunolabelled for BrdU and the cells incubated for an additional 24 h. Incorporated BrdU was detected by the BrdU Cell Proliferation Assay as instructed in the manufacture's protocol. The experiment was performed in biologically independent experiments (with three technical replicates).

Wound healing scratch assay

GFP-tagged HUVECs were seeded in 6-well plates at a concentration of 2×10^5 cells per well. After reaching 100% confluency, HUVECs were deprived of serum for 12 h and scratched with a sterile P200 pipette tip as previously described. After removal of the debris by repeated washes, cells were subjected to respective CM treatment and scratch wound closure was closely monitored by fluorescence microscopy (EVOS M7000 cell imaging system, ThermoFisher Scientific) capturing images of the same field with a 4X objective at 0 h and 24 h. The percentage of migrated area was calculated with Image J software (v1.53k) [77]. The experiment was performed in biologically independent experiments (with three different fields of view taken for the average).

In vitro tube formation assay

The effect of CM on angiogenic potential was assessed by the spontaneous formation of capillary-like structures by the GFP-tagged HUVECs. 96-well plates were coated with ice-cold Matrigel solution (#3533-005-02, 3533-005-02) and incubated at 37 ℃ for 60 min to allow the Matrigel to solidify. GFP-tagged HUVECs were harvested, suspended in serum-reduced (2%) endothelial growth medium, seeded in the Matrigel-coated wells at a density of 5×10^4 cells/well in 100 µl of respective CM/DMOG treatment solution. Images of the tubular structures were taken using a fluorescence microscopy (EVOS M7000 cell imaging system, ThermoFisher Scientific) capturing images of the same field with a 4X objective for every 3 h. The experiment was performed in biologically independent experiments and the relative tube length and relative number of tubes formed at 24 h were calculated using an angiogenesis plugin with Image J software (v1.53k) [78].

Endothelial barrier function study with Electrical Impedance spectroscopy (EIS)

An EIS approach was employed to study the influence of stroma secreted conditioned medium on the endothelial barrier function of HUVECs. The E16 plate (#5,469,830,001, Agilent, Germany) was mounted on to the xCELLigence RTCA (Agilent, Germany) for background reading. Later, HUVECs were trypsinized and 7000 cells per well was seeded. Respective treatment conditions with CM (technical duplicates) as mentioned above was added to the E16 plates with cells and kept for incubation at 37 °C for 30 min, for cells to equilibrate and adhere. Post cell adhesion, E16 plate containing cells was mounted on to the xCELLigence RTCA for impedance measurements. Live cell impedance was monitored every 15 min for a total period of 24 h. The experiment was performed in biologically independent experiments and the data is represented as cell index. Data acquisition and data analysis was performed using RTCA Software Pro (Agilent, Germany).

BeWO cell invasion through endothelial monolayer with electrical impedance spectroscopy (EIS)

The invasion of BeWo through the endothelial monolayer was studied with EIS measurements. The E16 plates were coated with 0.1% gelatin and let to incubate for an hour at 37 °C. Next, 100 µl of HUVEC growth medium was added to E16 plate for background measurement. The plate was mounted on to the xCELLigence RTCA (Agilent Technologies, Germany) for background reading. Later, HUVECs were trypsinized and 5000 cells per well were added to the E16 plates and kept for incubation at 37 °C for cells to equilibrate and adhere. Post 24 h, the cells were treated with respective treatment conditions with CM (Con / PlGF / siSGK1 / siSGK1 + PlGF) as mentioned above for 48 h. Ten hours prior treatment end point, E16 plates containing cells were clamped again onto the xCELLigence RTCA and placed in the incubator at 37 °C. Live cell impedance was monitored every 15 min for a total period of 10 h to ensure stromal cell monolayer formation.

Post treatment time point, the cell index measurement was paused and 2500 BeWo cells per 100 µl of 10% FBS DMEM were added. EIS cell index measurement was continued to monitor to the BeWo invasion through CM treated HUVEC monolayer. Live cell impedance was monitored every 30 min for a total period of 8 h. The experiment was performed in biologically independent experiments and the data is represented as normalized cell index relative to the time point BeWo cells were added to the HUVEC monolayer. Data acquisition and data analysis was performed using RTCA Software Pro (Agilent Technologies, Germany).

In silico data analysis

In silico analysis was performed on an open-access gene-expression data platform. The gene expression of *NFAT5* was verified by analysis of the normal endometrium at distinct phases of the menstrual cycle (*GDS2052*) [41]. To investigate the significance of *NFAT5* in PE pathogenesis, we obtained its gene expression data in human decidua of pre-symptomatic preeclamptic women and healthy pregnant women (*GDS3467*) [43].

Statistical analysis

Data are presented here as means ± SEM. n represents the number of independent experiments (biological replicates). All treatment groups are normalized with their respective control groups in EnSCs (Con) and HUVECs (Con-CM) respectively. Data represented were analysed for significance using student's unpaired two-tailed t-test with Welch's correction approach and One-way ANOVA. Results with $p < 0.05$ were considered statistically significant. Figures and statistical analysis were made in Graphpad Prism (v 7.0) and Inkscape (v 1.3).

Results

PlGF drives tonicity independent activation of NFAT5 in endometrial stromal cells

We first explored the spatio-temporal expression of *NFAT5* in the endometrium. Expression of *NFAT5* (Supplementary Fig. 1a) was found to be higher in the proliferative phase compared with the late secretory phase of the menstrual cycle (*GEO 2052*) [41]. Single cell analysis confirmed high *NFAT5* expression in the stromal population among the other endometrial cell types and extra villous trophoblast (Supplementary Fig. 1b & c). According to the Human Protein Atlas, NFAT5 is expressed throughout the endometrium and staining was highest in the perivascular area and blood vessels [79] (Supplementary Fig. 1d). We next assessed the involvement of NFAT5 in the etiology of PE pathogenesis. To address this, we manually mined expression levels of *NFAT5* obtained from gene expression studies of the first trimester decidua prior to the onset of PE compared with healthy pregnancies (*GEO 3467*) [43]. We found that *NFAT5* transcripts were upregulated in the decidua of pre-symptomatic women who developed PE later (Supplementary Fig. 1e). Taken together, the *in-silico* analysis reveals that endometrial NFAT5 expression is highest in the proliferative phase and is associated prior to the onset of PE.

PlGF is a member of the VEGF superfamily and aberrant expression is associated with abnormal blood vessel physiology *via* NFAT5 [52]. Thus, we sought to determine a putative link between PlGF on NFAT5 regulation in endometrial cells. EnSCs were treated with varying concentrations (titration of 2.5–50 ng/ml) of PlGF for 6 days. As illustrated in Supplementary Fig. 2a, *NFAT5* mRNA expression was highly upregulated by PlGF at a concentration of 20 ng/ml compared with the other concentrations tested. The time kinetics study revealed gene expression of *NFAT5* when EnSCs were treated with PlGF (20 ng/ml) were highest after 6 days of treatment (Fig. 1a). All proceeding experiments used PlGF at a concentration of 20 ng/ml for a treatment period of 6 days in EnSCs. Consistent with our mRNA data, PlGF also significantly upregulated NFAT5 protein levels in parallel (Fig. 1b-c and Supplementary Fig. 2b). Further, we examined PlGF activated NFAT5 spatial regulation in EnSCs using an immunofluorescence approach. Endogenous NFAT5 was localized to the cytosol in untreated EnSCs and was found to be translocated to the nucleus upon PlGF treatment (Fig. 1d). NFAT5 is well recognized to be activated under hyperosmolarity cellular stress (Hyp Osm), we compared its transcriptional activity in EnSCs by treating with Hyp Osm (800 mOsm/ml) medium for 3 h as a positive control (Supplementary Fig. 3a-c). Thus, we observed that PlGF can activate NFAT5 in EnSCs in a *tonicity independent* manner.

p38 MAPK regulated NFAT5 activation upregulates SGK1 expression in endometrial stromal cells

p38 Mitogen-Activated Protein Kinase (p38 MAPK), is known to activate NFAT5 transcriptional activation under hypertonic stimulus [80]. To verify the participation as an upstream target of NFAT5, we examined protein levels of total and phosphorylated levels of p38 MAPK following treatment with PlGF. Figure 2a-c and Supplementary Fig. 4 demonstrates the increased levels of total p38 MAPK protein, with significant upregulation of phosphorylated levels of p38MAPK. NFAT5 is a regulator for various angiogenic mediators and factors including; SGK1, HIF-1α and VEGF-A [52]. Next a further series of experiments tested if PlGF indeed contributed to the activation of these downstream targets. Our findings show both total and phosphorylated SGK1 protein levels were significantly upregulated in PlGF treated stromal cells (Fig. 2a, d-e). SGK1 is a known stimulator of

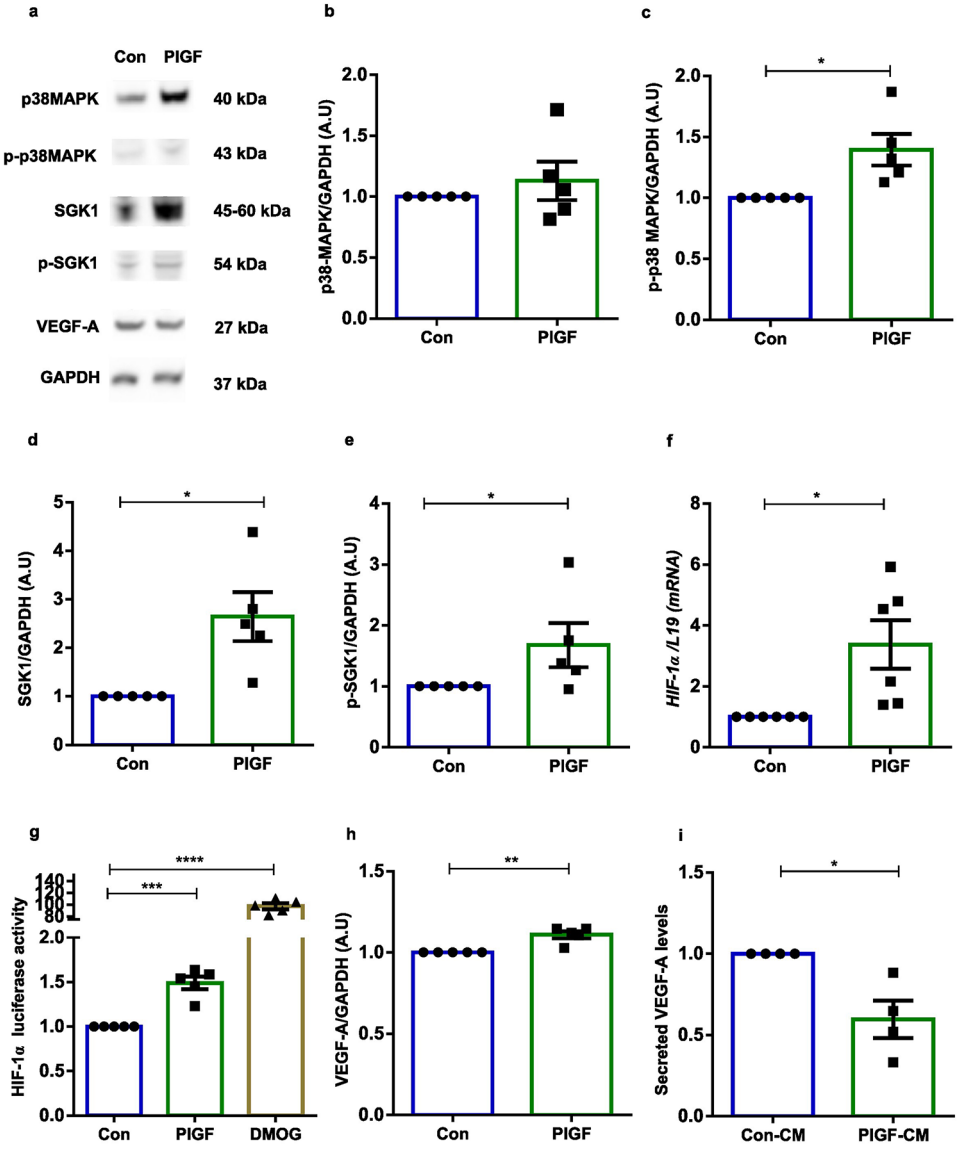

Fig. 2 PlGF-NFAT5 angiogenic signaling axis in EnSCs. (**a**) Original Western blots of total and phosphorylated levels of p38 MAPK, SGK1 and total VEGF-A targets with GAPDH as loading control in untreated (Con)and PlGF treated EnSCs. (**b**-**e**) Average protein expression levels of total and phosphorylated levels of p38 MAPK and SGK1 targets in untreated (Con) and PlGF treated EnSCs ($n = 5$, *, $p < 0.05$). (**f**) qPCR analysis of *HIF-1α* transcript levels in untreated (Con) and PlGF treated EnSCs. *L19* was used as a housekeeping gene ($n = 5$, *, $p < 0.05$). (**g**) Luciferase reporter assay measuring the HIF-1α promoter activity in untreated (Con), PlGF and DMOG (positive control for hypoxia, 0.5 mM for 24 h) treated EnSCs ($n = 5$, ***, $p < 0.001$, ****, $p < 0.0001$). (**h**) Immunoblotting showing average protein expression levels of VEGF-A (Con) in untreated and PlGF treated EnSCs ($n = 5$, **, $p < 0.01$). (**i**) Supernatant from untreated (Con) and PlGF treated EnSCs was collected and secreted VEGF-A levels were quantified with ELISA ($n = 5$, *, $p < 0.05$). Data represented here as arithmetic mean ± SEM. The treatment samples groups (PlGF) are represented after normalization with untreated control (Con). Significance was determined using student's unpaired two-tailed t-test with Welch's correction method. n represents the number of independent experiments (biological replicates)

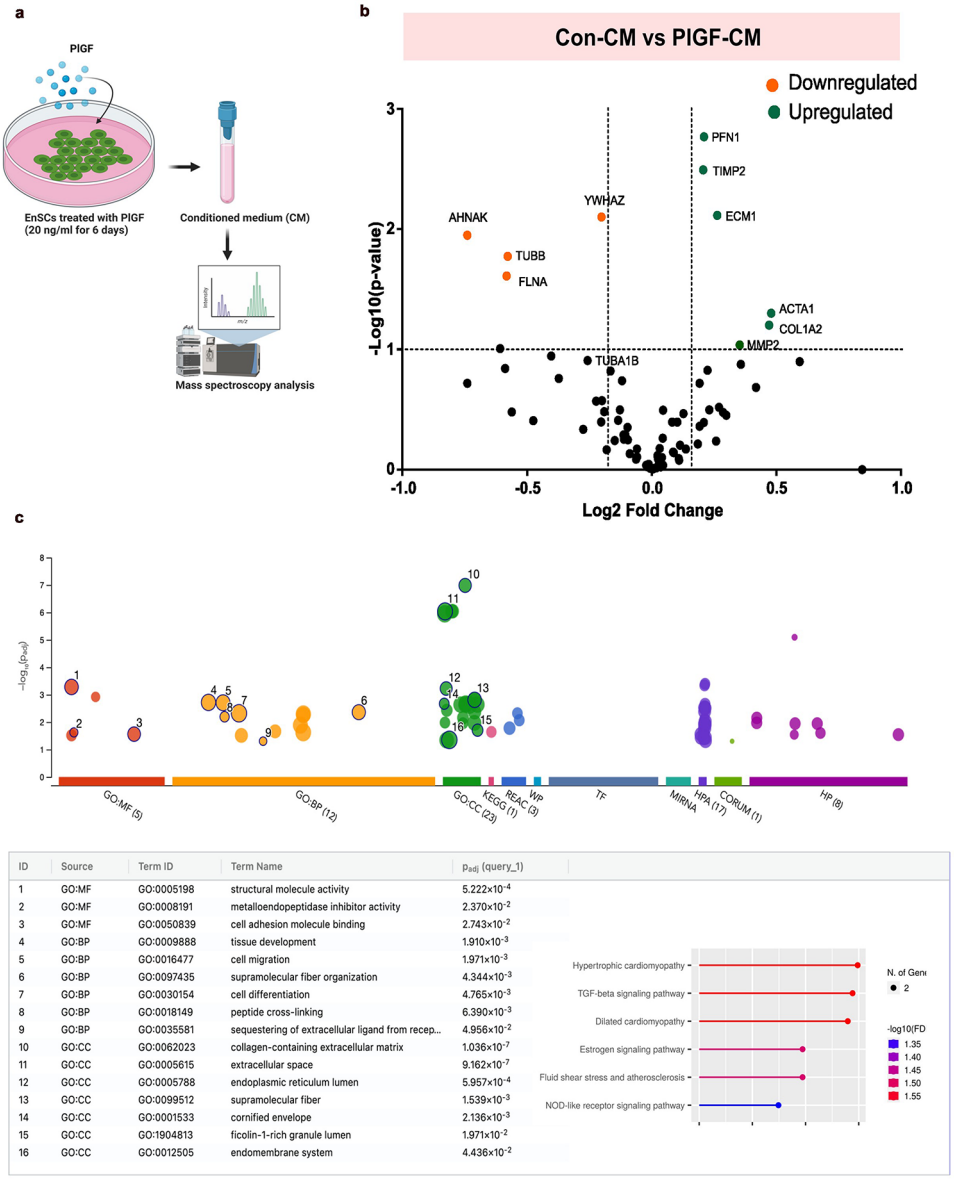

ID	Source	Term ID	Term Name	p_{adj} (query_1)
1	GO:MF	GO:0005198	structural molecule activity	5.222×10^{-4}
2	GO:MF	GO:0008191	metalloendopeptidase inhibitor activity	2.370×10^{-2}
3	GO:MF	GO:0050839	cell adhesion molecule binding	2.743×10^{-2}
4	GO:BP	GO:0009888	tissue development	1.910×10^{-3}
5	GO:BP	GO:0016477	cell migration	1.971×10^{-3}
6	GO:BP	GO:0097435	supramolecular fiber organization	4.344×10^{-3}
7	GO:BP	GO:0030154	cell differentiation	4.765×10^{-3}
8	GO:BP	GO:0018149	peptide cross-linking	6.390×10^{-3}
9	GO:BP	GO:0035581	sequestering of extracellular ligand from recep...	4.956×10^{-2}
10	GO:CC	GO:0062023	collagen-containing extracellular matrix	1.036×10^{-7}
11	GO:CC	GO:0005615	extracellular space	9.162×10^{-7}
12	GO:CC	GO:0005788	endoplasmic reticulum lumen	5.957×10^{-4}
13	GO:CC	GO:0099512	supramolecular fiber	1.539×10^{-3}
14	GO:CC	GO:0001533	cornified envelope	2.136×10^{-3}
15	GO:CC	GO:1904813	ficolin-1-rich granule lumen	1.971×10^{-2}
16	GO:CC	GO:0012505	endomembrane system	4.436×10^{-2}

Fig. 3 Proteomics profile of PlGF treated conditioned medium (CM) from EnSCs. (**a**) Schematics describing the experimental approach of mass spectrometry analysis on CM (supernatant) collected from EnSCs post 6 days treatment without (Con) and with PlGF (20 ng/ml). (**b**) Volcano plot showing significantly upregulated (green) and downregulated (orange) proteins in PlGF treated CM from EnSCs. Each point represents one protein; black points are the rest of the proteins obtained in the global proteomic analysis. The significance threshold range is 0.05 and the fold change threshold is -1 and + 1. (**c**) GO enrichment analysis of the protein signature depicting the enriched biological process and pathways associated with PlGF treated CM in EnSCs. n represents the number of independent experiments (biological replicates)

HIF-1α, a known modulator in angiogenic signaling [81, 82]. Elevated levels of *HIF-1α* transcripts were observed with PlGF treatment in stromal cells (Fig. 2f). Additionally, PlGF exerted a strong stimulating effect on HIF-1α promoter activity (luciferase) in EnSCs (Fig. 2g). DMOG treatment was used as positive control for HIF-1α promoter activation (0.5 mM for 24 h) [60].

To further validate the angiogenic pathway mediated by NFAT5 activation, we verified the intracellular and secreted protein levels of pro-angiogenic factor, VEGF-A. PlGF mediated NFAT5 stimulation significantly increased cellular VEGF-A protein levels in EnSCs (Fig. 2a-h). Surprisingly, the secreted protein levels of VEGF-A (Fig. 2i) in EnSCs supernatant (CM) was decreased compared with untreated control levels. These data identify the aberrant PlGF mediated angiogenic signaling in EnSCs with a decrease in secreted proangiogenic factor VEGF-A.

Secretome analysis reveals that PlGF treated CM is associated with pathological angiogenic signaling

To investigate if PlGF can dysregulate other angiogenic mediators in EnSCs, we sought to understand its comprehensive and global effect on stromal cell secreted factors. We utilized proteomics to characterize the supernatant (CM) from EnSCs. Liquid chromatography mass spectrometry (LC-MS) analysis was performed by comparing the protein cargo present in Con-CM ($n=3$) and PlGF-CM ($n=3$) collected from EnSCs post 6 days treatment with and without PlGF as described in Fig. 3a. This comparison revealed a total of 68 dysregulated secreted proteins. Differentially regulated proteins were shown in volcano plots as seen in Fig. 3b. A total of 36 upregulated and 32 downregulated differentially regulated proteins were identified in the CM as being associated with PlGF treatment in the EnSCs. Some of the significantly upregulated proteins (green) in PlGF-CM were actin and extra cellular matrix (ECM) associated components such as ECM-1, ACTA1, PFN1, COL1A2, MMP2 and inhibitors of the matrix metalloproteinases such as TIMP2. The significantly downregulated proteins (orange) include AHNAK, FLNA and YWHAZ. Other ECM associated proteins such as COL2A6, COL6A3, and COL3A1 were not differentially expressed based on the differential expression thresholds we used in this study, however we observed modest but significant changes in their expressions too. Gene Ontology (GO) analysis of the protein signature associated with supernatant from the PlGF treated cells identified pathways associated with structural remodelling, ECM modification and pathological vessel development (Fig. 3c). Thus, the proteomic analysis points to an anti-angiogenic signature mediated by PlGF.

HUVECs display abnormal 'hypersprouting' behaviour when treated with conditioned medium (CM)

Pathological PlGF is associated with poor vessel development in the retina [83]. We postulated that the paracrine signaling from PlGF treated endometrial cells would also support poor vessel formation. To test this conjecture, HUVECs were treated with CM collected from untreated or PlGF treated EnSCs (Fig. 4a). We then verified its effects on angiogenic checkpoints in HUVECs employing different functional assays. As seen in Fig. 4b, PlGF-CM significantly increased cell proliferation in HUVECs as evidenced with the BrdU ELISA assay. Further, a wound healing scratch assay with GFP-HUVECs showed reduced cell migration upon PlGF-CM treatment (Fig. 4c-d) and an in vitro tube formation assay showed no significant change in tube length between Con-CM and PlGF-CM treatment on HUVECs (Fig. 4e-f). However, PlGF-CM treated HUVECs displayed a greater number of endothelial cell branches pointing to an abnormal 'hypersprouting' behaviour (Fig. 4e-g). Hypersprouting behaviour in endothelial cells is a phenotype of deregulated Notch signaling [84]. To investigate Notch signaling in PlGF-CM mediated anti-angiogenic behaviour seen in HUVECs, gene expression levels of Notch signaling effectors such as Notch receptors (*Notch 1 and Notch 2*), ligands (*Dll4 and Jagged-1*) and target genes (*Hey 1 and Hes1*) were downregulated with PlGF-CM treated HUVECs (Fig. 4h-l and Supplementary Fig. 5a). Further, to substantiate the increase of hypersprouting and notch downregulation, we verified the protein levels of VEGF receptors and VEGF-A levels in HUVEC after CM treatment. PlGF-CM treated HUVECs showed enhanced VEGFR2 protein expression with downregulated levels of VEGFR1 and VEGF-A (Fig. 4m-n and Supplementary Fig. 5b). Thus, these results strongly suggest that PlGF-CM modulate hypersprouting in HUVECs *via* repression of notch signaling and upregulation of VEGFR2. Regulation and maintenance of the endothelial barrier during angiogenesis is critical for end organ function [85]. The influence of the stromal secreted factors on endothelial barrier function regulating vascular resistance and permeability is studied with an EIS approach. EIS measurements revealed an increase in cell index in HUVECs with PlGF-CM treatment, demonstrating an increase of junctional resistance and decrease in permeability between endothelial cells (Fig. 4o). Together, these data indicate that dysregulated PlGF-NFAT5-SGK1 signaling in stroma mediate negative angiogenic effects on HUVECs with an altered secretome signature.

Silencing of SGK1 improves secreted VEGF-A levels in EnSCs

Endometrial SGK1 plays a paramount role in endometrial physiology and for the maintenance of pregnancy. We therefore examined whether SGK1 is the key 'check point' molecule driving the stroma-endothelial paracrine pathway upon PlGF stimulation. SGK1 gene silencing was efficient, suppressing both total and phosphorylated SGK1 protein expression levels in EnSCs (Fig. 5a-c and Supplementary Fig. 6).

Similarly, SGK1 inhibition with PlGF again paralleled the effect on gene silencing, significantly downregulating both total and phosphorylated levels of SGK1 protein (Fig. 5a-c). Strikingly, silencing of SGK1 transcripts was also followed by significant decrease in *HIF-1α* mRNA levels and promoter activity in EnSCs (Fig. 5d-e). The effect was mimicked in EnSCs treated with siSGK1 + PlGF as well (Fig. 5d-e). DMOG treatment in EnSCs was used as a positive control (0.5 mM for 24 h). Intriguingly, attenuated SGK1 expression in EnSCs did not significantly alter total VEGF-A levels when using western blotting (Fig. 5a-f). However, SGK1 silencing improved secreted VEGF-A levels in the CM (Fig. 5g)

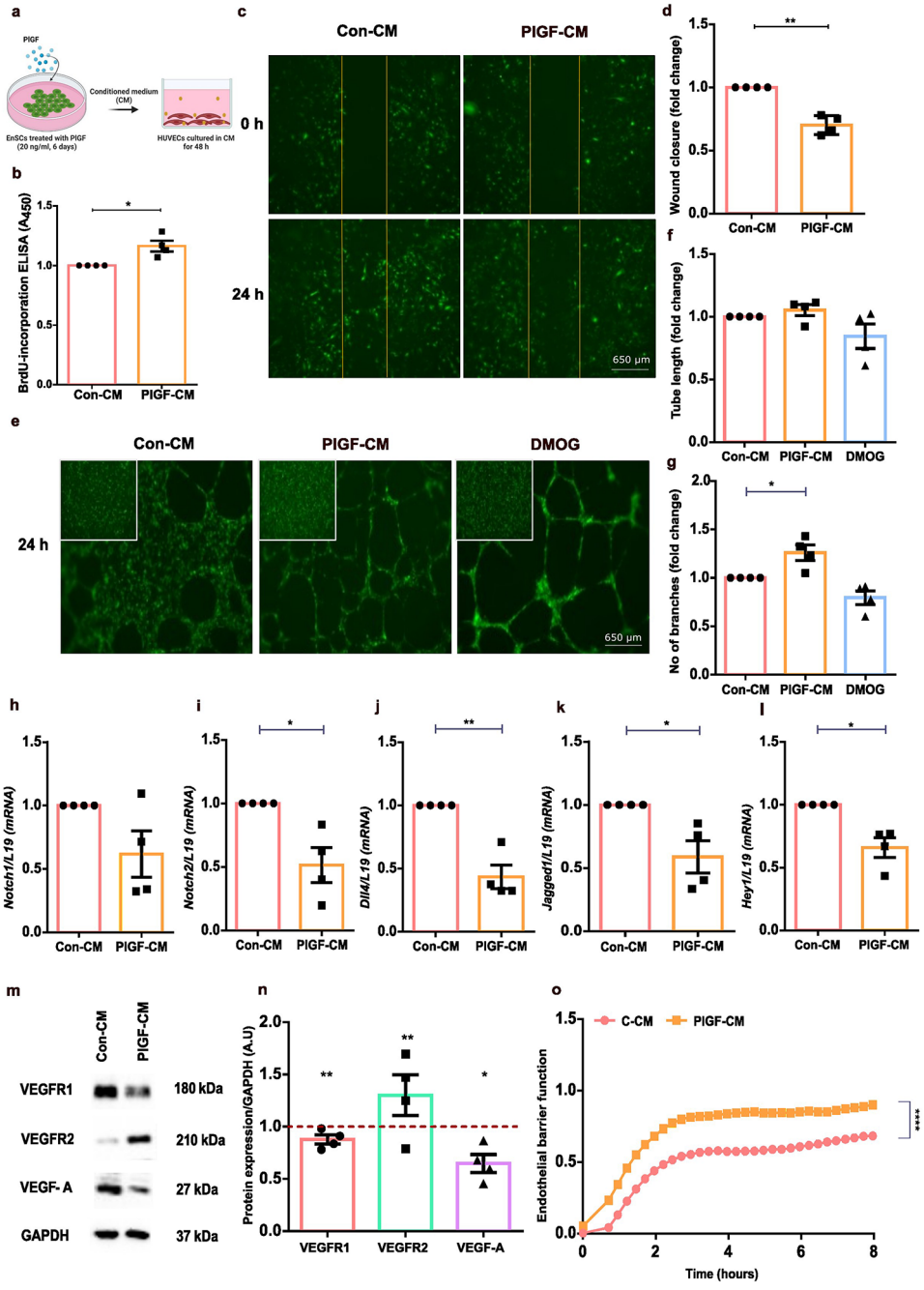

Fig. 4 Angiogenic effect of PlGF-NFAT5 signaling axis on HUVECs. (**a**) Schematics describing the experimental approach of CM treatment on HUVECs. (**b**) BrdU incorporated ELISA analysis for cell proliferation measured in Con-CM and PlGF-CM treated HUVECs ($n=4$, *, $p<0.05$). (**c**) Representative fluorescence microscopic images of wound healing scratch assay on Con-CM and PlGF-CM treated HUVECs at 0 and 24 h ($n=4$). Yellow line represents the wound area created. Scale bar: 650 µm. (**d**) Wound closure rate in Con-CM and PlGF-CM treated HUVECs at 24 h ($n=4$, **, $p<0.01$) explain normalization. (**e**) Representative fluorescence microscopic images of tube formation assay on a matrigel with Con-CM, PlGF-CM and DMOG (positive control; 0.5 mM for 24 h) treated HUVECs at 24 h ($n=4$). The insert displays HUVECs seeded on the matrigel at 0 h. Scale bar: 650 µm. (**f**) Tube formation assay analysis showing tube length in Con-CM, PlGF-CM and DMOG treated HUVECs at 24 h ($n=4$). (**g**) Tube formation assay analysis depicting number of branches in Con-CM, PlGF-CM and DMOG treated HUVECs at 24 h ($n=4$, *, $p<0.05$). (**h**-**l**) qPCR analysis of Notch receptors (*Notch 1 and Notch 2*), ligands (*Dll4 and Jagged-1*) and target genes (*Hey 1*) in Con-CM and PlGF-CM treated HUVECs. *L19* was used as a housekeeping control. ($n=4$, *, $p<0.05$, **, $p<0.01$). (**m**) Original Western blots of VEGFR1, VEGFR2 and VEGF-A targets with GAPDH as loading control in Con-CM and PlGF-CM treated HUVECs. (**n**) Average protein levels of VEGFR1, VEGFR2 and VEGF-A in Con-CM and PlGF-CM treated HUVECs ($n=4$, *, $p<0.05$, **, $p<0.01$). Data represented here as arithmetic mean ± SEM. The treatment samples groups (PlGF-CM) are represented after normalization with control (Con-CM). Significance was determined using student's unpaired two-tailed t-test with Welch's correction method. (**o**) EIS analysis of cell impedance values in Con-CM and PlGF-CM treated HUVEC monolayer representing endothelial barrier function ($n=4$, ****, $p<0.0001$). Significance was determined using student's unpaired two-tailed t-test with Welch's correction method for cell impedance values at 4 h. n represents the number of independent experiments (biological replicates)

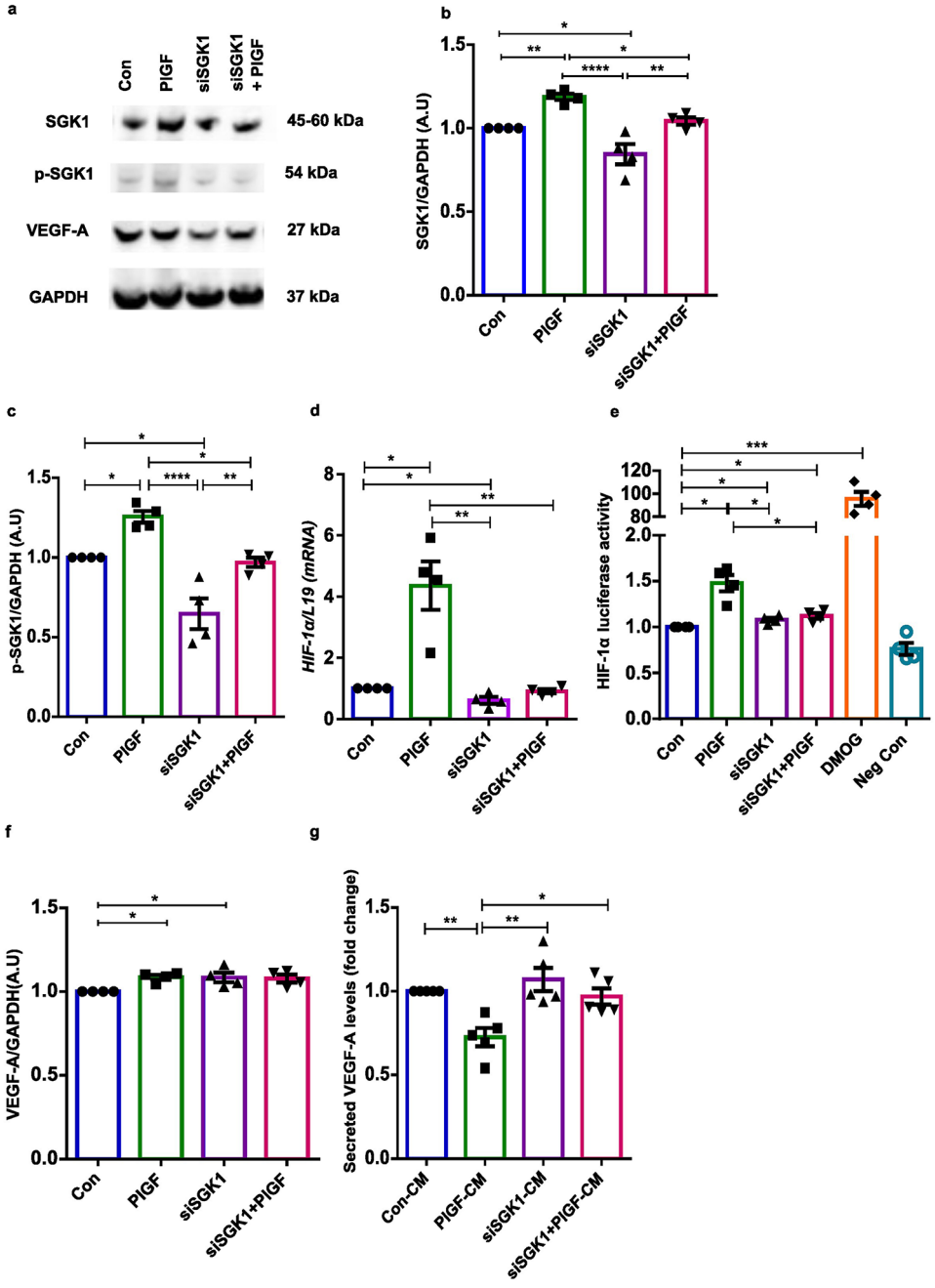

Fig. 5 Inhibition of SGK1 gene expression in EnSCs. (**a**) Original Western blots of total and phosphorylated levels of SGK1 and total VEGF-A targets with GAPDH as loading control in untreated (Con), PlGF and siSGK1 ± PlGF EnSCs. (**b**-**c**) Average protein levels of total and phosphorylated SGK1 in untreated (Con), PlGF and siSGK1 ± PlGF treated EnSCs ($n = 4$, * $p < 0.05$, ** $p < 0.01$, ***, $p < 0.001$, ****, $p < 0.0001$). (**d**) qPCR analysis of *HIF-1α* transcript levels in untreated (Con), PlGF and siSGK1 ± PlGF treated EnSCs ($n = 4$, * $p < 0.05$, ** $p < 0.01$). *L19* was used as a housekeeping control. (**e**) Luciferase reporter assay analysis of HIF-1α promoter activity in untreated (Con), PlGF, siSGK1 ± PlGF and DMOG (57 nM) treated EnSCs ($n = 4$, * $p < 0.05$, ***, $p < 0.001$). (**f**) Average protein levels of VEGF-A in untreated (Con), PlGF and siSGK1 ± PlGF treated EnSCs ($n = 4$, * $p < 0.05$, ** $p < 0.01$). (**g**) ELISA analysis measuring secreted VEGF-A protein levels in CM from untreated (Con), PlGF and siSGK1 ± PlGF treated EnSCs ($n = 4$, * $p < 0.05$, ** $p < 0.01$). Data represented here as arithmetic mean ± SEM. The treatment samples groups (PlGF/siSGK1/siSGK + PlGF) are represented after normalization with control (Con). Significance was determined using student's unpaired two-tailed t-test with Welch's correction method and One-way ANOVA. n represents the number of independent experiments (biological replicates)

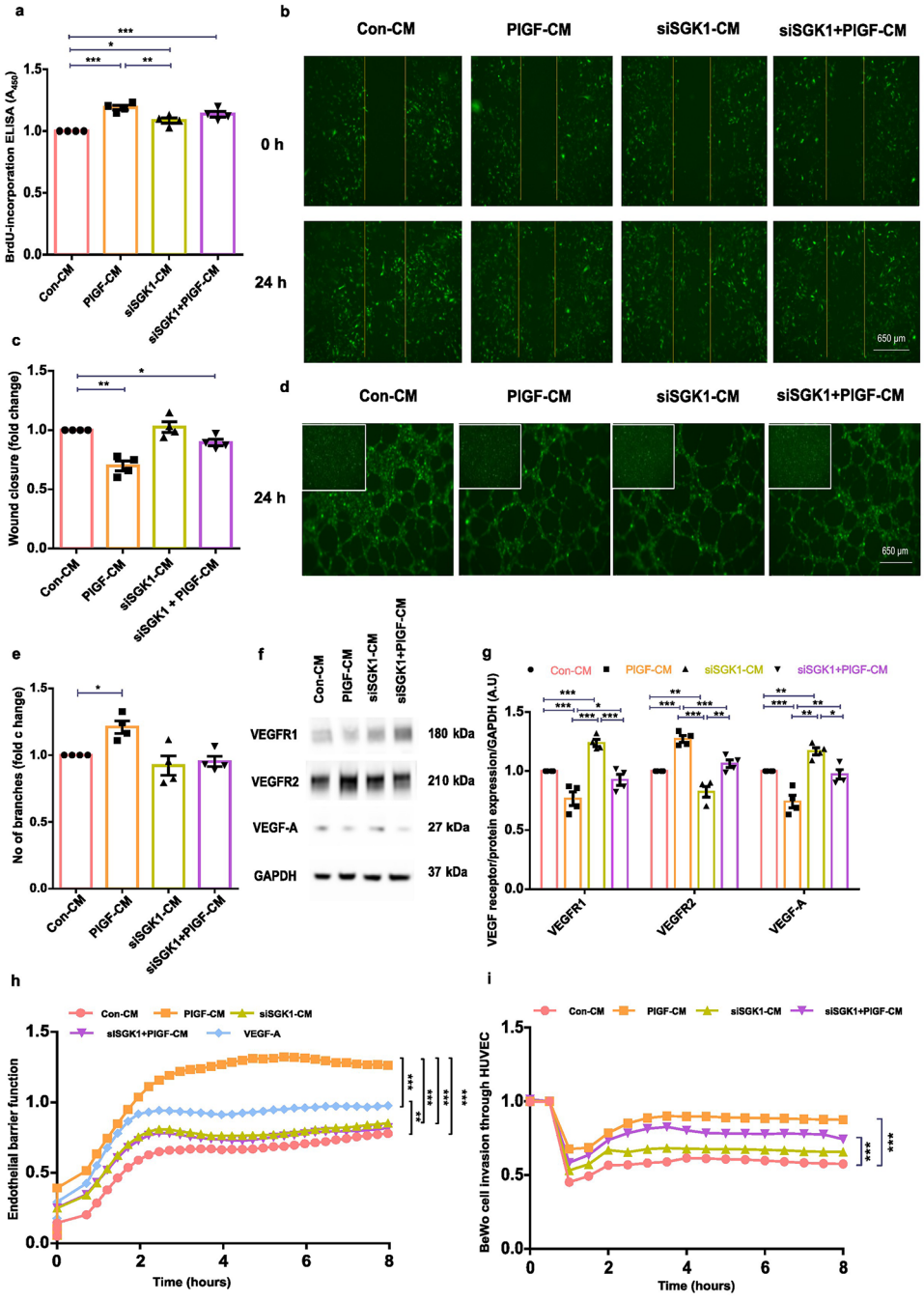

Fig. 6 (See legend on next page.)

and the VEGF-A protein signature (total and secreted) remained the same also in sample groups where siSGK1 inhibition was combined with PlGF treatment in EnSCs (Fig. 5a, f-g). These results confirm the key molecular role of SGK1 in the angiogenic communication pathway.

Inhibition of endometrial stromal SGK1 improves angiogenic behaviour of HUVECs

To explore the functional relevance of SGK1 in mediating the paracrine mechanism, HUVECs were treated with CM from EnSCs with SGK1 inhibition with and without PlGF treatment. siSGK1±PlGF-CM decreased cell proliferation and improved cell migration behaviour in HUVECs as seen with Con-CM (Fig. 6a -c). Further, the tube formation ability in HUVECs was improved both with siSGK1±PlGF-CM with decrease in number of branches observed (Fig. 6d-e). siSGK1±PlGF-CM treatment in HUVECs also showed an increase in notch receptors (*Notch 1 and Notch 2*), ligands (*Dll4 and Jagged-1*), and target genes (*Hey 1 and Hes1*), confirming

(See figure on previous page.)

Fig. 6 Silencing of SGK1 improved angiogenic effects in HUVECs. (**a**) BrdU ELISA analysis of cell proliferation in Con-CM, PlGF-CM and siSGK1 ± PlGF-CM treated HUVECs ($n = 4$, *, $p < 0.05$, **, $p < 0.01$). (**b**) Representative fluorescence microscopic images of wound healing scratch assay on Con-CM, PlGF-CM and siSGK1 ± PlGF-CM treated GFP-HUVECs at 0 and 24 h ($n = 4$). Yellow line represents the wound area created. Scale bar: 650 µm. (**c**) Wound scratch assay analysis showing wound closure rate in Con-CM, PlGF-CM and siSGK1 ± PlGF-CM treated GFP-HUVECs analysed with ImageJ at 24 h ($n = 4$, *, $p < 0.05$, **, $p < 0.01$). (**d**) Representative fluorescence microscopic images of tube formation assay on a matrigel with Con-CM, PlGF-CM and siSGK1 ± PlGF-CM treated GFP-HUVECs at 24 h ($n = 4$). The insert displays GFP-HUVECs seeded on the matrigel with respective treatment condition at 0 h. Scale bar: 650 µm. (**e**) Tube formation analysis showing number of branches in Con-CM, PlGF-CM and siSGK1 ± PlGF-CM treated GFP-HUVECs at 24 h ($n = 4$, *, $p < 0.05$). (**f**) Original western blots of VEGFR1, VEGFR2 and VEGF-A targets with GAPDH as loading control in Con-CM, PlGF-CM and siSGK1 ± PlGF-CM treated HUVECs. (**g**) Average protein expression levels of VEGFR1, VEGFR2 and VEGF-A in Con-CM, PlGF-CM and siSGK1 ± PlGF-CM treated HUVECs ($n = 4$, *, $p < 0.05$, **, $p < 0.01$, ***, $p < 0.001$). Data represented here as arithmetic mean ± SEM. The treatment samples groups (PlGF-CM/siSGK1-CM/siSGK + PlGF-CM) are represented after normalization with control (Con-CM). Significance was determined using student's unpaired two-tailed t-test with Welch's correction method and One-way ANOVA. (**h**) EIS analysis of cellular impedance in Con-CM, PlGF-CM, siSGK1 ± PlGF-CM and VEGF-A (40 ng/ml) treated HUVEC monolayer representing endothelial barrier function. The measurement reads for 8 h post CM treatment are represented here ($n = 4$, ***, $p < 0.001$). (**i**) EIS analysis of BeWo cell migration through HUVEC monolayer. Data represented here as normalized cell impedance values with respective to the BeWo addition time point to the HUVEC monolayer. The measurement reads for 8 h post BeWo addition are represented here ($n = 4$, ***, $p < 0.001$, ****, $p < 0.0001$). Significance was determined using student's unpaired two-tailed t-test with Welch's correction method for cell impedance values at 4 h. n represents the number of independent experiments (biological replicates)

rescue of notch signaling function upon SGK1 inhibition (Supplementary Fig. 7). With upregulation of notch signaling, the protein expression levels of VEGFR1/2 and VEGF-A in HUVECs were reversed with siSGK1 ± PlGF-CM (Fig. 6f-g and Supplementary Fig. 8). Thus, these data confirm SGK1 inhibition in EnSCs improves secreted angiogenic cues, attenuating the hypersprouting phenotype in HUVECs. In addition, cellular impedance analysis with EIS showed improved endothelial barrier function with increase in cell permeability under the influence of both siSGK1 ± PlGF-CM (Fig. 6h). HUVECs were treated with VEGF-A (40 ng/ml for 24 h) as positive stimulator for permeability.

Trophoblast invasion of the maternal blood vessels is critical for development of the placenta. Shallow or poor invasion of the maternal blood vessels by is associated with PE [86]. We postulated that aberrant PlGF signaling in the endometrial stromal in turn produces cues to prevent adequate trophoblast invasion. As seen in Fig. 6i, the BeWo invasion was impeded and associated with high resistance (i.e. higher cell index) in PlGF-CM treated HUVECs compared with Con-CM. Interestingly, SGK1 inhibition improved the PlGF driven poor BeWo invasion through the HUVEC monolayer as measured by the decrease in cell impedance values (Fig. 6i). Together, these findings emphasis the important role of stromal SGK1 regulation in mediating angiogenic stimulus during uterine angiogenesis.

Discussion

The physiological changes in the endometrium during the menstrual cycle are associated with profound angiogenesis [87]. Any impairment in endometrial milieu or disruptions in maternal vessel adaptations is considered to increase the risk of adverse pregnancy outcomes [5–7]. PE is characterized by abnormal spiral artery remodelling, angiogenic imbalance, defective placentation, placental ischemia, and oxidative stress at the maternal-fetal interface, thereby resulting in maternal endothelial dysfunction and end-organ damage [14, 15, 88]. Regardless of numerous proposed mechanisms, the underlying cause for PE is still unclear. Recently, several studies ratified the influence of maternal decidua in PE progression [14–16]. Gomez et al., identified transcriptomic alterations associated with defective decidualization in the endometrium from patients with a history of severe PE [16]. Similarly, Sufriyana et al., reported that endometrial maturation was abnormal prior to the onset of PE [89].

In our recent study, we also report a pathological role of endometrial PlGF contributing to an altered pre-pregnancy maternal microenvironment, by upregulating Rac1-PAK1 signaling axis resulting in increase of cell stiffness [40]. These studies emphasize the pre-pregnancy decidual contribution in PE pathogenesis and highlights the need for more prospective studies on endometrial health. In line with this, we hypothesized that the pathophysiological manifestation for poor placentation likely occurs well before pregnancy, possibly involving an abnormal endometrial vasculature. A variety of hormones, growth factors and cytokines participate in normal vascular development post menstruation and in vessel adaptation during decidualization [19, 23, 24, 90]. Many of these factors when present at abnormal levels could lead to endothelial dysfunction by inhibiting key signaling events and chronically promoting poor uterine vessels at the maternal site prior to pregnancy [19, 25]. Particularly, in this study we aimed to decipher the pathological role of endometrial PlGF in uterine vessel development during endometrial regeneration. PlGF, a known VEGF homolog is selectively associated with pathological angiogenesis and inflammation [27, 29, 30]. PlGF is well characterized for its role on blood vessels, but its effects on non-vascular cells is not well known [30, 33]. PlGF is temporally and spatially regulated in the endometrium, localized to glandular and luminal epithelial cells, with staining in the stromal cells surrounding the maternal

spiral arteries [26]. Hence, aberrant local production of PlGF in the surrounding stroma may have functional implications in endometrial vascularization and in spiral artery remodelling during early pregnancy events.

NFAT5 was identified as a regulator of cellular osmoadaptive responses under hypertonic stress conditions [91]. Besides its osmosensitive function, various reports demonstrate its potential protective role under non-hypertonic activation [46]. NFAT5 transcriptional functioning associated with deregulated pro-angiogenic factors is described in different pathogenesis. Yu et al., reported a positive correlation of NFAT5 expression in the highly vascularized glioblastoma tumours [45]. Increased NFAT5 activity enhanced glioblastoma cell-driven angiogenesis by mediating secretion of EGF like domain multiple 7 (EGFL7) via the miR-S38-3p axis [45]. High-salt mediated NFAT5/STAT3 signaling activation in breast cancer cell aids in proliferation and migration through activation of angiogenic factor VEGF-A [92]. In a similar study, Hollborn et al., suggest that hyperosmolarity stress induced NFAT5 stimulation aggravates neovascularization and oedema formation in retinal pigment epithelial cells via PlGF/VEGF-A signaling effectors [52]. In contrast, the pathological role of isotonic NFAT5 activation is poorly understood. Specifically, the expression kinetics of NFAT5 in endometrium and its potential role in uterine angiogenesis remain unexplored. The current study unravels the distinct regulation of tonicity independent NFAT5 activation in the endometrium. In EnSCs, PlGF induced NFAT5 mRNA and increased its nuclear abundance confirming its transcriptional activation. Additionally, the increase of NFAT5 immunoreactivity in endometrial tissues during the proliferative phase of the cycle in the perivascular region around the blood vessels emphasizes its importance in influencing uterine vessel formation.

p38 MAPK is one of the few kinases that is involved in regulating both nuclear translocation and in mediating transcriptional activation of NFAT5 [93, 94]. We report here that PlGF induces NFAT5 transcriptional activation in EnSCs through p38 MAPK signaling. NFAT5 has been reported to be a DNA binding transcriptional activator that controls various angiogenic genes such as SGK1, COX2 and VEGF-A [52, 95]. We show that increased NFAT5 transcription in EnSCs leads to enhanced SGK1 protein phosphorylation, thereby further positively mediating the angiogenic downstream signaling. In keeping with this finding Wang et al. have shown that increased placental SGK1 is associated with PE [96].

SGK1 downstream targets include HIF-1α and NF*k*B, which are known mediators in angiogenic signaling [54, 57, 58]. Since hypoxia is a well-known stimulus that promotes vessel growth [97, 98], we examined the role of this crucial molecular downstream target of SGK1. Our findings show enhanced levels of HIF-1α transcripts and increased promoter activity in EnSCs upon PlGF stimulation. Hypoxia is known to regulate various pro-survival pathways affecting VEGF secretion in vascular pathophysiology [98–100]. Hence, we further unravelled the signaling axis reporting increased cellular levels of pro-angiogenic factors VEGF-A in stromal cells. Previous studies have highlighted the role of VEGF in the early angiogenic processes associated with postmenstrual regeneration of the endometrium [101–103]. The temporal and spatial distribution of VEGF is essential for the rapid burst of angiogenesis that occurs at postmenstrual repair [101].

The endometrial stroma secretome acts in an autocrine and paracrine manner to facilitate decidual differentiation, maternal angiogenesis thus influencing trophoblast invasion and placentation [19, 23]. We show here aberrant PlGF primed EnSCs secretome (CM) by displaying low levels of secreted VEGF-A despite the increase in HIF-1α and cellular VEGF-A levels. The decrease in secreted protein levels of VEGF-A was a puzzling result, however it is thought that intracellularly activated VEGF-A (in EnSCs) can likely interact with the receptors located within the cell exhibiting an intracrine signaling, causing a decline in secretion levels of VEGF-A [104, 105]. Another possible mechanism could be the activation of autocrine signaling in EnSCs, where secreted VEGF-A follows a negative feedback loop binding to its extracellular receptors causing a decrease in the bioavailability of VEGF-A in the CM [106, 107]. Lastly, secreted PlGF upon HIF-1α activation in EnSCs could act as an antagonist to its structurally related analog VEGF-A. HIF-1α transcriptional activity is known to be a key regulator of PlGF secretion [108, 109]. In line with this, HIF-1α -PlGF activation could be conserved as bidirectional regulation in EnSCs. Therefore, the secreted PlGF could act as an antagonist for VEGF-A present in CM by formation of biologically inactive PlGF/VEGF heterodimers [110]. These proposed mechanisms are yet to be fully characterized.

During endometrial sprouting angiogenesis, growth factors and cytokines from the stroma and surrounding uterine microenvironment activate the quiescent endothelial cells lining the vasculature, to degrade the extracellular matrix and invade the surrounding tissue to form new capillaries [19, 20, 23]. Here, we aimed to better elucidate the effects of PlGF-induced secreted factors on HUVECs by verifying its effects on angiogenic sprouting behaviour in HUVECs. VEGF-A is known to be mitogenic for endothelial cells [111]. The binding of VEGF-A to its receptors on endothelial cells triggers a series of intracellular signaling events, that mediate cellular responses aiding in proliferation, migration and vascular permeability [111, 112]. The VEGF-A pathway is tightly

regulated and balanced in normal physiological conditions, but dysregulation of this pathway can contribute to various diseases, including cancer and vascular disorders [113, 114]. VEGF-A displays a concentration-dependent activity to induce endothelial cell proliferation, thus facilitating sprouting and anastomosis *via* a VEGF/Notch-dependent mechanism [84, 115]. In our study, PlGF-CM rendered a negative angiogenic modulation in HUVECs with impediment in proliferation, migration and pathological hypersprouting. VEGF-A and Notch signaling pathways often interact in a coordinated manner to fine-tune angiogenesis and vascular development [84, 116]. Low gene expression of notch effectors in PlGF-CM treated HUVECs, confirms poor notch regulation owing to low secreted VEGF-A by EnSCs. VEGF-A activates Dll4 expression in the tip cell by binding to VEGF receptors [115]. This receptor binding activates the Notch signaling pathway in the stalk cell leading to a suppression of the tip cell phenotype. Low levels of notch ligand (Dll4) and upregulation of VEGFR2 protein explains the hypersprouting behaviour observed in PlGF-CM treated HUVECs, causing failure in establishing proper balance between tip and stalk cells. Deranged Notch regulation between endothelial cells also resulted in downregulation of VEGFR1 and VEGF-A protein levels in HUVECs. In line with the reported findings, decreased expression of Notch and VEGFR1 was found in endothelial cells of decidua associated with early pregnancy loss [117]. The above data validates the crosstalk between the stroma and endothelial compartments aiding in cell-cell communication to regulate endometrial angiogenic function.

The proteomic characterization of CM secreted by EnSCs upon PlGF stimulation displayed upregulation of many ECM associated biomolecules. These molecules are also known to impinge angiogenesis by directly affecting endothelial cell phenotypes and functions [118]. Type I collagen is reported to play a major role in endothelial cell morphogenesis involving suppression of cAMP-dependent protein kinase A and induction of actin polymerization [119]. This finding is in keeping with our recent study, where we observed the PlGF-induced increase in both Type1 collagen and cell stiffness via increased actin polymerization [40]. Matrix metalloproteases (MMPs) are well known inflammatory mediators controlling endothelial proliferation and survival in pathological vessel modifications [120]. Using bioinformatic GO enrichment analysis, we show activation of pathways associated with pathological angiogenesis (atherosclerosis and hypertrophic cardiomyopathy) in the stromal secretome mediated by aberrant PlGF. The appearance of acute atherosis was found in the walls of spiral arteries of uteroplacental circulation in some PE cases [121, 122]. Acute atherosis lesions reportedly correlate with early stages of atherosclerosis [122]. Thus, we postulate the change in the composition of the ECM associated proteins together with angiogenic imbalances in PlGF-CM generates a pathological *inflammatory-like* microenvironment that modifies the angiogenic sprouting behaviour in HUVECs.

Establishment of a low-resistance vascular system is essential for adequate spiral artery remodelling and normal placentation [123]. In humans, it is estimated that between 50 and 100 spiral arteries are required to be transformed to support a healthy pregnancy [86, 124]. The importance of sufficient uterine vessel adaption is critical because by term (37 weeks) perfusion of the uterus increases from < 1% of cardiac output to 25%, of which 90% is carried through the limited number of physiologically transformed spiral arterioles into the intervillous space of the placenta [2, 123, 125]. Endothelial barrier function maintains vascular integrity by balancing vascular permeability and resistance [126]. We observed that low VEGF-A and high ECM associated biomolecules in PlGF-CM impaired barrier function in HUVECs (high cell impedance), resulting in poor permeability and increased vascular stiffness. This increase of vascular resistance and stiffness at the junctional interface of HUVECs impeded BeWo cell invasion. Therefore, high levels of endometrial PlGF could form high-resistant vessels in the endometrium resulting in insufficient trophoblast invasion as manifested in PE placentas.

SGK1 is recognized as a critical endometrial regulator participating in both uterine receptivity and pregnancy [55]. It is known to play a mechanistic role in maintaining the functional reproductive axis [55, 127]. However, to date, the exact role of SGK1 in endometrial vessel development remains unclear. Various studies report the critical role of SGK1 in regulating inflammation in vascular diseases. Xi et al., showed first evidence for a role of SGK1 in hypoxia mediated pulmonary hypertension by inducing pro-inflammatory reaction. Lack of SGK1 attenuated hypoxia induced pro-inflammation response and improved arterial remodelling [128]. Similarly, Baban et al., reported that activation of SGK1 signaling improved inflammation-mediated pro survival pathways, causing adverse cardiac remodelling in ischemic- reperfusion injury [129]. We report that PlGF treatment with SGK1 inhibition in EnSCs attenuated hypoxia and increased the secreted levels of VEGF-A. In addition, the corresponding CM improved endothelial migration, normal tube formation ability and vascular permeability as seen in Con-CM. Our study also cements the role of SGK1 as a key molecule, mediating PlGF induced angiogenic pathway by promoting hypoxia and differentially regulating angiogenic cues for pathological vessel development. HIF-1α overexpression is reported to be expressed in the PE placentas and known to regulate the production of sFlt-1 and soluble endoglin (sEng), causing the

angiogenic imbalance [130, 131]. Furthermore, HIF-1α overexpression reportedly induces a Hemolysis, Elevated Liver enzymes and Low Platelets (HELLP) syndrome-like phenotype and fetal growth restriction in pregnant mice [132]. These data help us to postulate the plausible role of dysregulated endometrial SGK1 in enhancing hypoxia during uterine vascularization and placentation as presented in PE. Also, our findings highlight the potential for selective inhibition of SGK1 in stroma to reverse the pathological switch activated by aberrant PlGF. This study uncovers a new role of SGK1 in PE pathogenesis and identifies SGK1 as an attractive therapeutic target.

Collectively, our findings support the conjecture that dysregulated endometrial PlGF could switch between the controlled physiological angiogenesis by disrupting the uterine stromal – endothelial paracrine mechanism, resulting in poor quality spiral artery modification thereby impeding trophoblast invasion and thus development of PE (Fig. 7). In keeping with this, Doppler studies showed a higher uterine artery pulsatility index during early gestation (weeks 11–13) and could identify at least 50% of patients who subsequently developed PE [133]. Interestingly, additional Doppler ultrasound studies have shown that during the late secretory phase, endometriosis is linked with increased sub-endometrial blood flow [134]. The inverse correlation between the amount of perfusion before pregnancy and the probability of pregnancy complications may, although untested, be relevant to other disorders including abnormal uterine bleeding, polycystic ovary syndrome and unexplained infertility. Notwithstanding, whilst we shed light on a new pathway, other contributing factors such as inadequate decidualization, deregulated uNK cell function, impaired activation of trophoblast interaction, trophoblast cell death, reprogramming /epigenetic changes (DNA methylation or post translational histone tail modifications) or a combination of the above may lead to dysregulation of spiral artery transformation and PE [16, 135–139].

Cyclic endometrial remodelling and menstruation is a pre-requisite for the human uterus in preparation for future pregnancy [140]. Hence, we posit that local endometrial disorders i.e. poor-quality uterine vessels (prior to pregnancy) will result in an unwarranted ripple effect with the 'crescendo' or end result being reduced placental function as presented in PE. Our findings presented here are further supported by a recent study employing single-cell transcriptomics to survey distinct molecular faces of PE subtypes [141]. Systematic molecular characterization revealed imbalances hallmarking angiogenic and extracellular matrix dysfunction in placentas from early onset

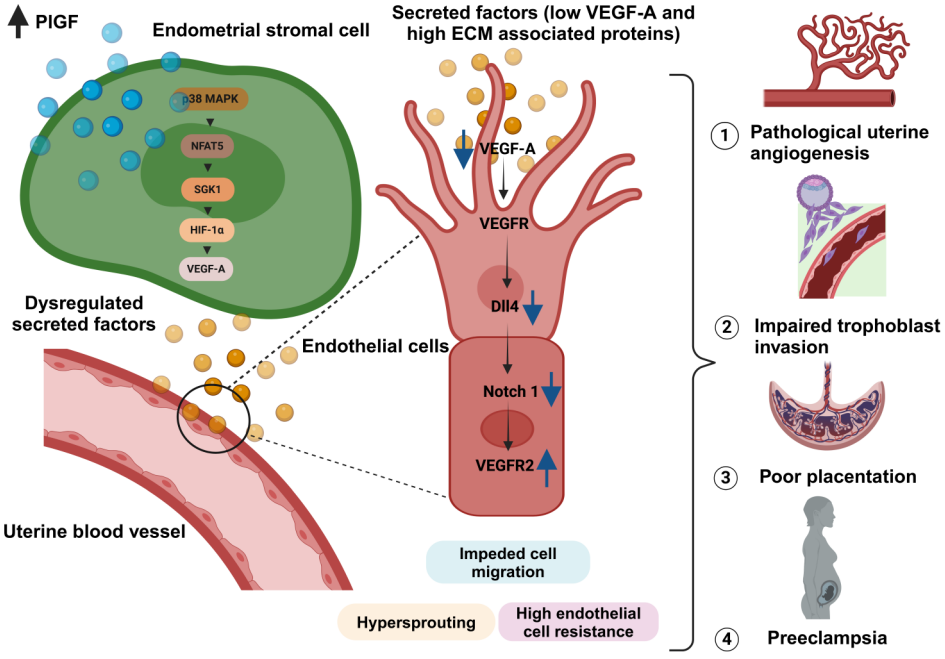

Fig. 7 Graphical abstract describing the effect of pathological PlGF levels in altered uterine endometrial angiogenesis and its plausible role in PE pathology. Aberrant levels of endometrial PlGF activates NFAT5-SGK1-VEGF-A signaling axis in uterine stromal cells. Activation of this signaling cascade presents negative angiogenic cues to endothelial cells, with deregulated secreted protein cargo (decreased angiogenic factor VEGF-A and increased ECM associated proteins). PlGF mediated secreted factors supports abnormal vessel development in HUVECs, with dysregulation of Notch-VEGF signaling. Aberrant PlGF triggered stromal-endothelial paracrine signaling results in hypersprouting, high cellular resistance and impaired BeWo invasion through HUEVCs. Hypersprouting and high cellular impedance in HUVECs confirm pathological uterine vascularization upon deregulated endometrial PlGF. Thus, we postulate such aberrant uterine angiogenesis prior to pregnancy will likely lead to poor quality maternal vessels, inadequate trophoblast invasion causing poor placentation as seen in PE pregnancy (Images created with BioRender)

PE. Intriguingly, stromal cells and vasculature reflected an inflamed, stressed, anti-angiogenic environment only in early PE groups. Thus, we could speculate that PE is primarily a disease of impaired endometrial preconditioning, which likely confers protection against abnormal hyperinflammation.

The correlation between abnormal endometrial PlGF and the corresponding circulating levels during early pregnancy driving abnormal pregnancy outcome remains unclear. PlGF, exists in at least four isoforms due to alternative mRNA splicing of the PlGF primary transcript [142, 143]. The main distinction amongst the four isoforms are that PlGF-1 and −3 are non-heparin binding and can (potentially) affect targets in a paracrine manner, whereas PlGF-2 and −4 have additional heparin-binding domains and most likely work in an autocrine way [142, 143]. The major isoforms are thought to be PlGF-1 and PlGF-2 and are thought to have different functions [143]. The addition of PlGF-1 to a spontaneously transformed first-trimester cytotrophoblast cell line stimulated cell proliferation whilst PlGF-2 had little effect [144]. In contrast, the addition of PlGF-1 had little effect on endothelial cell proliferation while this was inhibited by PlGF-2 [144]. Therefore, more careful analysis is required to delineate which isoform in the endometrium contributes to the pathogenesis of this disease. Our reanalysis of single-cell RNA sequencing of the human endometrium reveals that PlGF is expressed by various endometrial cell types (data not shown) with the highest expression levels observed in the stromal cells, endothelial cells and mesenchymal stem cells (MSCs) [145]. Intriguingly, the conditioned medium of PE placental MSCs impair trophoblast invasion and angiogenesis of endothelial cells, indicating a detrimental paracrine profile [146]. Furthermore, MSCs derived from the decidual component of PE placentas exhibited compromised function in response to oxidative stress and accelerated senescence compared with normotensive placentas [146–148]. In keeping with this, in our proteomic analysis we do see a modest upregulation of senesce marker β-galactosidase (data not shown). Taken together, we posit that aberrant expression of endometrial PlGF on MSCs could additionally deregulate the normal cellular activity, potentially leading to premature cellular senescence causing placental aging as seen in obstetric complications such as PE, IUGR and still birth [149, 150] and further work is required to validate this hypothesis.

Literature shows strong evidence on high levels of circulating PlGF in individuals with various diseases such as cancer (breast, melanoma, leukemia), auto-immune diseases (rheumatoid arthritis, Systemic Lupus Erythematosus), coronary heart disease, and neovascular age-related macular degeneration. Whether PlGF contributes to or is a result of these diseases remains to be determined [28, 29]. Furthermore, the knowledge on genetic determinants of circulating pathological levels of PlGF is limited. A recent study by Ruggerio et al., conducted the first genome-wide association study, to identify genetic variants that explain alterations in circulating PlGF concentrations [28]. The plausible candidate genes identified to be associated with PlGF circulating levels were *NRP1, FLT1 and RAPGEF5* [28]. Intriguingly these molecules have been implicated with different PE models [151–153]. Another study by Vodolazkaia et al., reported that genetic variants in *PlGF* rs2268613 gene may increase the PlGF plasma levels [154]. These findings thus provide new candidate genes and new insights into mechanisms by which PlGF is regulated in physiological and pathophysiological states.

PE is a complex condition involving multiple systems and various contributing factors [9]. Its development results from a combination of immunological, genetic and environmental influences, leading to systemic maternal endothelial dysfunction and impaired placental function [155]. Significant (high) risk factors include a history of PE, chronic hypertension, pre-existing diabetes mellitus, chronic kidney disease history and autoimmune conditions like antiphospholipid syndrome (APS) [155]. Additional risk (moderate) factors encompass advanced maternal age (>40 years), body mass index [BMI] ≥ 35 kg/m2, and the use of assisted reproductive technologies (ART/IVF) [155]. According to the NICE recommendations, the presence of one high-risk factor or more than one moderate risk factor is considered high risk for preeclampsia [13]. Interestingly, abnormal PlGF levels are also (independent of pregnancy) associated with some of these risk factors, such as diabetes, obesity and hypertension [156–159]. Interestingly, these conditions are also linked with increased SGK1 expression [160–163]. Taken together, these studies argue that certain genetic variations as previously stated or lifestyle factors may predispose women to abnormal PlGF levels before pregnancy, potentially augmenting the expression of the PlGF-NFAT5-SGK1 axis and promoting inadequate vessel quality in the endometrial microenvironment. Subsequently, during pregnancy, these compromised vessels may contribute to abnormal placentation, resulting in an imbalance in circulating angiogenic factors. In conclusion, our results shed light onto the new prospect and advances of PlGF-NFAT5-SGK1 signaling axis in endometrial stromal cells. While careful evaluation of the broad implications of PlGF is still necessary, this study identified both NFAT5 and SGK1 as promising targets for treatment strategies to improve vascularization prior to pregnancy and help improve adverse pregnancy outcome such as PE.

Supplementary Information

The online version contains supplementary material available at https://doi.org/10.1186/s40659-024-00526-w.

Supplementary Material 1

Supplementary Material 2

Acknowledgements

We thank Dr. Ana Velic from Proteome Center Tübingen (PCT) for performing the mass spec experiments and Quantitative Biology Centre Tübingen (QBiC) for proteomic data storage. We would like to thank Apl. Prof. Dr. Dorothea Alexander-Friedrich from the Department of Dental Medicine for providing access to the EIS equipment and Ms. Birgit Fehrenbacher from the Department of Dermatology for her help on confocal microscopy imaging.

Author contributions

M.S.S conceived and designed the study. M.S.S and J.P.R.X wrote the first draft. J.P.R.X, T.O, M.A, N.C and Y. S performed the experiments, bioinformatic analysis. analyzed the data and prepared figures. M.S.S, S.T, F.L and S.Y.B provided advice, equipment, resources, funds. All authors of the manuscript have read, edited and agreed to its content.

Funding

This work was supported by funding to M.S.S by Else Kröner-Fresenius-Stiftung (EKFS), intramural funds of Tübingen University the IZKF, the Athene award by the Federal Ministry of Education and Research (BMBF) and the Baden-Württemberg Ministry of Science as part of the Excellence Strategy of the German Federal and State Governments and by the Margarete von Wrangell (MvW 31-7635.41/118/3) habilitation scholarship co-funded by the Ministry of Science, Research and the arts (MWK) of the state of Baden-Württemberg and by the European Social Funds. We are grateful for the support from Open Access Publishing Fund of Tübingen University.
Open Access funding enabled and organized by Projekt DEAL.

Data availability

The proteomic datasets supporting the results in this article are available in the PRoteomics IDEntification database (PRIDE) with the accession number PXD051697. The source data behind the other data available in the figures can be found in the supplementary data file 2.

Declarations

Ethics approval and consent to participate

Not applicable.

Consent for publication

All authors approve for submission and confirm no conflict of interest.

Conflict interest

Part of this work is used in the Bachelor thesis of M.A, Master Thesis from N.A.C and PhD thesis of J.P.R.X. All other authors declare no conflict of interest.

Received: 10 May 2024 / Accepted: 26 June 2024
Published online: 17 August 2024

References

1. Zhang P. Decidual vasculopathy and spiral artery remodeling revisited II: relations to trophoblastic dependent and independent vascular transformation. J Maternal-Fetal Neonatal Med. 2020;1–7. https://doi.org/10.1080/14767058.2020.1718646.
2. Mori M, Bogdan A, Balassa T, Csabai T, Szekeres-Bartho J. The decidua-the maternal bed embracing the embryo-maintains the pregnancy. Semin Immunopathol. 2016;38:635–49. https://doi.org/10.1007/s00281-016-0574-0.
3. Wu HM, Chen LH, Hsu LT, Lai CH. Immune Tolerance of embryo implantation and pregnancy: the role of human decidual stromal cell- and embryonic-derived extracellular vesicles. Int J Mol Sci. 2022;23. https://doi.org/10.3390/ijms232113382.
4. Vento-Tormo R, Efremova M, Botting RA, Turco MY, Vento-Tormo M, Meyer KB, Park JE, Stephenson E, Polański K, Goncalves A, et al. Single-cell reconstruction of the early maternal-fetal interface in humans. Nature. 2018;563:347–53. https://doi.org/10.1038/s41586-018-0698-6.
5. Staff AC, Fjeldstad HE, Fosheim IK, Moe K, Turowski G, Johnsen GM, Alnaes-Katjavivi P, Sugulle M. Failure of physiological transformation and spiral artery atherosis: their roles in preeclampsia. Am J Obstet Gynecol. 2022;226:S895–906. https://doi.org/10.1016/j.ajog.2020.09.026.
6. Du L, Deng W, Zeng S, Xu P, Huang L, Liang Y, Wang Y, Xu H, Tang J, Bi S, et al. Single-cell transcriptome analysis reveals defective decidua stromal niche attributes to recurrent spontaneous abortion. Cell Prolif. 2021;54:e13125. https://doi.org/10.1111/cpr.13125.
7. Audette MC, Kingdom JC. Screening for fetal growth restriction and placental insufficiency. Semin Fetal Neonatal Med. 2018;23:119–25. https://doi.org/10.1016/j.siny.2017.11.004.
8. Levine RJ, Maynard SE, Qian C, Lim K-H, England LJ, Yu KF, Schisterman EF, Thadhani R, Sachs BP, Epstein FH, et al. Circulating angiogenic factors and the risk of Preeclampsia. N Engl J Med. 2004;350:672–83. https://doi.org/10.1056/NEJMoa031884.
9. Rana S, Lemoine E, Granger JP, Karumanchi SA, Preeclampsia. Pathophysiology, challenges, and perspectives. Circ Res. 2019;124:1094–112. https://doi.org/10.1161/circresaha.118.313276.
10. Conrad KP, Rabaglino MB, Post Uiterweer ED. Emerging role for dysregulated decidualization in the genesis of preeclampsia. Placenta. 2017;60:119–29. https://doi.org/10.1016/j.placenta.2017.06.005.
11. Albrecht ED, Babischkin JS, Aberdeen GW, Burch MG, Pepe GJ. Maternal systemic vascular dysfunction in a primate model of defective uterine spiral artery remodeling. Am J Physiol Heart Circ Physiol. 2021;320:H1712–23. https://doi.org/10.1152/ajpheart.00613.2020.
12. Wu P, Haththotuwa R, Kwok CS, Babu A, Kotronias RA, Rushton C, Zaman A, Fryer AA, Kadam U, Chew-Graham CA, et al. Preeclampsia and Future Cardiovascular Health: a systematic review and Meta-analysis. Circ Cardiovasc Qual Outcomes. 2017;10. https://doi.org/10.1161/circoutcomes.116.003497.
13. Khan B, Allah Yar R, Khakwani AK, Karim S, Arslan Ali H. Preeclampsia Incidence and its maternal and neonatal outcomes with Associated Risk factors. Cureus. 2022;14:e31143. https://doi.org/10.7759/cureus.31143.
14. Garrido-Gómez T, Castillo-Marco N, Cordero T, Simón C. Decidualization resistance in the origin of preeclampsia. Am J Obstet Gynecol. 2022;226:S886–94. https://doi.org/10.1016/j.ajog.2020.09.039.
15. Garrido-Gomez T, Quiñonero A, Dominguez F, Rubert L, Perales A, Hajjar KA, Simon C. Preeclampsia: a defect in decidualization is associated with deficiency of annexin A2. Am J Obstet Gynecol. 2020;222:376e371. 376.e317.
16. Garrido-Gomez T, Castillo-Marco N, Clemente-Ciscar M, Cordero T, Muñoz-Blat I, Amadoz A, Jimenez-Almazan J, Monfort-Ortiz R, Climent R, Perales-Marin A, et al. Disrupted PGR-B and ESR1 signaling underlies defective decidualization linked to severe preeclampsia. Elife. 2021;10. https://doi.org/10.7554/eLife.70753.
17. Yang M, Li H, Rong M, Zhang H, Hou L, Zhang C. Dysregulated GLUT1 may be involved in the pathogenesis of preeclampsia by impairing decidualization. Mol Cell Endocrinol. 2022;540:111509. https://doi.org/10.1016/j.mce.2021.111509.
18. Stevens DU, de Nobrega Teixeira JA, Spaanderman MEA, Bulten J, van Vugt JMG, Al-Nasiry. Understanding decidual vasculopathy and the link to preeclampsia: a review. Placenta. 2020;97:95–100. https://doi.org/10.1016/j.placenta.2020.06.020.
19. Ma Q, Beal JR, Bhurke A, Kannan A, Yu J, Taylor RN, Bagchi IC, Bagchi MK. Extracellular vesicles secreted by human uterine stromal cells regulate decidualization, angiogenesis, and trophoblast differentiation. Proc Natl Acad Sci U S A. 2022;119:e2200252119. https://doi.org/10.1073/pnas.2200252119.
20. Maas JW, Groothuis PG, Dunselman GA, de Goeij AF, Struyker Boudier HA, Evers JL. Endometrial angiogenesis throughout the human menstrual cycle. Hum Reprod. 2001;16:1557–61. https://doi.org/10.1093/humrep/16.8.1557.
21. Rogers PA, Donoghue JF, Walter LM, Girling JE. Endometrial angiogenesis, vascular maturation, and lymphangiogenesis. Reprod Sci. 2009;16:147–51. https://doi.org/10.1177/1933719108325509.
22. Chen W, Lu S, Yang C, Li N, Chen X, He J, Liu X, Ding Y, Tong C, Peng C, et al. Hyperinsulinemia restrains endometrial angiogenesis during decidualization in early pregnancy. J Endocrinol. 2019;243:137–48. https://doi.org/10.1530/joe-19-0127.

23. Ahn J, Yoon MJ, Hong SH, Cha H, Lee D, Koo HS, Ko JE, Lee J, Oh S, Jeon NL, et al. Three-dimensional microengineered vascularised endometrium-on-a-chip. Hum Reprod. 2021;36:2720–31. https://doi.org/10.1093/humrep/deab186.
24. Gnecco JS, Pensabene V, Li DJ, Ding T, Hui EE, Bruner-Tran KL, Osteen KG. Compartmentalized Culture of Perivascular Stroma and endothelial cells in a microfluidic model of the human endometrium. Ann Biomed Eng. 2017;45:1758–69. https://doi.org/10.1007/s10439-017-1797-5.
25. Duran CL, Abbey CA, Bayless KJ. Establishment of a three-dimensional model to study human uterine angiogenesis. Mol Hum Reprod. 2018;24:74–93. https://doi.org/10.1093/molehr/gax064.
26. Binder NK, Evans J, Salamonsen LA, Gardner DK, Kaitu'u-Lino TuJ, Hannan NJ. Placental growth factor is secreted by the human endometrium and has potential important functions during embryo development and implantation. PLoS ONE. 2016;11:e0163096. https://doi.org/10.1371/journal.pone.0163096.
27. Nejabati HR, Latifi Z, Ghasemnejad T, Fattahi A, Nouri M. Placental growth factor (PlGF) as an angiogenic/inflammatory switcher: lesson from early pregnancy losses. Gynecol Endocrinol. 2017;33:668–74. https://doi.org/10.1080/09513590.2017.1318375.
28. Ruggiero D, Nutile T, Nappo S, Tirozzi A, Bellenguez C, Leutenegger AL, Ciullo M. Genetics of PlGF plasma levels highlights a role of its receptors and supports the link between angiogenesis and immunity. Sci Rep. 2021;11:16821. https://doi.org/10.1038/s41598-021-96256-0.
29. Dewerchin M, Carmeliet P. PlGF: a multitasking cytokine with disease-restricted activity. Cold Spring Harb Perspect Med. 2012;2. https://doi.org/10.1101/cshperspect.a011056.
30. Li X, Jin Q, Yao Q, Zhou Y, Zou Y, Li Z, Zhang S, Tu C. Placental growth factor contributes to liver inflammation, angiogenesis, fibrosis in mice by promoting hepatic macrophage recruitment and activation. Front Immunol. 2017;8:801. https://doi.org/10.3389/fimmu.2017.00801.
31. Tudisco L, Orlandi A, Tarallo V, De Falco S. Hypoxia activates placental growth factor expression in lymphatic endothelial cells. Oncotarget. 2017;8:32873–83. https://doi.org/10.18632/oncotarget.15861.
32. Raevens S, Geerts A, Paridaens A, Lefere S, Verhelst X, Hoorens A, Van Dorpe J, Maes T, Bracke KR, Casteleyn C, et al. Placental growth factor inhibition targets pulmonary angiogenesis and represents a therapy for hepatopulmonary syndrome in mice. Hepatology. 2018;68:634–51. https://doi.org/10.1002/hep.29579.
33. Aoki S, Inoue K, Klein S, Halvorsen S, Chen J, Matsui A, Nikmaneshi MR, Kitahara S, Hato T, Chen X, et al. Placental growth factor promotes tumour desmoplasia and treatment resistance in intrahepatic cholangiocarcinoma. Gut. 2022;71:185–93. https://doi.org/10.1136/gutjnl-2020-322493.
34. Iwamoto H, Zhang Y, Seki T, Yang Y, Nakamura M, Wang J, Yang X, Torimura T, Cao Y. PlGF-induced VEGFR1-dependent vascular remodeling determines opposing antitumor effects and drug resistance to Dll4-Notch inhibitors. Sci Adv. 2015;1:e1400244. https://doi.org/10.1126/sciadv.1400244.
35. Lennikov A, Mukwaya A, Fan L, Saddala MS, De Falco S, Huang H. Synergistic interactions of PlGF and VEGF contribute to blood-retinal barrier breakdown through canonical NFκB activation. Exp Cell Res. 2020;397:112347. https://doi.org/10.1016/j.yexcr.2020.112347.
36. Apicella I, Cicatiello V, Acampora D, Tarallo V, De Falco S. Full functional knockout of placental growth factor by Knockin with an inactive variant able to Heterodimerize with VEGF-A. Cell Rep. 2018;23:3635–46. https://doi.org/10.1016/j.celrep.2018.05.067.
37. Luttun A, Tjwa M, Moons L, Wu Y, Angelillo-Scherrer A, Liao F, Nagy JA, Hooper A, Priller J, De Klerck B, et al. Revascularization of ischemic tissues by PlGF treatment, and inhibition of tumor angiogenesis, arthritis and atherosclerosis by anti-Flt1. Nat Med. 2002;8:831–40. https://doi.org/10.1038/nm731.
38. Maynard SE, Min JY, Merchan J, Lim KH, Li J, Mondal S, Libermann TA, Morgan JP, Sellke FW, Stillman IE, et al. Excess placental soluble fms-like tyrosine kinase 1 (sFlt1) may contribute to endothelial dysfunction, hypertension, and proteinuria in preeclampsia. J Clin Invest. 2003;111:649–58. https://doi.org/10.1172/jci17189.
39. Huang D, Liu G, Xu Z, Chen S, Wang C, Liu D, Cao J, Cheng J, Wu B, Wu D. The multifaceted role of placental growth factor in the pathogenesis and progression of bronchial asthma and pulmonary fibrosis: therapeutic implications. Genes Dis. 2023;10:1537–51. https://doi.org/10.1016/j.gendis.2022.10.017.
40. Raja Xavier JP, Rianna C, Hellwich E, Nikolou I, Lankapalli AK, Brucker SY, Singh Y, Lang F, Schäffer TE, Salker MS. Excessive endometrial PlGF- Rac1 signalling underlies endometrial cell stiffness linked to pre-eclampsia. Commun Biol. 2024;7:530. https://doi.org/10.1038/s42003-024-06220-7.
41. Talbi S, Hamilton AE, Vo KC, Tulac S, Overgaard MT, Dosiou C, Le Shay N, Nezhat CN, Kempson R, Lessey BA, et al. Molecular phenotyping of human endometrium distinguishes menstrual cycle phases and underlying biological processes in normo-ovulatory women. Endocrinology. 2006;147:1097–121. https://doi.org/10.1210/en.2005-1076.
42. Chen X, Jin X, Liu L, Man CW, Huang J, Wang CC, Zhang S, Li TC. Differential expression of vascular endothelial growth factor angiogenic factors in different endometrial compartments in women who have an elevated progesterone level before oocyte retrieval, during in vitro fertilization-embryo transfer treatment. Fertil Steril. 2015;104:1030–6. https://doi.org/10.1016/j.fertnstert.2015.06.021.
43. Founds SA, Conley YP, Lyons-Weiler JF, Jeyabalan A, Hogge WA, Conrad KP. Altered global gene expression in first trimester placentas of women destined to develop preeclampsia. Placenta. 2009;30:15–24. https://doi.org/10.1016/j.placenta.2008.09.015.
44. Cheung CY, Huang TT, Chow N, Zhang S, Zhao Y, Chau MP, Chan WC, Wong CCL, Boassa D, Phan S, et al. Unconventional tonicity-regulated nuclear trafficking of NFAT5 mediated by KPNB1, XPOT and RUVBL2. J Cell Sci. 2022;135. https://doi.org/10.1242/jcs.259280.
45. Yu H, Zheng J, Liu X, Xue Y, Shen S, Zhao L, Li Z, Liu Y. Transcription factor NFAT5 promotes Glioblastoma Cell-driven angiogenesis via SBF2-AS1/miR-338-3p-Mediated EGFL7 expression change. Front Mol Neurosci. 2017;10. https://doi.org/10.3389/fnmol.2017.00301.
46. Halterman JA, Kwon HM, Wamhoff BR. Tonicity-independent regulation of the osmosensitive transcription factor TonEBP (NFAT5). Am J Physiol Cell Physiol. 2012;302:C1–8. https://doi.org/10.1152/ajpcell.00327.2011.
47. Jeong GR, Im SK, Bae YH, Park ES, Jin BK, Kwon HM, Lee BJ, Bu Y, Hur EM, Lee BD. Inflammatory signals induce the expression of tonicity-responsive enhancer binding protein (TonEBP) in microglia. J Neuroimmunol. 2016;295–296:21–9. https://doi.org/10.1016/j.jneuroim.2016.04.009.
48. Zhao G, Aghakeshmiri S, Chen YT, Zhang HM, Yip F, Yang D. NFAT5-Mediated signalling pathways in viral infection and Cardiovascular Dysfunction. Int J Mol Sci. 2021;22. https://doi.org/10.3390/ijms22094872.
49. Muhammad K, Xavier D, Klein-Hessling S, Azeem M, Rauschenberger T, Murti K, Avots A, Goebeler M, Klein M, Bopp T, et al. NFAT5 controls the Integrity of Epidermis. Front Immunol. 2021;12:780727. https://doi.org/10.3389/fimmu.2021.780727.
50. Neubert P, Weichselbaum A, Reitinger C, Schatz V, Schröder A, Ferdinand JR, Simon M, Bär AL, Brochhausen C, Gerlach RG, et al. HIF1A and NFAT5 coordinate na(+)-boosted antibacterial defense via enhanced autophagy and autolysosomal targeting. Autophagy. 2019;15:1899–916. https://doi.org/10.1080/15548627.2019.1596483.
51. Lee N, Kim D, Kim WU. Role of NFAT5 in the Immune System and Pathogenesis of Autoimmune diseases. Front Immunol. 2019;10:270. https://doi.org/10.3389/fimmu.2019.00270.
52. Hollborn M, Fischer S, Kuhrt H, Wiedemann P, Bringmann A, Kohen L. Osmotic regulation of NFAT5 expression in RPE cells: the involvement of purinergic receptor signaling. Mol Vis. 2017;23:116–30.
53. Sahu I, Pelzl L, Sukkar B, Fakhri H, Al-Maghout T, Cao H, Hauser S, Gutti R, Gawaz M, Lang F. NFAT5-sensitive Orai1 expression and store-operated ca(2+) entry in megakaryocytes. Faseb j. 2017;31:3439–48. https://doi.org/10.1096/fj.201601211R.
54. Vanderhaeghen T, Beyaert R, Libert C. Bidirectional crosstalk between Hypoxia Inducible factors and glucocorticoid signalling in Health and Disease. Front Immunol. 2021;12:684085. https://doi.org/10.3389/fimmu.2021.684085.
55. Lang F, Rajaxavier J, Singh Y, Brucker SY, Salker MS. The Enigmatic Role of Serum & Glucocorticoid Inducible Kinase 1 in the Endometrium. Front Cell Dev Biol. 2020;8:556543–556543. https://doi.org/10.3389/fcell.2020.556543.
56. Sun N, Meng F, Xue N, Pang G, Wang Q, Ma H. Inducible miR-145 expression by HIF-1a protects cardiomyocytes against apoptosis via regulating SGK1 in simulated myocardial infarction hypoxic microenvironment. Cardiol J. 2018;25:268–78. https://doi.org/10.5603/CJ.a2017.0105.
57. Medina-Jover F, Gendrau-Sanclemente N, Viñals F. SGK1 is a signalling hub that controls protein synthesis and proliferation in endothelial cells. FEBS Lett. 2020;594:3200–15. https://doi.org/10.1002/1873-3468.13901.
58. Zarrinpashneh E, Poggioli T, Sarathchandra P, Lexow J, Monassier L, Terracciano C, Lang F, Damilano F, Zhou JQ, Rosenzweig A, et al. Ablation of SGK1 impairs endothelial cell migration and tube formation leading to decreased

neo-angiogenesis following myocardial infarction. PLoS ONE. 2013;8:e80268. https://doi.org/10.1371/journal.pone.0080268.
59. Chau K, Xu B, Hennessy A, Makris A. Effect of placental growth factor on trophoblast-endothelial cell interactions in Vitro. Reprod Sci. 2020;27:1285–92. https://doi.org/10.1007/s43032-019-00103-7.
60. Singh Y, Shi X, Zhang S, Umbach AT, Chen H, Salker MS, Lang F. Prolyl hydroxylase 3 (PHD3) expression augments the development of regulatory T cells. Mol Immunol. 2016;76:7–12. https://doi.org/10.1016/j.molimm.2016.06.003.
61. Hamdollah Zadeh MA, Glass CA, Magnussen A, Hancox JC, Bates DO. VEGF-mediated elevated intracellular calcium and angiogenesis in human microvascular endothelial cells in vitro are inhibited by dominant negative TRPC6. Microcirculation. 2008;15:605–14. https://doi.org/10.1080/10739680802220323.
62. Ayakannu T, Taylor AH, Willets JM, Brown L, Lambert DG, McDonald J, Davies Q, Moss EL, Konje JC. Validation of endogenous control reference genes for normalizing gene expression studies in endometrial carcinoma. Mol Hum Reprod. 2015;21:723–35. https://doi.org/10.1093/molehr/gav033.
63. Alauddin M, Salker MS, Umbach AT, Rajaxavier J, Okumura T, Singh Y, Wagner A, Brucker SY, Wallwiener D, Brosens JJ, et al. Annexin A7 regulates endometrial receptivity. Front Cell Dev Biol. 2020;8:770. https://doi.org/10.3389/fcell.2020.00770.
64. Okumura T, Raja Xavier JP, Pasternak J, Yang Z, Hang C, Nosirov B, Singh Y, Admard J, Brucker SY, Kommoss S, et al. Rel Family transcription factor NFAT5 upregulates COX2 via HIF-1α activity in Ishikawa and HEC1a cells. Int J Mol Sci. 2024;25. https://doi.org/10.3390/ijms25073666.
65. Schweitzer GG, Arias EB, Cartee GD. Sustained postexercise increases in AS160 Thr642 and Ser588 phosphorylation in skeletal muscle without sustained increases in kinase phosphorylation. J Appl Physiol (1985). 2012;113:1852–61. https://doi.org/10.1152/japplphysiol.00619.2012.
66. Endo A, Fukushima T, Takahashi C, Tsuchiya H, Ohtake F, Ono S, Ly T, Yoshida Y, Tanaka K, Saeki Y, et al. USP8 prevents aberrant NF-κB and Nrf2 activation by counteracting ubiquitin signals from endosomes. J Cell Biol. 2024;223. https://doi.org/10.1083/jcb.202306013.
67. Joubert R, Daniel E, Bonnin N, Comptour A, Gross C, Belville C, Chiambaretta F, Blanchon L, Sapin V. Retinoic acid Engineered amniotic membrane used as graft or homogenate: positive effects on corneal Alkali Burns. Invest Ophthalmol Vis Sci. 2017;58:3513–8. https://doi.org/10.1167/iovs.17-21810.
68. Wang Z, Yemanyi F, Blomfield AK, Bora K, Huang S, Liu CH, Britton WR, Cho SS, Tomita Y, Fu Z, et al. Amino acid transporter SLC38A5 regulates developmental and pathological retinal angiogenesis. Elife. 2022;11. https://doi.org/10.7554/eLife.73105.
69. Johnson BM, Johnson AM, Heim M, Buckley M, Mortimer B, Berry JL, Sewell-Loftin MK. Biomechanical stimulation promotes blood vessel growth despite VEGFR-2 inhibition. BMC Biol. 2023;21:290. https://doi.org/10.1186/s12915-023-01792-y.
70. Wu C, Liu H, Zhong D, Yang X, Liao Z, Chen Y, Zhang S, Su D, Zhang B, Li C, et al. Mapk7 deletion in chondrocytes causes vertebral defects by reducing MEF2C/PTEN/AKT signaling. Genes Dis. 2024;11:964–77. https://doi.org/10.1016/j.gendis.2023.02.012.
71. Pang H, Wu H, Zhan Z, Wu T, Xiang M, Wang Z, Song L, Wei B. Exploration of anti–osteosarcoma activity of asiatic acid based on network pharmacology and in vitro experiments. Oncol Rep. 2024;51. https://doi.org/10.3892/or.2023.8692.
72. Taylor SC, Posch A. The design of a quantitative Western blot experiment. Biomed Res Int. 2014;2014:361590–361590. https://doi.org/10.1155/2014/361590.
73. Poel Svd, Dreer M, Velic A, Macek B, Baskaran P, Iftner T, Stubenrauch F. Identification and functional characterization of Phosphorylation sites of the human papillomavirus 31 E8^E2 protein. J Virol. 2018;92:e01743–01717. https://doi.org/10.1128/JVI.01743-17.
74. Cox J, Mann M. MaxQuant enables high peptide identification rates, individualized p.p.b.-range mass accuracies and proteome-wide protein quantification. Nat Biotechnol. 2008;26:1367–72. https://doi.org/10.1038/nbt.1511.
75. Aguilan JT, Kulej K, Sidoli S. Guide for protein fold change and p-value calculation for non-experts in proteomics. Mol Omics. 2020;16:573–82. https://doi.org/10.1039/D0MO00087F.
76. Tyanova S, Temu T, Sinitcyn P, Carlson A, Hein MY, Geiger T, Mann M, Cox J. The Perseus computational platform for comprehensive analysis of (prote)omics data. Nat Methods. 2016;13:731–40. https://doi.org/10.1038/nmeth.3901.
77. Suarez-Arnedo A, Torres Figueroa F, Clavijo C, Arbeláez P, Cruz JC. Muñoz-Camargo, C. An image J plugin for the high throughput image analysis of in vitro scratch wound healing assays. PLoS ONE. 2020;15:e0232565. https://doi.org/10.1371/journal.pone.0232565.
78. DeCicco-Skinner KL, Henry GH, Cataisson C, Tabib T, Gwilliam JC, Watson NJ, Bullwinkle EM, Falkenburg L, O'Neill RC, Morin A, et al. Endothelial cell tube formation assay for the in vitro study of angiogenesis. J Vis Exp. 2014;e51312. https://doi.org/10.3791/51312.
79. Uhlén M, Björling E, Agaton C, Szigyarto CA, Amini B, Andersen E, Andersson AC, Angelidou P, Asplund A, Asplund C, et al. A human protein atlas for normal and cancer tissues based on antibody proteomics. Mol Cell Proteom. 2005;4:1920–32. https://doi.org/10.1074/mcp.M500279-MCP200.
80. Zhou X. How do kinases contribute to tonicity-dependent regulation of the transcription factor NFAT5? World J Nephrol. 2016;5:20–32. https://doi.org/10.5527/wjn.v5.i1.20.
81. Catela C, Kratsios P, Hede M, Lang F, Rosenthal N. Serum and glucocorticoid-inducible kinase 1 (SGK1) is necessary for vascular remodeling during angiogenesis. Dev Dynamics: Official Publication Am Association Anatomists. 2010;239:2149–60. https://doi.org/10.1002/dvdy.22345.
82. Talarico C, Dattilo V, D'Antona L, Menniti M, Bianco C, Ortuso F, Alcaro S, Schenone S, Perrotti N, Amato R. SGK1, the New Player in the game of resistance: Chemo-Radio Molecular Target and Strategy for Inhibition. Cell Physiol Biochem. 2016;39:1863–76. https://doi.org/10.1159/000447885.
83. Nguyen QD, De Falco S, Behar-Cohen F, Lam WC, Li X, Reichhart N, Ricci F, Pluim J, Li WW. Placental growth factor and its potential role in diabetic retinopathy and other ocular neovascular diseases. Acta Ophthalmol. 2018;96:e1–9. https://doi.org/10.1111/aos.13325.
84. Akil A, Gutiérrez-García AK, Guenter R, Rose JB, Beck AW, Chen H, Ren B. Notch Signaling in Vascular endothelial cells, angiogenesis, and Tumor Progression: an update and prospective. Front Cell Dev Biol. 2021;9. https://doi.org/10.3389/fcell.2021.642352.
85. Lakshmikanthan S, Sobczak M, Li Calzi S, Shaw L, Grant MB, Chrzanowska-Wodnicka M. Rap1B promotes VEGF-induced endothelial permeability and is required for dynamic regulation of the endothelial barrier. J Cell Sci. 2018;131. https://doi.org/10.1242/jcs.207605.
86. Whitley GS, Cartwright JE. Cellular and molecular regulation of spiral artery remodelling: lessons from the cardiovascular field. Placenta. 2010;31:465–74. https://doi.org/10.1016/j.placenta.2010.03.002.
87. Smith SK. Regulation of angiogenesis in the endometrium. Trends Endocrinol Metabolism. 2001;12:147–51. https://doi.org/10.1016/S1043-2760(01)00379-4.
88. Kornacki J, Olejniczak O, Sibiak R, Gutaj P, Wender-Ożegowska E. Pathophysiology of Pre-eclampsia-two theories of the development of the Disease. Int J Mol Sci. 2023;25. https://doi.org/10.3390/ijms25010307.
89. Sufriyana H, Wu YW, Su EC. Low- and high-level information analyses of transcriptome connecting endometrial-decidua-placental origin of preeclampsia subtypes: a preliminary study. Pac Symp Biocomput. 2024;29:549–63.
90. Dimitriadis E, White C, Jones R, Salamonsen L. Cytokines, chemokines and growth factors in endometrium related to implantation. Hum Reprod Update. 2005;11:613–30. https://doi.org/10.1093/humupd/dmi023.
91. Lee JH, Kim M, Im YS, Choi W, Byeon SH, Lee HK. NFAT5 induction and its role in Hyperosmolar Stressed Human Limbal epithelial cells. Investig Ophthalmol Vis Sci. 2008;49:1827–35. https://doi.org/10.1167/iovs.07-1142.
92. Amara S, Alotaibi D, Tiriveedhi V. NFAT5/STAT3 interaction mediates synergism of high salt with IL-17 towards induction of VEGF-A expression in breast cancer cells. Oncol Lett. 2016;12:933–43. https://doi.org/10.3892/ol.2016.4713.
93. Wu CC, Hsu SC, Shih HM, Lai MZ. Nuclear factor of activated T cells c is a target of p38 mitogen-activated protein kinase in T cells. Mol Cell Biol. 2003;23:6442–54. https://doi.org/10.1128/mcb.23.18.6442-6454.2003.
94. Gómez del Arco P, Martínez-Martínez S, Maldonado JL, Ortega-Pérez I, Redondo JM. A role for the p38 MAP kinase pathway in the nuclear shuttling of NFATp. J Biol Chem. 2000;275:13872–8. https://doi.org/10.1074/jbc.275.18.13872.
95. Chen S, Grigsby CL, Law CS, Ni X, Nekrep N, Olsen K, Humphreys MH, Gardner DG. Tonicity-dependent induction of Sgk1 expression has a potential role in dehydration-induced natriuresis in rodents. J Clin Investig. 2009;119:1647–58. https://doi.org/10.1172/JCI35314.
96. Wang D, Na Q, Song GY, Wang L. Human umbilical cord mesenchymal stem cell-derived exosome-mediated transfer of microRNA-133b boosts trophoblast cell proliferation, migration and invasion in preeclampsia by restricting SGK1. Cell Cycle. 2020;19:1869–83. https://doi.org/10.1080/15384101.2020.1769394.
97. Zhu H, Zhang S. Hypoxia inducible factor-1α/vascular endothelial growth factor signaling activation correlates with response to radiotherapy and

its inhibition reduces hypoxia-induced angiogenesis in lung cancer. J Cell Biochem. 2018;119:7707–18. https://doi.org/10.1002/jcb.27120.
98. Núñez-Gómez E, Pericacho M, Ollauri-Ibáñez C, Bernabéu C, López-Novoa JM. The role of endoglin in post-ischemic revascularization. Angiogenesis. 2017;20:1–24. https://doi.org/10.1007/s10456-016-9535-4.
99. Ahluwalia A, Tarnawski AS. Critical role of hypoxia sensor–HIF-1α in VEGF gene activation. Implications for angiogenesis and tissue injury healing. Curr Med Chem. 2012;19:90–7. https://doi.org/10.2174/092986712803413944.
100. Hu K, Babapoor-Farrokhran S, Rodrigues M, Deshpande M, Puchner B, Kashiwabuchi F, Hassan SJ, Asnaghi L, Handa JT, Merbs S, et al. Hypoxia-inducible factor 1 upregulation of both VEGF and ANGPTL4 is required to promote the angiogenic phenotype in uveal melanoma. Oncotarget. 2016;7:7816–28. https://doi.org/10.18632/oncotarget.6868.
101. Fan X, Krieg S, Kuo CJ, Wiegand SJ, Rabinovitch M, Druzin ML, Brenner RM, Giudice LC, Nayak. N.R. VEGF blockade inhibits angiogenesis and reepithelialization of endometrium. Faseb j. 2008;22:3571–80. https://doi.org/10.1096/fj.08-111401.
102. Cao C, Zhou Y, Zhang Y, Ma Y, Du S, Fan L, Niu R, Zhang Y, He M. GCN5 participates in KLF4-VEGFA feedback to promote endometrial angiogenesis. iScience. 2022;25:104509. https://doi.org/10.1016/j.isci.2022.104509.
103. Girling JE, Rogers PA. Regulation of endometrial vascular remodelling: role of the vascular endothelial growth factor family and the angiopoietin-TIE signalling system. Reproduction. 2009;138:883–93. https://doi.org/10.1530/rep-09-0147.
104. Wiszniak S, Schwarz Q. Exploring the Intracrine functions of VEGF-A. Biomolecules. 2021;11. https://doi.org/10.3390/biom11010128.
105. Bhattacharya R, Fan F, Wang R, Ye X, Xia L, Boulbes D, Ellis LM. Intracrine VEGF signalling mediates colorectal cancer cell migration and invasion. Br J Cancer. 2017;117:848–55. https://doi.org/10.1038/bjc.2017.238.
106. Lee S, Chen TT, Barber CL, Jordan MC, Murdock J, Desai S, Ferrara N, Nagy A, Roos KP, Iruela-Arispe ML. Autocrine VEGF signaling is required for vascular homeostasis. Cell. 2007;130:691–703. https://doi.org/10.1016/j.cell.2007.06.054.
107. Koch KR, Refaian N, Hos D, Schlereth SL, Bosch JJ, Cursiefen C, Heindl LM. Autocrine impact of VEGF-A on uveal melanoma cells. Invest Ophthalmol Vis Sci. 2014;55:2697–704. https://doi.org/10.1167/iovs.13-13254.
108. Tudisco L, Della Ragione F, Tarallo V, Apicella I, D'Esposito M, Matarazzo MR, De Falco S. Epigenetic control of hypoxia inducible factor-1α-dependent expression of placental growth factor in hypoxic conditions. Epigenetics. 2014;9:600–10. https://doi.org/10.4161/epi.27835.
109. Lazzara F, Trotta MC, Platania CBM, D'Amico M, Petrillo F, Galdiero M, Gesualdo C, Rossi S, Drago F, Bucolo C. Stabilization of HIF-1α in human retinal endothelial cells modulates expression of miRNAs and proangiogenic growth factors. Front Pharmacol. 2020;11:1063. https://doi.org/10.3389/fphar.2020.01063.
110. Eriksson A, Cao R, Pawliuk R, Berg SM, Tsang M, Zhou D, Fleet C, Tritsaris K, Dissing S, Leboulch P, et al. Placenta growth factor-1 antagonizes VEGF-induced angiogenesis and tumor growth by the formation of functionally inactive PlGF-1/VEGF heterodimers. Cancer Cell. 2002;1:99–108. https://doi.org/10.1016/s1535-6108(02)00028-4.
111. Abhinand CS, Raju R, Soumya SJ, Arya PS, Sudhakaran PR. VEGF-A/VEGFR2 signaling network in endothelial cells relevant to angiogenesis. J Cell Commun Signal. 2016;10:347–54. https://doi.org/10.1007/s12079-016-0352-8.
112. E G, Cao Y, Bhattacharya S, Dutta S, Wang E, Mukhopadhyay D. Endogenous vascular endothelial growth factor-A (VEGF-A) maintains endothelial cell homeostasis by regulating VEGF receptor-2 transcription. J Biol Chem. 2012;287:3029–41. https://doi.org/10.1074/jbc.M111.293985.
113. Braile M, Marcella S, Cristinziano L, Galdiero MR, Modestino L, Ferrara AL, Varricchi G, Marone G, Loffredo S. VEGF-A in Cardiomyocytes and Heart diseases. Int J Mol Sci. 2020;21. https://doi.org/10.3390/ijms21155294.
114. Apte RS, Chen DS, Ferrara N. VEGF in Signaling and Disease: Beyond Discovery and Development. Cell. 2019;176:1248–64. https://doi.org/10.1016/j.cell.2019.01.021.
115. Blanco R, Gerhardt H. VEGF and notch in tip and stalk cell selection. Cold Spring Harb Perspect Med. 2013;3:a006569. https://doi.org/10.1101/cshperspect.a006569.
116. Chen W, Xia P, Wang H, Tu J, Liang X, Zhang X, Li L. The endothelial tip-stalk cell selection and shuffling during angiogenesis. J Cell Commun Signal. 2019;13:291–301. https://doi.org/10.1007/s12079-019-00511-z.
117. Cöl-Madendag I, Madendag Y, Altinkaya S, Bayramoglu H, Danisman N. The role of VEGF and its receptors in the etiology of early pregnancy loss. Gynecol Endocrinol. 2014;30:153–6. https://doi.org/10.3109/09513590.2013.864272.
118. Mongiat M, Andreuzzi E, Tarticchio G, Paulitti A. Extracellular matrix, a hard player in Angiogenesis. Int J Mol Sci. 2016;17. https://doi.org/10.3390/ijms17111822.
119. Whelan MC, Senger DR. Collagen I initiates endothelial cell morphogenesis by inducing actin polymerization through suppression of cyclic AMP and protein kinase A. J Biol Chem. 2003;278:327–34. https://doi.org/10.1074/jbc.M207554200.
120. Wang X, Khalil RA, Matrix, Metalloproteinases. Vascular remodeling, and Vascular Disease. Adv Pharmacol. 2018;81:241–330. https://doi.org/10.1016/bs.apha.2017.08.002.
121. Kim JY, Kim YM. Acute atherosis of the uterine spiral arteries: clinicopathologic implications. J Pathol Transl Med. 2015;49:462–71. https://doi.org/10.4132/jptm.2015.10.23.
122. Pitz Jacobsen D, Fjeldstad HE, Johnsen GM, Fosheim IK, Moe K, Alnæs-Katjavivi P, Dechend R, Sugulle M, Staff AC. Acute atherosis lesions at the fetal-maternal Border: current knowledge and implications for maternal Cardiovascular Health. Front Immunol. 2021;12:791606. https://doi.org/10.3389/fimmu.2021.791606.
123. Sato Y, Fujiwara H, Konishi I. Mechanism of maternal vascular remodeling during human pregnancy. Reprod Med Biol. 2012;11:27–36. https://doi.org/10.1007/s12522-011-0102-9.
124. Allerkamp HH, Leighton S, Pole T, Clark AR, James JL. Synergistic regulation of uterine radial artery adaptation to pregnancy by paracrine and hemodynamic factors. Am J Physiol Heart Circ Physiol. 2023;325:H790–805. https://doi.org/10.1152/ajpheart.00205.2023.
125. Huang CC, Hsueh YW, Chang CW, Hsu HC, Yang TC, Lin WC, Chang HM. Establishment of the fetal-maternal interface: developmental events in human implantation and placentation. Front Cell Dev Biol. 2023;11:1200330. https://doi.org/10.3389/fcell.2023.1200330.
126. Claesson-Welsh L, Dejana E, McDonald DM. Permeability of the endothelial barrier: identifying and reconciling controversies. Trends Mol Med. 2021;27:314–31. https://doi.org/10.1016/j.molmed.2020.11.006.
127. Salker MS, Christian M, Steel JH, Nautiyal J, Lavery S, Trew G, Webster Z, Al-Sabbagh M, Puchchakayala G, Föller M, et al. Deregulation of the serum- and glucocorticoid-inducible kinase SGK1 in the endometrium causes reproductive failure. Nat Med. 2011;17:1509–13. https://doi.org/10.1038/nm.2498.
128. Xi X, Zhang J, Wang J, Chen Y, Zhang W, Zhang X, Du J, Zhu G. SGK1 mediates hypoxic pulmonary hypertension through promoting macrophage infiltration and activation. Anal Cell Pathol (Amst). 2019;2019(3013765). https://doi.org/10.1155/2019/3013765.
129. Baban B, Liu JY, Mozaffari MS. SGK-1 regulates inflammation and cell death in the ischemic-reperfused heart: pressure-related effects. Am J Hypertens. 2014;27:846–56. https://doi.org/10.1093/ajh/hpt269.
130. Nevo O, Soleymanlou N, Wu Y, Xu J, Kingdom J, Many A, Zamudio S, Caniggia I. Increased expression of sFlt-1 in in vivo and in vitro models of human placental hypoxia is mediated by HIF-1. Am J Physiol Regul Integr Comp Physiol. 2006;291:R1085–1093. https://doi.org/10.1152/ajpregu.00794.2005.
131. Sánchez-Elsner T, Botella LM, Velasco B, Langa C, Bernabéu C. Endoglin expression is regulated by transcriptional cooperation between the hypoxia and transforming growth factor-beta pathways. J Biol Chem. 2002;277:43799–808. https://doi.org/10.1074/jbc.M207160200.
132. Tal R, Shaish A, Barshack I, Polak-Charcon S, Afek A, Volkov A, Feldman B, Avivi C, Harats D. Effects of hypoxia-inducible factor-1alpha overexpression in pregnant mice: possible implications for preeclampsia and intrauterine growth restriction. Am J Pathol. 2010;177:2950–62. https://doi.org/10.2353/ajpath.2010.090800.
133. Plasencia W, Maiz N, Bonino S, Kaihura C, Nicolaides KH. Uterine artery Doppler at 11 + 0 to 13 + 6 weeks in the prediction of pre-eclampsia. Ultrasound Obstet Gynecol. 2007;30:742–9. https://doi.org/10.1002/uog.5157.
134. Xavier P, Beires J, Barros H, Martinez-de-Oliveira J. Subendometrial and intraendometrial blood flow during the menstrual cycle in patients with endometriosis. Fertil Steril. 2005;84:52–9. https://doi.org/10.1016/j.fertnstert.2005.01.114.
135. Wei X, Yang X. The central role of natural killer cells in preeclampsia. Front Immunol. 2023;14:1009867. https://doi.org/10.3389/fimmu.2023.1009867.
136. Mukherjee I, Dhar R, Singh S, Sharma JB, Nag TC, Mridha AR, Jaiswal P, Biswas S, Karmakar S. Oxidative stress-induced impairment of trophoblast function causes preeclampsia through the unfolded protein response pathway. Sci Rep. 2021;11:18415. https://doi.org/10.1038/s41598-021-97799-y.
137. Huppertz B. The critical role of abnormal trophoblast development in the etiology of Preeclampsia. Curr Pharm Biotechnol. 2018;19:771–80. https://doi.org/10.2174/1389201019666180427110547.

138. Lim JH, Kang YJ, Bak HJ, Kim MS, Lee HJ, Kwak DW, Han YJ, Kim MY, Boo H, Kim SY, et al. Epigenome-wide DNA methylation profiling of preeclamptic placenta according to severe features. Clin Epigenetics. 2020;12. https://doi.org/10.1186/s13148-020-00918-1.
139. Roberts VH, Webster RP, Brockman DE, Pitzer BA, Myatt L. Post-Translational Modifications of the P2X(4) purinergic receptor subtype in the human placenta are altered in preeclampsia. Placenta. 2007;28:270–7. https://doi.org/10.1016/j.placenta.2006.04.008.
140. Brosens JJ, Parker MG, McIndoe A, Pijnenborg R, Brosens IA. A role for menstruation in preconditioning the uterus for successful pregnancy. Am J Obstet Gynecol. 2009;200:e615611–616. https://doi.org/10.1016/j.ajog.2008.11.037.
141. Admati I, Skarbianskis N, Hochgerner H, Ophir O, Weiner Z, Yagel S, Solt I, Zeisel A. Two distinct molecular faces of preeclampsia revealed by single-cell transcriptomics. Med. 2023;4:687–e709687. https://doi.org/10.1016/j.medj.2023.07.005.
142. Yang W, Ahn H, Hinrichs M, Torry RJ, Torry DS. Evidence of a novel isoform of placenta growth factor (PlGF-4) expressed in human trophoblast and endothelial cells. J Reprod Immunol. 2003;60:53–60. https://doi.org/10.1016/s0165-0378(03)00082-2.
143. Nucci M, Poon LC, Demirdjian G, Darbouret B, Nicolaides KH. Maternal serum placental growth factor (PlGF) isoforms 1 and 2 at 11–13 weeks' gestation in normal and pathological pregnancies. Fetal Diagn Ther. 2014;36:106–16. https://doi.org/10.1159/000357842.
144. Ahmed A, Dunk C, Ahmad S, Khaliq A. Regulation of placental vascular endothelial growth factor (VEGF) and placenta growth factor (PlGF) and soluble Flt-1 by oxygen–a review. Placenta. 2000;21(Suppl A):S16–24. https://doi.org/10.1053/plac.1999.0524.
145. Wang W, Vilella F, Alama P, Moreno I, Mignardi M, Isakova A, Pan W, Simon C, Quake SR. Single-cell transcriptomic atlas of the human endometrium during the menstrual cycle. Nat Med. 2020;26:1644–53. https://doi.org/10.1038/s41591-020-1040-z.
146. Rolfo A, Giuffrida D, Nuzzo AM, Pierobon D, Cardaropoli S, Piccoli E, Giovarelli M, Todros T. Pro-inflammatory profile of preeclamptic placental mesenchymal stromal cells: new insights into the etiopathogenesis of preeclampsia. PLoS ONE. 2013;8:e59403. https://doi.org/10.1371/journal.pone.0059403.
147. Kusuma GD, Georgiou HM, Perkins AV, Abumaree MH, Brennecke SP, Kalionis B. Mesenchymal Stem/Stromal cells and their role in oxidative stress Associated with Preeclampsia. Yale J Biol Med. 2022;95:115–27.
148. Zheng S, Shi A, Hill S, Grant C, Kokkinos MI, Murthi P, Georgiou HM, Brennecke SP, Kalionis B. Decidual mesenchymal stem/stromal cell-derived extracellular vesicles ameliorate endothelial cell proliferation, inflammation, and oxidative stress in a cell culture model of preeclampsia. Pregnancy Hypertens. 2020;22:37–46. https://doi.org/10.1016/j.preghy.2020.07.003.
149. Scaife PJ, Simpson A, Kurlak LO, Briggs LV, Gardner DS, Broughton Pipkin F, Jones CJP, Mistry HD. Increased placental cell senescence and oxidative stress in women with Pre-eclampsia and Normotensive Post-term pregnancies. Int J Mol Sci. 2021;22. https://doi.org/10.3390/ijms22147295.
150. Zhang Y, Zhong Y, Yu Z, Cheng X, Zou L, Liu X. Single cell RNA-sequencing reveals the cellular senescence of placental mesenchymal stem/stromal cell in preeclampsia. Placenta. 2024;150:39–51. https://doi.org/10.1016/j.placenta.2024.03.014.
151. Yang X, Chen D, He B, Cheng W. NRP1 and MMP9 are dual targets of RNA-binding protein QKI5 to alter VEGF-R/ NRP1 signalling in trophoblasts in preeclampsia. J Cell Mol Med. 2021;25:5655–70. https://doi.org/10.1111/jcmm.16580.
152. Gray KJ, Saxena R, Karumanchi SA. Genetic predisposition to preeclampsia is conferred by fetal DNA variants near FLT1, a gene involved in the regulation of angiogenesis. Am J Obstet Gynecol. 2018;218:211–8. https://doi.org/10.1016/j.ajog.2017.11.562.
153. McGinnis R, Steinthorsdottir V, Williams NO, Thorleifsson G, Shooter S, Hjartardottir S, Bumpstead S, Stefansdottir L, Hildyard L, Sigurdsson JK, et al. Variants in the fetal genome near FLT1 are associated with risk of preeclampsia. Nat Genet. 2017;49:1255–60. https://doi.org/10.1038/ng.3895.
154. Vodolazkaia A, Yesilyurt BT, Kyama CM, Bokor A, Schols D, Huskens D, Meuleman C, Peeraer K, Tomassetti C, Bossuyt X, et al. Vascular endothelial growth factor pathway in endometriosis: genetic variants and plasma biomarkers. Fertil Steril. 2016;105:988–96. https://doi.org/10.1016/j.fertnstert.2015.12.016.
155. Zitouni H, Chayeb V, Ben Ali Gannoun M, Raguema N, Bendhaher S, Zouari I, Ben Abdennebi H, Guibourdenche J, Mahjoub T, Gaddour K, et al. Preeclampsia is associated with reduced renin, aldosterone, and PlGF levels, and increased sFlt-1/PlGF ratio, and specific angiotensin-converting enzyme Ins-Del gene variants. J Reprod Immunol. 2023;157:103924. https://doi.org/10.1016/j.jri.2023.103924.
156. Becker-Greene D, Li H, Perez-Cremades D, Wu W, Bestepe F, Ozdemir D, Niosi CE, Aydogan C, Orgill DP, Feinberg MW, et al. MiR-409-3p targets a MAP4K3-ZEB1-PLGF signaling axis and controls brown adipose tissue angiogenesis and insulin resistance. Cell Mol Life Sci. 2021;78:7663–79. https://doi.org/10.1007/s00018-021-03960-1.
157. Heimberger S, Mueller A, Ratnaparkhi R, Perdigao JL, Rana S. Angiogenic factor abnormalities and risk of peripartum complications and prematurity among urban predominantly obese parturients with chronic hypertension. Pregnancy Hypertens. 2020;20:124–30. https://doi.org/10.1016/j.preghy.2020.04.004.
158. Mesquita J, Santos FM, Sousa JP, Vaz-Pereira S, Tavares-Ratado P, Neves A, Mesquita R, Tomaz CT. Serum and vitreous levels of Placenta Growth factor in Diabetic Retinopathy patients: correlation with Disease Severity and Optical Coherence Tomographic parameters. Cureus. 2024;16:e54862. https://doi.org/10.7759/cureus.54862.
159. Wang Y, Ding Y, Zhuang Q, Luan J. Comparison of the cytokines levels in aqueous humor in vitrectomized eyes versus non-vitrectomized eyes with diabetic macular edema. Int Ophthalmol. 2024;44:220. https://doi.org/10.1007/s10792-024-03136-3.
160. Sierra-Ramos C, Velazquez-Garcia S, Vastola-Mascolo A, Hernández G, Faresse N. Alvarez De La Rosa, D. SGK1 activation exacerbates diet-induced obesity, metabolic syndrome and hypertension. J Endocrinol. 2020;244:149–62. https://doi.org/10.1530/joe-19-0275.
161. Xu H, Li J, Jin L, Zhang D, Chen B, Liu X, Lin X, Huang Y, Ke Z, Liu J, et al. Intrauterine hyperglycemia impairs endometrial receptivity via up-regulating SGK1 in diabetes. Sci China Life Sci. 2022;65:1578–89. https://doi.org/10.1007/s11427-021-2035-2.
162. Hill MA, Yang Y, Zhang L, Sun Z, Jia G, Parrish AR, Sowers JR. Insulin resistance, cardiovascular stiffening and cardiovascular disease. Metabolism. 2021;119:154766. https://doi.org/10.1016/j.metabol.2021.154766.
163. Norlander AE, Saleh MA, Pandey AK, Itani HA, Wu J, Xiao L, Kang J, Dale BL, Goleva SB, Laroumanie F, et al. A salt-sensing kinase in T lymphocytes, SGK1, drives hypertension and hypertensive end-organ damage. JCI Insight. 2017;2. https://doi.org/10.1172/jci.insight.92801.

Publisher's Note

Supplementary Information

Placental growth factor mediates pathological uterine angiogenesis by activating the NFAT5-SGK1 signaling axis in the endometrium: Implications for preeclampsia development.

Supplementary 1

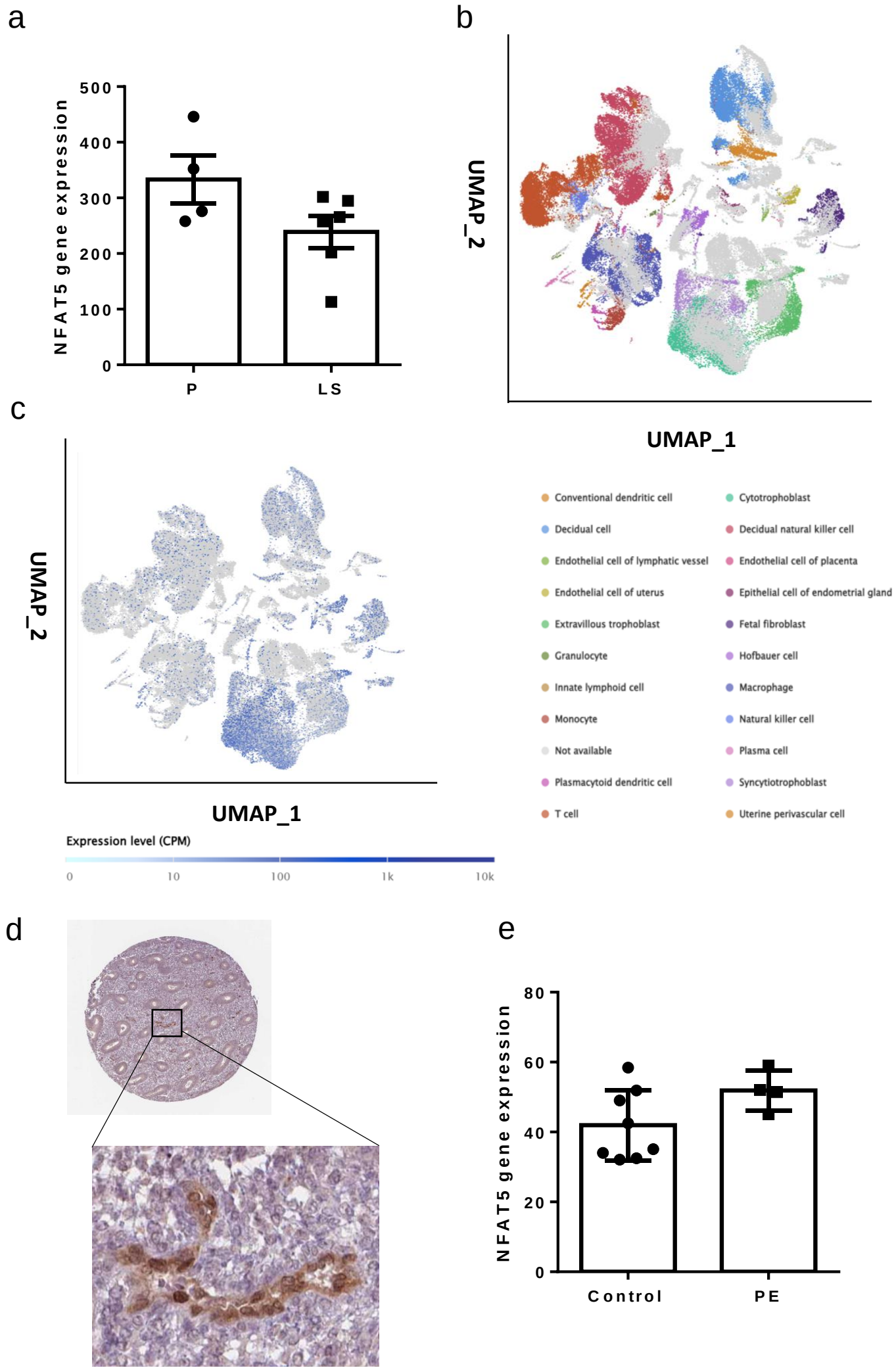

Supplementary Figure 1: a. NFAT5 gene expression value across the menstrual cycle in the proliferative (P) and late secretory (LS) phase (*GDS 2052*). b-c. UMAP projections of the dataset from Single-cell reconstruction of the early maternal-fetal interface in humans, b represents cell lineages of the decidua and placenta, c represents NFAT5 expression across the different decidual and placental cell population.d. NFAT5 protein expression on endometrial tissue samples analyzed from Human Protein Atlas. NAFT5 is expressed throughout the endometrium and staining was highest in the stroma near to the blood vessels e. NFAT5 gene expression value in the pre-symptamatic deciduas of PE patients compared with healthy (control) pregnant deciduas (*GDS 3467*).

Supplementary 2

a

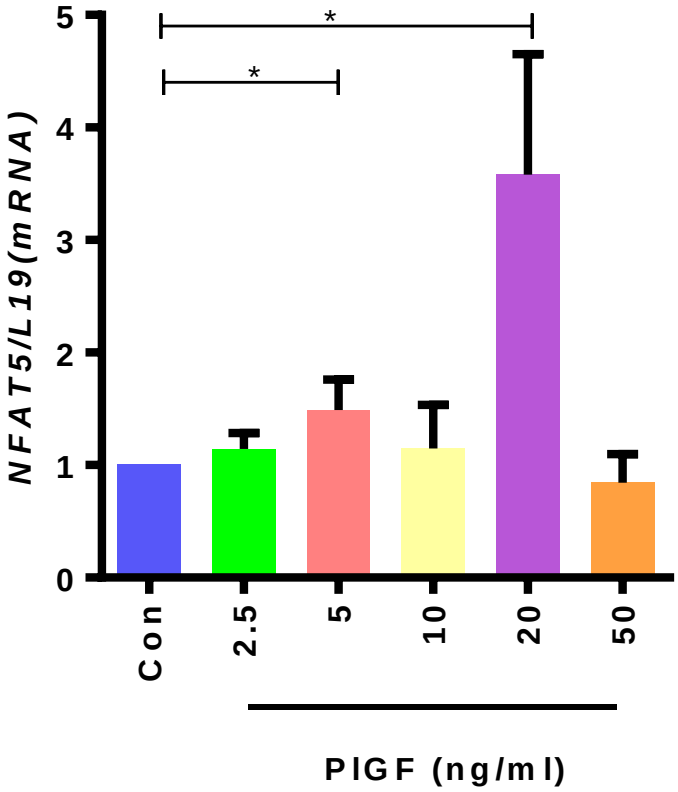

b

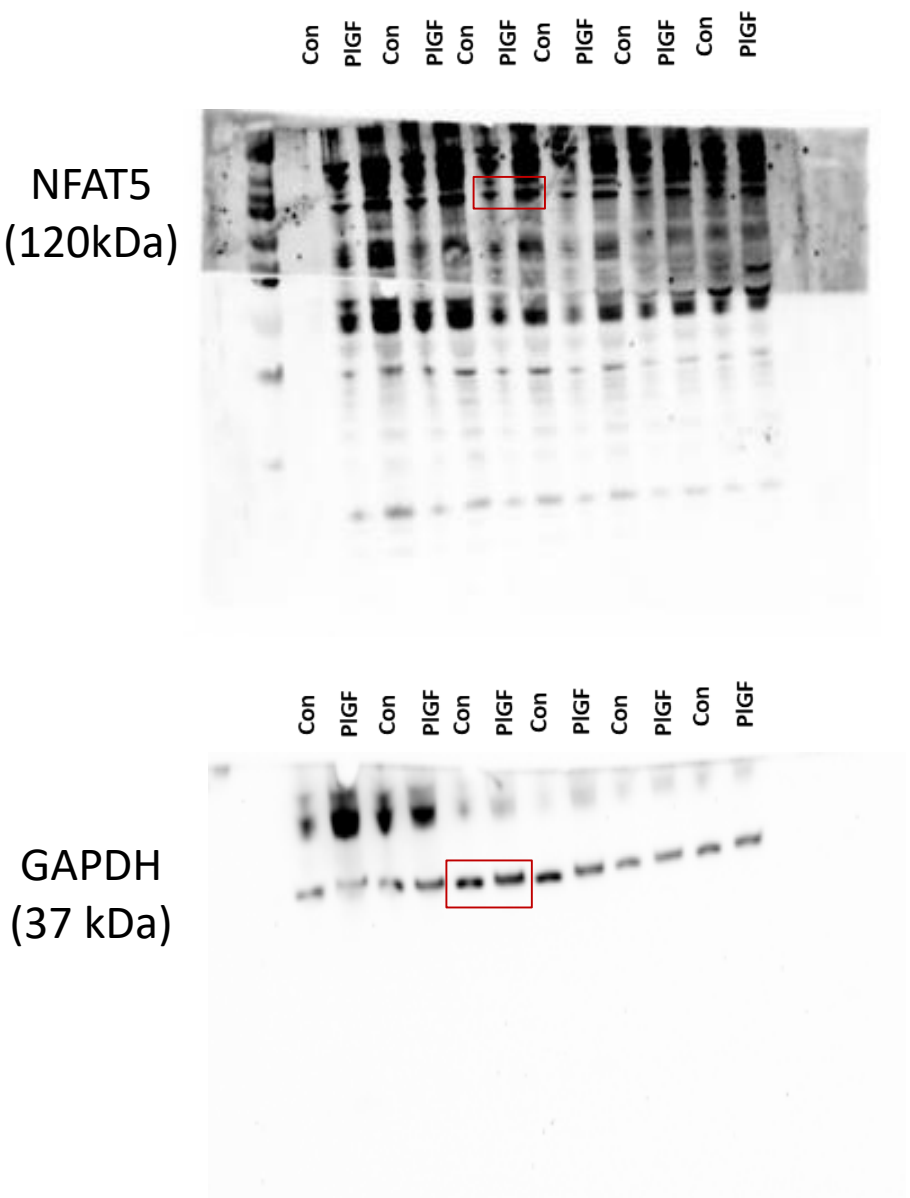

Supplementary Figure 2: a. qPCR determining NFAT5 expression in EnSCs treated with varying concentrations of PlGF (2.5 -50 ng/ml) for 24 hours. (n=4, *, $p < 0.05$) b. Original western blot membrane of blots represented in figure 1b.

Supplementary 3

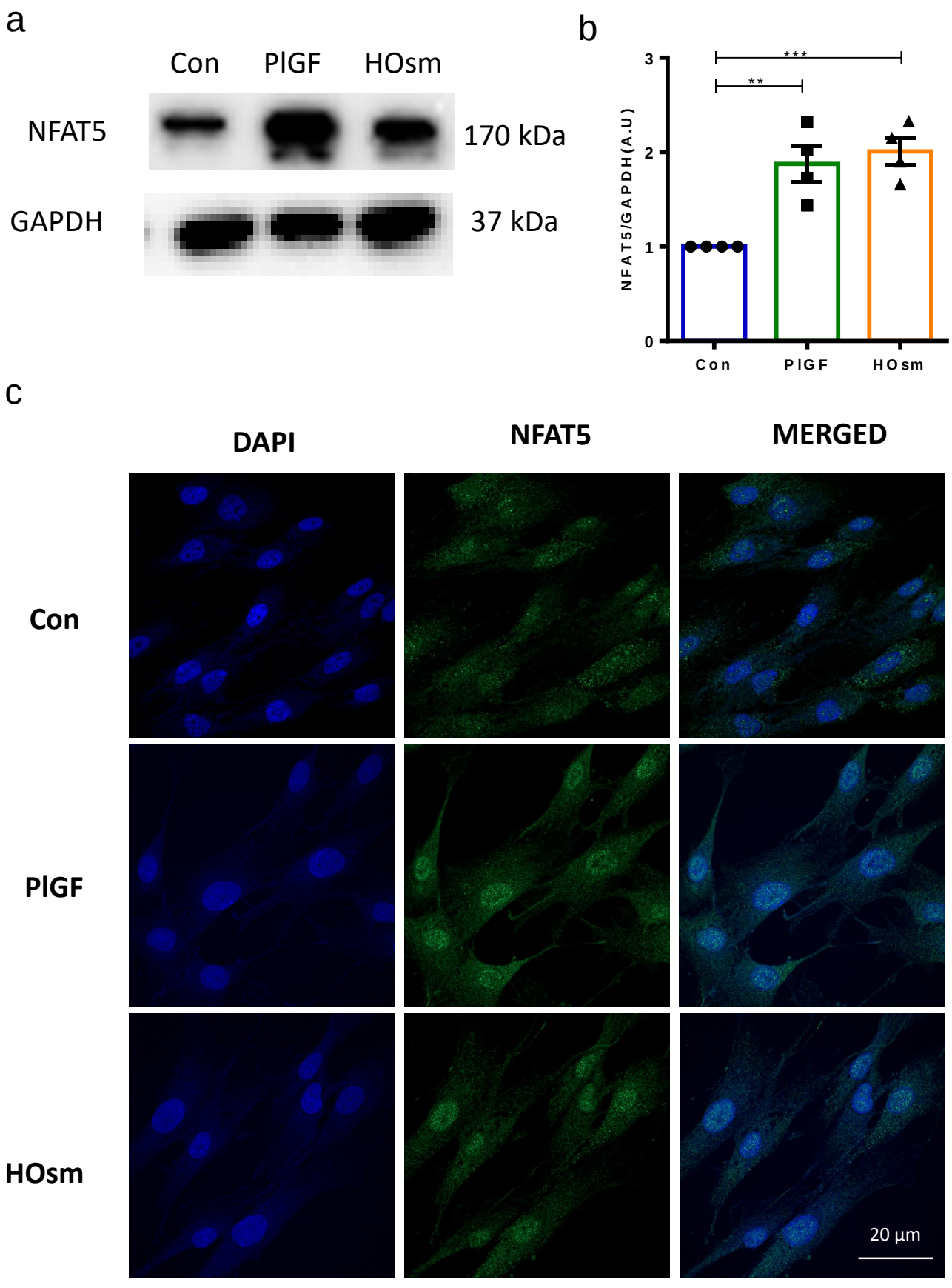

Supplementary 3: a. Original Western blot analysis of NFAT5 protein with GAPDH as loading control in untreated (Con), PlGF and HOsm treated EnSCs. b) Average NFAT5 protein levels after 6 days treatment with PlGF and 3 h treatment with Hosm (n=4, **, p 0.01, ***, p < 0.001). The samples are represented after normalization with untreated control (Con) (n=3). c) Immunofluorescence images confirms nuclear translocation of NFAT5 from the cytosol when activated by HOsm (n=3). Scale bar: 20 µm. Data represented as arithmetic mean ± SEM. Significance was determined using student's unpaired two-tailed t-test with Welch's correction method.

Supplementary 4

p-p38 MAPK (43 kDa)

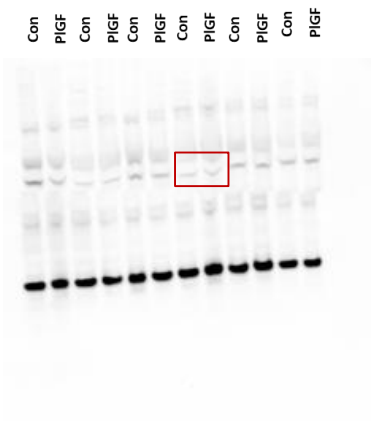

GAPDH (37 kDa)

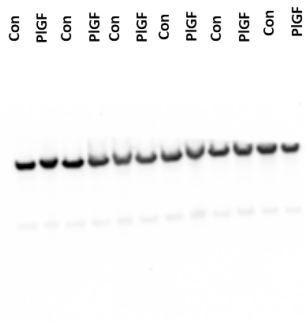

SGK1 (45-50 kDa)

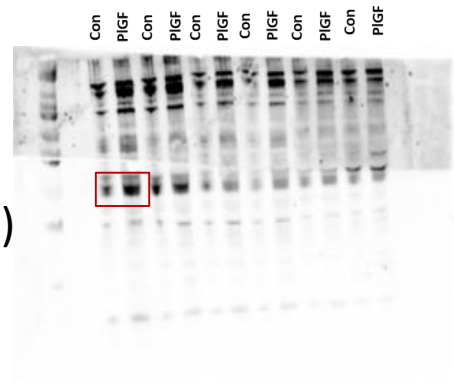

GAPDH (37 kDa)

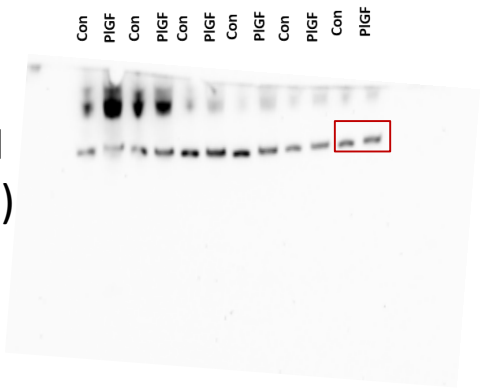

p-SGK1 (54 kDa)

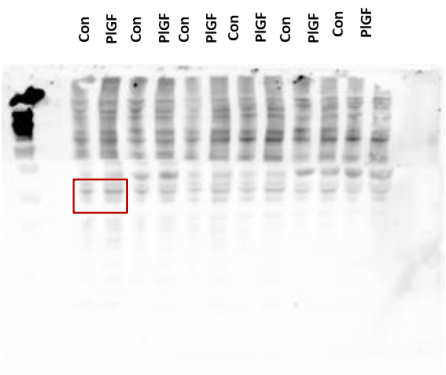

VEGF-A (27 kDa)

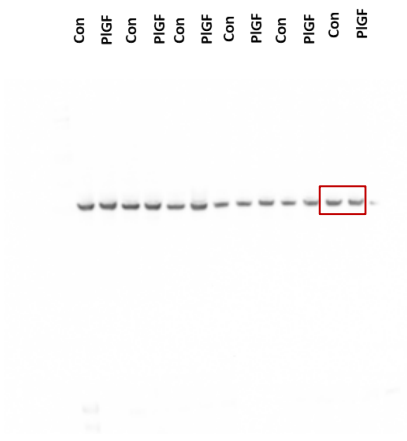

p38 MAPK (40 kDa)

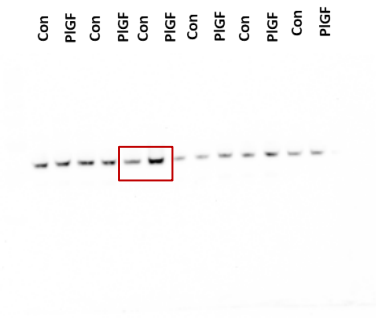

GAPDH (37 kDa)

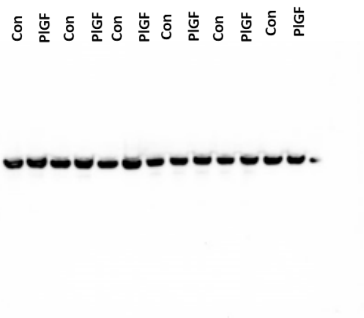

Supplementary Figure 4 : Original western blot membrane of blots represented in figure 2a.

Supplementary 5

a

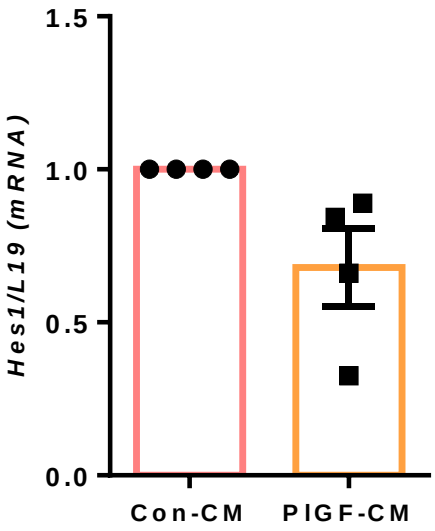

b

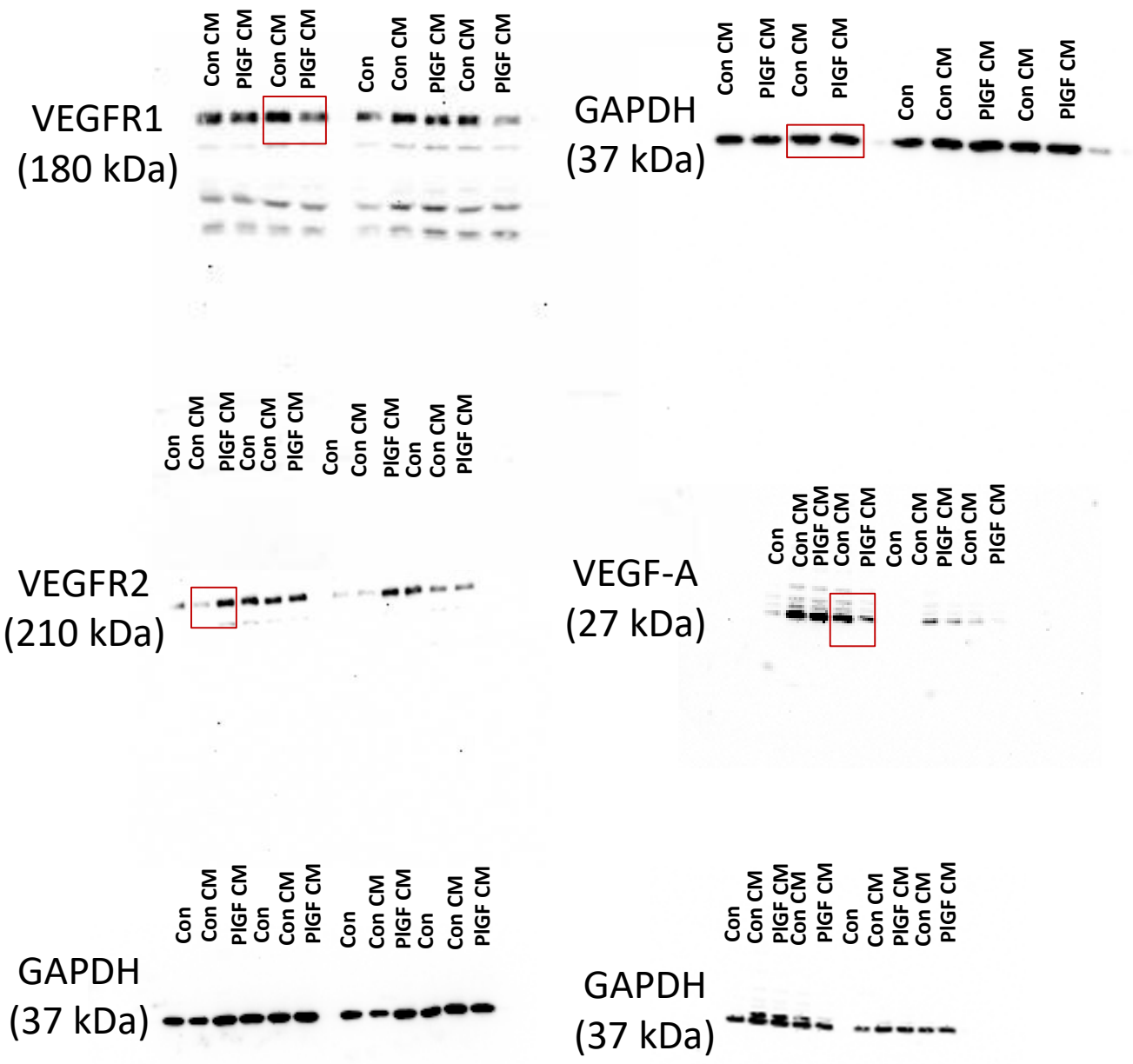

Supplementary Figure 8 : a. . qPCR analysis of Notch target gene (*Hes 1*) in Con-CM and PlGF-CM treated HUVECs. *L19* was used as a housekeeping control. (n=4). b. Original western blot membrane of blots represented in figure 4m.

Supplementary 6

SGK1
(45-60 kDa)

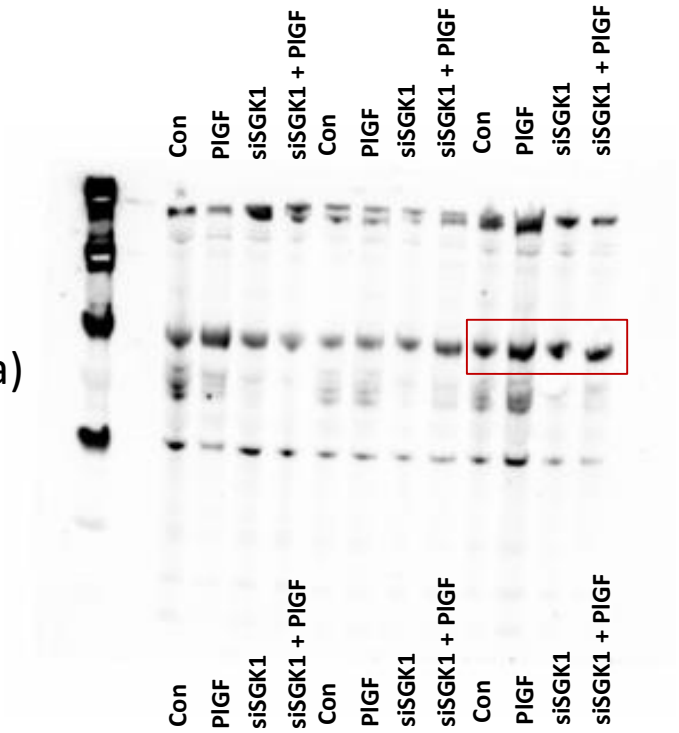

p-SGK1
(54 kDa)

VEGF-A
(27 kDa)

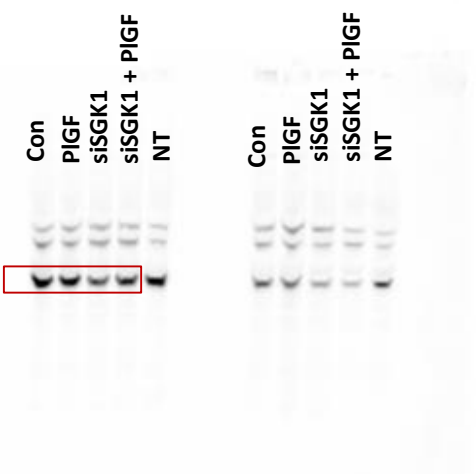

GAPDH
(37 kDa)

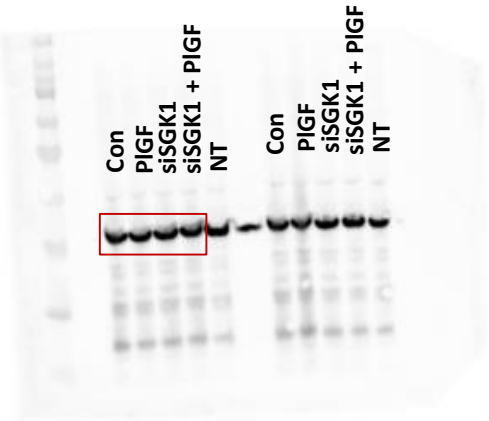

Supplementary Figure 8 : Original western blot membrane of blots represented in figure 5a.

Supplementary 7

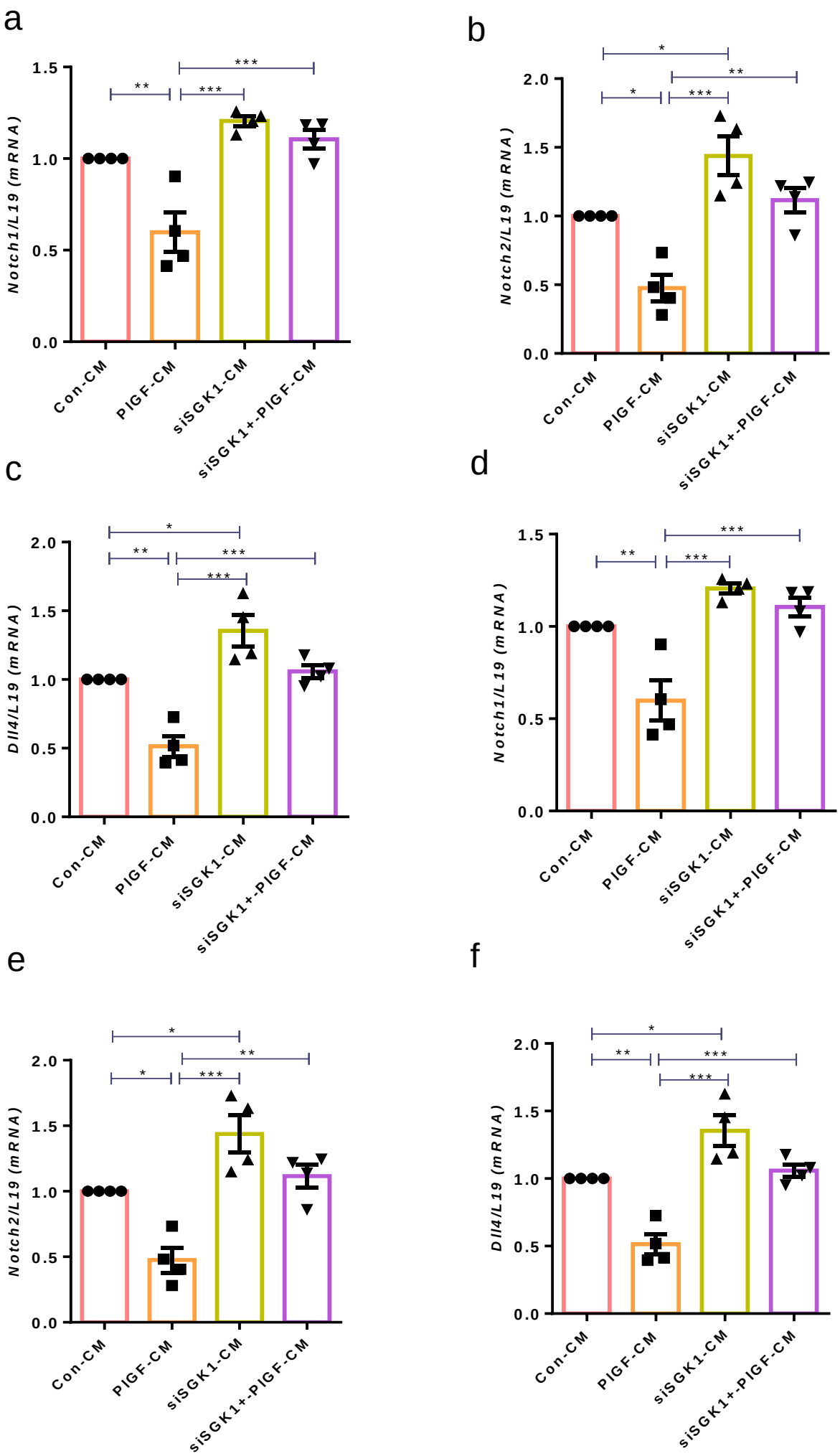

Supplementary Figure 7 : a-f. qPCR analysis of Notch receptors (*Notch1 and Notch2*), ligands (*Dll4 and Jagged-1*) and target genes (*Hey1and Hes1*) in Con-CM and PlGF-CM treated HUVECs. *L19* was used as a housekeeping control. (n=4, *, p<0.05, **, p < 0.01).

Supplementary 8

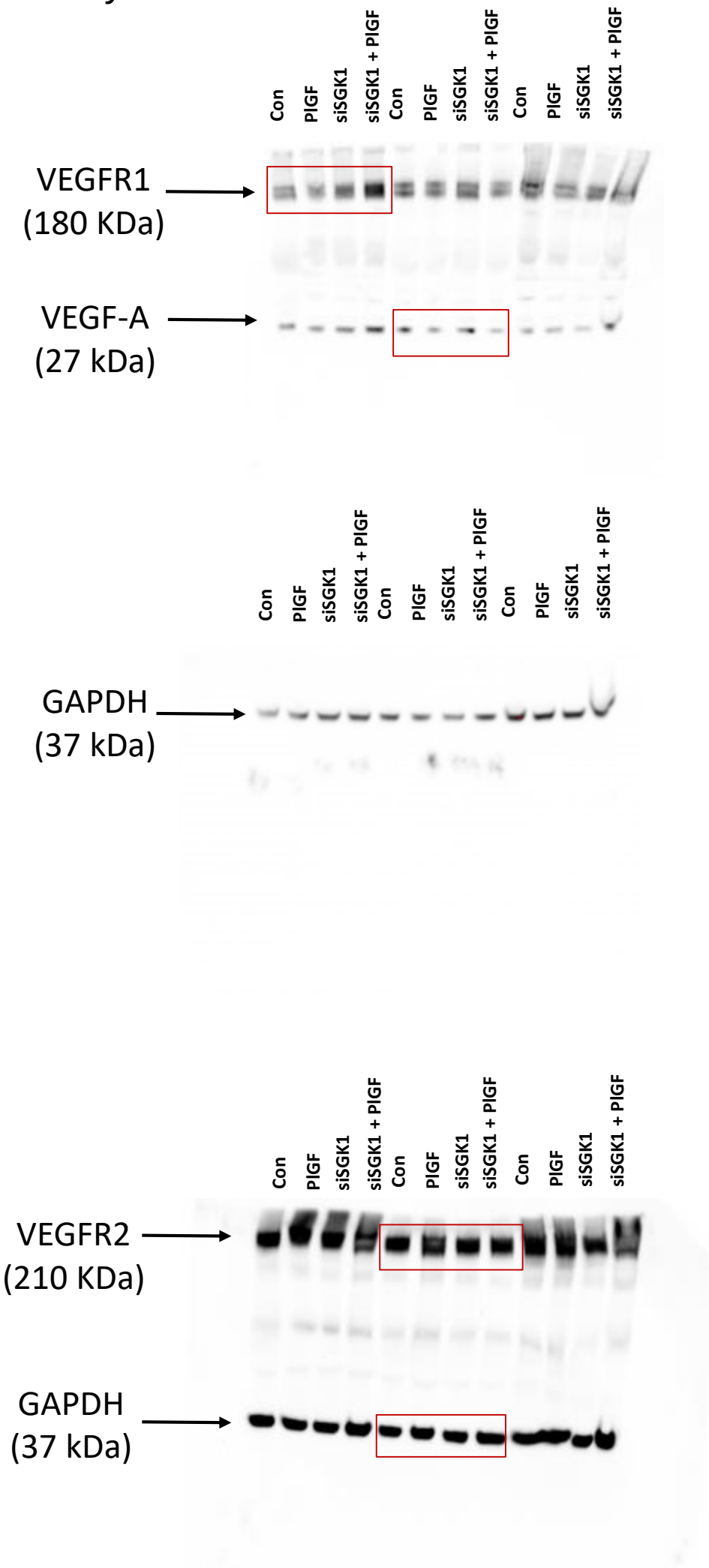

Supplementary Figure 8 : Original western blot membrane of blots represented in figure 6f.

International Journal of
Molecular Sciences

MDPI

Article

Rel Family Transcription Factor NFAT5 Upregulates COX2 via HIF-1α Activity in Ishikawa and HEC1a Cells

Toshiyuki Okumura [1,2], Janet P. Raja Xavier [1], Jana Pasternak [1], Zhiqi Yang [1], Cao Hang [1], Bakhtiyor Nosirov [3], Yogesh Singh [1,4], Jakob Admard [4], Sara Y. Brucker [1], Stefan Kommoss [1], Satoru Takeda [2], Annette Staebler [5], Florian Lang [6] and Madhuri S. Salker [1,*]

1 Department of Women's Health, Tübingen University Hospital, D-72076 Tübingen, Germany; tokumura@juntendo.ac.jp (T.O.); janet.raja-xavier@med.uni-tuebingen.de (J.P.R.X.); jana.pasternak@med.uni-tuebingen.de (J.P.); caohang3@gmail.com (C.H.); yogesh.singh@med.uni-tuebingen.de (Y.S.); sara.brucker@med.uni-tuebingen.de (S.Y.B.); stefan.kommoss@diakoneo.de (S.K.)
2 Department of Obstetrics and Gynecology, Faculty of Medicine, Juntendo University, Tokyo 113-8421, Japan; stakeda@juntendo.ac.jp
3 Department of Cancer Research, Luxembourg Institute of Health, L-1210 Luxembourg, Luxembourg
4 Institute of Medical Genetics and Applied Genomics, Eberhard Karls University, D-72074 Tübingen, Germany; jakob.admard@med.uni-tuebingen.de
5 Institute of Pathology, Eberhard Karls University, D-72074 Tübingen, Germany; annette.staebler@med.uni-tuebingen.de
6 Institute of Physiology, Eberhard Karls University, D-72074 Tübingen, Germany; florian.lang@uni-tuebingen.de
* Correspondence: madhuri.salker@med.uni-tuebingen.de; Tel.: +49-7071-29-78264

Abstract: Nuclear factor of activated T cells 5 (NFAT5) and cyclooxygenase 2 (COX2; *PTGS2*) both participate in diverse pathologies including cancer progression. However, the biological role of the NFAT5-COX2 signaling pathway in human endometrial cancer has remained elusive. The present study explored whether NFAT5 is expressed in endometrial tumors and if NFAT5 participates in cancer progression. To gain insights into the underlying mechanisms, NFAT5 protein abundance in endometrial cancer tissue was visualized by immunohistochemistry and endometrial cancer cells (Ishikawa and HEC1a) were transfected with NFAT5 or with an empty plasmid. As a result, NFAT5 expression is more abundant in high-grade than in low-grade endometrial cancer tissue. RNA sequencing analysis of NFAT5 overexpression in Ishikawa cells upregulated 37 genes and downregulated 20 genes. Genes affected included cyclooxygenase 2 and hypoxia inducible factor 1α (*HIF1A*). NFAT5 transfection and/or treatment with HIF-1α stabilizer exerted a strong stimulating effect on HIF-1α promoter activity as well as COX2 expression level and prostaglandin E2 receptor (PGE2) levels. Our findings suggest that activation of NFAT5—HIF-1α—COX2 axis could promote endometrial cancer progression.

Keywords: endometrial cancer; hypoxia inducible factor 1α; cyclooxygenase 2

Citation: Okumura, T.; Raja Xavier, J.P.; Pasternak, J.; Yang, Z.; Hang, C.; Nosirov, B.; Singh, Y.; Admard, J.; Brucker, S.Y.; Kommoss, S.; et al. Rel Family Transcription Factor NFAT5 Upregulates COX2 via HIF-1α Activity in Ishikawa and HEC1a Cells. *Int. J. Mol. Sci.* **2024**, *25*, 3666. https://doi.org/10.3390/ijms25073666

Academic Editors: Nam Deuk Kim and Maria Valeria Catani

Received: 1 August 2023
Revised: 14 March 2024
Accepted: 19 March 2024
Published: 25 March 2024

1. Introduction

Endometrial cancer (EnCa) is a frequent gynecological neoplasia and its incidence rate has increased in the past years, especially in developed or high-income countries [1,2]. In 2020, the reported global incidence of EnCa was 417,367 and about 2.2% of newly diagnosed cancer cases in that year, making it the sixth most commonly diagnosed cancer [3]. In contrast to breast and cervical cancers, which are expected to decline significantly by 2030, EnCa is expected to increase over the next decade [2,4,5]. The largest incident rate has been reported in women aged 65–79 years [6]; however, alarmingly, EnCa is increasing among younger age groups (25–49 years and 50–59 years) as well [7,8]. Risk factors for EnCa include ethnicity (in particular Caucasians), poor diet (high salt/sugar) obesity,

nulliparity, polycystic ovarian syndrome, estrogen-only hormone replacement therapy (HRT), comorbidities such as hypertension or diabetes, and genetic predisposition (Lynch and Cowden syndromes) [9–11]. As the world's population increases, together with an ageing population and the prevalence of risk factors, the number of individuals with EnCa is expected to increase further.

EnCa is a hormone-sensitive disease thought to arise due to excessive estrogenic stimulation of the endometrial lining of the uterus [4], though estrogen-independent pathways are also known to participate in carcinogenesis. This aberrant stimulation leads to mitogenic activation by hijacking physiological cellular mechanisms (i.e., the down regulation of checkpoint mechanisms, thus leading to uncontrolled proliferation), ultimately leading to malignant transformation and metastasis [11]. Cancer can advance when it acquires six biological hallmarks of cancer development, including: persistent proliferation signaling, evasion of growth suppressors, resistance to cell death, immortality, induction of angiogenesis, and activation of invasion and migratory pathways [11,12]. The molecular mechanisms behind these events involve a complex interplay of genetic, epigenetic, and environmental factors that lead to the uncontrolled growth and division of cells [9,13]. The survival outcomes are poor in patients with advanced disease, and hence, there is an urgent need for identification and discovery of new molecular targets to improve the survival of patients with EnCa.

Nuclear factor of activated T cells 5 (NFAT5/TonEBP) is a member of the Rel family of transcriptional activators, which also includes nuclear factor κappa B (NFκB) and NFAT1–4. NFAT5 has a DNA binding domain that is in sequence homology with the rel homology domain (RHD) [14]. In contrast to its other isoforms (NFAT1–4), NFAT5 lacks a calcineurin-binding domain outside of its DNA binding domain [14]. The NFAT5 protein contains a leucine-rich nuclear export sequence (NES) followed by a proline-rich transactivation domain (AD1) at the N-terminal. Further, it has low-complexity glutamine and serine/threonine-rich regions (AD2 and AD3) at the C- terminal end. The three activation domains (AD1, AD2, and AD3) act in coordination in response to hypertonicity [15,16]. NFAT5 is expressed in tissues that are often subjected to osmotic stress, such as the renal medulla, eyes, and skin [17–19]. Separately from the well-known osmoprotective role of NFAT5 in the renal medulla, NFAT5 is also activated in a *tonicity-independent* manner, having broader implications in development, immune function, and cellular stress responses [14]. Aberrant NFAT5 levels contribute to several pathologies, including hypoxia [20], vascular calcification [16,21], diabetes [22], inflammation [15,23], chronic kidney disease [24], bacterial infection [25], and are seen in breast and lung cancer [26–28]. NFAT5 is also highly expressed in mouse, ovine, and human placenta and throughout gestation in the mouse embryo, suggesting its critical role during embryonic development and fetal maturation [29]. NFAT5's involvement in cancer pathogenesis is not as extensively studied as other transcription factors; however, there is evidence suggesting its potential impact on tumor development. Studies have explored its involvement in breast cancer, renal cell carcinoma, and glioblastoma [30–32]. NFAT5 has been implicated in promoting cell survival and proliferation in breast cancer cells via secretion of pro-angiogenic factors [30]. High expression of NFAT5 levels in renal cell carcinoma has been correlated with various clinicopathological features, including tumor stage, grade, and metastasis [31]. This suggests NFAT5's potential role in the aggressiveness and progression of tumor pathophysiology. These findings suggest a potential role for NFAT5 in cancer pathogenesis; however, it has not yet been described in EnCa.

Hypoxia (insufficient oxygen) is a common feature of most tumors [33,34]. Hypoxia-inducible factors (HIFs) are often upregulated in cancer microenvironments and are known to aggravate tumorigenesis by inducing epithelial–to–mesenchymal transition (EMT) and induce a stem-cell-like phenotype, thus promoting cell survival [34,35]. A hypoxic environment can exacerbate tumorigenesis but is also involved in reducing therapeutic efficacy of chemotherapeutic agents [17,36]. Thus, identifying new factors inducing and driving hypoxia signaling in cancer progression is important in the development of new thera-

peutic targets for EnCa. Several studies show that cellular activation of NFAT5 favors transcriptional activation of HIF-1α [20,25,37]. NFAT5 and HIF-1α are known to coordinate together [25]. As highlighted by Yang et al., coordinated functional regulation between NFAT5 and HIF-1α is critically important in the pathogenesis of hypoxic-ischemic encephalopathy [20]. The cooperation of NFAT5 and HIF-1α in the pathophysiology of EnCa has not yet been defined.

In kidney and colon cancer models, NFAT5 has been shown to upregulate cyclooxygenase 2 (COX2; *PTGS2*) [38,39], an enzyme of paramount functional importance in both normal and malignant endometrial tissue [40,41]. Strikingly, inflammation-associated COX2 activation is also known to enhance HIF-1α activity in some tumor models such as breast and lung cancer [42,43]. HIF-1α-dependent COX2 activation is shown to promote proliferation, inflammation, and tumor metastasis [44]. It is currently unknown if NFAT5 is present in endometrium and if there is a putative link to NFAT5 activation and HIF-1α/COX2 signaling axis in EnCa progression.

The present study thus explored whether NFAT5 is expressed in human endometrial cancer tissue, whether NFAT5 expression in endometrial cancer cells is sensitive to HIF-1α, and investigated whether NFAT5 activation influences the expression of HIF-1α and COX2 signaling cascade in EnCa pathogenesis.

2. Results

The present study explored the expression and function of the transcription factor NFAT5 in endometrial cancer. A total of 26 cases were selected at random (between 2014–2016, Table 1). From the cohort, $n = 15$ were over the age of 60 and the vast majority of the cases had a post-menopausal status. Of the cases investigated the $n = 24$ were classified as Endometriod and two were Serous histotype.

Table 1. Clinical characteristics of study cohort.

Clinical Characteristics	Total	NFAT5 Score			*p*-Value
		1	2	3	
Age > 60 years	15 (100%)	5(33.3%)	6 (40%)	4 (26.7%)	$p = 0.941$
Age < 60 years	11 (100%)	3 (27.3%)	5 (45.5%)	3 (27.3%)	
Premenopausal	7 (100%)	3 (42.9%)	3 (42.9%)	1 (14.3%)	
Postmenopausal	19 (100%)	5 (26.3%)	8 (42.1%)	6 (31.6%)	$p = 0.599$
Endometriod	24 (100%)	8 (33.3%)	9 (37.5%)	7 (29.2%)	$p = 0.228$
Serous	2 (100%)	0 (0%)	2 (100%)	0 (0%)	
Grade 1/2	15 (100%)	8 (53.3%)	7 (46.7%)	0 (0%)	$p < 0.001$
Grade 3	11 (100%)	0 (0%)	4 (36.4%)	7 (63.6%)	
pT1a	15 (100%)	7 (46.7%)	7 (46.7%)	1 (6.7%)	$p = 0.091$
pT1b	6 (100%)	0 (0%)	3 (50%)	3 (50%)	
pT2	2 (100%)	1 (50%)	0 (0%)	1 (50%)	
pT3a	3 (100%)	0 (0%)	1 (33.3%)	2 (66.7%)	
pT1a	15 (100%)	7 (46.7%)	7 (46.7%)	1 (6.7%)	$p = 0.014$
>pT1b	11 (100%)	1 (9.1%)	4 (36.4%)	6 (54.5%)	
Regional Nodes pN0	21 (100%)	7 (33.3%)	10 (47.6%)	4 (19%)	$p = 0.176$
Regional Nodes pN1	5 (100%)	1 (20%)	1 (20%)	3 (60%)	
Metastatsis 0	20 (100%)	7 (35%)	10 (50%)	3 (15%)	$p = 0.043$
Metastatsis 1	6 (100%)	1 (16.7%)	1 (16.7%)	4 (66.7%)	
Lymph Vessel L0	19 (100%)	8 (42.1%)	7 (36.8%)	4 (21.1%)	$p = 0.114$
Lymph Vessel L1	7 (100%)	0 (0%)	4 (57.1%)	3 (42.9%)	

The overall score of the staining intensity typically has the following categories: weak (score 1), moderate (score 2), and strong (score 3) [45]. Immunostaining was performed on formalin fixed, paraffin-embedded (FFPE) archival endometrial tumor tissue and investigated for NFAT5 expression. As apparent from immunohistochemistry (Figure 1a and Table 1) in low-grade (G1, G2) endometrial cancer tissue, NFAT5 staining showed low to intermediate cytoplasmic intensity (score 1) in the tumor cells, which is less than the moderate staining in neighboring endothelial cells (score 2) serving as an internal reference. In contrast, NFAT5 expression shows a strong and block-like expression pattern in high-grade endometrioid carcinomas (G3) with particularly strong staining in the perivascular area and on the leading edge. The staining intensity is clearly homogenous and stronger (score 3) than in the adjoining endothelial cells (moderate intensity, score 2). Benign endometrium showed intense expression (score 3) in proliferating glands and reduced or low expression (score 1) in non-proliferating cells in the secretory phase. We observed a significant association between a higher grade and intense NFAT5 staining ($p < 0.001$). Additionally, with cases diagnosed with pT1b and higher (i.e., invasion into the outer half of the myometrium), we noticed a significant association with an increase of NFAT5 staining ($p = 0.014$). An increase with NFAT5 staining is also significantly associated with metastasis ($p = 0.043$). The staining pattern of NFAT5 was similar in other G1 and the G3 cases verified in this study (Supplementary Figure S1).

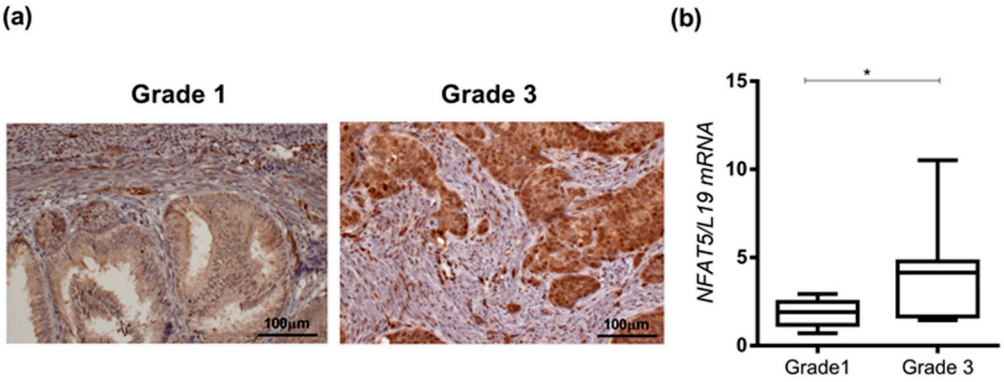

Figure 1. NFAT5 expression in Grades 1 and 3 endometrial cancer tissues. (**a**). Representative images of NFAT5 immunohistochemistry expression analysis in Grade 1 ($n = 15$) and Grade 3 ($n = 11$) endometrial cancer tissue. Staining shows excessive NFAT5 expression in Grade 3 tumor samples compared to Grade 1. Scale bar—100 µm. (**b**). In parallel, mRNA expression level of *NFAT5* from FFPE tissue samples was quantified by qRT-PCR, *, $p < 0.05$ based on unpaired *t*-test. Data were normalized to ribosomal housekeeping gene, *L19*.

In parallel, total RNA was collected from the same FFPE blocks and subjected to qRT-PCR. RNA data revealed that *NFAT5* transcript levels were also significantly higher in G3 (aggressive) tumor tissues (Figure 1b, *, $p = 0.0130$) compared to low-grade G1 tumor tissues.

To gain further insight into the role of NFAT5 overexpression in high-grade endometrial cancer, we used Ishikawa cells, a well-used model of adenocarcinoma cancer [46]. Total RNA was harvested from four independent cultures, following transfection with either NFAT5 overexpression plasmid or an empty vector for 24 h.

After accounting for variations between cultures, the effect of NFAT5 overexpression on the gene expression pattern in Ishikawa cells was observed to be highly consistent. Based on FDR < 0.05 and log2FC $\geq$ 0.3 (corresponding to actual fold change $\geq$ 1.23), we identified 57 differently regulated genes that were significantly altered upon NFAT5 overexpression in Ishikawa cells (Figure 2a), of which 37 genes were upregulated and 20 genes were downregulated. Genes upregulated significantly upon NFAT5 overexpression in Ishikawa cells include leucine-rich repeat containing G protein-coupled receptor 6 (*LGR6*) (log2FC = 1.749), *NFAT5* (log2FC = 2.705), prostaglandin-endoperoxide synthase 2 (*PTGS2*,

which encodes for COX2 protein) (log2FC = 0.320), netrin 4 (*NTN4*) (log2FC = 0.476), and angiogenin (*ANG*) (log2FC = 0.566). NFAT5 overexpression in Ishikawa downregulated genes like ankyrin repeat domain 1 (*ANKRD1*) (log2FC = −0.855) coding, a transcription factor that positively regulates apoptosis [47] and amine oxidase copper containing 3 (*AOC3*) (log2FC = −0.358), which at low levels is associated with poor prognosis in cancers [48]. Although *HIF1A* (log2FC = 0.104, FDR < 0.05) and estrogen receptor 1 (*ESR1*) (log2FC = −0.22, FDR < 0.05) were not differentially expressed based on the differential expression thresholds we used in this study, we observed modest but significant changes in their expressions too upon NFAT5 overexpression. The log2 fold change values of differential gene expression between the control and NFAT5 overexpression in Ishikawa, for genes of interest, are represented in Figure 2b. Taken together, these results show there is an increase of *PTGS2* and *HIF1A* transcripts after overexpression of NFAT5 in Ishikawa. The complete set of differently expressed genes are shown in Supplementary Table S1. In order to examine the role of molecules predicted to be involved in the pathways relevant for cancer progression, we used Ingenuity Pathway Analysis (IPA), a bioinformatics tool from QIAGEN, to examine the underlying molecular mechanisms. Supplementary Figure S2 points to a strong association with activation of PTGS2 (COX2) signaling upon NFAT5 overexpression in Ishikawa cells.

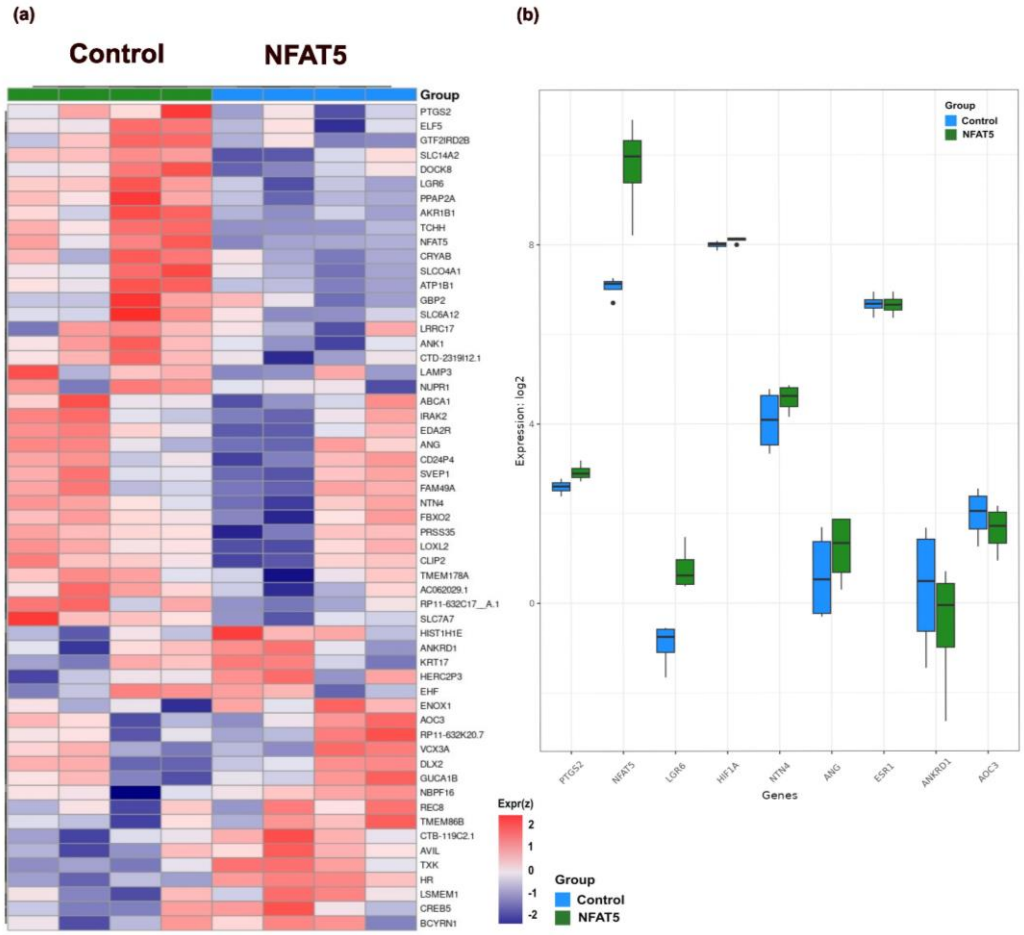

Figure 2. Gene expression alteration in Ishikawa cells with NFAT5 overexpression. (**a**). Heatmap shows gene expression alteration by NFAT5 overexpression in Ishikawa cells (FDR < 0.05 and log2FC ≥ 0.3). Upregulation and downregulation of genes are shown by red and blue color coding, respectively. (**b**). Box and whisker plots of log2 fold change of genes of interest in control and NFAT5 overexpressed Ishikawa cells.

To test whether induction of NFAT5 expression in Ishikawa cells is sensitive to hypoxia, cells were treated with a known cell permeable prolyl-4-hydroxylase (PHD) inhibitor [49],

dimethyloxalylglycine (DMOG) (0.5 mM DMOG for 24 h). PHD is involved in degradation of HIF-1α and during hypoxia, PHD is blocked due to limited oxygen, leading to HIF-1α stabilization and an increase in downstream target gene activation [49]. DMOG is known to suppress PHD activity and stabilize HIF-1α levels, thus maintaining hypoxic environment both in vitro and in vivo conditions [49–51]. Ishikawa was treated with DMOG for 24 h and total RNA was extracted. qRT-PCR was performed for NFAT5 gene expression analysis. As shown in Figure 3a (n = 6; *, p = 0.0107), DMOG treatment was indeed followed by a significant increase of *NFAT5* transcript levels. Western blotting was employed to test whether the stimulation of NFAT5 transcription was followed by an increase of protein expression. As illustrated in Figure 3b and Supplementary Figure S3 (n = 6; ****, $p < 0.0001$), the effect of DMOG on *NFAT5* transcript levels was paralleled by a highly significant increase in NFAT5 protein abundance in Ishikawa cells.

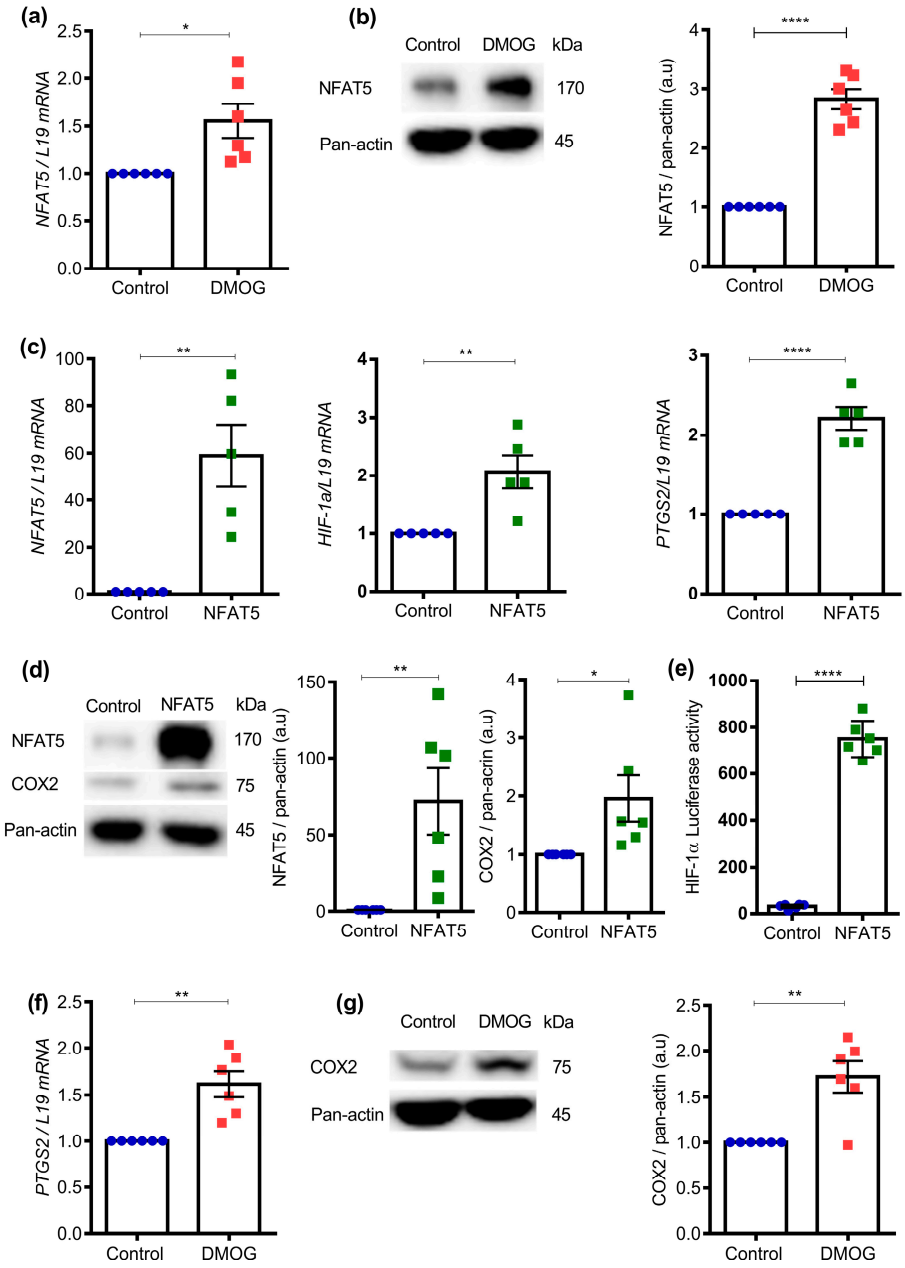

Figure 3. Effect of NFAT5 on COX2 transcript and protein levels in Ishikawa cells. (**a**). Ishikawa cells were treated with 0.5 mM DMOG for 24 h. mRNA expression level of *NFAT5* was quantified by qRT-

PCR. Data were normalized to *L19* and presented as mean ± SEM. ($n = 6$; *, $p < 0.05$). (**b**). NFAT5 protein abundance was investigated by SDS-PAGE and western blot analysis. Ishikawa cells were treated with 0.5 mM DMOG for 24 h. Data were normalized to each corresponding level of pan-actin and shown as mean ± SEM. ($n = 6$; ****, $p < 0.0001$, a.u: arbitrary unit). (**c**). mRNA expression level of *NFAT5*, *HIF1A*, and *PTGS2* were quantified by qRT-PCR. Ishikawa cells were transfected with NFAT5 overexpression plasmid for 24 h ($n = 5$; **, $p < 0.01$, ****, $p < 0.0001$). (**d**). NFAT5 and PTGS2 protein abundance were investigated by SDS-PAGE and western blot analysis using the indicated antibodies. Ishikawa cells were transfected with NFAT5 overexpression plasmid for 24 h ($n = 6$; *, $p < 0.05$; **, $p < 0.01$). (**e**). Luciferase activity of HIF-1α that was normalized to renilla post Ishikawa cells transfected with NFAT5 overexpression plasmid for 24 h ($n = 6$; ****, $p < 0.0001$). (**f**). mRNA expression level of *PTGS2* was quantified by qRT-PCR. Ishikawa cells were treated with 0.5 mM DMOG for 24 h ($n = 6$; **, $p < 0.01$). (**g**). COX2 protein abundance was investigated by SDS-PAGE and western blot analysis using the indicated antibodies. Ishikawa cells were treated with 0.5 mM DMOG for 24 h ($n = 6$; **, $p < 0.01$).

To gain insight into whether enhanced expression of NFAT5 can induce the HIF-1α signaling axis, Ishikawa cells were first transfected with either NFAT5 overexpression plasmid or an empty vector for 24 h and then subjected to qRT-PCR. As illustrated in Figure 3c ($n = 5$; **, $p = 0.002$, **, $p = 0.005$, ****, $p < 0.0001$), NFAT5 transfection was followed by the expected up-regulation of *NFAT5* transcript levels and by a significant increase of *HIF1A* and *PTGS2* transcript levels. As illustrated in Figure 3d and Supplementary Figure S3 ($n = 6$; *, $p = 0.037$; **, $p = 0.008$), the effect of NFAT5 transfection on *NFAT5* and *PTGS2* transcript levels was paralleled by a similar increase of NFAT5 and COX2 protein abundance. As shown in Figure 3e ($n = 6$; ****, $p < 0.0001$), NFAT5 overexpression significantly increased HIF-1α activity, as measured by hypoxia response elements (HRE)-luciferase. These data suggest that NFAT5 can induce *HIF1A* transcription and activity in Ishikawa cells. Further, HIF-1α activation can increase COX2 levels in colon cancer cells [43,52]. To test this hypothesis in endometrial carcinoma cells, the next series of experiments tested whether COX2 expression is sensitive to DMOG (i.e., hypoxia). As illustrated in Figure 3f ($n = 6$; **, $p = 0.001$), DMOG treatment in Ishikawa cells was followed by a significant increase of *PTGS2* transcript levels. Following an increase of *PTGS2* gene expression, we observed an increase of COX2 protein abundance (Figure 3g and Supplementary Figure S3, $n = 6$; **, $p = 0.001$) upon DMOG treatment in Ishikawa cells.

NFAT5 has been shown to upregulate *PTGS2* gene expression (COX2) [33,34]. In turn, COX2 activation is also known to enhance HIF-1α activity in breast and lung cancer [37,38]. To address whether NFAT5 overexpression can lead to a more aggressive state, we monitored cell cycle progression, cell proliferation, and cell migration in Ishikawa cells transfected with NFAT5 plasmid. The examination of the cell cycle profile (Figure 4a, $n = 7$; *, $p = 0.012$) revealed a higher proportion of cells in the S phase upon NFAT5 overexpression, indicating an augmentation in DNA replication compared to the control. Cells present at G0/G1 phase of the cycle showed no difference between the control and NFAT5-transfected population. Further, we observed fewer numbers of NFAT5-transfected cells at the G2/M phase compared to the control cells. As shown in Figure 4b ($n = 4$; **, $p = 0.002$), the overexpression of NFAT5 resulted in a significant increase in cell proliferation as established with BrdU ELISA. Furthermore, the wound healing assay demonstrated a significant enhancement in cell migration in Ishikawa cells at 24 h post scratch following NFAT5 overexpression (Figure 4c,d, $n = 4$; **, $p = 0.002$).

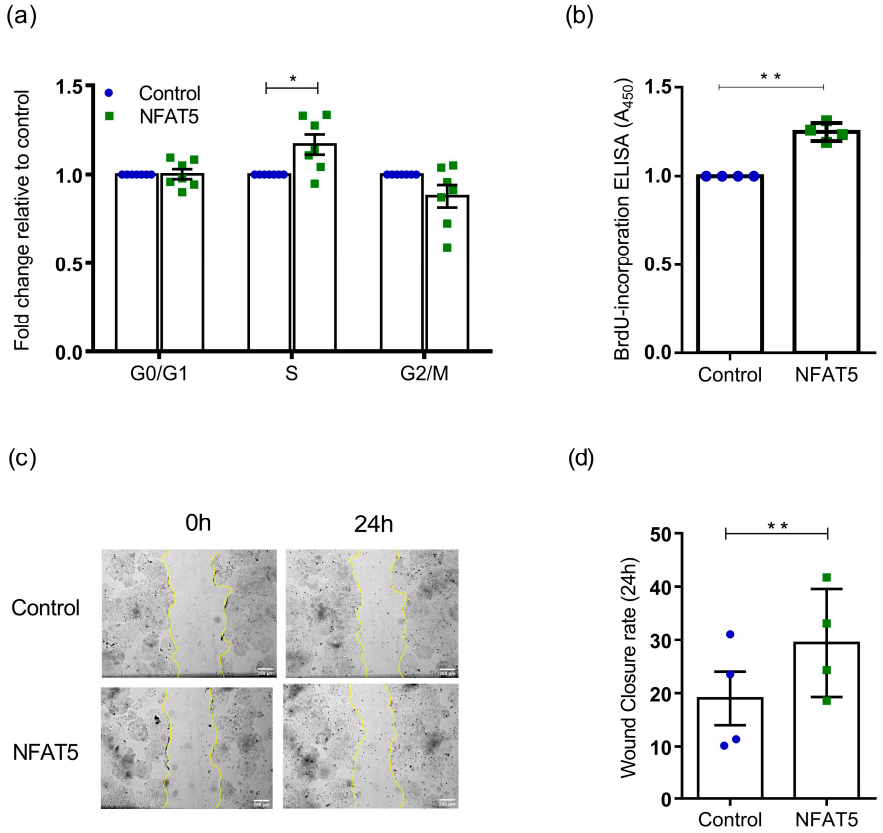

Figure 4. Effect of NFAT5 overexpression in Ishikawa biological activity. (**a**). FACS assisted cell cycle analysis on control and NFAT5 overexpressed Ishikawa cells ($n = 7$; *, $p < 0.05$). (**b**). Cell proliferation analysis on control and NFAT5 overexpressed Ishikawa cells with BrdU ELISA assay ($n = 4$; **, $p < 0.01$). Data were normalized to each control and shown as mean ± SEM. (**c**). Representative bright field images of wound healing scratch assay on the control and NFAT5-overexpressed Ishikawa cells. (**d**). Wound closure rate on the control and NFAT5 overexpressed Ishikawa cells 24 h post scratch ($n = 4$; **, $p < 0.01$), scale bar—200 μm.

To test if there is positive feedback between NFAT5 and hypoxia, we transfected Ishikawa cells with NFAT5 overexpression plasmid followed by DMOG treatment or DMOG alone. As a result (Figure 5a, $n = 6$; *, $p = 0.0117$; **, $p = 0.0064$), we observed significantly higher *NFAT5* and *PTGS2* transcript levels compared with only DMOG treatment. As illustrated in Figure 5b–d and Supplementary Figure S4 ($n = 5$; *, $p < 0.05$; **, $p < 0.01$; ***, $p < 0.001$, ****, $p < 0.0001$), the effect of NFAT5 transfection and DMOG treatment was paralleled by a similar increase of NFAT5 and COX2 protein abundance compared to cells treated with DMOG alone. To explore the putative link with NFAT5 and hypoxia, HIF-1α promoter activity was thus quantified by dual-luciferase reporter assays with prior 24 h NFAT5 transfection and/or treatment with DMOG. As illustrated in Figure 5e ($n = 6$; **, $p = 0.005$), NFAT5 transfection and DMOG treatment in Ishikawa cells both exerted a strong stimulating effect on HIF-1α promoter activity, which was further increased by combined NFAT5 transfection and DMOG treatment. These results were also paralleled by an increase in secreted PGE_2 levels in Ishikawa cells with a significant difference observed in cells with combined NFAT5 transfection and DMOG treatment Figure 5f ($n = 4$; *, $p = 0.024$, $p = 0.012$).

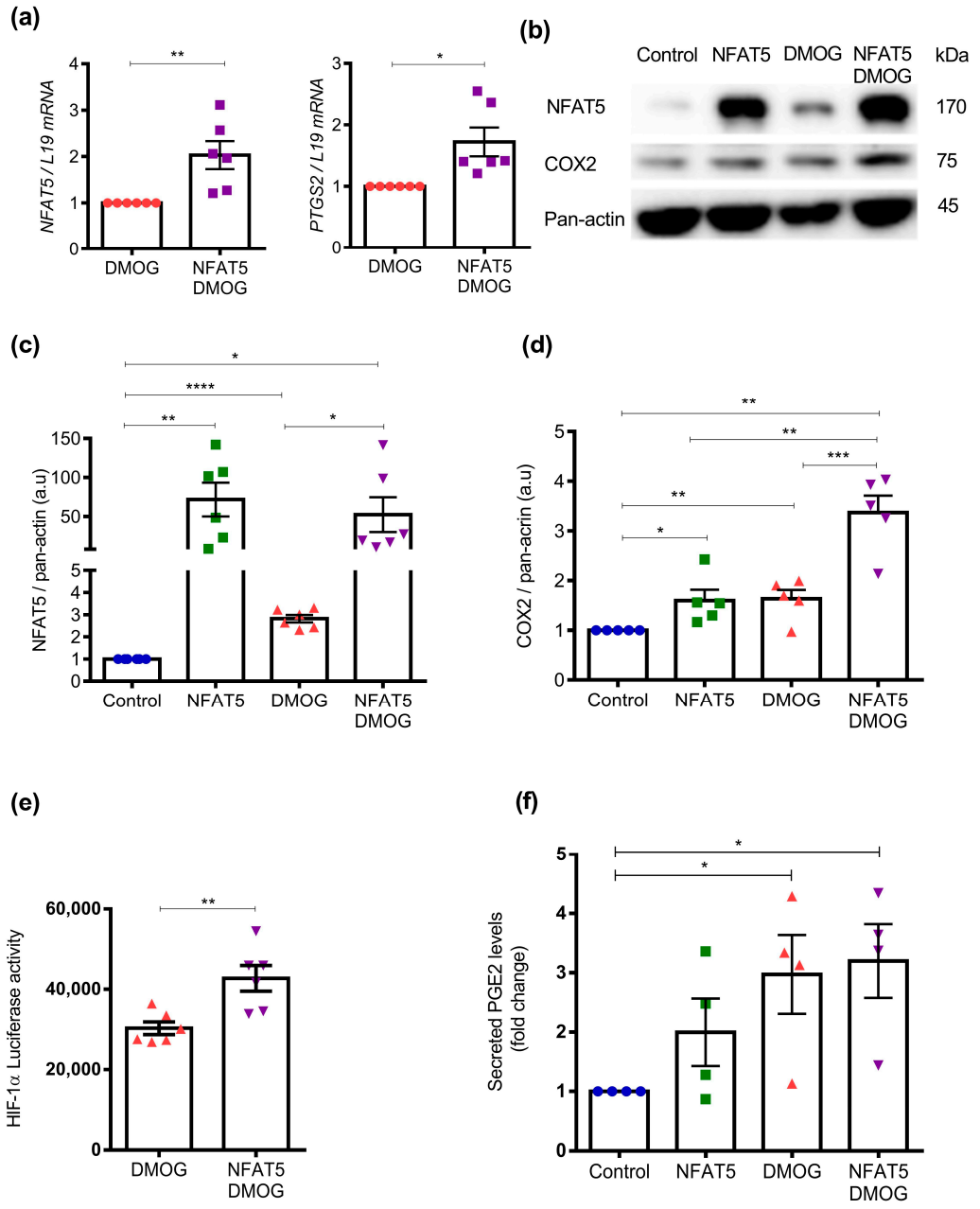

Figure 5. Synergistic effect of NFAT5 overexpression and DMOG on COX2 transcript and protein levels in Ishikawa cells. (**a**). mRNA expression level of *NFAT5* and *PTGS2* quantified by qRT-PCR. Ishikawa cells were treated with 0.5 mM DMOG for 24 h post with or without 24 h transfection with NFAT5 overexpression plasmid. Data were normalized to L19 and presented as mean ± SEM. (NFAT5, $n = 6$; *, $p < 0.05$; **, $p < 0.01$). (**b–d**). NFAT5 and COX2 protein abundance were investigated by SDS-PAGE and western blot analysis using the indicated antibodies. Ishikawa cells were subjected to with or without NFAT5 transfection followed by treatment with or without DMOG. Data were normalized to each corresponding level of pan-actin and shown as mean ± SEM. ($n = 5$; *, $p < 0.05$; **, $p < 0.01$; ***, $p < 0.001$, ****, $p < 0.0001$, a.u: arbitrary unit). (**e**). Effect of hypoxia on HIF-1α induction with or without NFAT5 transfection using Luciferase promoter assay. Data shown as mean ± SEM. ($n = 6$; **, $p < 0.01$). (**f**). Effect on PGE2 levels with or without NFAT5 transfection, followed by treatment with or without DMOG (0.5 mM, 24 h). Data shown as mean ± SEM. ($n = 4$; *, $p < 0.05$).

In order to test whether NFAT5 overexpression is sensitive to hypoxia in an alternative endometrial cell line, HEC1a cells were initially transfected with either an NFAT5 overexpression plasmid or an empty vector for a duration of 24 h. Subsequently, the cells were

treated with or without DMOG at a concentration of 0.5 mM for an additional 24 h. Supplementary Figure S5a demonstrates that the NFAT5 overexpression followed by DMOG treatment did induce an increase in NFAT5 protein expression higher than that following only DMOG treatment in HEC1a cells ($n = 3$, *, $p = 0.014$). Furthermore, analysis of HIF-1α promoter activity showed a significant elevation upon NFAT5 overexpression and a further increase upon DMOG treatment (Supplementary Figure S5b, $n = 4$, ***, $p < 0.001$). Investigation on HEC1a migratory potential upon NFAT5 overexpression revealed an increase in cell migration at 24 h with the wound scratch assay (Supplementary Figure S5c). Taken together, these results confirm NFAT5 responsive hypoxia induction in HEC1a, verifying NFAT5 relevance in other adenocarcinoma cell lines.

3. Discussion

There has been an astonishing increase of reports describing the role of NFAT5 in tonicity-independent manner with its effects in cell development and human diseases [27,28,53–55]. NFAT5 is a pleiotropic stress protein with a protective role in cellular adaption to osmotic stress, bacterial infection, and genotoxin-induced DNA damage [18,56]. NFAT5-mediated pathological responses can result in human pathologies such as autoimmune diseases, acute kidney injury, hepatocellular carcinoma, atherosclerosis, and obesity [15,56–58]. Importantly, downregulation of NFAT5 reduces inflammation and thereby renders a protective role in preventing these diseases [15]. NFAT5, as a protective factor, is well studied; however, its role in endometrium and tumor progression and metastasis is still in its infancy.

In our study, we report that expression of NFAT5 was significantly higher in more aggressive (G3) endometrial cancer tissues than in corresponding non-tumor, low-grade (G1) tissues. Staining was highest around blood vessels and the leading edge. Our study was using a small proof-of-concept cohort and further larger clinical cohorts are required to validate our findings. To gain further insight of NFAT5 overexpression and establish a comprehensive analysis of aberrantly expressed genes after NFAT5 overexpression in Ishikawa cells (well used model cells of endometrial adenocarcinoma [59]), RNA-sequencing was performed. NFAT5 plasmid transfection into Ishikawa cells upregulated 37 genes and downregulated 20 genes. In keeping with its established role, many of the NFAT5-regulated genes were related to osmoregulation and/or support cell survival in hypertonic environment (e.g., aldo-keto reductase family 1 member b (*AKR1B1*), solute carrier family 6 member 12 (*SLC6A12*), and ATPase Na^+/K^+ transporting subunit beta 1 (*ATP1B1*) [19,60]. Interestingly, altered genes after NFAT5 overexpression in Ishikawa cells included *PTGS2* and *HIF1A*. Given the hypoxia-sensitivity of NFAT5 expression, we posit that local hypoxia of advanced cancer tissue contributes to or even accounts for upregulation of NFAT5 expression in EnCa [25,53,61].

It has been established that HIF-1α regulates oxygen homeostasis in the tumor microenvironment and can elevate COX2 expression by regulating it at transcriptional level [52,62]. Further, it has also been linked with increased levels of PGE_2 and cancer progression [52]. These results are in concordance with our findings reported here. Along this line, NFAT5 transfection in Ishikawa cells exerted a strong stimulating effect on HIF-1α promoter activity. Furthermore, the HIF-1α-stabilizing prolylhydroxylase inhibitor, DMOG, significantly increased *NFAT5* transcript levels and protein abundance in Ishikawa cells. Thus, our results show that NFAT5 upregulates *HIF1A* transcription and promoter activity in Ishikawa cells. Further, the stimulation of HIF-1α via NFAT5 with DMOG augments the response, and thus establishes a positive feedback loop.

COX2 is a well-known mediator of pro-tumorigenic inflammation. It is upregulated in many cancers and is involved in tumor progression [63,64]. COX2 is responsible for the synthesis of prostanoids (prostaglandins, prostacyclin, and thromboxane) from the precursor arachidonic acid [65]. Prostaglandins trigger the release of proinflammatory chemokines [66,67]. Indeed, it is now well established that inflammation is a critical and enabling characteristic of tumorigenesis [68]. Our results show an increased trend

of PGE_2 levels upon NFAT5-COX2 signaling activation in Ishikawa cells. The ELISA approach employed in this study holds some limitations such as its inability to detect low levels of secreted PGE_2 or that considering its rapid half-life, it is not able to detect PGE_2 quickly [69]. Therefore, we propose the future utility of liquid-chromatograph-based mass spectroscopy (LC-MS/MS) approaches evaluating these lipid molecules. Meanwhile, it is also worthy to analyze if other isoforms of prostanoids are regulated upon NFAT5-mediated COX2 activation.

This synergism towards tumor progression and metastasis makes COX2 a potential therapeutic target. Since chemoresistance is very closely associated with hypoxia and COX2 overexpression in tumor, inhibiting of COX2 activity may result in increased effectiveness of cancer therapies (chemotherapy and radiation) [70]. Furthermore, selective inhibition of COX2 with nimesulide was successful in able to reducing tumor formation in a mouse hypoxic tumor model. Further work is warranted to verify if this can be confirmed in humans [71].

We show that NFAT5 transfection and DMOG treatment were followed by significant increases of transcript levels and protein abundance of COX2, another signaling molecule sensitive to hypoxia [52,72]. NFAT5 has previously been shown to increase the expression of serum/glucocorticoid regulated kinase 1 (SGK1) [54,73], which is known to trigger the degradation of the inhibitor protein IκBα, thus allowing nuclear translocation of the transcription factor NFκB [74]. Genes up-regulated by NFκB activation include *PTGS2* [58] and *HIF1A* [25]. Intriguingly, NFAT5 has been suggested to play a role in EMT, a process where epithelial cells adopt to a mesenchymal phenotype [31]. EMT is associated with increased invasiveness and metastatic potential of cancer cells [75]. Whether NFAT5 plays a direct role in EMT progression in endometrial cells remains to be tested.

Based on the above results, we propose that overexpression of NFAT5 might have an important role in the progression of EnCa even though the exact mechanism on enhanced NFAT5 expression corresponding with tumor aggression is unknown. There are several possible risk factors associated. EnCa is strongly associated with obesity, poor diet, and sedentary lifestyle [1,10,76]. A high-salt diet induces over-expression of inflammatory mediators, adhesive molecules, and coagulation mediators [76,77]. It was shown that a high-salt diet increased NFAT5, activating macrophages and fibrin deposition [78]. Further, excessive salt is reported to alter the expression of many pro-inflammatory cytokines such as TNF, IL-6, and PGE_2 mediated via NFAT5 transcriptional activity [79].

Similarly, high glucose uptake contributes to elevated NFAT5 levels and contributes to pathophysiology, as observed earlier in diabetic retinopathy and diabetes mellitus [22,80,81]. High levels of NFAT5 are associated with the development of obesity and insulin resistance. Lee at al. reported greater than a 50-fold increase in NFAT5 expression in response to high-fat diet in mouse models [57]. It has been demonstrated that NFAT5 can epigenetically suppress the transcriptional activity of peroxisome proliferator-activated receptor gamma (PPARγ), which modulates nutrient and energy metabolism [57]. Hence, it could be postulated that in obese women, characterized expansion of adipose tissue could cause pathological conditions like hypoxia and hypothermic resistance, which mediates elevated NFAT5 expression. Thus, high dietary salt/sugar/fat consumption might upregulate NFAT5, thereby contributing to local inflammation and promoting a tumorigenic-potential-like microenvironment.

Apart from dietary or lifestyle factors, genetic predisposition to dysregulated NFAT5 activity could also be a high risk factor. Single-nucleotide polymorphisms (SNPs) in NFAT5 introns with *cis*-expression quantitative trait loci that affect its transcriptional function are reported [14]. These SNPs are associated with the risk of high blood pressure, diabetes mellitus, diabetic nephropathy, and inflammation, suggesting that genetic variation in NFAT5 transcription might contribute to pathological phenotypes [14,22,56,82]. Further work is required to confirm these findings in relation to EnCa.

In summary, our study indicates that high levels of NFAT5 are associated with more aggressive endometrial cancers. Further, overexpression of NFAT5 leads to activation of

HIF-1α and COX2 followed by higher PGE2 levels, which may support the development of more aggressive tumors. Even though the exact underlying mechanism that drives aberrant expression of NFAT5 in tumor tissues remains elusive, the advent of selective COX2 inhibitors as anti-cancer therapies could be a useful tool for EnCa. In conclusion, NFAT5 is expressed in high-grade endometrial tumor tissue and upregulates many genes including *HIF1A* and *PTGS2*, which may participate in malignant tumor pathogenesis.

4. Materials and Methods

4.1. Clinical Sample Collection

A series of 26 endometrial carcinomas (Table 1) from FFPE tumor samples (obtained from surgical specimens, retrospective samples from 2014–2016) from the Women's University Hospital of Tübingen (Tübingen, Germany) were ethically obtained. All carcinomas were centrally reviewed by gynecologic pathology subspecialty pathologists to ensure that the tumor was correctly subtyped based on well-established pathological criteria.

4.2. Immunohistochemistry

Immunostaining was performed on formalin fixed, paraffin-embedded archival tissue. The paraffin blocks were sliced into 2.5 µm thick sections onto glass slides. The slides were loaded onto the automated slide stainer on the VENTANA BenchMark Series Instruments (Roche Diagnostics, Mannheim, Germany) for staining. The paraffin sections were deparaffinized with Ez prep (#950-102, Roche Diagnostics). Antigen retrieval was achieved by incubating slides with CC1 (#950124, Roche Diagnostics) for 64 min at 37 °C. Endogenous peroxidases were quenched by incubating the slides with pre-primary peroxidase inhibitors. The slides were then incubated with a primary antibody for NFAT5 (#NB120-3446, Novus Bio, Wiesbaden-Nordenstadt, Germany, 1:250) for 20 min at 37 °C. The bound primary antibody was detected using an OptiView DAB IHC Detection Kit (#760-700, Roche Diagnostics) following the manufacture's protocol. The immunohistochemical reaction was assessed with Nikon Eclipse E200 light microscope with Nikon DS-Fi1 digital camera (Nikon, Amstelveen, The Netherlands). Complete negative staining equals a score of 0, 0–10% score 1, 10–50% score 2, and >50% score 3. This analysis was independently performed by 2 pathologists (A.S., I.P.).

4.3. Cell Culture

Two well-differentiated endometrial carcinoma cell lines Ishikawa (type 1 endometrialcarcinoma, ECACC #99040201, Sigma-Aldrich, Taufkirchen, Germany, RRID: CVCL_2529) and HEC1a (type2 endometrial adenocarcinoma, #HTB-112, ATCC, Wesel, Germany, RRID: CVCL_0293) were cultured in a humidified atmosphere of 5% CO_2 at 37 °C in Dulbecco's modified Eagle's medium F-12 (DMEM: F12) (#11039-021, Invitrogen, Darmstadt, Germany), which was phenol-free and supplemented with 10% (*v*/*v*) FBS (#10270-106, Invitrogen); the FBS was replenished every 48 h. Cells were passaged when the confluency reached at 80%. When performing experiments, cells were cultured in DMEM: F12 phenol-free supplemented with 2% (*v*/*v*) FBS medium containing antibiotics. Cells were treated with dimethyloxalylglycine (DMOG) (#D3695; Sigma-Aldrich, 0.5 mM) for 24 h. All work was carried out in a Class I laminar flow hood. Cells were routinely tested for mycoplasma and always gave a negative result.

4.4. Plasmid DNA Transfection

Ishikawa or HEC1a cells were plated in 6-well plates at a density of 200,000 cells per well in 2% media as described above. Ishikawa cells were transfected with plasmid DNA (2.5 ng/µL) encoding human NFAT5 in pcDNA6V5-HisC vector [54] by using Lipofectamine LTX DNA transfection reagent (#15338-100, Invitrogen) according to the manufacturer's protocol. After 24 h the transfection mix was removed and the cells were treated with DMOG (0.5 mM) for another 24 h. Control cells remained untreated. Post treatment cells were collected for downstream analysis.

4.5. RNA Sequencing and Data Analysis

Total RNA samples were extracted by using miRNeasy Mini kit (#217084, QIAGEN, Hilden, Germany) according to the manufacturer's protocol. RNA concentration and quality were measured by using a photometric measurement of nucleic acid approach with Varioskan LUX (Thermo Fisher Scientific, Sindelfingen, Germany). RNA quality was assessed with an Agilent 2100 Bioanalyzer system (Agilent Technologies, Waldbronn, Germany). Samples with high RNA integrity (>8) were selected for library construction. Using the NEBNext Ultra II Directional RNA Library Prep Kit (#E7760S, New England Biolabs GmbH, Frankfurt am Main, Germany) for Illumina and 100 ng of total RNA for each sequencing library, poly(A) selected sequencing libraries were generated according to the manufacturer's instructions. All libraries were sequenced on the Illumina NovaSeq 6000 (Illumina, San Diego, CA, USA) platform in paired-end mode with read length 50 bp and at a depth of approx. 70 million clusters each. Library preparation and sequencing procedures were performed by the same individual and a design aimed to minimize technical batch effects was chosen. Quality of raw RNA-seq data in FASTQ files was assessed using ReadQC (https://github.com/imgag/ngs-bits) to identify potential sequencing cycles with low average quality and base distribution bias. Reads were pre-processed with skewer (version 0.2.2) and aligned using STAR (version 2.5.4a) allowing spliced read alignment to the human reference genome (GRCh37). Alignment quality was analyzed using MappingQC (https://github.com/imgag/ngs-bits) and visually inspected with Broad Integrative Genome Viewer (IGV, version 2.3.1). Based on the Ensemble genome annotation (GRCh37 v75), read counts for all genes were obtained using subread (version 1.6.0).

For differential expressed gene (DEGs) analysis, raw gene read counts were filtered to only retain genes with at least 1 cpm (count per million) in at least two samples, leaving > 15,000 genes for determining differential expression in the pair-wise comparisons be-tween experimental groups. The analysis was performed with edgeR [83–85] (version 3.40.2) that uses a statistical framework based on negative binomial distributions and gene-wise testing using generalized linear models. Genes with absolute log2FC $\geq$ 0.3, and false discover rate (FDR) < 0.05 were considered DEGs and used for downstream analysis. Functional enrichment analysis of DEGs were performed by using gprofiler2 [86] in R by using default parameter values. The gprofiler2 R package utilizes the hypergeometric test, along with correction for multiple testing, to detect statistically significant (over-represented) functional annotations from diverse set of resources such as GO [87], KEGG [88], Reactome [89], and human disease annotations [90] etc., all through a single command. In this paper, we have shown only the top 10 functional terms on the corresponding plots and have provided the complete list in the Supplementary Table S1.

4.6. Ingenuity Pathway Analysis (IPA)

Pathway enrichment analysis on NFAT5 overexpression in Ishikawa cells was analysied with a web-based bioinformatics application, Qiagen IPA platform. Data were analyzed with the use of QIAGEN IPA (QIAGEN Inc., https://digitalinsights.qiagen.com/IPA).

4.7. Messenger RNA (mRNA) Extraction and Quantitative Real-Time Reverse Transcriptase PCR (qRT-PCR)

Total RNA was extracted from cells using TRizol^{TM} reagent (#15596026, Invitrogen). One µg of total RNA was utilized to synthesize cDNA using the MaximaTM H Minus cDNA Synthesis Master Mix with dsDNase (#M1681, Invitrogen). mRNA concentration was measured by using a Nanodrop. qRT-PCR was performed on the QuantStudio 3 Real-Time PCR System (Invitrogen) by using sets of gene-specific primers (Table 2). The cycling conditions were; hold stage for 20 s at 95 °C and PCR stage with 40 cycles of 1 s at 95 °C and 20 s at 60 °C. The relative differences in PCR product amounts were quantified by the $2^{-\Delta\Delta CT}$ method [91], using ribosomal L19 (*L19*) as an internal control [92]. Experiments were performed in triplicate. Melting curve was utilized to confirm amplification speci-

ficity. All the gene-specific primers used in this study was designed using Primer-BLAST (NCBI) [93] and purchased from Sigma-Aldrich.

Table 2. List of the human primer sequences used in the study.

Gene	Primer Sequence
L19	Forward (5′-3′): GCGGAAGGGTACAGCCAA
	Reverse (5′-3′): GCAGCCGGCGCAAA
NFAT5	Forward (5′-3′): GAGCAGAGCTGCAGTAT
	Reverse (5′-3′): AGCTGAGAAAGCACATAG
PTGS2	Forward (5′-3′): GCTCAAACATGATGTTTGCATTC
	Reverse (5′-3′): GCTGGCCCTCGCTTATGA
HIF1A	Forward (5′-3′): TCTGGACTTGCCTTTCCTTCTC
	Reverse (5′-3′): AACTTATCTTTTTCTTGTCGTTCGC

4.8. Western Blotting

Whole cell protein lysate was extracted from Ishikawa cells using Laemmli buffer as previously reported [94]. Whole cell protein lysates were heated at 95 °C for 5 min. Extracts were then loaded on to a 10% sodium dodecyl sulfate polyacrylamide gel (SDS-PAGE) using the XCell SureLock® Mini-Cell apparatus (Invitrogen) followed by electrophoresis. The protein from the gel was transferred onto polyvinylidenefluoride membrane (#10600023, VWR International GmbH, Ulm, Germany). After air drying the membranes, they were activated in 100% methanol and subsequently blocked using 5% milk for 1 h at room temperature (RT). Membranes were probed overnight at 4 °C with antibodies: human NFAT5 antibody (1:1000, #NB20-3446, Novus Bio), human COX2 antibody (1:1000, #160106, Cayman Chemical, Ann Arbor, MI, USA), human pan-actin antibody (HRP-conjugate) (1:1000, #12748, Cell Signaling Technology, Frankfurt am Main, Germany) was used as loading control. After 3 × 15 min washing with 1 × TBST, the membranes were incubated with HRP-conjugated anti-rabbit secondary antibody (1:2000, #7074s, Cell Signaling Technology) at RT for 1 h. Next, after second 3 × 15 min washes, protein bands were detected using a chemiluminescent detection kit (#34580, SuperSignal™ West Pico PLUS Chemiluminescent Substrate, Thermo Fisher Scientific) and visualized by using iBright™ Imaging System (Invitrogen). Bands were quantified with ImageJ Software 1.53k (National Institutes of Health, Bethesda, MD, USA) [59,94].

4.9. Luciferase Reporter Assay

Ishikawa or HEC1a cells were seeded onto 24-well plates at a density of 5×10^4 cells/well with 10% FBS DMEM and allowed to attach for 24 h. Next, cells were transfected with HIF-1α vector (#87261, Addgene, Watertown, MA, USA) using Lipofectamine LTX with Plus reagent (#15338100, Invitrogen) as per the manufacturer's instruction. After transfection for 24 h, cells were subjected to NFAT5 overexpression transfection followed by DMOG treatment as described above. The reporter activation was determined using the Dual-Luciferase Reporter Assay System (#E2920, Promega, Madison, WI, USA) according to the manufacturer's instructions.

Briefly, growth medium was removed and cells were washed with PBS. Subsequently, cells were lysed for 15 min at room temperature using 1× passive lysis buffer. Lysed cells were used for determination of luciferase activity. LAR II reagent was added to each well, and firefly luminescence was measured using a microplate reader (LUX VARIOSKAN, Thermo Fisher Scientific). Next, Stop & Glo reagent was added to each well and renilla luciferase activity was measured using a microplate reader. Three replicate wells were used for each analysis, and the results were normalized to the activity of renilla luciferase.

4.10. Enzyme-Linked Immunosorbent Assay (ELISA)

After transfection of Ishikawa cells with NFAT5 plasmid followed by DMOG treatment as stated above, the culture medium was harvested and stored at −80 °C. The collected

cultured medium was processed for ELISA by using human prostaglandin E2 ELISA Kit (#KHL1701, Invitrogen) following the manufacturer's instructions. The absorbance was measured with Varioskan LUX spectrophotometer (Thermo Fisher Scientific).

4.11. Cell-Cycle Anaylsis with Flow Cytometry

The effect of NFAT5 overexpression on Ishikawa cell cycle progression was studied with FACS approach. After treatment with NFAT5 overexpression plasmid as described above, cells and medium were collected into a 15 mL centrifuge tube and spun down at 600× *g* for 5 min. The supernatant was discarded and 1 mL of −20 °C ice-cold ethanol (#20821.330, VWR International GmbH), PBS (#D8537, Sigma-Aldrich) mixture (3:1) was added to the pellet during vortexing. The mixture was kept at −20 °C overnight, the next day washed with PBS again, 250 µL PI mix containing 50 µg/mL PI (#P4864, Sigma-Aldrich) and 100 µg/mL RNase A (#R4642, Sigma-Aldrich) were added, incubated for 30 min at 37 °C, and subjected to flow cytometry (BD LSRFortessa™ Cell Analyzer, BD Biosciences, Heidelberg, Germany) for cell cycle analysis. The data were analyzed by FlowJo™ software 10.8.1 (FlowJo, Ashland, OR, USA).

4.12. BrdU ELISA Cell Profileration Assay

The effect of NFAT5 overexpression on Ishikawa proliferation was measured using BrdU cell proliferation assay (#QIA58, Sigma-Aldrich). Post treatment with NFAT5 overexpression plasmid as described above, the cells were immunolabelled for BrdU and the cells incubated for an additional 24 h. Incorporated BrdU was detected by the BrdU cell proliferation assay as instructed in the manufacture protocol. Fluorescence was measured using a microplate reader (LUX VARIOSKAN, Thermo Fisher Scientific).

4.13. Wound Scratch Assay

Ishikawa/HEC1a cells were seeded in six-well plates at a concentration of 200 × 10^3 cells per well. After reaching 100% confluency, cells were deprived of serum for 24 h and scratched with a sterile P200 pipette tip (#613-1096, VWR International GmbH) as previously described [59]. After removal of the debris by repeated washes, cells were subjected to respective treatment (control/NFAT5 overexpression) and scratch wound closure was closely monitored by microscopy (EVOS M7000 cell imaging system, Thermo Fisher Scientific) capturing bright field images of the same field with a 4× objective at 0 h and 24 h. The percentage of wound are closure was calculated with ImageJ software.

4.14. Statistics

The data are given as arithmetic mean ± SEM, the number of independent biological experiments were denoted as *n*. The data were analyzed for significance using un-paired Student's *t*-test using GraphPad Prism (GraphPad Software 7.0, San Diego, CA, USA). Statistical significance was considered when p value was less than < 0.05. the clinical table was analyzed using Stata statistical software version 17.2 (StataCorp LLC, College Station, TX, USA). We compared categorical variables using χ^2 tests.

Supplementary Materials: The supporting information can be downloaded at: https://www.mdpi.com/article/10.3390/ijms25073666/s1.

Author Contributions: T.O., J.P.R.X., M.S.S., Z.Y., C.H., B.N., Y.S. and J.A. performed experiments and/or analyzed data; B.N., Y.S. and J.A., performed the RNA sequencing and data analysis; J.P., S.Y.B., S.K. and A.S. recruited and consented patients, performed immunohistochemistry and performed data analysis; M.S.S., S.Y.B., S.T. and F.L. provided resources and funding; M.S.S. and F.L. developed the concepts/experiments and wrote the original draft. All authors have read and agreed to the published version of the manuscript.

Funding: This work was supported by funding to M.S.S., Else Kröner-Fresenius-Stiftung 2019_A140, the IZKF (2510-0-0) and the joint initiative between the EU and the Ministerium für Wissenschaft, Forschung und Kunst Baden-Württemberg (DE) Margarete von Wrangell-Habilitationsprogramm für

Frauen (31-7635.41/118/3). To F.L. the Open Access Publishing Fund of Tuebingen University. T.O was supported by the Juntendo University Medical Research Exchange Program.

Institutional Review Board Statement: The study was conducted in accordance with the Declaration of Helsinki, and approved by the Tübingen University Medical Ethics Committee issued study/ethical approval for this study (protocol code—707/2022B02) on 01 December 2022.

Informed Consent Statement: Informed consent was obtained from all subjects involved in the study.

Data Availability Statement: Expression data have been submitted to the Gene Expression Omnibus (GEO) repository with accession number GSE134319. The remaining data presented in this study are available upon reasonable request from the corresponding author.

Acknowledgments: We thank Dr. André Koch with his help with preparation of the clinical patient table. We also thank Karen Greif on her technical assistance in staining patient tissue samples.

Conflicts of Interest: The authors declare that they have no conflicts of interests.

References

1. Raglan, O.; Kalliala, I.; Markozannes, G.; Cividini, S.; Gunter, M.J.; Nautiyal, J.; Gabra, H.; Paraskevaidis, E.; Martin-Hirsch, P.; Tsilidis, K.K.; et al. Risk factors for endometrial cancer: An umbrella review of the literature. *Int. J. Cancer* **2019**, *145*, 1719–1730. [CrossRef] [PubMed]
2. Crosbie, E.J.; Kitson, S.J.; McAlpine, J.N.; Mukhopadhyay, A.; Powell, M.E.; Singh, N. Endometrial cancer. *Lancet* **2022**, *399*, 1412–1428. [CrossRef] [PubMed]
3. Leone Roberti Maggiore, U.; Spanò Bascio, L.; Alboni, C.; Chiarello, G.; Savelli, L.; Bogani, G.; Martinelli, F.; Chiappa, V.; Ditto, A.; Raspagliesi, F. Sentinel lymph node biopsy in endometrial cancer: When, how and in which patients. *Eur. J. Surg. Oncol.* **2024**, *50*, 107956. [CrossRef] [PubMed]
4. Makker, V.; MacKay, H.; Ray-Coquard, I.; Levine, D.A.; Westin, S.N.; Aoki, D.; Oaknin, A. Endometrial cancer. *Nat. Rev. Dis. Primers* **2021**, *7*, 88. [CrossRef] [PubMed]
5. Charo, L.M.; Plaxe, S.C. Recent advances in endometrial cancer: A review of key clinical trials from 2015 to 2019. *F1000Research* **2019**, *8*, 849. [CrossRef] [PubMed]
6. Wu, Y.; Sun, W.; Liu, H.; Zhang, D. Age at Menopause and Risk of Developing Endometrial Cancer: A Meta-Analysis. *BioMed Res. Int.* **2019**, *2019*, 8584130. [CrossRef]
7. Siegel, R.L.; Miller, K.D.; Jemal, A. Cancer statistics, 2019. *CA Cancer J. Clin.* **2019**, *69*, 7–34. [CrossRef]
8. Son, J.; Carr, C.; Yao, M.; Radeva, M.; Priyadarshini, A.; Marquard, J.; Michener, C.M.; AlHilli, M. Endometrial cancer in young women: Prognostic factors and treatment outcomes in women aged ≤40 years. *Int. J. Gynecol. Cancer* **2020**, *30*, 631–639. [CrossRef]
9. Wong, A.; Ngeow, J. Hereditary Syndromes Manifesting as Endometrial Carcinoma: How Can Pathological Features Aid Risk Assessment? *BioMed Res. Int.* **2015**, *2015*, 219012. [CrossRef] [PubMed]
10. Onstad, M.A.; Schmandt, R.E.; Lu, K.H. Addressing the Role of Obesity in Endometrial Cancer Risk, Prevention, and Treatment. *J. Clin. Oncol.* **2016**, *34*, 4225–4230. [CrossRef] [PubMed]
11. Cai, Y.; Wang, B.; Xu, W.; Liu, K.; Gao, Y.; Guo, C.; Chen, J.; Kamal, M.A.; Yuan, C. Endometrial Cancer: Genetic, Metabolic Characteristics, Therapeutic Strategies and Nanomedicine. *Curr. Med. Chem.* **2021**, *28*, 8755–8781. [CrossRef] [PubMed]
12. Gong, H.; Nie, D.; Li, Z. Targeting Six Hallmarks of Cancer in Ovarian Cancer Therapy. *Curr. Cancer Drug Targets* **2020**, *20*, 853–867. [CrossRef] [PubMed]
13. Terzic, M.; Aimagambetova, G.; Kunz, J.; Bapayeva, G.; Aitbayeva, B.; Terzic, S.; Laganà, A.S. Molecular Basis of Endometriosis and Endometrial Cancer: Current Knowledge and Future Perspectives. *Int. J. Mol. Sci.* **2021**, *22*, 9274. [CrossRef] [PubMed]
14. Choi, S.Y.; Lee-Kwon, W.; Kwon, H.M. The evolving role of TonEBP as an immunometabolic stress protein. *Nat. Rev. Nephrol.* **2020**, *16*, 352–364. [CrossRef]
15. Lee, N.; Kim, D.; Kim, W.U. Role of NFAT5 in the Immune System and Pathogenesis of Autoimmune Diseases. *Front. Immunol.* **2019**, *10*, 270. [CrossRef] [PubMed]
16. Zhou, X. How do kinases contribute to tonicity-dependent regulation of the transcription factor NFAT5? *World J. Nephrol.* **2016**, *5*, 20–32. [CrossRef]
17. Ma, S.; Zhao, Y.; Lee, W.C.; Ong, L.T.; Lee, P.L.; Jiang, Z.; Oguz, G.; Niu, Z.; Liu, M.; Goh, J.Y.; et al. Hypoxia induces HIF1α-dependent epigenetic vulnerability in triple negative breast cancer to confer immune effector dysfunction and resistance to anti-PD-1 immunotherapy. *Nat. Commun.* **2022**, *13*, 4118. [CrossRef] [PubMed]
18. Muhammad, K.; Xavier, D.; Klein-Hessling, S.; Azeem, M.; Rauschenberger, T.; Murti, K.; Avots, A.; Goebeler, M.; Klein, M.; Bopp, T.; et al. NFAT5 Controls the Integrity of Epidermis. *Front. Immunol.* **2021**, *12*, 780727. [CrossRef]
19. Chen, B.L.; Li, Y.; Xu, S.; Nie, Y.; Zhang, J. NFAT5 Regulated by STUB1, Facilitates Malignant Cell Survival and p38 MAPK Activation by Upregulating AQP5 in Chronic Lymphocytic Leukemia. *Biochem. Genet.* **2021**, *59*, 870–883. [CrossRef] [PubMed]

20. Yang, X.L.; Zeng, M.L.; Shao, L.; Jiang, G.T.; Cheng, J.J.; Chen, T.X.; Han, S.; Yin, J.; Liu, W.H.; He, X.H.; et al. NFAT5 and HIF-1α Coordinate to Regulate NKCC1 Expression in Hippocampal Neurons After Hypoxia-Ischemia. *Front. Cell Dev. Biol.* **2019**, *7*, 339. [CrossRef]
21. Lang, F.; Guelinckx, I.; Lemetais, G.; Melander, O. Two Liters a Day Keep the Doctor Away? Considerations on the Pathophysiology of Suboptimal Fluid Intake in the Common Population. *Kidney Blood Press. Res.* **2017**, *42*, 483–494. [CrossRef] [PubMed]
22. Cen, L.; Xing, F.; Xu, L.; Cao, Y. Potential Role of Gene Regulator NFAT5 in the Pathogenesis of Diabetes Mellitus. *J. Diabetes Res.* **2020**, *2020*, 6927429. [CrossRef] [PubMed]
23. Aramburu, J.; López-Rodríguez, C. Regulation of Inflammatory Functions of Macrophages and T Lymphocytes by NFAT5. *Front. Immunol.* **2019**, *10*, 535. [CrossRef] [PubMed]
24. Leibrock, C.B.; Alesutan, I.; Voelkl, J.; Pakladok, T.; Michael, D.; Schleicher, E.; Kamyabi-Moghaddam, Z.; Quintanilla-Martinez, L.; Kuro-o, M.; Lang, F. NH_4Cl Treatment Prevents Tissue Calcification in Klotho Deficiency. *J. Am. Soc. Nephrol.* **2015**, *26*, 2423–2433. [CrossRef] [PubMed]
25. Neubert, P.; Weichselbaum, A.; Reitinger, C.; Schatz, V.; Schroder, A.; Ferdinand, J.R.; Simon, M.; Bar, A.L.; Brochhausen, C.; Gerlach, R.G.; et al. HIF1A and NFAT5 coordinate Na(+)-boosted antibacterial defense via enhanced autophagy and autolysosomal targeting. *Autophagy* **2019**, *15*, 1899–1916. [CrossRef]
26. Meng, X.; Li, Z.; Zhou, S.; Xiao, S.; Yu, P. miR-194 suppresses high glucose-induced non-small cell lung cancer cell progression by targeting NFAT5. *Thorac. Cancer* **2019**, *10*, 1051–1059. [CrossRef] [PubMed]
27. Xu, J.; Wang, H.; Shi, B.; Li, N.; Xu, G.; Yan, X.; Xu, L. Exosomal MFI2-AS1 sponge miR-107 promotes non-small cell lung cancer progression through NFAT5. *Cancer Cell Int.* **2023**, *23*, 51. [CrossRef]
28. Zhen, H.; Yao, Y.; Yang, H. SAFB2 Inhibits the Progression of Breast Cancer by Suppressing the Wnt/β-Catenin Signaling Pathway via NFAT5. *Mol. Biotechnol.* **2023**, *65*, 1465–1475. [CrossRef]
29. Arroyo, J.A.; Teng, C.; Battaglia, F.C.; Galan, H.L. Determination of the NFAT5/TonEBP transcription factor in the human and ovine placenta. *Syst. Biol. Reprod. Med.* **2009**, *55*, 164–170. [CrossRef] [PubMed]
30. Amara, S.; Alotaibi, D.; Tiriveedhi, V. NFAT5/STAT3 interaction mediates synergism of high salt with IL-17 towards induction of VEGF-A expression in breast cancer cells. *Oncol. Lett.* **2016**, *12*, 933–943. [CrossRef] [PubMed]
31. Chernyakov, D.; Groß, A.; Fischer, A.; Bornkessel, N.; Schultheiss, C.; Gerloff, D.; Edemir, B. Loss of RANBP3L leads to transformation of renal epithelial cells towards a renal clear cell carcinoma like phenotype. *J. Exp. Clin. Cancer Res.* **2021**, *40*, 226. [CrossRef] [PubMed]
32. Yu, H.; Zheng, J.; Liu, X.; Xue, Y.; Shen, S.; Zhao, L.; Li, Z.; Liu, Y. Transcription Factor NFAT5 Promotes Glioblastoma Cell-driven Angiogenesis via SBF2-AS1/miR-338-3p-Mediated EGFL7 Expression Change. *Front. Mol. Neurosci.* **2017**, *10*, 301. [CrossRef] [PubMed]
33. Dzhalilova, D.S.; Makarova, O.V. HIF-Dependent Mechanisms of Relationship between Hypoxia Tolerance and Tumor Development. *Biochemistry* **2021**, *86*, 1163–1180. [CrossRef] [PubMed]
34. Bai, R.; Li, Y.; Jian, L.; Yang, Y.; Zhao, L.; Wei, M. The hypoxia-driven crosstalk between tumor and tumor-associated macrophages: Mechanisms and clinical treatment strategies. *Mol. Cancer* **2022**, *21*, 177. [CrossRef] [PubMed]
35. Tam, S.Y.; Wu, V.W.C.; Law, H.K.W. Hypoxia-Induced Epithelial-Mesenchymal Transition in Cancers: HIF-1α and Beyond. *Front. Oncol.* **2020**, *10*, 486. [CrossRef] [PubMed]
36. Qin, X.; Li, C.; Guo, T.; Chen, J.; Wang, H.T.; Wang, Y.T.; Xiao, Y.S.; Li, J.; Liu, P.; Liu, Z.S.; et al. Upregulation of DARS2 by HBV promotes hepatocarcinogenesis through the miR-30e-5p/MAPK/NFAT5 pathway. *J. Exp. Clin. Cancer Res.* **2017**, *36*, 148. [CrossRef] [PubMed]
37. Li, J.; Zhang, J.; Xie, F.; Peng, J.; Wu, X. Macrophage migration inhibitory factor promotes Warburg effect via activation of the NFkappaB/HIF1alpha pathway in lung cancer. *Int. J. Mol. Med.* **2018**, *41*, 1062–1068. [CrossRef]
38. Hidalgo-Estévez, A.M.; Stamatakis, K.; Jiménez-Martínez, M.; López-Pérez, R.; Fresno, M. Cyclooxygenase 2-Regulated Genes an Alternative Avenue to the Development of New Therapeutic Drugs for Colorectal Cancer. *Front. Pharmacol.* **2020**, *11*, 533. [CrossRef] [PubMed]
39. Kirkby, N.S.; Chan, M.V.; Zaiss, A.K.; Garcia-Vaz, E.; Jiao, J.; Berglund, L.M.; Verdu, E.F.; Ahmetaj-Shala, B.; Wallace, J.L.; Herschman, H.R.; et al. Systematic study of constitutive cyclooxygenase-2 expression: Role of NF-κB and NFAT transcriptional pathways. *Proc. Natl. Acad. Sci. USA* **2016**, *113*, 434–439. [CrossRef] [PubMed]
40. Shukla, V.; Kaushal, J.B.; Sankhwar, P.; Manohar, M.; Dwivedi, A. Inhibition of TPPP3 attenuates β-catenin/NF-κB/COX-2 signaling in endometrial stromal cells and impairs decidualization. *J. Endocrinol.* **2019**, *240*, 417–429. [CrossRef] [PubMed]
41. Lyndin, M.; Kravtsova, O.; Sikora, K.; Lyndina, Y.; Kuzenko, Y.; Awuah, W.A.; Abdul-Rahman, T.; Hyriavenko, N.; Sikora, V.; Romaniuk, A. COX2 Effects on endometrial carcinomas progression. *Pathol. Res. Pract.* **2022**, *238*, 154082. [CrossRef] [PubMed]
42. Yan, X.; Jiao, S.C.; Zhang, G.Q.; Guan, Y.; Wang, J.L. Tumor-associated immune factors are associated with recurrence and metastasis in non-small cell lung cancer. *Cancer Gene Ther.* **2017**, *24*, 57–63. [CrossRef] [PubMed]
43. Piasecka, D.; Braun, M.; Mieszkowska, M.; Kowalczyk, L.; Kopczynski, J.; Kordek, R.; Sadej, R.; Romanska, H.M. Upregulation of HIF1-α via an NF-κB/COX2 pathway confers proliferative dominance of HER2-negative ductal carcinoma in situ cells in response to inflammatory stimuli. *Neoplasia* **2020**, *22*, 576–589. [CrossRef]

44. Ding, Y.; Zhuang, S.; Li, Y.; Yu, X.; Lu, M.; Ding, N. Hypoxia-induced HIF1α dependent COX2 promotes ovarian cancer progress. *J. Bioenerg. Biomembr.* **2021**, *53*, 441–448. [CrossRef] [PubMed]
45. Cizkova, K.; Foltynkova, T.; Gachechiladze, M.; Tauber, Z. Comparative Analysis of Immunohistochemical Staining Intensity Determined by Light Microscopy, ImageJ and QuPath in Placental Hofbauer Cells. *Acta Histochem. Cytochem.* **2021**, *54*, 21–29. [CrossRef] [PubMed]
46. Eritja, N.; Chen, B.J.; Rodríguez-Barrueco, R.; Santacana, M.; Gatius, S.; Vidal, A.; Martí, M.D.; Ponce, J.; Bergadà, L.; Yeramian, A.; et al. Autophagy orchestrates adaptive responses to targeted therapy in endometrial cancer. *Autophagy* **2017**, *13*, 608–624. [CrossRef] [PubMed]
47. Takahashi, A.; Seike, M.; Chiba, M.; Takahashi, S.; Nakamichi, S.; Matsumoto, M.; Takeuchi, S.; Minegishi, Y.; Noro, R.; Kunugi, S.; et al. Ankyrin Repeat Domain 1 Overexpression is Associated with Common Resistance to Afatinib and Osimertinib in EGFR-mutant Lung Cancer. *Sci. Rep.* **2018**, *8*, 14896. [CrossRef] [PubMed]
48. Ahmad Zawawi, S.S.; Mohd Azram, N.A.S.; Sulong, S.; Zakaria, A.D.; Lee, Y.Y.; Che Jalil, N.A.; Musa, M. Identification of AOC3 and LRRC17 as Colonic Fibroblast Activation Markers and Their Potential Roles in Colorectal Cancer Progression. *Asian Pac. J. Cancer Prev.* **2023**, *24*, 3099–3107. [CrossRef] [PubMed]
49. Singh, Y.; Shi, X.; Zhang, S.; Umbach, A.T.; Chen, H.; Salker, M.S.; Lang, F. Prolyl hydroxylase 3 (PHD3) expression augments the development of regulatory T cells. *Mol. Immunol.* **2016**, *76*, 7–12. [CrossRef] [PubMed]
50. Chen, R.; Ahmed, M.A.; Forsyth, N.R. Dimethyloxalylglycine (DMOG), a Hypoxia Mimetic Agent, Does Not Replicate a Rat Pheochromocytoma (PC12) Cell Biological Response to Reduced Oxygen Culture. *Biomolecules* **2022**, *12*, 541. [CrossRef] [PubMed]
51. Yuan, Q.; Bleiziffer, O.; Boos, A.M.; Sun, J.; Brandl, A.; Beier, J.P.; Arkudas, A.; Schmitz, M.; Kneser, U.; Horch, R.E. PHDs inhibitor DMOG promotes the vascularization process in the AV loop by HIF-1a up-regulation and the preliminary discussion on its kinetics in rat. *BMC Biotechnol.* **2014**, *14*, 112. [CrossRef] [PubMed]
52. Xue, X.; Shah, Y.M. Hypoxia-inducible factor-2alpha is essential in activating the COX2/mPGES-1/PGE2 signaling axis in colon cancer. *Carcinogenesis* **2013**, *34*, 163–169. [CrossRef] [PubMed]
53. Serman, Y.; Fuentealba, R.A.; Pasten, C.; Rocco, J.; Ko, B.C.B.; Carrion, F.; Irarrazabal, C.E. Emerging new role of NFAT5 in inducible nitric oxide synthase in response to hypoxia in mouse embryonic fibroblast cells. *Am. J. Physiol. Cell Physiol.* **2019**, *317*, C31–C38. [CrossRef] [PubMed]
54. Sahu, I.; Pelzl, L.; Sukkar, B.; Fakhri, H.; Al-Maghout, T.; Cao, H.; Hauser, S.; Gutti, R.; Gawaz, M.; Lang, F. NFAT5-sensitive Orai1 expression and store-operated Ca^{2+} entry in megakaryocytes. *FASEB J.* **2017**, *31*, 3439–3448. [CrossRef] [PubMed]
55. Maouyo, D.; Kim, J.Y.; Lee, S.D.; Wu, Y.; Woo, S.K.; Kwon, H.M. Mouse TonEBP-NFAT5: Expression in early development and alternative splicing. *Am. J. Physiol. Renal Physiol.* **2002**, *282*, F802–F809. [CrossRef]
56. Packialakshmi, B.; Hira, S.; Lund, K.; Zhang, A.H.; Halterman, J.; Feng, Y.; Scott, D.W.; Lees, J.R.; Zhou, X. NFAT5 contributes to the pathogenesis of experimental autoimmune encephalomyelitis (EAE) and decrease of T regulatory cells in female mice. *Cell. Immunol.* **2022**, *375*, 104515. [CrossRef]
57. Lee, H.H.; Jeong, G.W.; Ye, B.J.; Yoo, E.J.; Son, K.S.; Kim, D.K.; Park, H.K.; Kang, B.H.; Lee-Kwon, W.; Kwon, H.M.; et al. TonEBP in Myeloid Cells Promotes Obesity-Induced Insulin Resistance and Inflammation Through Adipose Tissue Remodeling. *Diabetes* **2022**, *71*, 2557–2571. [CrossRef] [PubMed]
58. He, W.; Zhang, M.; Zhao, M.; Davis, L.S.; Blackwell, T.S.; Yull, F.; Breyer, M.D.; Hao, C.M. Increased dietary sodium induces COX2 expression by activating NFkappaB in renal medullary interstitial cells. *Pflugers Arch.* **2014**, *466*, 357–367. [CrossRef] [PubMed]
59. Alauddin, M.; Okumura, T.; Rajaxavier, J.; Khozooei, S.; Pöschel, S.; Takeda, S.; Singh, Y.; Brucker, S.Y.; Wallwiener, D.; Koch, A.; et al. Gut Bacterial Metabolite Urolithin A Decreases Actin Polymerization and Migration in Cancer Cells. *Mol. Nutr. Food Res.* **2020**, *64*, 1900390. [CrossRef] [PubMed]
60. Johnson, Z.I.; Doolittle, A.C.; Snuggs, J.W.; Shapiro, I.M.; Le Maitre, C.L.; Risbud, M.V. TNF-α promotes nuclear enrichment of the transcription factor TonEBP/NFAT5 to selectively control inflammatory but not osmoregulatory responses in nucleus pulposus cells. *J. Biol. Chem.* **2017**, *292*, 17561–17575. [CrossRef] [PubMed]
61. Xia, X.; Qu, B.; Li, Y.M.; Yang, L.B.; Fan, K.X.; Zheng, H.; Huang, H.D.; Gu, J.W.; Kuang, Y.Q.; Ma, Y. NFAT5 protects astrocytes against oxygen-glucose-serum deprivation/restoration damage via the SIRT1/Nrf2 pathway. *J. Mol. Neurosci.* **2017**, *61*, 96–104. [CrossRef] [PubMed]
62. Chen, W.-T.; Hung, W.-C.; Kang, W.-Y.; Huang, Y.-C.; Su, Y.-C.; Yang, C.-H.; Chai, C.-Y. Overexpression of cyclooxygenase-2 in urothelial carcinoma in conjunction with tumor-associated-macrophage infiltration, hypoxia-inducible factor-1α expression, and tumor angiogenesis. *APMIS* **2009**, *117*, 176–184. [CrossRef] [PubMed]
63. Garg, R.; Blando, J.M.; Perez, C.J.; Lal, P.; Feldman, M.D.; Smyth, E.M.; Ricciotti, E.; Grosser, T.; Benavides, F.; Kazanietz, M.G. COX-2 mediates pro-tumorigenic effects of PKCε in prostate cancer. *Oncogene* **2018**, *37*, 4735–4749. [CrossRef] [PubMed]
64. Zheng, Y.; Comaills, V.; Burr, R.; Boulay, G.; Miyamoto, D.T.; Wittner, B.S.; Emmons, E.; Sil, S.; Koulopoulos, M.W.; Broderick, K.T.; et al. COX-2 mediates tumor-stromal prolactin signaling to initiate tumorigenesis. *Proc. Natl. Acad. Sci. USA* **2019**, *116*, 5223–5232. [CrossRef] [PubMed]
65. Alexanian, A.; Sorokin, A. Cyclooxygenase 2: Protein-protein interactions and posttranslational modifications. *Physiol. Genom.* **2017**, *49*, 667–681. [CrossRef] [PubMed]

66. Greenhough, A.; Smartt, H.J.; Moore, A.E.; Roberts, H.R.; Williams, A.C.; Paraskeva, C.; Kaidi, A. The COX-2/PGE2 pathway: Key roles in the hallmarks of cancer and adaptation to the tumour microenvironment. *Carcinogenesis* **2009**, *30*, 377–386. [CrossRef] [PubMed]
67. Nasry, W.H.S.; Rodriguez-Lecompte, J.C.; Martin, C.K. Role of COX-2/PGE2 Mediated Inflammation in Oral Squamous Cell Carcinoma. *Cancers* **2018**, *10*, 348. [CrossRef] [PubMed]
68. Greten, F.R.; Grivennikov, S.I. Inflammation and Cancer: Triggers, Mechanisms, and Consequences. *Immunity* **2019**, *51*, 27–41. [CrossRef] [PubMed]
69. Gandhi, A.S.; Budac, D.; Khayrullina, T.; Staal, R.; Chandrasena, G. Quantitative analysis of lipids: A higher-throughput LC-MS/MS-based method and its comparison to ELISA. *Future Sci. OA* **2017**, *3*, Fso157. [CrossRef]
70. Kefayat, A.; Ghahremani, F.; Safavi, A.; Hajiaghababa, A.; Moshtaghian, J. C-phycocyanin: A natural product with radiosensitizing property for enhancement of colon cancer radiation therapy efficacy through inhibition of COX-2 expression. *Sci. Rep.* **2019**, *9*, 19161. [CrossRef] [PubMed]
71. Li, X.H.; Li, J.J.; Zhang, H.W.; Sun, P.; Zhang, Y.L.; Cai, S.H.; Ren, X.D. Nimesulide inhibits tumor growth in mice implanted hepatoma: Overexpression of Bax over Bcl-2. *Acta Pharmacol. Sin.* **2003**, *24*, 1045–1050.
72. Gui, D.; Li, Y.; Chen, X.; Gao, D.; Yang, Y.; Li, X. HIF1 signaling pathway involving iNOS, COX2 and caspase9 mediates the neuroprotection provided by erythropoietin in the retina of chronic ocular hypertension rats. *Mol. Med. Rep.* **2015**, *11*, 1490–1496. [CrossRef] [PubMed]
73. Chen, S.; Grigsby, C.L.; Law, C.S.; Ni, X.; Nekrep, N.; Olsen, K.; Humphreys, M.H.; Gardner, D.G. Tonicity-dependent induction of Sgk1 expression has a potential role in dehydration-induced natriuresis in rodents. *J. Clin. Investig.* **2009**, *119*, 1647–1658. [CrossRef] [PubMed]
74. Lang, F.; Shumilina, E. Regulation of ion channels by the serum- and glucocorticoid-inducible kinase SGK1. *FASEB J.* **2013**, *27*, 3–12. [CrossRef] [PubMed]
75. Roche, J. The Epithelial-to-Mesenchymal Transition in Cancer. *Cancers* **2018**, *10*, 52. [CrossRef] [PubMed]
76. Wang, X.; Glubb, D.M.; O'Mara, T.A. Dietary Factors and Endometrial Cancer Risk: A Mendelian Randomization Study. *Nutrients* **2023**, *15*, 603. [CrossRef] [PubMed]
77. Balan, Y.; Packirisamy, R.M.; Mohanraj, P.S. High dietary salt intake activates inflammatory cascades via Th17 immune cells: Impact on health and diseases. *Arch. Med. Sci.* **2022**, *18*, 459–465. [CrossRef] [PubMed]
78. Ma, P.; Li, G.; Jiang, X.; Shen, X.; Li, H.; Yang, L.; Liu, W. NFAT5 directs hyperosmotic stress-induced fibrin deposition and macrophage infiltration via PAI-1 in endothelium. *Aging* **2020**, *13*, 3661–3679. [CrossRef]
79. Schröder, A.; Leikam, A.; Käppler, P.; Neubert, P.; Jantsch, J.; Neuhofer, W.; Deschner, J.; Proff, P.; Kirschneck, C. Impact of salt and the osmoprotective transcription factor NFAT-5 on macrophages during mechanical strain. *Immunol. Cell Biol.* **2021**, *99*, 84–96. [CrossRef] [PubMed]
80. Madonna, R.; Giovannelli, G.; Confalone, P.; Renna, F.V.; Geng, Y.J.; De Caterina, R. High glucose-induced hyperosmolarity contributes to COX-2 expression and angiogenesis: Implications for diabetic retinopathy. *Cardiovasc. Diabetol.* **2016**, *15*, 18. [CrossRef] [PubMed]
81. Hernández-Ochoa, E.O.; Robison, P.; Contreras, M.; Shen, T.; Zhao, Z.; Schneider, M.F. Elevated extracellular glucose and uncontrolled type 1 diabetes enhance NFAT5 signaling and disrupt the transverse tubular network in mouse skeletal muscle. *Exp. Biol. Med.* **2012**, *237*, 1068–1083. [CrossRef]
82. Padmanabhan, S.; Caulfield, M.; Dominiczak, A.F. Genetic and Molecular Aspects of Hypertension. *Circ. Res.* **2015**, *116*, 937–959. [CrossRef]
83. Robinson, M.D.; McCarthy, D.J.; Smyth, G.K. edgeR: A Bioconductor package for differential expression analysis of digital gene expression data. *Bioinformatics* **2010**, *26*, 139–140. [CrossRef]
84. McCarthy, D.J.; Chen, Y.; Smyth, G.K. Differential expression analysis of multifactor RNA-Seq experiments with respect to biological variation. *Nucleic Acids Res.* **2012**, *40*, 4288–4297. [CrossRef]
85. Chen, Y.; Lun, A.T.; Smyth, G.K. From reads to genes to pathways: Differential expression analysis of RNA-Seq experiments using Rsubread and the edgeR quasi-likelihood pipeline. *F1000Research* **2016**, *5*, 1438. [CrossRef]
86. Chicco, D.; Jurman, G. A brief survey of tools for genomic regions enrichment analysis. *Front. Bioinform.* **2022**, *2*, 968327. [CrossRef]
87. Thomas, P.D.; Ebert, D.; Muruganujan, A.; Mushayahama, T.; Albou, L.P.; Mi, H. PANTHER: Making genome-scale phylogenetics accessible to all. *Protein Sci.* **2022**, *31*, 8–22. [CrossRef]
88. Kanehisa, M.; Goto, S. KEGG: Kyoto encyclopedia of genes and genomes. *Nucleic Acids Res.* **2000**, *28*, 27–30. [CrossRef]
89. Fabregat, A.; Sidiropoulos, K.; Viteri, G.; Forner, O.; Marin-Garcia, P.; Arnau, V.; D'Eustachio, P.; Stein, L.; Hermjakob, H. Reactome pathway analysis: A high-performance in-memory approach. *BMC Bioinform.* **2017**, *18*, 142. [CrossRef]
90. Schriml, L.M.; Mitraka, E.; Munro, J.; Tauber, B.; Schor, M.; Nickle, L.; Felix, V.; Jeng, L.; Bearer, C.; Lichenstein, R.; et al. Human Disease Ontology 2018 update: Classification, content and workflow expansion. *Nucleic Acids Res.* **2019**, *47*, D955–D962. [CrossRef]
91. Livak, K.J.; Schmittgen, T.D. Analysis of relative gene expression data using real-time quantitative PCR and the 2(-Delta Delta C(T)) Method. *Methods* **2001**, *25*, 402–408. [CrossRef] [PubMed]

92. Ayakannu, T.; Taylor, A.H.; Willets, J.M.; Brown, L.; Lambert, D.G.; McDonald, J.; Davies, Q.; Moss, E.L.; Konje, J.C. Validation of endogenous control reference genes for normalizing gene expression studies in endometrial carcinoma. *Mol. Hum. Reprod.* **2015**, *21*, 723–735. [CrossRef] [PubMed]
93. Ye, J.; Coulouris, G.; Zaretskaya, I.; Cutcutache, I.; Rozen, S.; Madden, T.L. Primer-BLAST: A tool to design target-specific primers for polymerase chain reaction. *BMC Bioinform.* **2012**, *13*, 134. [CrossRef] [PubMed]
94. Salker, M.S.; Singh, Y.; Durairaj, R.R.P.; Yan, J.; Alauddin, M.; Zeng, N.; Steel, J.H.; Zhang, S.; Nautiyal, J.; Webster, Z.; et al. LEFTY2 inhibits endometrial receptivity by downregulating Orai1 expression and store-operated Ca^{2+} entry. *J. Mol. Med.* **2018**, *96*, 173–182. [CrossRef]

Rel family transcription factor NFAT5 upregulates COX2 *via* HIF-1α activity in Ishikawa and HEC1a cells

Toshiyuki Okumura[1,2], Janet Raja Xavier[1], Jana Pasternak[1], Zhiqi Yang[1], Cao Hang[1], Bakhtiyor Nosirov[4], Yogesh Singh[1,3], Jakob Admard[3], Sara Y. Brucker[1], Stefan Kommoss[1], Satoru Takeda[2], Annette Staebler[5], Florian Lang[6] and Madhuri S. Salker[1]*

Supplementary Information

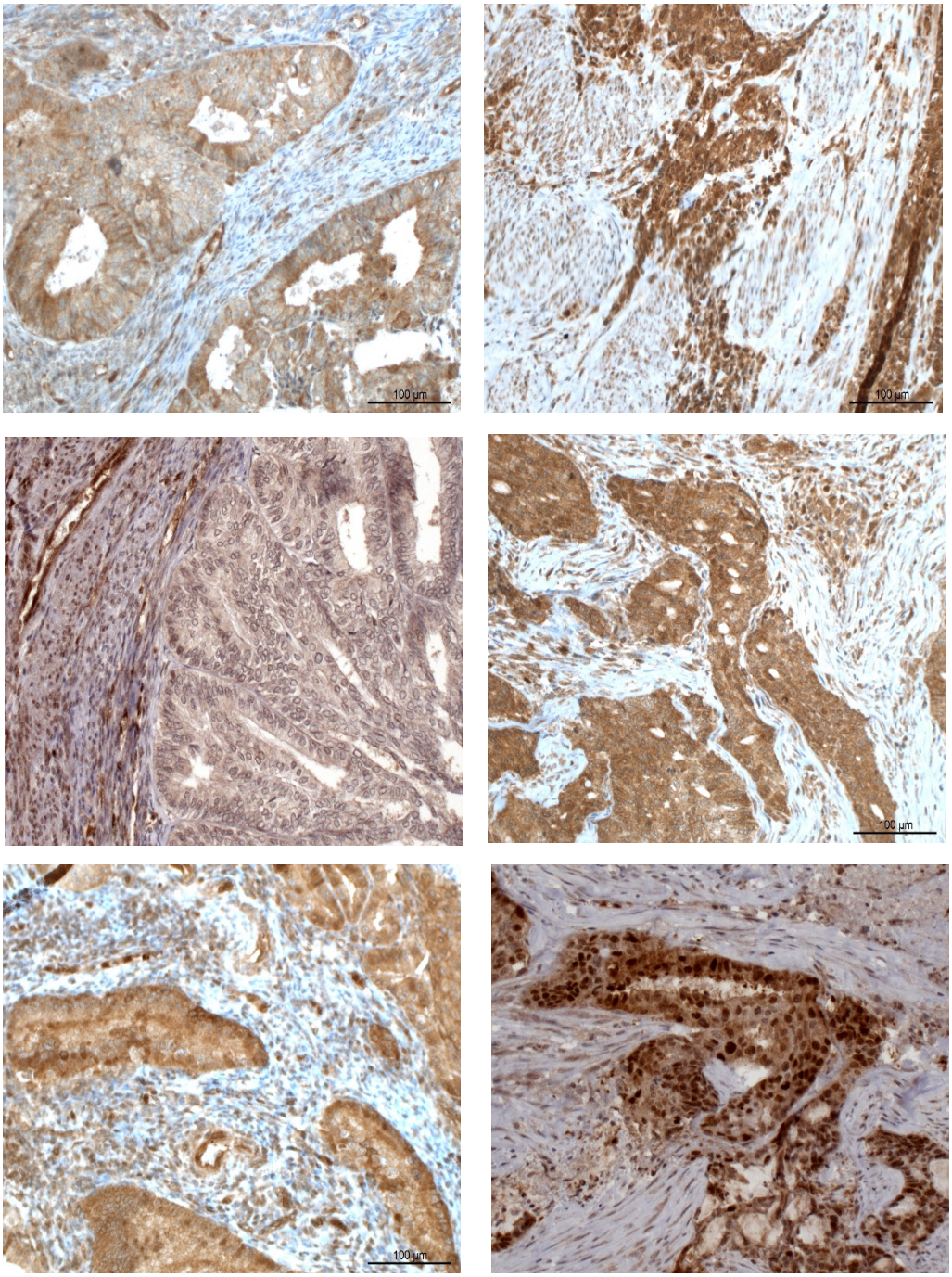

Figure S1. Representative immunohistochemistry images of NFAT5 staining in cases of grade 1 and grade 3 adenocarcinomas.

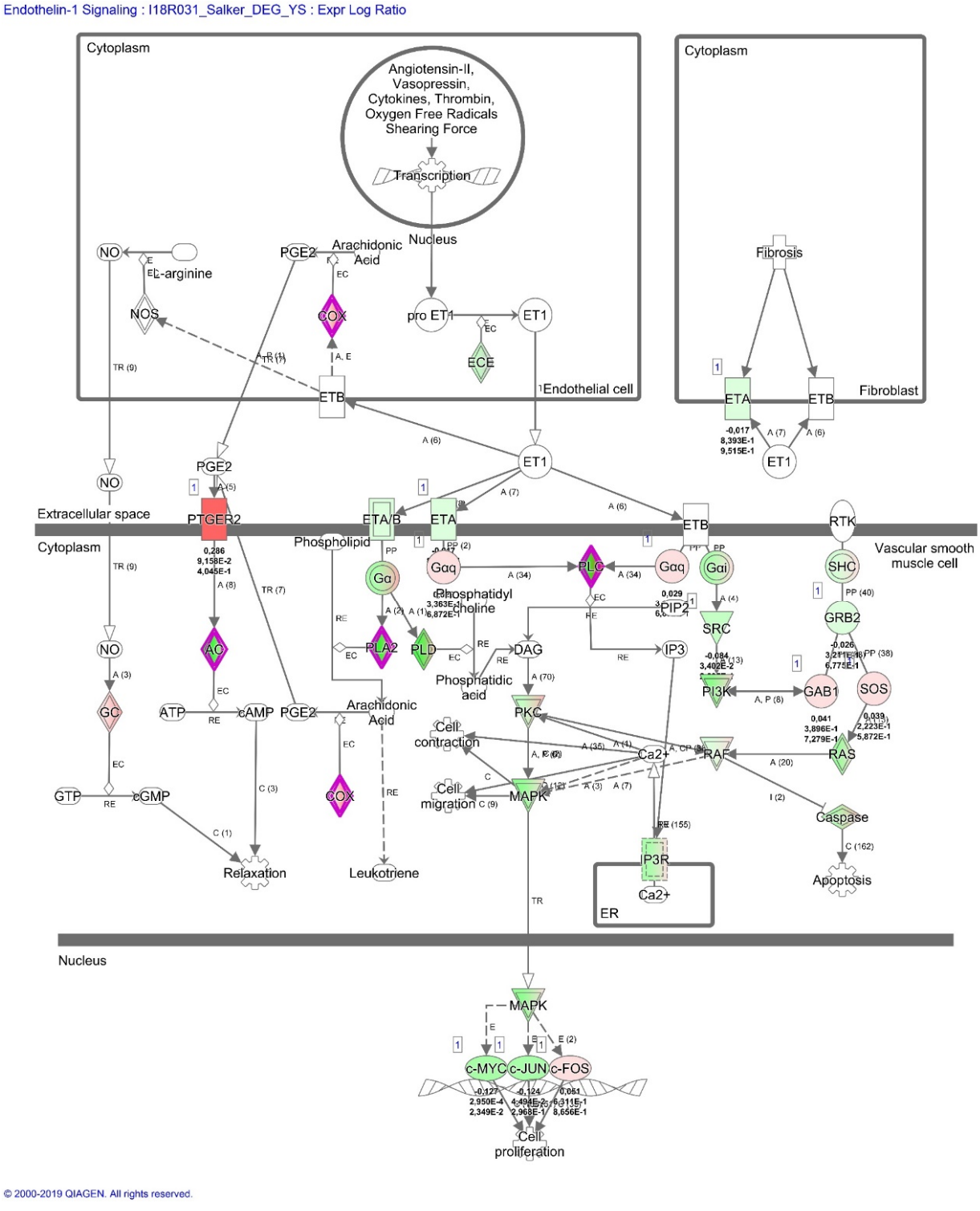

Figure S2. QIAGEN Ingenuity Pathway Analysis with RNA sequencing data (Con/NFAT5 overexpressed) from Ishikawa cells revealed the associated cellular signaling pathway activated. NFAT5 overexpression points to the activation of PTGS2 (COX2) signaling.

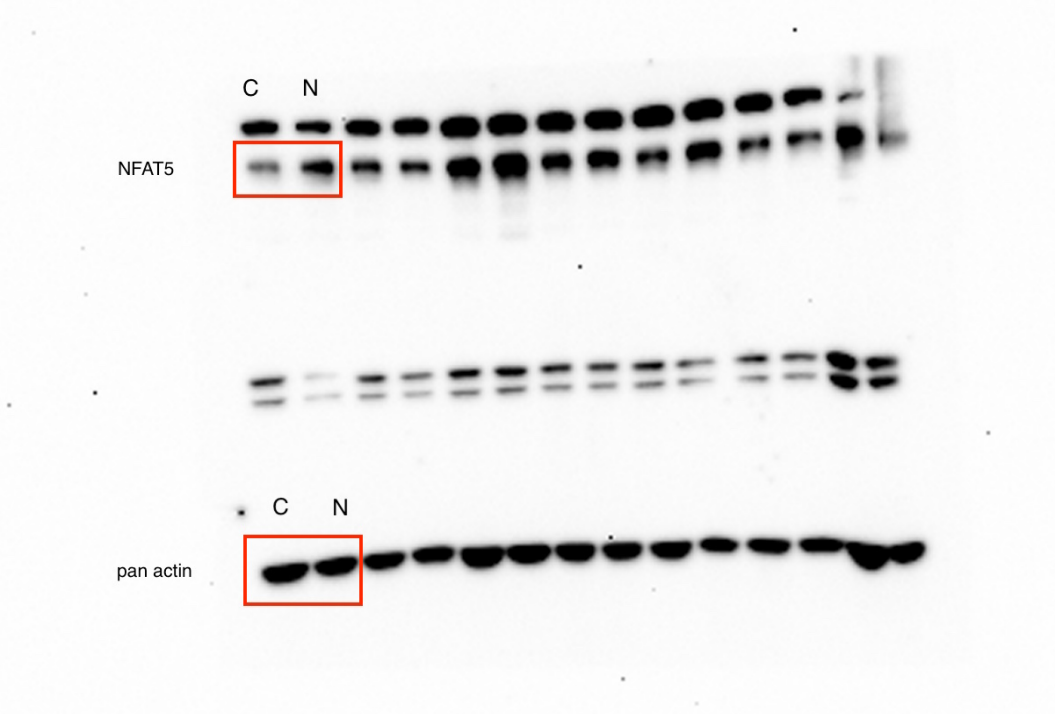

Figure S3. Original western blot membranes of blots represented in figure 3.

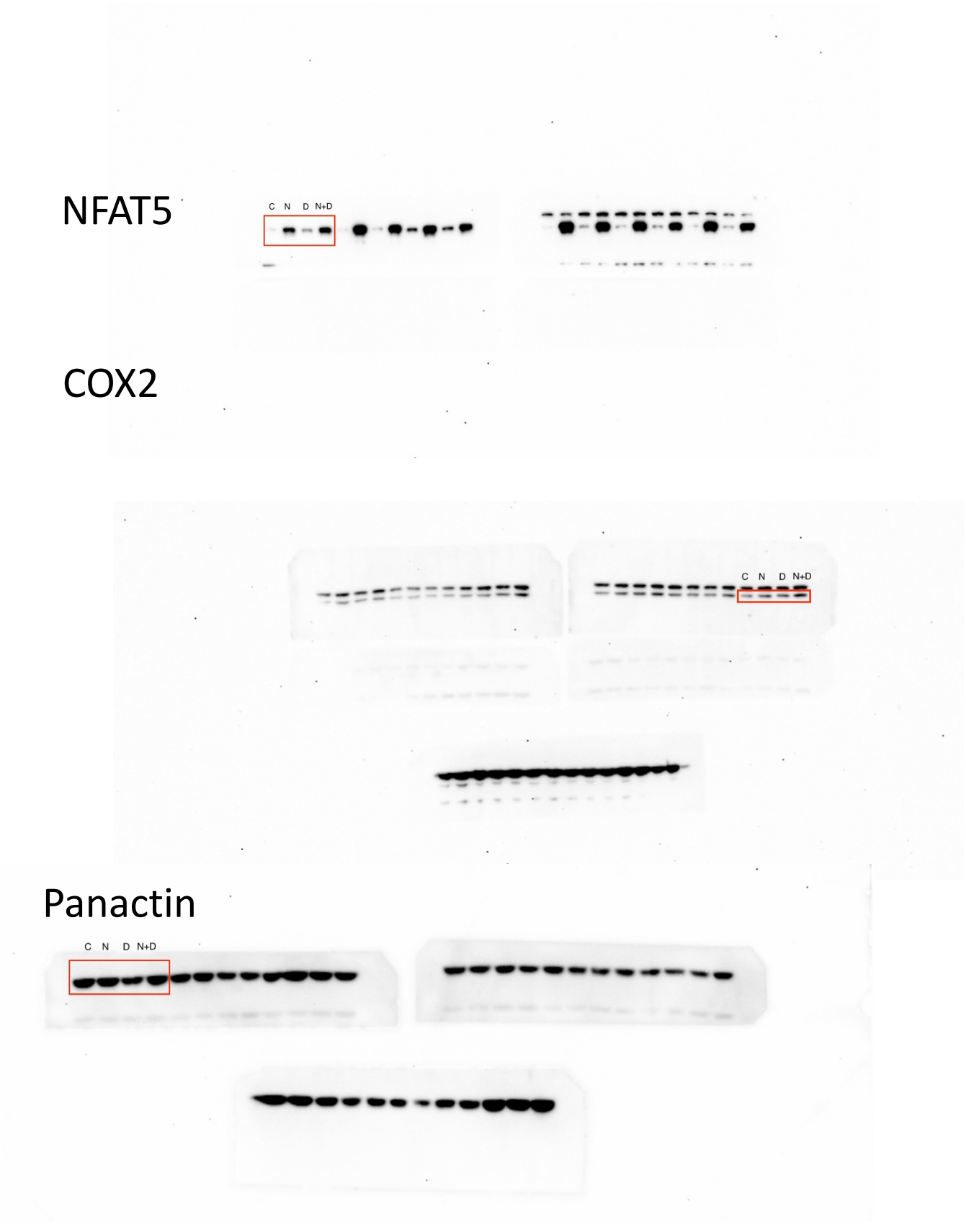

Figure S4. Original western blot membranes of blots represented in figure 5.

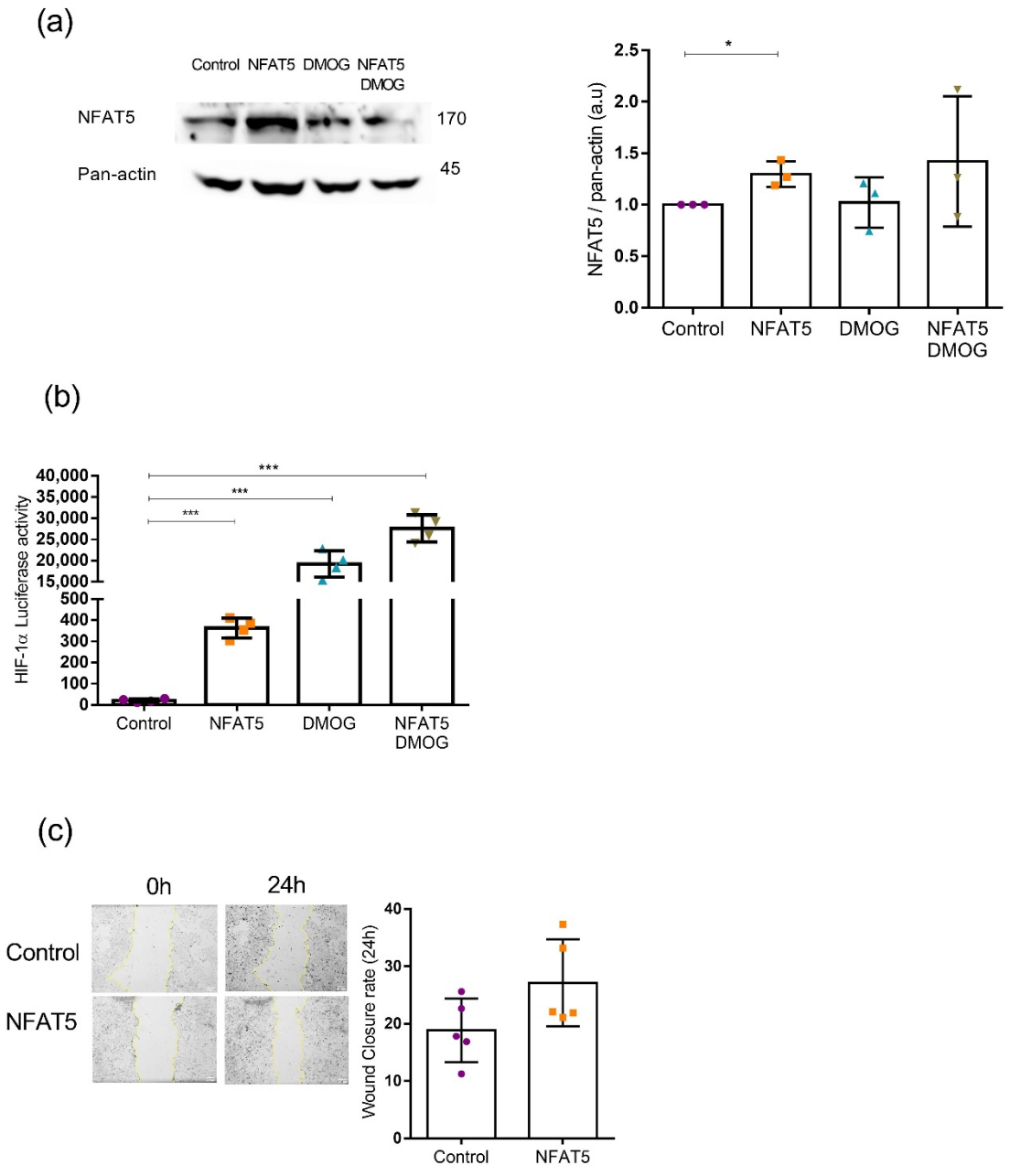

Figure S5. Effect of NFAT5 overexpression in HEC1a cells. HEC1a cells were treated with 0.5 mM DMOG for 24 hours, after 24 hours transfection with NFAT5 overexpression plasmid. (a). NFAT5 protein abundance were investigated by western blot analysis (n=3, *, P, <0.05). (b) HIF-1α promoter activation upon NFAT5 transfection in verified with luciferase reporter assay (n=4, ***, P<0.001). (c) Effect of NFAT5 overexpression on HEC1a cell migration was verified with wound healing scratch assay (n=5). Representative bright field images and wound closure rate 24 hours post scratch.